Universitat Autònoma de Barcelona

The role of the oncogene Prostate Tumor Overexpressed-1 and the regulation of mRNA translation in Prostate Cancer progression and chemoresistance

Verónica Cánovas Hernández

UNIVERSITAT AUTÒNOMA DE BARCELONA

DEPARTAMENTO DE BIOQUÍMICA Y BIOLOGÍA MOLECULAR

PROGRAMA DE DOCTORADO EN

BIOQUÍMICA, BIOLOGÍA MOLECULAR Y BIOMEDICINA

The role of the oncogene Prostate Tumor Overexpressed-1 and the regulation of mRNA translation in Prostate Cancer progression and chemoresistance

Tesis presentada por Verónica Cánovas Hernández para optar al grado de Doctor por la Universitat Autònoma de Barcelona.

Trabajo realizado en el Grupo de Investigación Biomédica en Urología del Institut de Recerca del Hospital Vall d'Hebron, bajo la dirección de la Dra. Rosanna Paciucci.

Tesis doctoral adscrita al Departamento de Bioquímica y Biología Molecular de la Universitat Autònoma de Barcelona, bajo la tutoría de la Dra. Anna Meseguer.

La doctoranda,

Verónica Cánovas Hernández

La directora,

Dra. Rosanna Paciucci

La tutora,

Dra. Anna Meseguer

Agradecimientos

Gracias a mi familia Collserola. A mis buenas compañeras de laboratorio y amigas (Yolanda, Valentina), de pasillo (Luz, Laia, Aroa, Ana, Carla, Elena, Irene, Blanca, Laura, Lucía, Tati, Mireia, Gabriel, Alfonso, Yoelsis, Marta, Maria José, Pedro, Kim, Eva, Ana, Paula ….) a todos los estudiantes que han pasado por el laboratorio (Marga, Adriana, Blanca, Vicente, Enric, Sandra, Lidia, Estela, Daniele, Laura, Marc), y especialmente a Rosanna. Gracias por vuestras enseñanzas, consejos, por crear un entorno de trabajo agradable y en ocasiones muy divertido y contribuir a que vuestras experiencias sean parte hoy de mis experiencias. Gracias también al resto de investigadores, sobre todo a Miguel Segura por su enorme paciencia, grandes consejos y críticas constructivas. No me olvido de los celadores (Ray, Pilar, Tao, Xavi), coordinación (Eulalia, Rosa), mantenimiento y técnicos (Rashida, Nuria), gracias por el soporte y cariño recibido durante estos años, porque sin vuestro trabajo el nuestro no sería posible. Gracias al Dr. Sonenberg por brindarme la oportunidad de realizar una estancia en su laboratorio y especialmente, gracias al Dr. Mehdi por su ayuda en el día a día del laboratorio, su paciencia y por mantener y transmitir en todo momento una actitud calmada y positiva, a pesar del más horrible de los días, cuando piensas que tu trabajo ha sido en balde.

A mi tesoro más preciado: amigos, los encontrados por el camino durante mi paso por Barcelona (entre ellos Gabi ☺) y a mis Biofriends murcianos y adoptados (Blanca, Joni, Juanjo, Rafa, Miriam, Pablo, Santi, Mari Paz, Javi, Gloria, Antonio) por acompañarme durante todos estos años y hacer los momentos más simples inolvidables. OS ADORO FAMILIA BIOFRIENDS.

A mis padres por su educación, consejos y paciencia, porque sin vuestro esfuerzo y apoyo nada de esto hubiera sido posible. A toda mi familia, también a los Guijarro Carrillo, por apoyarme y ayudarme en este nuevo reto. A la memoria de mi abuelo Antonio, por endulzarme la vida con sus "solano" e inculcarme el valor del esfuerzo y la perseverancia.

Y sobre todo a mi compañero de vida, Pedro, por haber creído siempre en mí, aconsejarme y apoyarme en todas las decisiones importantes durante estos más de 10 años. Gracias por tus mejores sonrisas y por acompañarme durante esta etapa permitiendo descubrir junto a ti esta hermosa Cataluña.

A todos y cada uno de vosotros, un millón de gracias.

A mi tierra…

“En Murcia hablan el más bello catalán del mundo”

http://www.laverdad.es/murcia/ciudad-murcia/201609/04/murcia-hablan-bello-catalan-20160904012144-v.html

“Dadme un punto de apoyo y moveré el mundo”

Arquímedes

Index

INDEX OF FIGURES

ABBREVIATIONS

A

AAH: atypical adenomatous hyperplasia

ABC: ATP-binding cassette

ADT: androgen deprivation therapy

ALDH1A1: aldehyde dehydrogenase 1 family member A1

AMACR: α-methylacyl-CoA racemase

AP2: activator protein 2

AR: androgen receptor

ARE: androgen responder element

ARV7*:* androgen receptor splice variant 7

ATF6: activating transcription factor 6

B

BHP: benign prostate hyperplasia

BSA: bovine serum albumin

C

CBP: CREB-binding protein

CCNG2: cyclin G2

CHD-1: cadherin 1

ChIP: chromatin immunoprecipitation

CRPC: castration resistant prostate cancer

CSCs: cancer stem cells

CTC: circulating tumor cell

CZ: central zone

D

DAB2IP: DAB2 interacting protein

DBS: double strand break

DDA: DNA-damaging agent

DDR: DNA damage response

DHT: dihydrotestosterone

DKK1: dickkopf WNT signaling pathway inhibitor 1

DMSF: distant-metastasis free survival

DMSO: dimethyl sulfoxide

Dox: doxycycline

DR: docetaxel resistant

DRE: digital rectal examination

DS: docetaxel sensitive

E

eIF4E: eukaryotic initiation factor 4E

eIF4E-BP: EIF4E binding protein (also known 4EBP)

EMT: epithelial-mesenchymal transition

EPCA: early prostate cancer antigen

ESC: embryonic stem cells

ESCC: esophageal squamous cell carcinoma

ETS: erythroblast transformation-specific

ETV5: ETS variant 5

F

FISH: fluorescence in situ hybridization

G

GC: genomic classifier

GFP: green fluorescence protein

GPS: genomic prostate score

GS: Gleason score

GSTP1: glutathione S-transferase pi 1

H

h: hours

HDAC: histone deacetylase

HES1: hes family bHLH transcription factor 1

HEY1: hes related family bHLH transcription factor with YRPW motif 1

HGPIN: high-grade prostatic intraepithelial neoplasia

HPV: human papillomavirus

I

ICN: intracellular Notch

IGF-1: insulin-like growth factor 1

IHC: immunohistochemistry

J

JNK: Jun N-terminal kinase

K

KD: dissociation constant

KLK1: kallikrein 1

KLK2: kallikrein 2

KRT: cytokeratin

L

lncRNAs: long non-coding RNAs

LSCC: lung squamous cell carcinoma.

LV: lentiviral vectors

M

MED25: mediator complex subunit 25

mHNPC: metastatic hormone-naïve prostate cancer

MMPs: methaloproteinases

mTOR: mechanistic target of rapamycin

N

NGS: next generation sequencing

NKX3: NK3 homeobox 1

NLS: nuclear localization signal

NMR: nuclear magnetic resonance

O

O/N: over night

OS: overall survival

P

PARP1: poly ADP-ribose polymerase-1

PBS: phosphate-buffered saline

PCa: prostate cancer

PCA3: prostate cancer antigen 3

PDCD4: programmed cell death protein 4

PDT: population doubling time

PEA3: polyoma enhancer activator 3

PI3K: phosphatidylinositol-4,5-bisphosphate 3-kinase

PI3KCA: PI3K catalytic subunit alpha

PIN: prostatic intraepithelial neoplasia

PKC: protein kinase C

PolyPro: polysome profiling

PSA: prostate specific antigen

PSADT: PSA doubling time

PTEN: phosphatase and tensin homolog

PTOV1: prostate tumor overexpressed 1

PTOV1-AS1: PTOV1 antisense 1

PTOV1-AS2: PTOV1 antisense 2

PZ: peripheral zone

R

RA: retinoic acid

RACK1: receptor for activated C kinase 1

RAR: retinoic acid receptor

RFP: red fluorescence protein

RFS: relapse free survival

RiboPro: ribosome profiling

RPM: revolutions per minute

RPS6: ribosomal protein S6

RT: room temperature

S

SDS-PAGE: sodium dodecyl sulfate polyacrylamide gel electrophoresis

SFE: sphere forming efficiency

SHARP: SMRT/HDAC1-associated repressor protein

SP: side population

SP1: specificity protein 1

SPOC: Spen paralog and ortholog C-terminal

SPOP: speckle type BTB/POZ protein

STAT6: signal transducer and activator of transcription 6

T

TAD: transactivation domain

TGFβ1: transforming growth factor beta 1

TICs: tumor initiating cells

TMPRSS2: Transmembrane Protease, Serine 2

TNM: tumor, node and metastasis

TOP: terminal oligopyrimidine

TSL: transcript support level

TZ: transition zone

U

uPA: urokinase-type plasminogen activator

uPAR: receptor of uPA

UTR: untranslated terminal region

V

V: volts

VSMCs: vascular smooth muscle cells

VWA: von Willebrand factor A

Chapter 1:

INTRODUCTION

Cathedral of Murcia.

"The Cathedral of Murcia dates back to 1394 and continued to grow until the 18th century. It is an imposing building in a range of Gothic and baroque styles. With three naves, a restored choir and 23 side chapels, it is filled with treasures and artworks. The belltower rises up for four floors and, with its weathervane on top, is the tallest campanile in Spain. The façade is truly resplendent with carved detail on every surface. Highlights include the Door of Apostles, the polygonal Velez Chapel and the Door of Chains…."

1. Natural history, genetic alterations and current treatments of primary and metastatic prostate cancer

1.1 Anatomy and histology of the normal prostate

The human prostate is a glandular organ of the male reproductive system situated beneath the bladder and just in front of the rectum. The base of the prostate is in continuity with the bladder and the prostate ends at the apex before becoming the striated external urethral sphincter. The most important function of the prostate is the production of a milky fluid that makes up around 20 to 30 percent of the semen, together with sperm cells from the testicles and fluids from other glands. The muscles of the prostate also ensure that the semen is forcefully pressed into the urethra and then expelled outwards during ejaculation. The prostate is enclosed by a capsule composed of collagen, elastin and large amounts of smooth muscle and is composed of 3 different anatomical zones [1]:

- The central zone (CZ), which is the area that surrounds the ejaculatory ducts, is about 25% of the prostate volume. Only a very small percentage of prostate cancers begin here.
- The peripheral zone (PZ) that is located at the posterior of the gland, closest to the rectal wall, and represents the 70% of the prostate volume. The PZ is the area that is palpated on digital rectal examination (DRE) and the majority of prostate intraepithelial neoplasias (PIN) and prostatic carcinomas originate from this region.
- The transition zone (TZ) represents about 5-10% of the prostate volume. TZ is directly below the bladder and surrounds the transitional urethra. The epithelium consists of transitional cells similar to bladder epithelium. Most of benign prostate hyperplasia (BHP) occurs in this region and 20-30% of prostate cancers begin in this zone [2].
- Anterior fibromuscular stroma is located anterior to the urethra and extends into the transition zone.

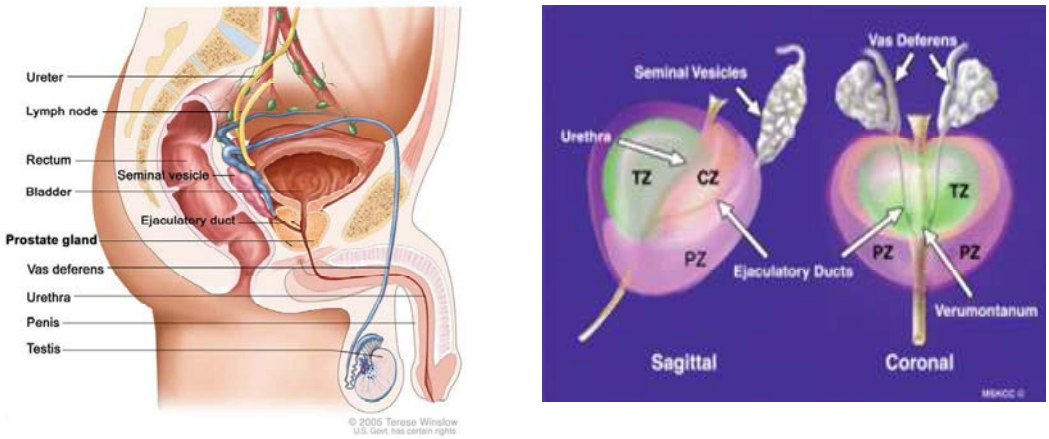

Figure 1. Anatomy of the normal prostate. Image from Geneva Foundation for Medical Education and Research.

Histologically, the prostate is composed of epithelial acini arranged in a fibromuscular stromal network [3]. The tubuloalveolar gland have pseudostratified columnar epithelium. Prostatic epithelium is composed of different cell types, including basal, luminal, neuroendocrine and intermediate cells that share properties of both luminal and basal cells. Luminal cells directly surround the lumen and produce secretory proteins such as prostate specific antigen (PSA), express cytokeratin 8 (KRT8), KRT18, and high levels of the androgen receptor (AR). The basal cells are aligned between the luminal cells and the basement membrane and express markers such as KRT5, KRT14 and p63 but express AR at low or undetectable levels. Neuroendrocrine cells are less common and secrete neurotrophic factors. Intermediate cells express both the basal and luminal lineage markers. Each gland is surrounded by connective tissue and smooth muscle. The stroma accounts for about 70% of the prostate mass. During ejaculation, the smooth muscle contracts and leads to the expulsion of the glandular content. The prostatic secretion is slightly acidic (pH 6.4) and forms about 20% of semen volume. It contains factors that contribute to motility of sperm cells and uterus stimulation, as well as Zn^{2+}, citrate, phosphatases and proteases which are responsible of liquefaction of the semen and crucial for the molecular synchronization of the functional cascade triggered by ejaculatory stimuli [4].

The development, maturation and maintenance of the prostate require regulation by androgens [5]. Testosterone, the principal androgen secreted by the fetal and adult testes, can undergo irreversible 5α-reduction to dihydrotestosterone (DHT) which mediates many of the differentiating, growth-promoting and functional actions of androgens. The 5 α-reductase enzyme is necessary for proper prostate development and survival. In

individuals lacking a functional 5 α-reductase gene, the prostate is small or undetectable [6]. In addition, chemical castration results in a loss of 70% of the prostate secretory epithelial cells with no affectation of basal epithelia and stromal cell populations [6].

1.2 Prostate Cancer

1.2.1 General concepts and risk factors

Prostate Cancer (PCa) is the most common male malignancy and the second major cause of cancer deaths in men of EEUU, and the third one in Spain. However, its incidence differs among Countries due to coverage of prostate-specific antigen (PSA) screening [7]. PCa incidence is increasing mainly because of population ageing and the widespread introduction of the PSA screening test [8]. The majority of PCa are adenocarcinomas derived from the gland cells of the prostate. Other unusual types of PCa include sarcomas, small cell carcinomas, neuroendocrine tumors and transitional cell carcinomas [9].

The most important risk factors for PCa are: age, ancestry, family history and genetic changes [10].

- Age: PCa is rarely seen in men younger than 40 years, but the chance of having PCa rises rapidly after age 50. Approximately 10% of PCa cases are diagnosed in men younger than 56 years and about 6 out of 10 cases are found in men older than 65.

- Ancestry: The risk of developing and dying from PCa is higher among African-American men than in men of other races. The risk is lowest among Asian men. The reasons for these racial/ethnic differences are not clear.

- Family history: PCa has a heritable component. Inherited gene changes cause about 5 to 10% of PCa cases. Risk also increases when a first-degree relative is diagnosed with PCa before age 65 years. Several inherited mutated genes have been linked to hereditary prostate cancer, including mutations in genes related with normal development of the prostate gland (HOXB13) and mutations in several tumor suppressor genes such as HPC1, BRCA1 and BRCA2 [10].

- Acquired genes mutations: the majority of gene mutations related to prostate carcinogenesis seem to develop during a man's life rather than having been inherited.

Somatic alterations arise in prostate cells including activation of oncogenes and loss of function of tumor suppressor genes. Genetic alterations will be discussed in detail in a subsequent section.

Other potential modifiers of PCa risk are endogenous hormones, including both androgens and estrogens. It has been reported that individuals with castrated levels of testosterone before puberty do not develop PCa [11]. In addition, genetic variations in androgen biosynthesis and metabolism have been linked to prostate carcinogenesis [12].

1.2.2 Natural history of prostate cancer

So far, two premalignant lesions are considered as precursors of prostatic adenocarcinoma: the high grade prostatic intraepithelial neoplasia (HGPIN) and the atypical adenomatous hyperplasia (AAH) [13]. PIN is predominantly located in the peripheral zone of the prostate, the area in which most clinically important prostate cancers are found, and PIN, like PCa, is often multifocal. PIN is classified in two grades according to architectural and cytological characteristics: low grade- (grade I) and high grade- (grade II and III) PIN. At the histological level, PIN is characterized by the appearance of luminal epithelial hyperplasia, reduction in basal cells, enlargement of nuclei and nucleoli and nuclear atypia. In HGPIN, the basal cell layer is disrupted or fragmented as demonstrated by high-molecular-weight cytokeratin immunolabeling, whereas in PCa there is a complete loss of the basal cell layer (**Figure 2**). PIN and PCa share several nuclear properties, such as amount of DNA, chromatin texture, chromatin distribution, nuclear perimeter, diameter, and nuclear abnormalities. AAH can be diagnosed throughout the prostate, but it is most often located in the transition zone of the prostate in intimate association with benign nodular hyperplasia. AAH is a lesion characterized by a proliferation of small acinar structures that mimics adenocarcinoma because of histological similarities.

Prostate carcinogenesis is mediated by the accumulation of genetic and epigenetic aberrations. These molecular changes can result from altered AR transcriptional activity, changes in chromatin architecture, error-prone DNA repair or defective cell division that can be inherited. All together, these processes confer survival and growth advantage to the transformed cell. PCa preferably metastasizes to bones, where it forms characteristic osteoblastic lesions rather than osteolytic lesion, although other common sites of secondary metastasis are lung, liver and pleura. Molecular and cytogenetic analyses of

multiple metastases in the same patients show that they are clonally related, suggesting that metastatic PCa may arise from individual clones during cancer progression [14].

PCa presents two important features that directly affect its study and clinical management: it is a heterogeneous and multifocal disease. Within the tumor can coexist different benign glands, PIN and neoplastic foci of different grade of malignancy. In addition, different neoplastic foci can present distinct molecular and clinical features, and are often genetically distinct [15]. About 80% of radical prostatectomy specimens showed separate foci of cancer and in addition, around of 70% also present PIN lesions [16].

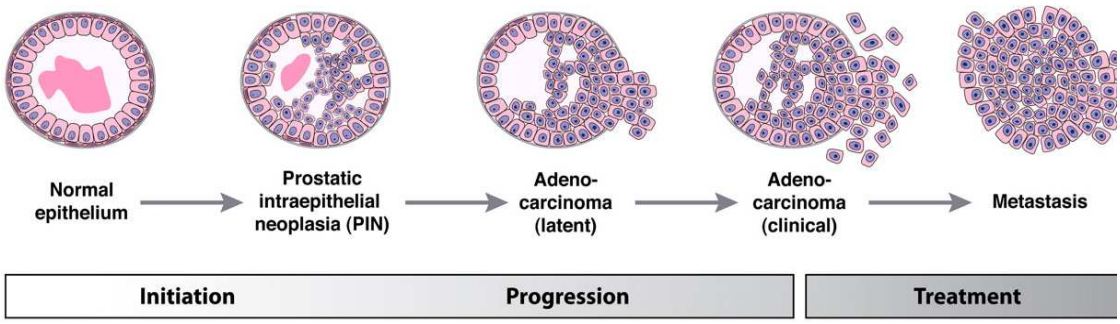

Figure 2. Stages of progression of prostate cancer. Figure adapted from Shen *et al.* [17]

1.2.3 Genetic and epigenetic alterations in prostate cancer

PCa is a clinically and genetically heterogeneous disease. Next-generation sequencing has allowed the characterization of the clonal hierarchy of genomic lesions in prostate tumors, providing information about carcinogenesis. From initiation of hormone-naïve PCa to its progression towards therapeutic resistance and death, various combinations of genetic and epigenetic events occur. A number of important somatic alterations have been identify as gains or losses of chromosomal regions, including gains at 8q and losses at 3p, 8p, 10q, 13q and 17p [17]. The most frequent molecular subtypes of localized PCa present *ETS* gene rearrangements, most commonly as *TMPRSS2-ERG*, in association with mutations of *TP53* (**Figure 3**). Less frequent are subtypes with mutations in *SPOP/CHD1* genes, and several other smaller subtypes [18]. Deletions at 10q24 region including *PTEN* locus and gains at 8q24 region including *MYC* have been shown to promote further disease progression. Of note, several of these genetic alterations, such as *MYC* overexpression, have also been observed in HGPIN lesions supporting the precursor relationship of these lesions [19, 20]. ETS-rearranged tumors are

prone to be enriched in genomic alterations in the PI3K and p53 signaling pathways, whereas other genomic alterations predominate in SPOP-mutant cancers. Deletions at the *TP53* locus are very frequent (25% to 40%) in PCa samples, with point mutations in 5% to 40% of cases [21]. These alterations have been reported in 25% to 30% of clinically localized cancers, suggesting that dysregulation of *TP53* may occur relatively early in the disease timeline.

The mutations in the *SPOP* gene, that encodes for the substrate-recognition component of a Cullin 3-based E3-ubiquitin ligase, have been identified as a key genomic event involved in the natural carcinogenesis of hormone naïve PCa without any androgen driven gene fusions [18]. Mutations in *SPOP* occur in up to 15% of PCa and are mutually exclusive with *TMPRSS-ERG* fusions and other *ETS* rearrangements. *SPOP* mutations are found in HGPIN adjacent to adenocarcinoma, and likely represent early events in the natural history of PCa. In addition, *SPOP* mutant tumors generally lack lesions in the PI3K pathway (*PTEN*) or in *TP53* and are associated to deletions of *CHD1* at 5q21, a chromodomain helicase DNA-binding protein. *SPINK1*, a secreted serine peptidase inhibitor, is overexpressed in a subset of *ETS*-negative cancers (10%) including *SPOP*-mutant cancers (**Figure 3**). Therefore, *SPOP* mutations are considered as a driver lesion restricted to *ETS* negative tumors.

Metastatic tumors show a significant *de novo* activity of androgen signaling, that involves *AR* gene point mutations, alteration in its splicing, gene amplifications, mostly observed in cancers treated with androgen deprivation therapy (**Figure 3**). These alterations are found in association to *ETS* rearrangements and *PTEN* deletions, but are not detected in tumors with *CHD1/SPOP* alterations [19, 20]. Metastatic tumors also show a significant increase in *PTEN* lesions and other PI3K pathway components besides an overall increase in genomic aberrations.

Epigenetic modifications are also believed to represent important contributing factors in prostate carcinogenesis [22]. Some of the earliest molecular events commonly reported in human primary PCa are the CpG island promoter methylation of *GSTP1* gene [17]. Additionally, trimethylation of lysine residue 27 of histone H3 (H3K27-me3) have been associated with prostate carcinogenesis through the repression of tumor suppressor genes such as *DAB2IP*, a member of the Ras GTPase family.

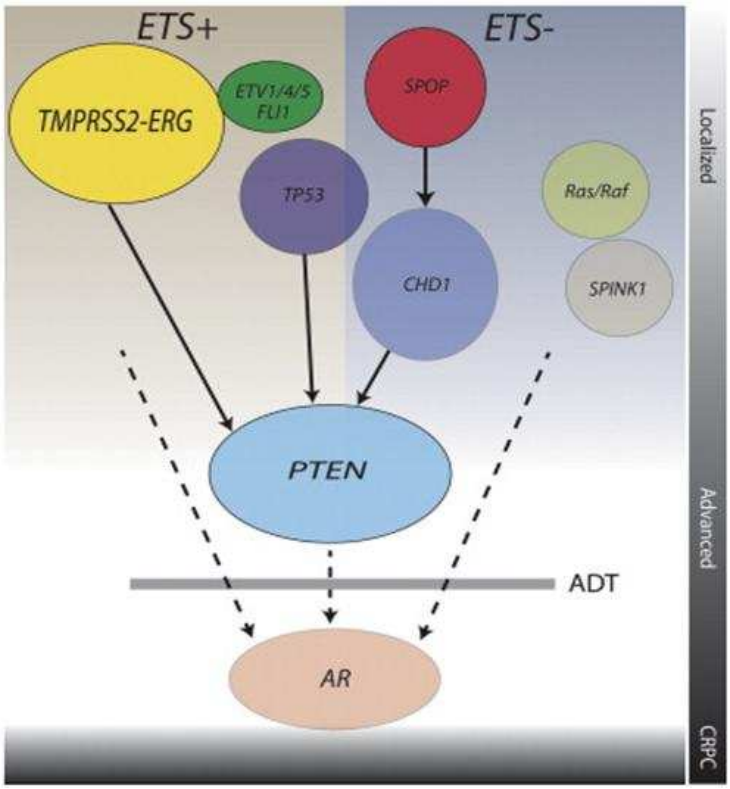

Figure 3. Genetic landscape of localized and advanced prostate cancer. Genes with common genomic lesions (including mutation, rearrangement, or copy number alteration) are shown. Solid arrows designate a temporal relationship between events; presumptive "early" lesions are at the top, with "later" lesions below. From Barbieri *et al.* [21].

1.2.4 Early detection, prognosis and risk stratification of prostate cancer

Today, the early detection of PCa is based in the screening with the prostate-specific antigen (PSA) blood test, followed by digital rectal examination (DRE) or transrectal ultrasound (TRUS) [8]. PSA is a kallikrein-related serine protease that is produced in normal prostate secretions, but is released into the blood as a consequence of the disruption of the normal prostate architecture. However, a definitive diagnosis depends on histopathologic verification and requires a prostate biopsy. Following biopsy, histopathological grading of prostate tissue is performed by Gleason scoring which classifies tumors from most to least differentiated. In addition, patients are also diagnosed according to the TNM classification that records the primary and regional nodal extent of the tumor and the absence or presence of metastases.

A. Histopathological grading prostate cancer: Gleason system

The Gleason system, introduced in 1966 by Donald F. Gleason, is one of the most worldwide accepted grading systems used as predictors of prognosis in patients with PCa [23]. Five grades were proposed based on architectural features and not on cytological atypia, cell counts or mitotic rates as most tumor grading systems (**Figure 4**).

- Pattern 1 was defined as very well-differentiated, closely packed, small, uniform glands in circumscribed masses.
- Pattern 2 had less well-circumscribed masses consisting of well-differentiated glands, variable in size and shape. A ‘‘mild degree’’ of cribriform patterning was permitted.
- Pattern 3 showed diffuse penetration of the stroma by malignant well-differentiated glands. This included variable cribriform patterns, single cells and cords or masses of cells.
- Pattern 4 consisted of tumors with a diffuse growth of large polygonal cells resembling clear cell carcinoma of the kidney.
- Pattern 5 was restricted to undifferentiated carcinoma with little or no glandular differentiation resembling small cell carcinoma of the lung or carcinoma simplex.

Due to the heterogeneity of PCa, the biopsy Gleason score (GS) consists of the Gleason grade of the most extensive pattern plus the highest pattern, regardless its extent [8]. The original Gleason grading system has suffered some modifications so far. Some of the most important changes are that grade 4 criteria were expanded to include poorly formed glands. It has been found that any cribriform morphology in PCa is associated with a less favorable outcome. This has led to the concept that all cribriform cancer and glomeruloid structures should be graded as pattern 4. It was recommended for needle biopsies that the secondary pattern, if of higher grade, had to be included in the score even if this was less than 5% of the tumor volume. The original Gleason system had scores ranging from 2 to 10, but with the 2005 modifications, needle biopsy scores could only range from 6 to 10. This meant that the lowest score that could be reported for well-differentiated tumors was 6, giving an incorrect message to patients that their cancer was moderately differentiated. In an attempt to address this, there was consensus at the 2014 International Society of Urological Pathology (ISUP) conference that GSs should be replaced by five grades: grade 1 (GS 3+3 or ≤6), grade 2 (GS 3+4), grade 3 (GS 4+3), grade 4 (GS 4+4, 3+5 and 5+3) and grade 5 (GS 9–10). Grade groups can now be

reported in addition to the overall or global Gleason score of a prostate biopsy or radical prostatectomy [8].

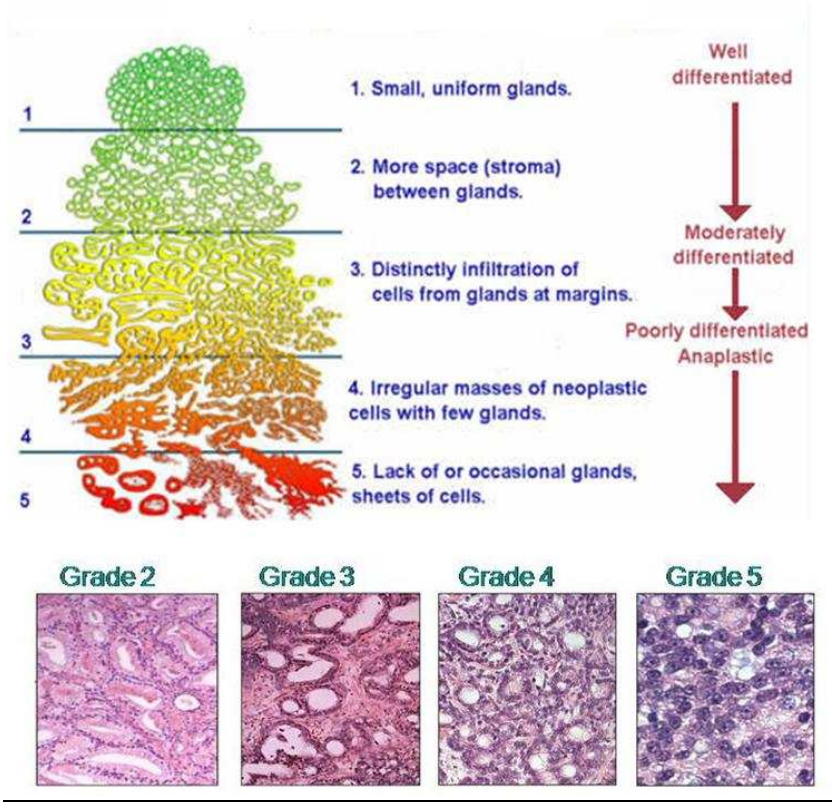

Figure 4. Gleason grading system.

B. Anatomic classification of prostate cancer: TNM system

TNM classification is based in anatomic disease extent. T category describes the primary tumor site, from organ-confined to fully invasive (T1-4). N category describes the regional lymph node involvement (N0 or 1) and M category describes the presence or otherwise of distant metastases (M0 and 1 a-c) [24] (**Tabla 1**).

Stage	Definition
Primary tumor	
TX	Primary tumor cannot be assessed
T0	No evidence of primary tumor
T1	Clinically, the tumor is neither palpable nor visible with imaging
T1a	Tumor is an incidental histologic finding in 5% or less of tissue resected
T1b	Tumor is an incidental histologic finding in more than 5% of tissue resected
T1c	Tumor identified with needle biopsy (eg, because of an elevated PSA level)
T2	Tumor confined within the prostate
T2a	Tumor involves one-half of one lobe or less
T2b	Tumor involves more than one-half of one lobe but not both lobes
T2c	Tumor involves both lobes
T3	Tumor extends through the prostate capsule
T3a	Extracapsular extension (unilateral or bilateral)
T3b	Tumor invades seminal vesicle(s)
T4	Tumor is fixed or invades adjacent structures other than seminal vesicles: bladder neck, external sphincter, rectum, levator muscles, and/or pelvic wall
Regional lymph nodes	
NX	Regional lymph nodes were not assessed
N0	No regional lymph node metastasis
N1	Metastasis in regional lymph node(s)
Distant metastasis	
MX	Distant metastasis cannot be assessed (not evaluated with any modality)
M0	No distant metastasis
M1	Distant metastasis
M1a	Nonregional lymph node(s)
M1b	Bone(s)
M1c	Other site(s) with or without bone disease

Table 1. TNM classification of prostate cancer.

A combination of TNM classification for staging of PCa and the European Association of Urology (EAU) risk group classification, based on grouping patients with a similar risk of biochemical recurrence after local treatment, are used to classify low-risk, intermediate-risk of high-risk PCa (**Table 2**).

Low-risk	Intermediate-risk	High-risk	
	Definition		
PSA < 10 ng/mL	PSA 10–20 ng/mL	PSA > 20 ng/mL	any PSA
and GS < 7	or GS 7	or GS >7	any GS
and cT1-2a	or cT2b	or cT2c	cT3–4 or cN+
Localised	Localised	Localised	Locally advanced

GS = Gleason score; PSA = prostate-specific antigen.

Table 2. EAU risk groups for biochemical recurrence of localized and advanced prostate cancer. From Mottet 2017 [8].

1.2.4.1 Biomarkers for early diagnosis of prostate cancer

Screening for PCa remains one of the most controversial topics in the urologic literature. Since PSA screening has been widely implemented for PCa detection, the incidence of locally advanced PCa, metastasis and death have dramatically decreased. However, the presence of PSA in serum is sensitive but not specific for PCa, especially

when levels are moderately elevated between 4 and 10 ng/mL. A number of benign conditions (e.g. prostatitis and BPH) can increase PSA levels. In addition, PSA blood screening is also associated with overdiagnosis and overtreatment of low-risk cancers that are unlikely to progress. Therefore, in order to discern indolent and aggressive disease PCa screening requires tools that improve the limited specificity and risk stratification of PSA test and have a higher specificity for clinically significant disease [25].

A. Serum biomarkers

A growing armamentarium of novel biomarkers for risk prediction in the detection and prognosis of PCa has emerged in recent years due to recognized limitations of conventional biomarkers, such as the determination of total blood PSA levels. With this aim, several derivatives of PSA have been evaluated for their presence in serum, including age-specific total PSA cutoffs, total PSA density (PSA levels divided by the volume of the prostate transition zone), total PSA velocity (the total of PSA evaluation in one year), isoforms of PSA-messenger RNA, and PSA doubling time (PSADT) (the time over which a man's PSA level doubles) [25]. Additionally, different forms of PSA such as free PSA and bound PSA (complexed to α2-macroglobulin, α1-protease inhibitor or α1-antichymotrypsin), and [-2]pro-prostate-specific antigen, a proform of PSA, can be measured [26, 27]. The determination of these three forms of PSA constitute the Prostate Health Index, or *phi score*, calculated as follows: $([-2]\text{proPSA} / \text{free PSA}) * (\sqrt{\text{total PSA}})$. It is useful for distinguishing PCa from benign prostatic condition in men with PSA in the 4-10 ng/mL range and negative digital rectal examination. In addition, other diagnostic biomarkers used in the pre-biopsy setting are included in the 4Kscore Test (total PSA, free PSA, intact PSA, and human kallikrein protein 2) [26]. The main utility of the 4Kscore is to find clinically significant PCa and to minimize unnecessary biopsies in previously undiagnoses patients.

Additional proteins measured in serum have emerged as promising PCa biomarkers. Early prostate cancer antigen (EPCA) and EPCA-2 are integral elements of the nuclear matrix that were demostrated to be upregulated in PCa patients and, in the case of EPCA-2, able to differentiate men with non-organ-confined PCa from those with organ-confined disease and may therefore be helpful to identify aggressive PCa [28].

B. *Tissue biomarkers*

Diagnosis of PCa may be supported by elevated immunostaining for α-methylacyl-CoA racemase (AMACR) combinated with the absence of p63 staining (a basal cell marker) to diagnose inconclusive cases [29]. Methylation status of the enzyme glutathione S-transferase 1 (GSTP1) have been shown to accurately detect PCa. GSTP1 was unmethylated in normal human tissues and BPH but was hypermethylated in PCa specimens [30].

Due to the heterogeneity of PCa, a combination of biomarkers may provide a better predictive value. More recently, several genomic signatures such as oncotypeDX Genomic Prostate Score (GPS) have been validated to predict the subsequent risk of adverse oncologic outcome following treatment with radical prostatectomy [26, 31]. These biopsy-based assays are based on detection of different genes associated with PCa aggressiveness before treatment of patients (**Table 3**). This test is commonly used for an appropiate selection of men for active surveillance and it is useful for patients who have a diagnosis of PCa but the aggressiveness of the tumor is not known.

Stromal Group	Cellular Organization Group	Androgen Group	Proliferation	Reference Genes
BGN	FLNC	FAM13C	TPX2	ARF1
COL1A1	GSN	KLK2		ATP5E
SFRP4	TPM2	AZGP1		CLTC
	GSTM2	SRD5A2		GPS1
				PGK1

Table 3. OncotypeDX GPS. The aggregate expression of 5 reference genes is used to normalize the expression of the 12 cancer-related genes. Individual group scores are calculated (stromal, cellular organization, androgen and proliferation score) and algorithmically combined to calculated the GPS. A negative coefficient in the calculation of the GPS is associated with better outcome whereas a positive coefficient is associated with poorer outcome. Figure adapted from [31].

C. *Urine biomarkers*

Prostate cancer antigen 3 (PCA3), a non-coding prostate specific mRNA, is overexpressed at high levels in PCa tissues compared with benign prostate tissue. The PCA3 assay is based on a PCR nucleic acid amplification test that measures the ratio of the concentration of PCA3 to PSA mRNA in post-DRE first-catch urine samples. The PCA3 test combined with other genetic data, such as *TMRPSS2-ERG* fusion, is a potential way to improve accuracy for PCa diagnosis when the two markers are combined [32].

1.2.4.2 Biomarkers for disease progression and post-treatment risk stratification

Identification of appropriate biomarkers to predict patients' prognosis and treatment success is of dire need. Today, some tests are available to predict disease progression in men with advanced disease and to determine which men have the highest risk of cancer recurrence after definitive therapy.

Some classical parameters such as PSA and PSADT have been shown to be independent prognostic factors for overall survival (OS) in metastatic castration resistant prostate cancer (CRPC) [33]. In addition, reduction in PSA velocity (half-life dynamics) with docetaxel-based therapies is indicative of favorable prognosis over time. However, rapid PSA kinetics in men with asymptomatic metastatic CRPC is a poor prognostic factor and may suggest a need for aggressive therapy such as docetaxel to prevent the onset of symptomatic disease [33]. It is important to consider that some prostate cancers, particularly those with neuroendocrine features, produces little or any PSA and thus other biomarkers should be explored.

Additionally, tests based in a genomic signature have emerged in recent years to predict the likelihood of clinical disease recurrence. The Decipher test uses a gene-expression panel of 22 genes involved in cell proliferation, migration, tumor motility, androgen signaling and immune system evasion to determine a genomic classifier (GC) risk score [32]. It predicts the likelihood of disease recurrence at 5 years after prostatectomy in men with adverse pathological conditions, such as seminal vesicle invasion or extracapsular extension, on final post-prostatectomy pathology.

In recent years, the release of circulating tumor cells (CTCs) and cell-free DNA from the primary tumor site or from metastasis into the circulation have emerged as promising PCa biomarkers of cancer progression for non-invasive characterization of disease and molecular stratification of patients [34]. For instance, the AR splice variant *ARV7,* a truncated form of the AR lacking the ligand binding domain, was isolated from patients with no response or lower response rates to AR-directed therapies (abiraterone and enzalutamide) although no evidences suggest its role in resistance to taxanes chemotherapies. The CellSearch CTC test analyzes the expression of specific epithelial cell-adhesion markers to discern CTCs from normal blood cells [32]. However, the lack of specificity of epithelial cell-adhesion markers or inadequacies in cell recovery restricts the widespread use of this kit.

Despite significant progress in the research of PCa biomarkers for prostate cancer management, a number of patients are still overdiagnosed with indolent PCa while others die from aggressive disease diagnosed too late or barely respond to current therapies. Therefore, future effort is required for the identification of new biomarkers that provide better predictive value and improve personalized PCa therapy.

1.2.5 Treatment options for prostate cancer

An early diagnosis and treatment of PCa is associated with better outcomes. The majority of newly diagnosed localized (80%) or regional tumors (12%) are successfully treated by surgery (radical prostatectomy) or irradiation, and their 5-year survival is nearly 100% (**Figure 5**) [8, 35, 36]. For men with metastatic PCa at the time of diagnosis, their 5-year survival is only 28.2% [36]. The first-line therapy for patients with both metastatic hormone-naïve PCa and high-risk localized disease is androgen deprivation therapy (ADT) [37]. The initial response to ADT is very effective in reducing PCa and metastatic growth. The deprivation of serum testosterone leads to reduced levels of dihydrotestosterone (DHT) and the androgen-dependent tumor cells undergo apoptosis. However these responses are seldom sustained in the long term and eventually the disease recurs and progresses to a castration-resistant prostate cancer (CRPC) in most cases (**Figure 5**) [38, 39]. CRPC is defined by castrate serum testosterone levels less than 50 ng/dL or 1.7 nmol/L plus biochemical progression (three consecutive rises in PSA >2 ng/mL one week apart) or radiologic progression (appearance of new metastatic lesions) [40]. The median survival of men with metastatic CRPC ranges from 15 to 36 months [41]. Kirby and cols determined that approximately 9.5% to 53% of men with advanced PCa will develop CRPC within 5 years. However, considering those studies that defined CRPC in terms of a rise in PSA levels following castration, the prevalence ranges from 10% to 20% and around 84% of those will have metastases at the time of CRPC diagnosis. Of those with no metastases present at time of CRPC diagnosis, 33% likely will develop metastases within 2 years [41].

Until 2010, the gold standard treatment in US for CRPC patients was docetaxel chemotherapy, 75 mg/m^2 in three weekly doses combined with prednisone 5 mg twice a day up to 10 cycles [40, 42]. Docetaxel is a taxol that prevents microtubule de-polymerization and mitotic division. Microtubules are components of the cellular cytoskeleton which are fundamental for separating chromosomes during mitosis, for the

control of intracellular trafficking of proteins, organelles and vesicles, and are very important structures for cell proliferation and migration [43]. In the last three years, the use of docetaxel has been introduced in the clinics in combination with androgen suppression with the aim to enhance the effects of androgen deprivation in eliminating the cancer cell populations with more proliferative capacities [44]. Results from this combined-therapy are still scarce, however it appears to be more efficient and patients ameliorate their survival free from CRPC [44-46]. In addition, the findings that tumors in men with CRPC are still largely dependent on AR signaling, upregulate its expression, constitutively activate AR splice variants, or re-activate AR signaling via alternative pathways, have stimulated the development of more specific anti androgen drugs [47]. These include the androgen biosynthesis inhibitor abiraterone and the AR antagonist enzalutamide and ARN-509 (apalutamide), a newer antagonist with higher activity currently in Phase III Clinical Trial [37, 48-51]. Additional new drugs have been approved over the past few years, including second-generation taxols such as cabazitaxel, immunotherapeutic sipuleucel-T or alpharadin (also known as radium-223) and multiple new compounds are under evaluation [52-54] (**Figure 5**). Despite the moderate increase in therapeutic options, resistance to therapies in CRPC remains a critical point in the clinical management of patients as evidenced by the modest survival benefits offered by each of these treatments.

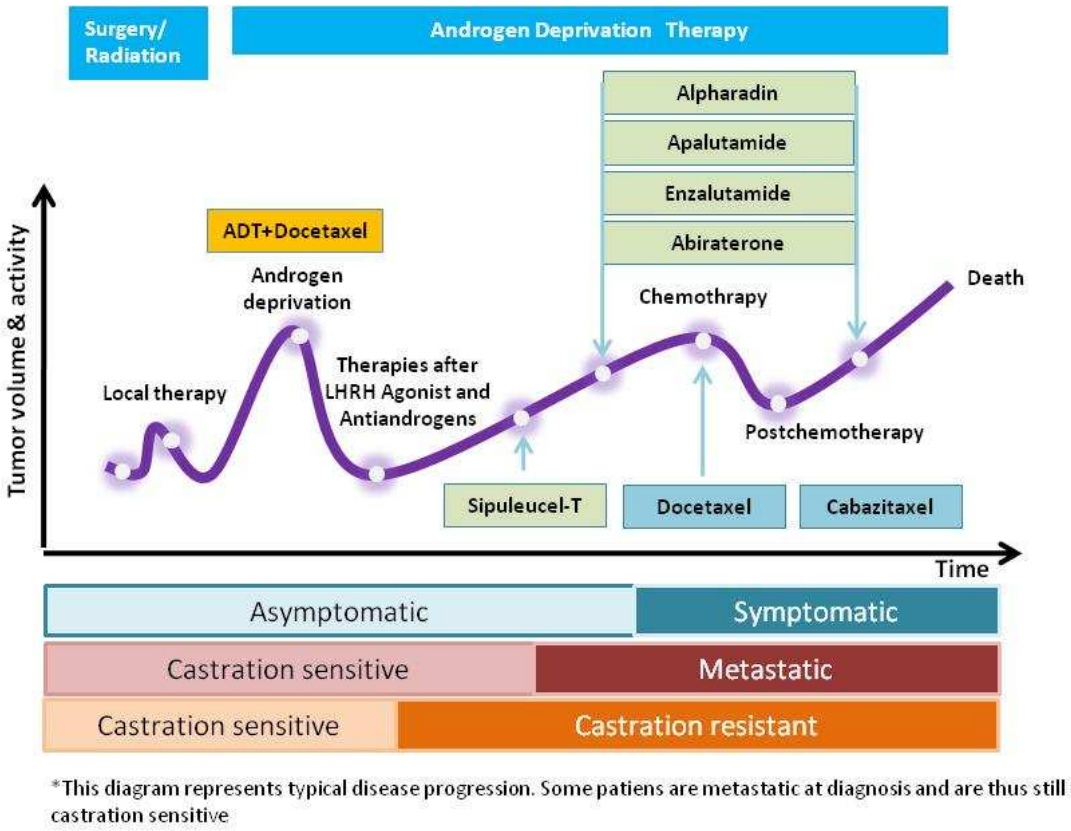

Figure 5. Disease progression and current therapies in prostate cancer.

1.2.6 Mechanisms of therapeutic resistance to docetaxel treatment in CRPC

Several strategies are deployed by cancer cells to overcome the lack of androgen, that consequently induce a progression of the cancer to CRPC, including molecular adaptations of the AR, ligands, and AR signaling regulators as well as tumor microenvironment modifications [39]. The therapeutic impact of taxanes based chemotherapies (docetaxel and cabazitaxel) on patient survival is still essential in the management of advanced PCa for patients who failed AR-targeting strategies.

Docetaxel prevents microtubule de-polymerization and results in apoptosis and G2/M cell cycle arrest. Recent data suggest that taxanes can also affect AR signaling by inhibiting ligand-induced AR nuclear translocation and downstream transcriptional activation of its target genes, confirming a role for microtubules in AR trafficking to the nucleus [55]. However, AR nuclear translocation and signaling was not inhibited in cells with acquired β-tubulin mutations that prevent taxanes-induced microtubule stabilization [56, 57]. Mechanistically, the resistance to docetaxel has been associated to overexpression of ATP-binding cassette (ABC) transporter molecules, altered expression

of alternative β-tubulin isoforms and survival factors, diminishing docetaxel efficacy [35, 58-60].

Docetaxel resistance has also been associated with Epithelial-Mesenchymal transition (EMT) induction [61-63], a process associated with invasive, migratory tumor cells and metastasis. EMT is characterized by changes in gene expression profile, including decreased expression of epithelial genes such as *CDH1* and increased expression of mesenchymal genes such as *SNAI1, CDH2* and *VIM* [64-66]. Three major families of transcription factors control EMT: *ZEB1/ZEB2*, zinc finger *SNAI1* / *SNAI2,* and basic helix-loop-helix families (e.g. *TWIST1*). These transcriptional factors repress the expression of *CDH1* and other epithelial markers and induce the expression of mesenchymal markers. Upregulation of *ZEB1* and its repression action on *CDH1* in docetaxel resistant prostate cancer cells was shown to be a driver of EMT and docetaxel resistance [62]. The exposure of docetaxel sensitive PCa cells to TGFβ1, an EMT inducer in PCa, increased their survival in the presence of docetaxel. In CRPC patients treated with docetaxel, the expression of E-cadherin was decreased in patients not responding to therapy compared to control, suggesting that EMT process might be a major player in the establishment and maintenance of resistance to docetaxel [62]. In addition, *JUN, SNAI1*, and *NOTCH2 / SHH* (sonic hedgehog) signaling pathways have been implicated in the development of resistance to docetaxel or paclitaxel [67-69]. However, despite the intense research, the mechanisms of PCa resistance to docetaxel are not completely understood and more investigations are required to design targeted therapies able to overcome the insurgence of resistance.

2. Prostate Tumor Overexpressed-1 (PTOV1)

PTOV1 is a conserved adaptor protein overexpressed in PCa. Since its discovery by our group, the number of binding partners and associated cellular functions has increased and helped to identify PTOV1 as regulator of gene expression at transcription and translation levels. Increasing evidence demonstrates the oncogenic role of PTOV1 in different types of cancer [70-72]. However, the function of this protein and the molecular mechanisms by which influences the initiation, maintenance and progression of neoplasia have not been sufficiently explored.

2.1 The gene structure

Prostate Tumor Overexpressed-1 (PTOV1) was first described as gene and protein overexpressed in prostate tumors and preneoplastic lesions of HGPIN [73]. The gene was assigned to chromosome 19q13.3 by FISH analysis on human metaphase chromosomes. This region harbors a large number of androgens modulated and PCa related genes, including the proteases prostate specific antigen, kallikrein 1 (KLK1), kallikrein related peptidase 2 (KLK2) [74], the apoptotic regulator BCL2 associated X (BAX) [75], kallikrein related peptidase 11 (TLSP) [76] or kallikrein related peptidase 6 (Zyme/Neurosin) [77].

The gene *PTOV1* spans 9.51 Kb and includes 12 exons of which exons 3 to 6 code for the first *PTOV* homology block, or A domain, and exons 7 to 12 for the second block, or B domain [73] (**Figure 6A**). At least three transcripts with transcript support level (TSL) 1, supported by at least one non-suspect mRNA, resulting from differential splicing have been described [78]. The first and second one include 1,587 bps (NM_017432) and 1,577 (NM_001305105) bps, respectively, and both translate for a protein of 416 residues [78]. Variant number three includes 1,443 bps (NM_001305108) and initiates translation at an alternate start codon. This variant translates for a shorter protein of 374 amino acids that has distinct N- and C-termini. These differences likely affect the function of the final product.

PTOV1 gene has two antisense transcripts, known as *PTOV1*-AS1 and *PTOV1*-AS2 transcribed from the opposite strand that were initially classified as transcriptional noise [79]. More recently, they have been classified as a class of long non-coding RNAs (lncRNAs), a set of RNAs with important functions in transcriptional and post-transcriptional gene regulation. Antisense transcripts compete with microRNAs (miRNAs) for binding to target mRNA and thus act as miRNA competitive inhibitors or 'miRNA sponges'. Very recently, *PTOV1*-AS1 has been involved in cancer proliferation via inhibition of the function of miR-1207-5p [80]. *PTOV1*-AS1 suppresses heme oxygenase-1 (HO-1) expression by increasing the enrichment of HO-1 mRNA in miR-1207-5p-mediated miRISC.

A related gene containing one *PTOV*-domain, identified as *PTOV2*, was discovered on the same chromosome, 14 Kb upstream from the putative first exon of *PTOV1* [73]. *PTOV2* was later found to correspond to the subunit 25 of the Mediator complex, MED25, composed of up to thirty proteins, a transcription coactivator essential for the eukaryotic RNA polymerase II complex regulation of transcription in all eukaryotes [81-83]. This coactivator is also referred to as the vitamin D receptor interacting protein

(DRIP) or as the thyroid hormone receptor-associated proteins (TRAP) [84]. The Mediator is required for the transcription of most class II genes in yeasts and mammals and acts as a bridge between the RNA polymerase II and the activating transcription factors [84]. MED25 was also previously identified as p78/Arc92 /ACID1 [82, 85]. In this thesis, we will refer to *PTOV2* as *MED25*.

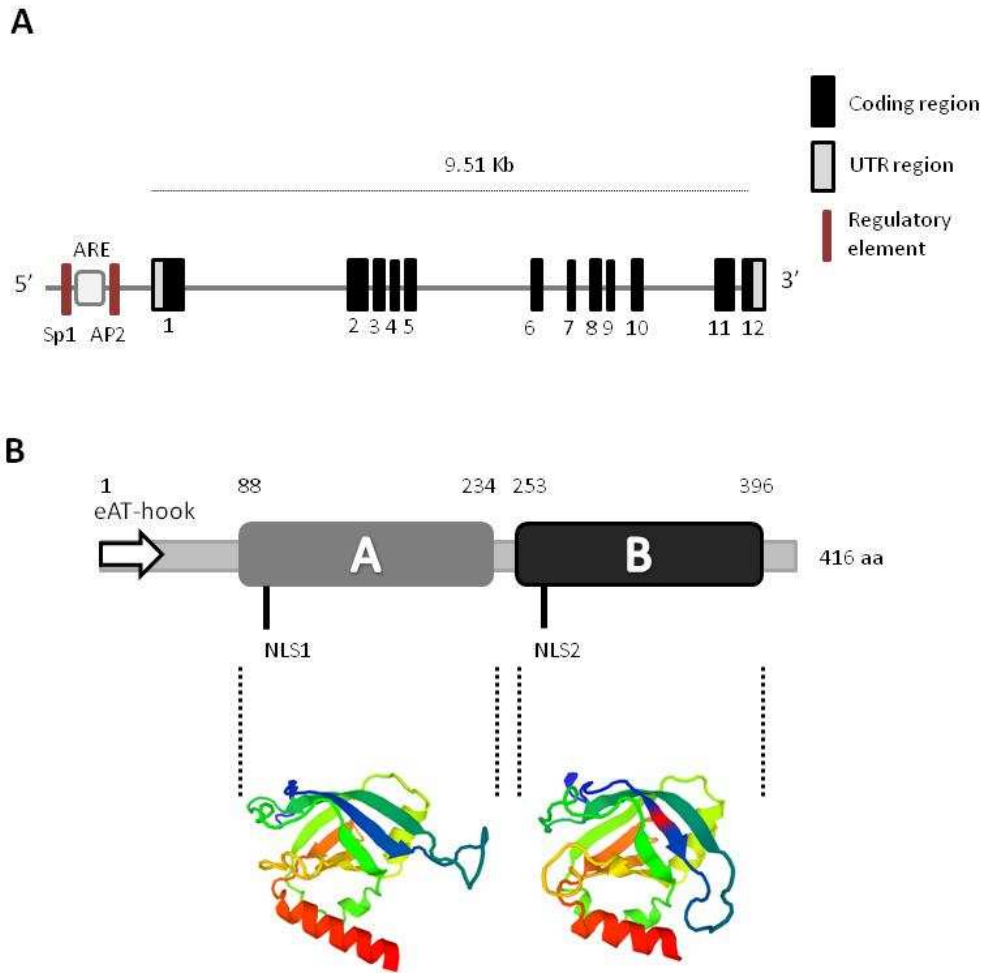

Figure 6. Gene and protein structure of PTOV1. **(A)** The gene includes 12 coding exons and two untranslated regions (UTR). In the putative promoter region, the localization of regulatory sites for ARE (Androgen Responsive Element), SP1 (Specificity protein 1), and AP2 (Activator protein 2) are shown (not in scale). **(B)** Protein organization showing the A and B domains, the Nuclear Localization Sequences (NLS1 and NLS2) and the extended AT-hook (eAT-hook) motif (not in scale). The three-dimensional structure of the A and B domains based on the Swiss Model, is shown in color [86].

The orthologous *PTOV1* gene in *Drosophila melanogaster* (acc. AC013074) shows a similar modular arrangement, but a lower degree of similarity between the two domains A and B (33% identity; 57% similarity) [73]. The orthologous *MED25* gene, found on chromosome 3R at 3Mb from *PTOV1*, was also predicted to encode a protein with a single PTOV block embedded within an 863-amino acid protein.

The putative promoter region of *PTOV1* reveals the presence of consensus sequences for transcription factors SP1 and AP2 and a putative Androgen Responder Element (ARE), similar to those observed in the *PSA* gene. In agreement with these observations, PTOV1 expression is androgen-responsive [73]. This has been confirmed in vascular smooth muscle cells (VSMCs) where the gene was suggested to play a critical role in androgen related atherogenesis in the human aorta through the regulation of proliferation of neointimal VSMCs [87].

2.3 The protein structure

PTOV1 is an adaptor, conserved in vertebrates (mammals and fish) and in arthropods (insects), although not in fungi (yeasts). The protein interacts with a number of factors both in the nucleus and the cytoplasm to regulate gene expression at transcription and post-transcriptional levels and to promote cancer cell proliferation and motility.

The predicted protein, 416 aminoacids long, reflects the structure of the gene and presents two highly homologous domains arranged in tandem, identified as A domain (146 amino acids) and B domain (143 amino acids), that show 66% identity and 79% similarity among each other [73, 86] (**Figure 6B**). The protein presents two putative nuclear localization signals (NLS), one in the A domain and the second in the B domain. NMR technology revealed the structure of the PTOV domain of MED25 [88-90] (**Figure 7A**). This domain (391–543) exhibits high sequence identity with the A and B domains of human PTOV1 (81% and 73%, respectively) (**Figure 7B** and **C**). The secondary structure of MED25 forms a seven-stranded β-barrel framed by three α-helices [89, 90] and presents two different positively electrostatic charged regions that appear to be important for its binding to the transactivation domain (TAD) of the RNA Polymerase II (**Figure 7A**).

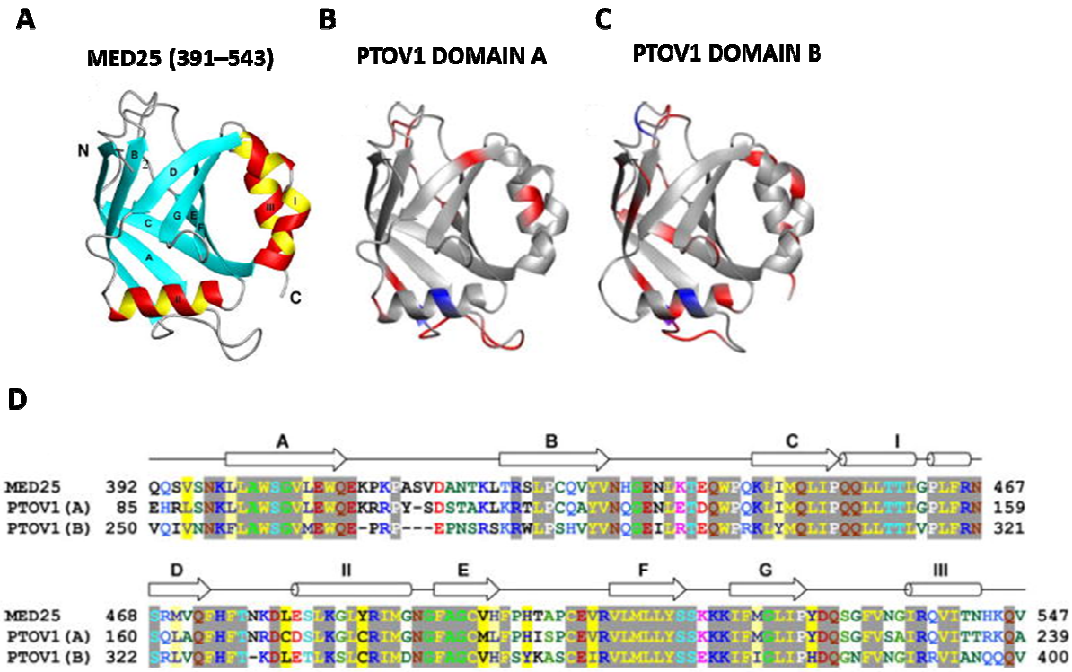

Figure 7. PTOV domain in MED25 exhibits high sequence identity with the A and B domains of human PTOV1. (**A)** Ribbon diagram of the lowest-energy conformer of MED25(391–543): *α*-helices I, II and III are shown in *red* and *yellow*, *β*-strands A to G are shown in *cyan*, and other polypeptide segments are shown in *gray*. (**B)** Ribbon diagram of the homology model of the PTOV1 N-terminal domain. Residues which are conserved in both ACID domains as well as MED25 (391–543) are depicted in *grey*. Residues which are conserved in the two PTOV1 ACID domains are shown in *red*, while residues which are not conserved in the two ACID domains are shown in *blue*. Substitutions among the following groups of residues are considered as being conserved: (i) Leu, Val, Ile, Ala, Phe, Met; (ii) Glu, Asp; (iii) Arg, Lys; (iv) Ser, Thr, Cys. (**C)** Same as (**b)** but for the homology model of the PTOV1 C-terminal domain. **(D)** Sequence alignment of human MED25 and PTOV1 fragments comprising the ACID domains. The regular secondary structure elements of MED25 (391–543) are indicated above the alignment. The figure was generated with the program Chroma v1.0 (http://www.llew.org.uk/chroma/) using its default coloring scheme: negative (*red*), positive (*dark blue*), charged (*magenta*), polar (*light blue*), Ser/Thr (*cyan*), tiny (*light green*), small (*dark green*), aliphatic (*grey on yellow*), aromatic (*blue on yellow*), big (*violet on pale yellow*), hydrophobic (*black on yellow*). Figure adapted from Eletsky, Ruyechan et al. [89].

The PTOV domain in MED25 shares structural similarity with the β-barrel domains of the Spen paralog and ortholog C-terminal (SPOC) domain of SMRT/HDAC1-associated repressor protein (SHARP) and Ku70/Ku80 heterodimer [88-90]. These proteins are involved double-stranded DNA break repair, transcriptional activation and repression by interaction with histone deacetylase complexes. For instance, SHARP has been identified as a component of the Notch co-repressor complex [91].

Very recently, an extended (e)AT-hook motif was identified in PTOV1, suggesting a function as nucleic acid binding protein (**Figure 6B**) [92]. Classical AT-hook motifs in proteins can bind nucleic acids at AT-rich sequences in the minor groove of the DNA, and are characteristics of proteins associated with chromatin remodeling, histone

modifications, insulator functions and proposed to anchor chromatin-modifying proteins [93, 94]. However, the (e)AT-hook discovered at the first N-terminal 43 amino acids of PTOV1 is a new functional AT-hook-like motif that differs in the basic amino acid patches from the canonical G-R-P (glycine-arginine-proline) core. This motif showed higher RNA binding affinity compared to DNA [92].

2.4 PTOV1 expression in cancer tissues

Most functions of PTOV1 have been surmised in pathological conditions, such as cancerous cells and tissues, although its expression has also been detected in normal tissues [73, 87, 95, 96]. However, scarce information is available about its function at those sites.

In HGPIN lesions associated with prostate carcinomas, PTOV1 expression is increased compared to the normal prostate epithelium [71, 97]. This higher expression was found helpful to discriminate those premalignant lesions associated with cancer, suggesting the potential value of PTOV1 detection in the early diagnosis of PCa [71]. Of interest, the proportions of Ki-67 positive nuclei and the levels of PTOV1 in HGPIN areas adjacent to cancer lesions are higher than those found in HGPIN areas away from the cancer, supporting the concept of *field cancerization* or *field effect* in prostatic carcinogenesis [97, 98]. More recently, the expression of PTOV1 in AAH, a proliferative lesion of the transition zone of the prostate that morphologically resembles low grade carcinoma, has been associated with PCa [99].

In prostate adenocarcinoma 71% of T2 and T3 stages overexpressed PTOV1 [72]. This overexpression was limited to the cytoplasm in 59% of samples whereas a strong expression was detected both in the nucleus and the cytoplasm in the remaining samples, with a small proportion of tumors showing a strong nuclear staining and weak cytoplasmic staining. More recently, metastatic primary tumors and metastatic lesions were shown to express significantly higher levels of PTOV1 compared to non-metastatic tumors [100, 101]. PTOV1 stained intensely in the nucleus of local and distal (bones) metastatic cells [101]. This high expression of PTOV1 significantly associated to the Ki67 index suggesting its participation in an active proliferative status. Remarkably, this relationship was stronger in tumors with nuclear PTOV1 staining. These findings are supported by observations *in vitro*, where in quiescent PCa cells, PTOV1 localized in the cytoplasm but after serum stimulation it partially translocated to the nucleus at the

beginning of the S phase [72]. The transfection of PTOV1 forced PC3 cells to enter the S phase with a subsequently increase in the levels of cyclin D1, indicating that the overexpression of PTOV1 can directly increase the proliferation of PCa cells.

More recently, numerous reports have described the overexpression of PTOV1 in different types of tumors. These included tumors of the breast, pancreas, liver, colon, kidney, bladder, laryngeal, cerebral gliomas and ovary [96, 99, 102-105]. The association between its overexpression and high grade of malignancy was strong in primary hepatocellular carcinoma, epithelial ovarian cancer, breast cancer and clear cell renal carcinomas, where PTOV1 expression was closely correlated with the clinic-pathological characteristics and tumor aggressiveness [70, 96, 102, 103, 105].

2.5 PTOV1 transcriptional regulatory functions

Homology models of PTOV domain in MED25 and human PTOV1 have shown that amino acid residues involved in TAD binding in MED25 are generally conserved in PTOV1, suggesting that both domains may serve as activator-binding modules [90]. In contrast to MED25, PTOV1 did not interact with the Mediator complex [85]. The differential biological activities of PTOV in MED25 and PTOV1 were suggested to be due to modulation of protein-protein interactions patterns by some amino acid residues which are differently grouped peripherally around the charged surface region [88, 89]. The retinoic acid (RA) was shown to activate the response of its receptor (RAR) through MED25 that, through its VWA domain, interacts with the Mediator and, through the PTOV domain, binds to the activators (histone acetyltransferase CBP) [106]. These observations suggest a role for the PTOV domain of MED25 in chromatin remodeling and pre-initiation complex assembly to recruit activators to the basal transcriptional machinery [85]. Additional evidences confirmed that the PTOV domain of MED25 is responsible for binding the TAD domain of several transcription factors, including ETV5 (ERM), a PEA3 member of ETS-related transcription factors [107], the nuclear receptor Hepatocyte Nuclear Factor 4 alpha [108], the transcription factor ATF6 alpha [109], a master regulator of endoplasmic reticulum (ER) stress response genes, the *retinoic acid receptor* (RAR) [110], STAT6 and chromatin remodelers [111]. Because PTOV1, in contrast to MED25, did not interact with the Mediator complex [85], its action may plausibly modulate, or hamper, the MED25 activator-binding PTOV module in those cells where it is overexpressed, as described below for the *RAR*. In agreement with the

above observations, PTOV1 was recently identified as a regulator of transcription of several genes including the *RAR, HES1, HEY1*, and *Dickkopf-1*.

2.5.1 The Retinoic Acid Receptor promoter

Retinoids are promising chemotherapeutics that inhibit cell growth by inducing apoptosis, senescence and differentiation of cancer cells [112, 113]. Unfortunately, intrinsic or acquired resistance to these agents frequently occurs after cancer therapy [114]. The formation of the complex MED25-RAR and RA, induces the stimulation of *RAR* promoter activity [106]. PTOV1 was shown to suppress the MED25-enhanced *RAR* activity by binding the activator CREB-binding protein (CBP) [110]. Thus, the expression of PTOV1 prevented CBP binding to MED25 inducing a repression of the *RAR* promoter. CBP belongs to a family of large multifunctional transcriptional coactivators that through their acetyl transferase action modify histones and other proteins, regulating a large number of transcription activators and cellular functions [115]. Both PTOV1 and MED25 proteins interact with the acetyl transferase CBP through the PTOV domain [100, 110]. Chromatin immunoprecipitation (ChIP) assays showed that PTOV1 itself is not recruited to the RA-responsive *RARβ2* promoter. Instead, the increased PTOV1 expression inhibited CBP chromatin binding by forming a chromatin-free PTOV1-CBP interaction that sequesters away CBP from MED25 [110]. In this context, in response to RA the LIM family member Zyxin was shown to interact and cooperate with PTOV1 in RAR repression, by forming a ternary complex with CBP and PTOV1 that antagonized with MED25 for CBP binding [116]. These data suggest a potential molecular mechanism for PTOV1 in RA resistance.

2.5.2 The HES1 and HEY1 promoters

Notch is an evolutionarily conserved signaling pathway that regulates cell fate, tissue homeostasis, cell differentiation, proliferation and growth [117]. Activation of the receptor induces the intracellular Notch (ICN) receptor to enter the nucleus where it acts as a transcription factor for numerous targets, including *HES1* and *HEY1* genes, two well known downstream regulators of the pathway [118, 119]. In the absence of ICN, a transcriptional repressor complex, that include SMRT/NCoR and HDAC1, is formed on target promoters [120].

Aberrant Notch signaling has been detected in different types of cancer to suppress or activate cancer progression depending on the cell context and tumor type [121-123]. In PCa, its role in progression has been studied *in vitro* and *in vivo* with contradictory results [124-126]. In metastatic prostate tumors PTOV1 is significantly overexpressed and represses the transcription of the downstream targets of Notch, the *HES1* and *HEY1* genes, by interacting with SMRT, RBP-Jκ, NCoR, HDAC1 and HDAC4 [100]. PTOV1 is bound to the chromatin of these promoters when Notch is inactive. Its repressive action was reverted by trichostatin A (TSA), an HDAC inhibitor, indicating the requirement for the activity of HDACs. Interestingly, the repression by PTOV1 was abolished by the overexpression of CBP, in agreement with previous reports showing that *HES1* transcription was activated by CBP [127]. PTOV domain shares structural similarity with the SPOC domain of SHARP, a known component of the Notch repressor complex [91, 128], and thus PTOV1 may be a facultative additional Notch co-repressor restricted to cancerous events. Additional *in vivo* evidence supports the role of PTOV1 as a negative regulator of the Notch pathway [100]. In the *Drosophila melanogaster* wing model, the expression of the human PTOV1 exacerbated Notch deletion mutant phenotypes and suppressed the effects of constitutively active Notch. In human tissues, the normal prostate epithelium revealed high levels of expression of HES1 and HEY1 proteins, supporting activated Notch signaling, whereas metastatic samples expressed significantly lower levels of these proteins, suggesting a Notch repressed state [100]. In contrast, the expression of PTOV1 in the normal prostate epithelium was mostly absent, but the protein was significantly overexpressed in metastatic samples. In human PCa cell lines, the downregulation of PTOV1 induced an upregulation of the endogenous *HEY1* and *HES1* genes, and reciprocally, the ectopic expression of PTOV1 in PCa cells and HaCaT keratinocytes, where Notch acts as tumor suppressor, caused the inhibition of expression of *HEY1* and *HES1* genes [129, 130]. All together, these observations support a pro-oncogenic role for PTOV1 as a negative regulator of Notch signaling in PCa progression. They also support a tumor-suppressor function of Notch in PCa, similarly to previous reports in skin, myeloid leukemia, and cervical carcinoma cells [121, 129, 131].

2.5.3 The Dickkopf-1 promoter

Aberrant activation of Wnt/β-catenin signaling was reported in breast cancer and strong evidence point to a possible epigenetic silencing of negative regulators of Wnt,

although the regulatory mechanisms underlying these epigenetic changes are poorly understood [132]. Very recently, PTOV1 expression was shown to activate Wnt/β-catenin signaling in breast cancer [133]. In the canonical Wnt pathway, binding of Wnt ligand to frizzled receptors and lipoprotein receptor-related protein-5 or 6 (LRP5/6) co-receptors initiates a cascade, which results in the β-catenin activation, its nuclear translocation and the transcription of target genes [134]. *Dickkopf-1* (*DKK1*) is a negative regulator of Wnt signaling. Silencing its expression was tightly associated with DNA hypermethylation and histone deacetylation [135, 136]. *DKK1* methylation has been reported in 27% of breast cancer cell lines and 19% of breast cancer patients [137].

In human breast carcinoma, high levels of PTOV1 expression correlated with high levels of nuclear β-catenin and low levels of DKK1 [133]. The overexpression of PTOV1 in breast cancer cell lines induced the nuclear translocation of β-catenin and increased β-catenin/TCF transcriptional activity. PTOV1 overexpression repressed *DKK1* transcription via the recruitment of HDACs to the promoter and a concomitant decrease of histone acetylation [133]. Treatment with TSA reverted the repression of *DKK1*. These findings suggest a role for PTOV1 as a novel epigenetic regulator of the Wnt/β-catenin pathway in breast tumorigenesis.

2.6 PTOV1 interactions and regulation of other cellular functions

PTOV1 has been detected at different subcellular locations, including sub-membrane sites, lipid rafts, cytoplasm, especially the perinuclear region, and in the nucleus. These locations are likely associated with different interacting proteins involved in several cellular processes [138]. It is not clear how each interaction contributes to a role of dysregulated PTOV1 expression in cancer progression. **Figure 8** summarizes the interactions of PTOV1 with other proteins in relationship with the functions described for each protein. Groups including transcriptional regulation and DNA replication, cell cycle regulation-mitotic functions contain numerous interactors. Similarly, groups including protein synthesis, ubiquitination and membrane trafficking functions contain at least three interactors. Together, these observations indicate that PTOV1 participates in different cellular events at different subcellular locations.

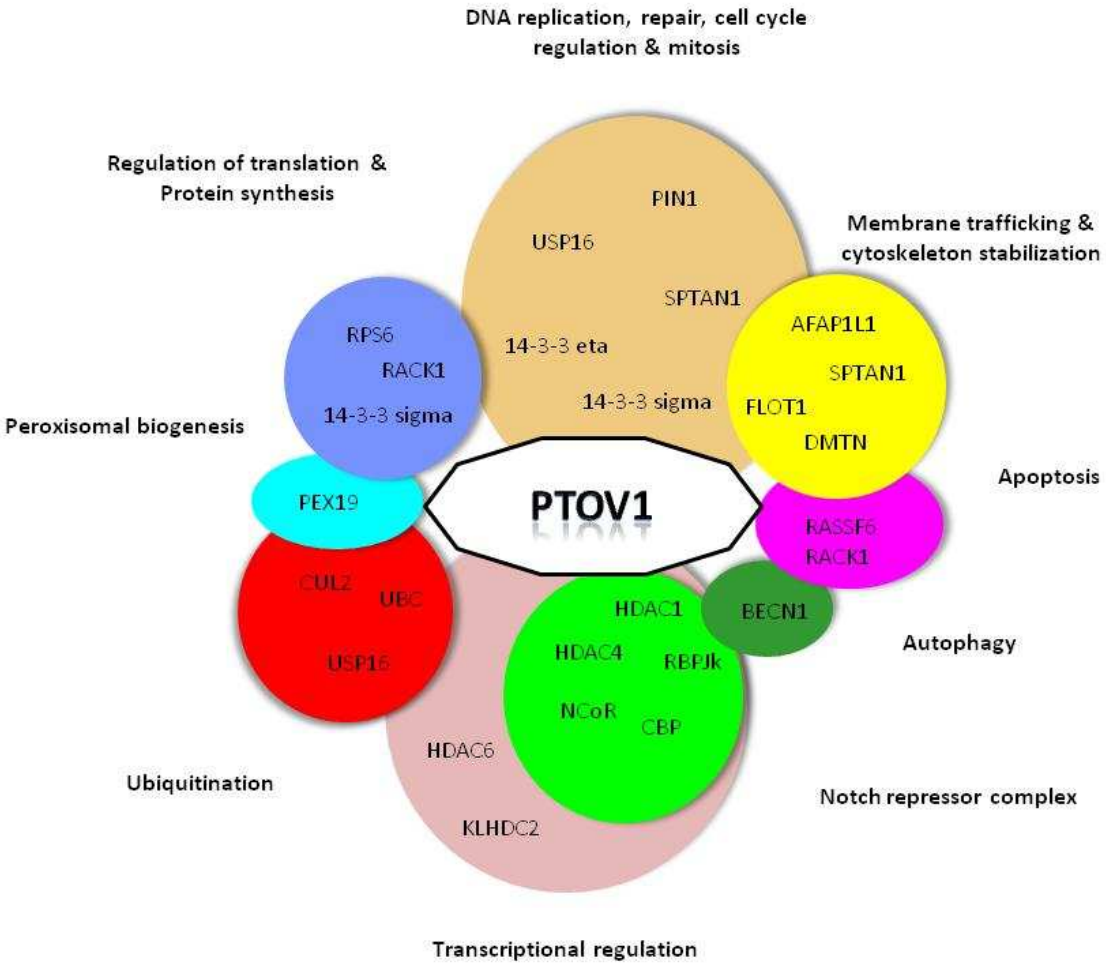

Figure 8. Scheme representing interactions of PTOV1 with other proteins in relationship with the functions described for each protein.

2.6.1 BUZ/Znf-Ubp domains of the histone deacetylase 6, HDAC6

The BUZ (binder of ubiquitin zinc finger) domain, also known as the Znf-UBP (zinc finger-ubiquitin-specific processing protease domain), is present in a subfamily of ubiquitin-specific processing proteases (USPs), the E3 ubiquitin ligase BRCA1-associated protein 2 (BRAP2) and in the histone deacetylase 6 (HDAC6) [139, 140]. The BUZ domain is a sequence-specific protein-binding module that recognizes the free C-termini of proteins. Through its C-terminal sequence (RGMGG), PTOV1 interacts with the BUZ domain of HDAC6 with a low KD value, that means a high-affinity interaction, that required the Gly-Gly motif present at the C-terminal of HDAC6 [141]. HDAC6 although it has been detected in the nucleus, it is mostly a cytoplasmic deacetylase that catalyzes the cleavage of the acetyl group of ε-amino groups of lysines and can regulate growth factor-induced chemotaxis by association with the cytoskeleton [142]. The role of

HDAC6 in tumor progression is controversial. Some evidences suggest an oncogenic role [143-147] whereas several reports suggest a tumor suppressor-like function [148, 149].

2.6.1 Flotillin-1

PTOV1 was shown to interact with the lipid-raft-associated protein Flotillin-1 [150] a protein that belongs to the Reggie/Flotillin family. Lipid rafts play a central role in membrane trafficking and signaling [151]. Flotillin-1, localized to non-caveolar lipid-rafts [152], has been involved in neuronal regeneration [153], and in insulin signaling in adipocytes, where it generates a signal crucial in the regulation of glucose uptake in adipocytes [154]. In PCa cells, Flotillin-1 interacts with the B domain of PTOV1, as expected the two proteins colocalized in lipid rafts and, surprisingly, in the nucleus [150]. After a mitogenic stimulus, Flotillin-1 entered the nucleus concomitantly with PTOV1 shortly before the beginning of the S phase. The overexpression of Flotillin-1 caused a significant increase in cell proliferation, and both PTOV1 and Flotillin-1 are required for PCa proliferation. However, while the presence of PTOV1 and an intact carboxy terminus of Flotillin-1 are required for its nuclear entry, the depletion of Flotillin-1 did not affect the nuclear localization of PTOV1 [150]. In additional work, Flotillin-1 was shown to be required for the stability and function of the Aurora B kinase in mitosis [155]. These data suggest that PTOV1 may drive PCa progression in part through the regulation of expression and nuclear localization of Flotillin-1 necessary to support Aurora B kinase mitotic function.

Additional recent reports confirmed the pro-oncogenic effects of increased Flotillin-1 levels in tumors [156-158] and its action in promoting invasion and metastasis through EMT, activation of NF-kB, Wnt/β-catenin and TGF-β pathways [156, 157]. Flotillin-1 is an important regulator of H-ras activation and invasion in triple-negative breast cancer and its expression inversely correlates with patient disease-free survival rates [158]. In gastric cancer, Flotillin-1 overexpression was shown to be the result of miR-485-5p downregulation that correlated with poor prognosis [159]. These findings suggest that the interaction of PTOV1 with Flotillin-1 might amplify its action in tumor progression.

2.6.3 Receptor of Activated protein C Kinase, RACK1

PTOV1 was shown to interact with RACK1, also known as guanine nucleotide binding protein beta polypeptide 2-like 1, GNB2L1 [101]. Data from our group demonstrated that PC3 cells stimulated with IGF-1 or phorbol esthers, showed PTOV1 and RACK1 colocalized at membrane ruffles [101]. RACK1 interacted with full-length PTOV1 and with the B domain, but not with the A domain, suggesting un-equivalent functions between the two PTOV1 domains. The PTOV1-RACK interaction was localized on 40S ribosomes by polysome profiling experiments in PC3 cells. Significantly, PTOV1 failed to co-sediment with the 40S ribosomal subunit in RACK1 knockdown cells, indicating that RACK1 is necessary for the association of PTOV1 with ribosomes [101]. In addition, PTOV1 co-immunoprecipitated and colocalized with the ribosomal protein S6 (RPS6) corroborating its interaction with ribosomes. The overexpression of PTOV1 caused a significant stimulation of c-Jun protein synthesis without affecting its mRNA levels.

Although RACK1 was first described to interact with Protein Kinase C (PKC) isoforms [160, 161], also interacts with numerous proteins and is involved in a diverse array of cellular processes. These include apoptosis regulation of insulin receptor and IGF-1R signaling, cell spreading, cell proliferation, STAT3 activation, and UV radiation [162-164]. In addition, it is now known that RACK1 is a part of the 40S small ribosomal subunit and localized at the head of the 40S subunit close to the mRNA exit channel [165], suggesting that it may function as a molecular link connecting cell signaling with the protein translation machinery. RACK1 was described to recruit active PKCβII on ribosomes to phosphorylate eukaryotic initiation factor 6 (eIF6) that allows the assembly of the 80S ribosome on the pre-initiation mRNA complex [166, 167]. RACK1 has been described as an adaptor required for the PKC-mediated phosphorylation of Ser129 of JNK [168]. More recently, the recruitment of JNK by RACK1 has been identified as part of a mechanism underlying the quality control of newly synthesized proteins under stress conditions [169]. After stress induction, RACK1 recruits activated JNK to 40S on actively translating ribosomes to phosphorylates the elongation factor eEF1A2, which in turn promotes the ubiquitination and degradation of damaged newly synthesized polypeptides [169].

RACK1 overexpression has been reported in different tumors and it was found to be a differential diagnostic biomarker and predictor for poor clinical outcome in breast and pulmonary carcinomas [170-172]. In hepatocellular carcinoma it promotes chemoresistance and tumor growth by localization on ribosomes and phosphorylation of

eukaryotic initiation factor 4E (eIF4E), preferential translation of cyclin D1, Myc, survivin and Bcl-2 [173]. These findings indicate that the increased expression of PTOV1 in cancer and its ability to bind to RACK1 on ribosomes and to increase protein synthesis, especially c-Jun translation, may be an efficient way for this protein to promote cancer progression.

3. mRNA translation regulation in prostate cancer

A growing body of evidence supports the idea that deregulation of translational control plays a central role promoting cellular transformation and tumor development. Aberrant regulation of key oncogenic pathways induces rapid and dramatic translational reprogramming both by increasing overall protein synthesis and by modulating specific mRNA networks. However, further investigation is needed to explore novel mechanism of translational control during cancer progression and development of resistance to current treatments.

3.1 Regulation of mRNA translation

The process of protein synthesis is tightly controlled in eukaryotic cells mostly at the initiation of translation and it is a key point in cancer development and progression. Tumors have developed different strategies to satisfy their rapid proliferation and growth requirements, including the deregulation of this initial step of mRNA translation to obtain increased rates of protein synthesis and eventually tumor progression [174-176]. In the canonical initiation of translation, numerous hormones and growth factors may induce phosphorylation of PI3K with the consequent activation of downstream AKT and mTOR kinases that trigger the synthesis of proteins (**Figure 9**). mTOR protein is found in two different complexes, mTOR complex 1(mTORC1) and TOR complex 2 (mTORC2). The activation of mTORC1 mediates the phosphorylation of eIF4E-BP1, ribosomal protein S6 kinase 1 (S6K1) and eIF4G. Hyperphosphorylation of eIF4E-BPs, the substrate with the most recognised impact on translation, release eIF4E that can bind to mRNAs and activate cap-dependent translation [177]. Conversely, in adverse growth conditions mTORC1 is inhibited and the consequent decrease in 4EBP phosphorylation reduces translation. PDCD4 inhibits translation initiation through interaction with translation initiation eIF4A and blocks its incorporation into the eukaryotic translation initiation factor 4F (eIF4F) complex [178].

The majority of cellular mRNAs initiate translation by a mechanism called 'cap-dependent' that depends on the recognition of the 7-methylguanosine-triphospho-5′ ribonucleoside, also called 'cap', located at the 5' end of most mRNAs. The 5' cap structure of the mRNA is recognized by eIF4F complex, which contains the mRNA 5'cap-binding protein eIF4E, the ATP-dependent helicase eIF4A, and eIF4G, a large scaffolding protein (**Figure 9**). This complex is directed to the 5' end of the mRNA via eIF4E, eIF4A and eIF4B, a RNA binding protein which functionally interacts with eIF4F and eIF4A potentiating their RNA helicase activities [179]. Together, the eIF4F complex with eIF4A and eIF4B participate in melting the mRNA 5' secondary structure to facilitate ribosome binding. eIF4G then recruits the 40S small ribosomal subunit to the mRNA through binding to the eIF3 complex, that is associated with eIF2/Met-tRNA/GTP, forming the 43S initiation complex. This complex scans the mRNA in a 5′→3′ direction until it recognizes the AUG start codon. Then, the complex is joined by a 60S subunit to form an elongation-competent 80S ribosome [180, 181]

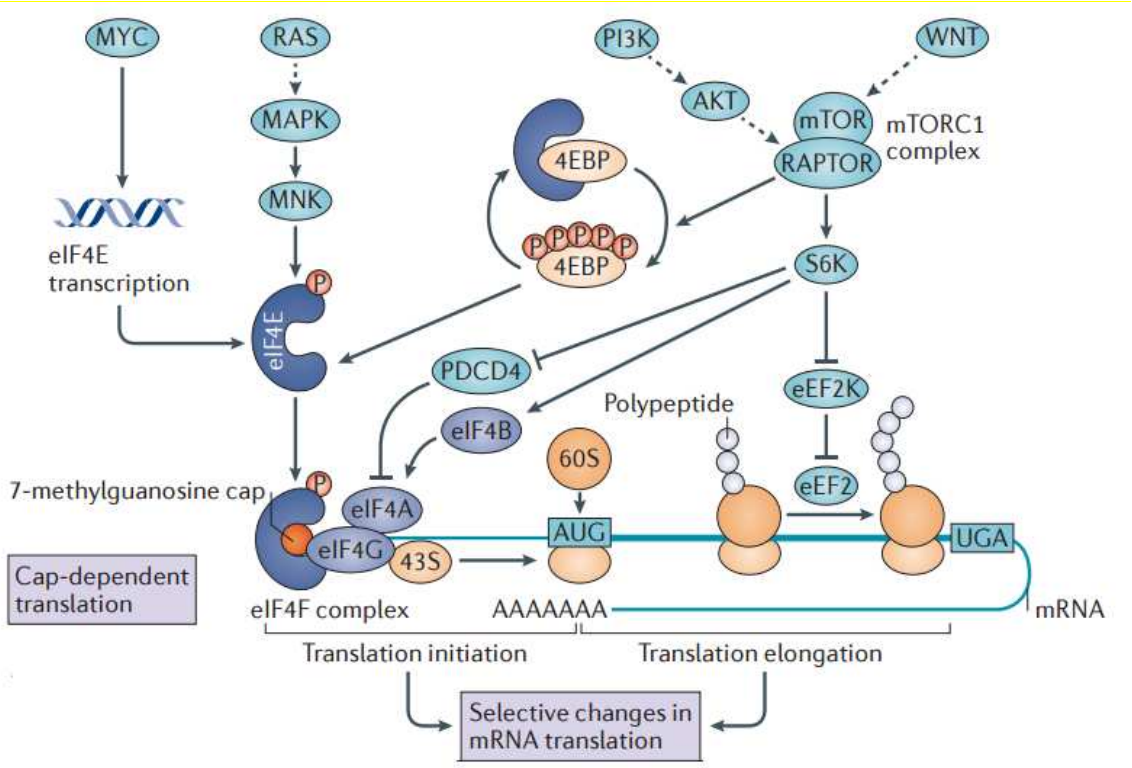

Figure 9. Numerous hormones and growth factors and oncogenic signaling pathways can activates mRNA translation at the initiation and elongation steps. Translation initiation is the main rate-limiting step of protein synthesis and typically relies on the ability of the eIF4F complex to bind to the 5' 7-methylguanosine cap present on mature mRNAs. eIF4F complex comprises cap-binding protein eIF4E, the scaffolding protein eIF4G and the helicase eIF4A. The eIF4F complex drives translation initiation through

the ability of eIF4E to bind to the 5' cap and interact with eIF4G, which recruits the 43S ribosomal pre-initiation complex (comprising a 40S ribosomal subunit, the eIF2–GTP–Met-tRNAi Met ternary complex, eIF3 and several additional accessory factors). Upon recruitment of the 43S complex to the 5' untranslated region of mRNA, it scans in the 5' to 3' direction until reaching a start codon, a process facilitated by eIF4A helicase unwinding of secondary structures and promoted by ribosomal protein S6 kinase (S6K)-dependent stimulation of eIF4A activity through inhibition of programmed cell death protein 4 (PDCD4) and activation of eIF4B. Image adapted from Truitt *et al*. [182].

3.2 Translation deregulation in cancer

As mentioned above translation initiation might be significantly modulated in cancer cells. In 1990 it was put into evidence for the first time a link between translation initiation and cancer by showing that the overexpression of eIF4E in rodent fibroblasts induced their transformation [183]. Since then, many evidences for the deregulation of translation initiation in cancer have emerged. **Table 4** illustrates the numerous eIFs, ribosomal proteins and other factors that are being found with increasing frequency associated with aberrant translation of human cancers.

Factor	U/D effect	Human cancer	Reference
eIF4B	upregulation	Diffuse large B-cell lymphoma	[184]
eIF4E	upregulation	Breast Cancer, Node-positive breast cancer patients, Gastric cancer, Acute myeloid leukemia, Nasopharyngeal carcinoma	[185],[186],[187] [188], [189]
peIF4E	upregulation	Penile squamous cell carcinoma	[190]
eIF5A	upregulation	Colorectal cancer	[191]
eIF5A2	upregulation	Bladder Cancer	[192]
eIF3e (Int6)(p48)	downregulation	Glioblastoma	[193]
eIF3i	upregulation	Colon Cancer, Hepatocellular carcinoma	[194], [195]
eIF3c	upregulation	Colon Cancer	[196]
p4EBP1	upregulation	Breast Cancer, Lung Cancer, Laryngeal carcinoma	[197], [198], [199]
RPL39L	upregulation	Hepatocellular carcinoma	[200]
RPL22	downregulation	T-acute lymphoblastic leukemia	[201]
RPMPS-1/S27	upregulation	Breast Cancer, Melanoma	[202]
RPL6	upregulation	Gastric cancer	[203]

Table 4. Eukaryotic initiation factors and ribosomal proteins altered in cancer.

In cancer cells, the activation of PI3K/AKT/mTOR mostly derives from mutations/deletions in the tumor suppressor *PTEN*, a negative regulator of PI3K/AKT function very frequently deleted in several types of human cancers, including lymphomas, metastatic breast cancer, colorectal cancer and prostate cancer [204-206]. In PCa, a key role for the PI3K-AKT-mTOR signaling axis in the development and maintenance of this neoplasia is put into evidence by the frequent rate of point mutations and loss of expression of PTEN, in primary PCa. Data from genomic profiling of PCa specimens identified the activation of the PI3K pathway in nearly half of primaries and all metastatic lesions examined, with loss of PTEN function primarily through copy-number loss rather than point mutation although the *PI3KCA* oncogene was not commonly mutated [19-21]. Intense investigation is ongoing to identify specific, ATP-competitive inhibitors of mTOR to use in metastatic drug-resistant tumors [207, 208].

3.3 From transcriptome to proteome: focusing on the translatome

The need to understand the mechanisms implicated in the establishment of cancer, has stimulated a great effort to develop precise technologies of analysis. The majority of efforts focused in the study of gene expression by measuring separately RNA and proteins. With the blooming of *–omic* era and the development of high-throughput methods for measuring mRNA expression (e.g. microarrays, RNA-sequencing), tools for analyzing mRNA expression have become widespread. It is commonly considered as a general yardstick that changes in mRNA abundance are proportional to changes in protein synthesis, but numerous exceptions are known which are partly due to the regulation of translation. A study carried out in yeast comparing proteomic and transcriptomic data showed that the correlation was insufficient for prediction of protein expression levels from mRNA transcript analysis, with differences in some genes of more than 20-fold [209]. In addition, no correlation between mRNA and protein expression was observed within the same human lung adenocarcinomas samples [210]. Ingolia *et al*. [211] using a new high-throughput technique called “Ribo-seq” demonstrated that in response to starvation in yeast some genes were transcribed but not translated. The results from our studies also support that changes in mRNA abundance are not always proportional to changes in protein synthesis. As explained above, PTOV1 interacts with RACK1 and ribosomes and stimulates the expression of the oncogene c-Jun by

promoting its translation without affecting its mRNA levels [101]. The above evidences illustrate that protein levels are not always a faithful reflection of mRNA concentrations and implementing additional direct analyses of mRNA translation can provide a more accurate and complete measure of gene expression. As mentioned above, control of translation appears to be a major regulatory step in normal and abnormal cell growth, cell proliferation, cancer initiation, and metastasis. Understanding the molecular basis of translational deregulation in cancer will hopefully contribute to the development of novel anticancer therapeutic strategies.

The technological gap between our abilities to quantify the transcriptome and the proteome has been solved with the emergence and readjustment of new approaches that provide genome wide information on protein synthesis. It is now possible not only detect RNA and protein molecules in the cell but determine which protein molecules are being synthesized in the cell at any given moment. These new approaches, including polysome profiling and ribosome profiling, take advantage of the recent advances in sequencing technology, to provide global measurements of translation.

3.3.1 Polysome profiling

The polysome profiling (PolyPro) is based on the principle that actively translating mRNAs are typically associated with multiple ribosomes, forming polysomes. In constrast, translationally inactive mRNAs are sequestered as messenger ribonucleoprotein (mRNP) particles or associated with a single ribosome (monosome). The ribosome density is used here as a predictor of protein levels. It is well known that ribosomes are characterized by their sedimentation properties in sucrose density gradients and the pioneering studies using this technique dates back to 1960's [212, 213]. Depending on the density of polysomes, it means the number of ribosomes bound to a transcript, they can be separated in a linear sucrose gradient by ultracentrifugation according to the number of ribosomes they contain (**Figure 10**). However, the resurgence of the PolyPro as a high-throughput method for simultaneosly monitoring the translation state and level of individual mRNAs is not described until many years later [214-217]. Combining sucrose gradient centrifugation with differential screening using arrays or coupled to next generation of sequencing (NGS) enables simultaneous analysis of both transcriptional (total RNA) and translational regulation (polysome-bounded RNA) as a tool for obtaining wide-genome information.

3.3.2 Ribosome profiling

The ribosome profiling, or Ribo-seq, is an innovative technique for monitoring translation *in vivo* worked up in the laboratory of Jonathan Weissman at University of California, San Francisco [211]. The ribosome profiling start out from the well known ability of ribosomes to protect mRNA fragments from nuclease digestion [218] and coupled this one with the emerged sequencing technology: the deep sequencing of these ribosome protected mRNA fragments generated after nuclease digestion (**Figure 10**). A translating ribosome encloses a ~30 nt portion of the mRNA template and protects it from nuclease digestion. Therefore, it is possible to obtain a pool of fragments of mRNA after nuclease digestion of ribosomes from living cells. These fragments are the so-called ribosome protected fragments or footprint (RPFs) and provide information about the specific position of ribosomes in the mRNA copies of a cell population. This information is rewarding because the association of a RNA transcript with a ribosome does not necessarily mean that the transcript is being translated. In certain situations, the ribosome could be stalled or associated with the 5'UTR [219-221].

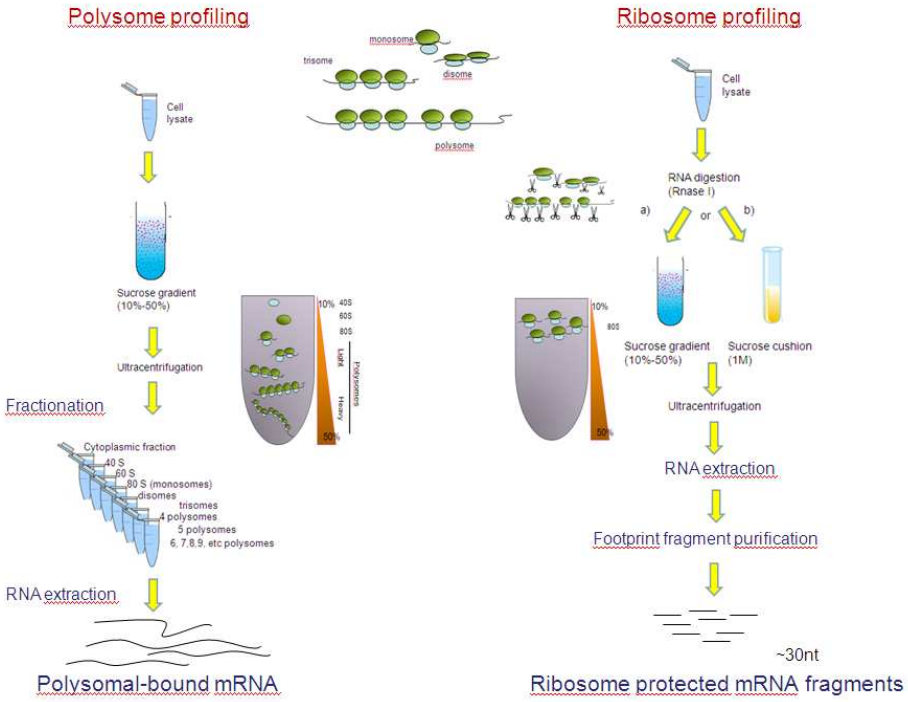

Figure 10. Techniques for monitoring protein translation.

Chapter 2:

HYPOTHESIS

Mar Menor y La Manga

“The Mar Menor lagoon is one of the most important ecological singularities in the Mediterranean area. The Mar Menor is -in spite of its name- Europe's biggest salt water lagoon, and it is separated from the Mediterranean Sea by La Manga, a strip of land which is 22km long. At the same time, it is an area where many economic and industrial activities meet. The sum of the impacts of mining, agriculture and urban development in the surroundings to the lagoon during the last decades has affected its ecosystem….”

Metastatic PCa is a deadly disease. Patients that progress to a castration-resistant status are usually treated with docetaxel, and eventually develop resistance to the medication. Therefore, one major question is to identify the mechanisms responsible for this resistance and discover specific targets to improve present therapies. In addition, to know in advance which patients will not benefit from the docetaxel therapy, will avoid useless toxic treatments of non-responders.

Previous evidences from our group and new findings from others support an important role for PTOV1 in the progression of different types of cancer to a metastatic disease with poor prognosis [100, 102, 104]. The overexpression of PTOV1 in castration resistant prostate cancer cells increases proliferation, cell migration and invasion. Mechanistically, we have shown that PTOV1 interacts with RACK1 and ribosomes and promotes selective translation of mRNAs, including the oncogene *JUN*. Both RACK1 and c-Jun are proteins associated to invasion, EMT and chemoresistance in different types of tumors [173, 222, 223].

In addition, as highlighted in the Introduction section, the mRNA translation process is decisive in prostate cancer progression and the metastatic process. However, little information is available about the role of the deregulation of translation in chemoresistance.

According to our previous observations, we formulated the following hypotheses:

i) The widely observed overexpression of PTOV1 in aggressive tumors and in metastatic prostate cancer, its promoting activity on the expression of oncogenic proteins and pathways, suggest a relevant role for this protein in driving prostate cancer progression and chemotherapy resistance.

ii) Specific mRNAs are selectively translated during the progression of cancer to the development of the resistant tumor. Analyzing the translatome (genome-wide pool of translated mRNAs associated with polysomes) in drug resistant prostate cancer cells, in comparison with the transcriptome, may identified differentially translated proteins critical for the process of resistance.

Chapter 3:

OBJECTIVES

Bando de la Huerta

"Bando de la Huerta is a tradition dating back to 1851 that remains alive and kicking today. Bando de la Huerta, declared Festival of International Tourist Interest in 2012, is a celebration of countryside traditions, which are deeply rooted in the history of this city. Murcians take on to the streets that day dressed with the traditional costume in an explosion of color and joy. Everyone participates in this festival, either as part of the parade or simply enjoying the vibrant vibe of every city corner…"

One main objective of this thesis is to study PTOV1 function in prostate cancer progression and its role in the development and maintenance of resistance to current therapies, mainly chemotherapy with taxanes. A second main objective is to study the role of translation deregulation in aggressive prostate cancer, in particular in the cells that become resistant to most conventional therapies in metastatic prostate cancer.

Specific objectives:

(i) Analyze the role of PTOV1 as an inductor of the epithelial-mesenchymal transition and in tumorigenesis in prostate cancer and identify the molecular mechanisms mediating this capacity.

(ii) Analyze the specific role of PTOV1 in promoting docetaxel resistance in metastatic prostate cancer and identify the molecular mechanisms and signaling pathways involved, using two docetaxel-resistant PCa cell lines with gain of function or knockdown of PTOV1 *in vitro*.

(iii) Analyze the status of mRNA translation in androgen-independent and docetaxel-resistant prostate cancer cells using the polysome profiling approach coupled to RNA-sequencing to identify new markers for diagnosis and novel players involved in the establishment of resistance.

Chapter 4:

MATERIAL AND METHODS

The Roman Theatre museum *–Cartagena (Murcia)*

"The Roman Theatre of Cartagena was built at the end of the 1st Century BC when Cartagena was a Roman colony, in the era of Emperor Augustus. The theatre was not discovered until 1987 and many of the finds are in the Archaeological Museum. The terraced seats were built into the northern side of La Concepcion hill which had been excavated to create seating for 6000. Santa Maria La Vieja Cathedral was built in the 13th Century from materials taken from the Roman theatre. By the sixteenth century, however, the theatre had been lost to fire and its remains built over. Well hidden by the town of Cartagena as it grew over the ruins it was not discovered again until 1987. The town was asked to vote as to whether or not, the buildings standing there in 1987 should remain, or be torn down to find the ruins. The town voted in favor of the excavation and reconstruction of the Roman Theatre…"

1. Cellular cultures

1.1 Cell lines

All cells lines were purchased from the American Type Culture Collection, Manassas, VA, USA.

a) **HEK293T*:*** is an epithelial cell line derived from human embryonic kidney 293 cells. This cell line expresses the oncogenic T antigen of the SV40 virus and is competent to replicate vectors carrying the SV40 region of replication. It is widely used for retroviral production, gene expression and protein production.

b) **MDCK:** is an epithelial cell line derived from a kidney of a normal adult female canine.

c) **RWPE-1:** is a non-neoplastic cell line derived from adult human prostatic epithelial cells from a white male donor immortalized with human papillomavirus 18 (HPV-18) encoding the oncogenic E7 proteins. RWPE-1 cells neither grow in agar nor form tumors when injected into nude mice.

d) **LNCaP:** is a human prostate epithelial cell line isolated in 1977 from a needle aspiration biopsy of a left supraclavicular lymph node of a 50-year-old Caucasian male with metastatic prostate carcinoma. The cells express the androgen receptor, estrogen receptor and PSA and are androgen responsive. Cells also express KRT8, KRT18, and KRT20, wild type (WT) p53 and PTEN inactivation. Of note, this cell line contains a T877A mutation in the AR coding sequence that gives it promiscuous binding affinity to many steroid compounds. It is a slow growing cell line with a population doubling time (PDT) around 60-72 hours and has a karyotype of 33 to 91 chromosomes (modal of 76–91). LNCaP xenografts shows a modest 50% success rate with a tumor doubling time of 86 hours [224].

e) **Du145**: is a human epithelial prostate cancer cell line derived from a metastasis in the brain. The cells do not express PSA and are androgen non-responsive. PDT is approximately 29 hrs. It is a highly rearranged cell line containing 58 to 63 chromosomes per metaphase spread (modal of 64). Structural abnormalities include rearrangements to approximately 70% of the 22 different autosomal chromosomes including the t(11q12q), del(11)(q23), 16q+, del(9)(p11) and del(1)(p32). Du145 cells form grade II adenocarcinoma and metastasize to a variety of organs, including spleen, lung, and liver.

f) **PC3**: is a human epithelial prostate cancer cell line derived from a bone metastasis of a grade IV prostate adenocarcinoma from a 62-year-old Caucasian male. This cell line is similar to Du145 cells in that it is hormone insensitive and presents no AR or PSA mRNA/protein, and forms adenocarcinomas in nude mice. The line is highly aneuploid with a near-triploid with a modal number of 62 chromosomes and a doubling time of approximately 33 hours. It expresses aberrant p53 with a C deletion in codon 138 causing a nonsense codon at 169 (causing a loss of heterozygosity) and is PTEN deficient.

The docetaxel-resistant cellular models Du145 and PC3 were kindly provided by Dr. Begoña Mellado (Laboratory and Medical Oncology Department, Hospital Clínic in Barcelona). DR-Du145 and DR-PC3 were selected by culturing cells with docetaxel in a dose-escalation manner using 72h exposures during 1 year and 6 months, respectively. Initial culture was 5 nM docetaxel. Surviving cells were cultured and concentration of docetaxel was increased to 10, 25, 50, 100 and 250 nM. In parallel, parental Du145 and PC3 cells were exposed to DMSO (vehicle solution) in the same dose-escalation manner.

LNCaP andogen independent (AI) and androgen dependent (AD) were obtained from the Anna C. Ferrari's laboratory at the Division of Neoplasic Diseases, Department of Medicine, Mount Sinai School of Medicine, New York. Briefly, the androgen-independent subline LNCaP AI was derived over a period of 6 months by continuous culture of the LNCaP cells in RPMI medium deprivated of androgens, containing 10% charcoal stripped heat-inactivated FBS.

Although Du145 and PC3 cell lines were originally described to be androgen-receptor (AR) negative, recent studies reported expression of the AR protein in both cell lines and its induction after DHT treatment [225]. However, the upregulation of AR protein did not activate AR-reponsive reporter genes and the authors proposed Du145 and PC3 cell lines should be considered as "androgen non-responsive" instead of "AR-negative".

1.2 Cell culture methods and reagents

Cells were cultured at 37°C in an atmosphere of 5% CO_2. MDCK were cultured in the Eagle's Minimum Essential Medium (BioWest, Nuaillé, France), HEK293T were

cultured in DMEM (BioWest), Du145 cells and LNCaP cells were cultured in RPMI-1640 (BioWest) and PC3 were cultured in F12K nutrient mixture medium (Thermo Fisher Scientific, Waltham, MA, USA). Media were supplemented with 10% fetal bovine serum (FBS), 2 mM L-glutamine, 100 U of penicillin/mL, 100 µg of streptomycin/mL, and 0.1 mM non essential amino acids (all from BioWest). LNCaP AI subline was cultured in RPMI-1640 containing 10% charcoal-stripped (Sigma Aldrich USA), heat-inactivated FBS and above supplements. Docetaxel resistant cell lines were kept with 2.5 nM of docetaxel (Sigma-Aldrich, St. Louis, MO). Wnt3a conditioned medium was kindly provided by D. Arango (Vall d'Hebron Institut of Research, Barcelona). Briefly, mouse L1-Wnt3a (ATCC® CRL2647™) cells were cultured in DMEM supplemented with 10% FBS and 0.4 mg/ml G418. After 4 days, medium was collected, filtered and store at 4ºC. Fresh medium was added to cells and cultured for another 3 days. Medium was collected, filtered and mixed with the first batch of medium. For long storage, Wnt3a-conditioned medium was store in aliquots at -20ºC. To activate Wnt signaling pathway, Du145 cells were cultured for 24 h with Wnt3a-conditioned medium diluted 1:1 with supplemented RPMI medium. Where indicated, cells were treated for 24 h with 30 µM JNK inhibitor II (Calbiochem) or 60 µM iCRT14 (Tocris Bioscience).

For cryopreservation, two million cells were frozen slowly in 1 mL of cold FBS plus 10% DMSO and they were immediately placed on ice. Cells were stored 1 day at -20ºC, then stored at -80ºC for a few days and for long storage, vials were transferred to a liquid-nitrogen freezer to maintain temperatures below -160ºC. For the recovery of cryopreserved cells, frozen vial was thawed rapidly in a 37ºC water bath and immediately diluted in pre-warmed complete culture medium. Cells were centrifugated at 400 xG for 5 min, resuspended in complete culture medium and seeded into an appropriate flask.

1.3 Production of lentiviral vectors and cellular transduction

Lentiviral vectors (LV) are a kind of retroviruses derived from human immunodeficiency virus (HIV). Lentiviruses are transmitted as single-stranded, positive-sense, envelope RNA viruses. Upon entry into the target cell, the viral RNA genome is reverse transcribed into double-stranded DNA that integrates into the genome. Lentiviruses are widely used for the efficient delivery and stable integration of transgenes or interference RNA sequences. The latter allows for the long-term knockdown of the targeted host mRNA by sequence-specific degradation (RNA interference, or RNAi)

[226]. We have used virally produced vectors to knockdown the expression of PTOV1 in several prostate cancer cell lines. In this method of RNAi the production of LV is achieved by transient transfection of a plasmid set into HEK293T cells, which contain the SV40 T-antigen that increases efficiency for vector production. Three different components included in different plasmids are used to build replication-defective recombinant chimeric lentiviral particles (**Figure 11**):

i. The transfer vector contains the plasmid encoding the insert of interest. This sequence is flanked by long terminal repeats (LTRs) that facilitate host genome integration. To improve safety, transfer vectors are all replication incompetent.
ii. The packaging vector: codes for the internal structural and enzymatic protein. In our laboratory we used 2nd generation system, in which five of the nine HIV-1 genes were eliminated leaving the *gag* and *pol* frames, which encode for the structural and enzymatic components of the virion, respectively, and the *tat* and *rev* genes, fulfilling transcriptional and post-transcriptional functions.
iii. Envelope vector: codes for the envelope glycoprotein. The G protein of the Vesicular Stomatitis Virus is the most widely used.

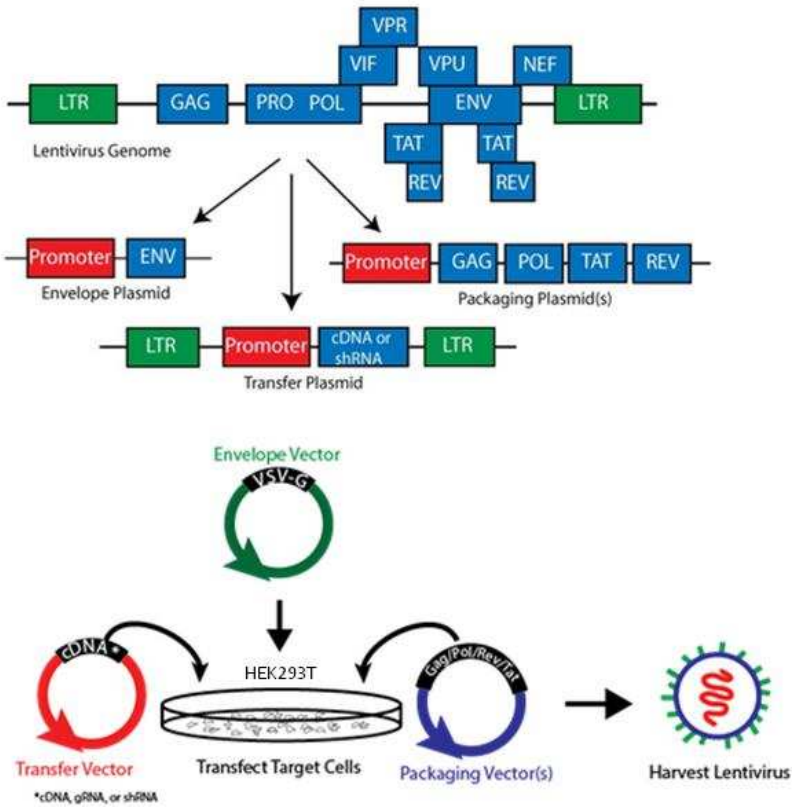

Figure 11. Second generation lentiviral vectors. Lentiviral genome is edited down and distributed across three plasmids: envelope, packaging and transfer plasmid. For viral production, plasmids are transfected into HEK293T cells.

The protocol used for the production of LV was the following:

Four millions HEK293T cells were seeded in a 10 cm culture dish in complete DMEM medium. Twenty-four hours later, cells were transfected using $CaPO_4$ precipitation method. Two tubes were prepared:

- Tube A: Transfer plasmid (12 µg), packaging plasmid (8 µg), envelope plasmid (4 µg), 60 µL 2.5 M CaCl2, and sterile water were added to complete a final volume 500 µL. Mix well.
- Tube B: 500 µL of 2 times concentrated (2X) Hepes Buffered Saline (HBS) solution pH: 7 (280 mM NaCl, 1.5 mM PO4, 50 mM HEPES) were added to a 50 mL falcon tube.

The content of tube A was added to tube B, drop wise and slowly while constantly bubbling the solution in tube B. The mixture was incubated 20 minutes at room temperature (RT). One mL of the transfection mixture was added to cells in drops. Plates were swirled and incubated 6 h at 37ºC. Then the medium was removed, 10 mL fresh complete medium were added and plates were incubated O/N at 37ºC. The first harvest of supernatant was collected and 6 mL fresh complete medium were added to cells. Cells were incubated O/N at 37ºC. Supernatants from 4 plates were pooled, filtered through a 0.22 µm filter and concentrated by ultracentrifugation 1.5 h at 89,000 xG at 4ºC. Pellets containing viral particles were resuspended in 1 mL of suitable cell medium and stored at -80ºC for long storage. Next day, a second harvest of supernatants was collected and processed as above.

For cells transduction, 700,000 cells were seeded in a 10 cm culture dishes the day before transduction. The vial containing concentrated LV was resuspended in 7 mL of appropriate medium (depending on the cell line) plus 10 µg/mL of polybrene, to facilitate transduction, and added to cells. After 24 h, complete fresh medium was added. Transduced cells were selected by treatment with 1 µg/mL puromycin for 4 days.

1.4 Cell transfections

The transfection is a powerful tool used to deliver DNA or RNA into eukaryotic cells for the study and control of gene expression. In transient transfections, many copies of the exogenous gene are present in the cytoplasm that lead to high levels of the expressed protein. The expression of the transfected gene is usually analyzed between 24 and 96 hours after the transfection. For transient transfections, we used X-tremeGene 9 DNA transfection reagent (Roche) and OptiMEM Reduced Serum Medium (ThermoFisher Scientif) as DNA diluent. The protocol used was the following:

Cells were seeded the day before transfection in their appropriate media to an 80% confluence on the day of transfection (**Table 5**). Twenty-four hours later, the plasmid DNA was added with the diluent in a sterile tube and vortexed. The X-tremeGENE 9 transfection reagent was added and mixed by vortexing (**Table 5**). After incubation for 20 min at RT, the medium was removed and an appropriate amount of diluent added. The transfection complex was added to the cells in a dropwise manner. Plates were incubated for 4 h at 37ºC after which the transfection complex was removed and fresh medium was added.

Type of plate	Number of cells	Diluent (µL)	DNA (µg)	Ratio reagent: DNA	Transfection Reagent (µL)	Final Volume (Diluent,mL)
12 well	100.000 200.000 (LNCaP)	100	1.5	3:1	4.5	1
6 well	400.000 800.000 (LNCaP)	200	4.5	3:1	13.5	2

Table 5. Information about transient transfection conditions with X-tremeGene 9 DNA transfection reagent.

2. Functional assays

2.1 Proliferation assay

One simple method to determine differences in proliferation or the indirect quantification of cell death is the staining of attached cells with crystal violet dye, which binds to proteins and DNA. Adherent cells that undergo cell death lose their adherence and are subsequently lost from the plate. For these assays cells (4×10^3 cells/well) were

seeded on collagen-coated 96-well plates in sextuplicates. At the indicated time points, cells were fixed in 4% formaldehyde solution, washed with PBS and stained with 0.5% crystal violet. Crystals were dissolved with 15% acetic acid and optical density was read at 590 nm.

2.2 Cytotoxicity assay

Cells (4×10^3 cells/well) were seeded on collagen-coated 96-well plates in sextuplicates. After 24 h, cells were treated with solvent (control) or the drug at different concentrations for 48 h for Du145 cells and 72 h for PC3 cells. Fresh medium with the drug was replaced every day. At the indicated time points, cells were fixed, washed with PBS and stained with 0.5% crystal violet. Crystals were dissolved with 15% acetic acid and optical density was read at 595 nm. Docetaxel (Sigma-Aldrich) and Cabazitaxel (kindly provided by D. Begoña Mellado, Hospital Clinic, Barcelona) were diluted in DMSO at 1 mg/mL and aliquots were store at -20ºC. Doxycycline, minocycline hydrocloride and methacycline hydrocloride (Sigma-Aldrich) were diluted in sterile water at 10 mg/mL and store at -20ºC.

2.3 Viability assay: trypan blue exclusion test

The Trypan blue exclusion test is used to determine the number of viable cells present in a cell suspension. It is based on the principle that live cells possess intact cell membranes that exclude certain dyes, such as Trypan blue. Therefore, it allows a direct identification and quantification of live (unstained) and dead (blue) cells in a given population. Briefly, 24 h after transduction with lentiviral particles, cells were seeded (5×10^4 cells/well) on 24-well plates in triplicates. After 72 h, cells were collected and stained with Trypan blue to identify dead cells by cell counting. Cell viability was calculated as the number of viable cells divided by the total number of cells.

2.4 Clonogenic assay

Clonogenic assay, or colony formation assay, is an *in vitro* cell survival assay based on the ability of a single cell to grow into a colony (macroscopically visible or with at least 50 cells). The assay essentially tests every cell in the population for its ability to undergo "unlimited" divisions. Briefly, cells were seeded at low concentration ($3x10^3$

cells/well) in 6 wells plates in triplicates. After 7 days, cells were fixed in 4% formaldehyde solution and stained with 0.5 % crystal violet, photographed, and scored.

2.5 Spheres formation assay

The use of sphere-forming assays provides a widely recognized *in vitro* method for the identification and characterization of tumor initiating cells (TICs), also called cancer stem cells (CSCs) [227]. A tumorsphere is a solid, spherical formation developed from the proliferation of one cancer stem/progenitor cell. Cells are grown in serum-free, non-adherent conditions in order to enrich the cancer stem/progenitor cell population as only cancer stem/progenitor cells can survive and proliferate in this environment. The protocol is detailed below:

Cells were seeded ($4x10^3$ Du145 cells/well or $2x10^3$ PC3 cells/well) in 24-well ultra low attachment culture plates (Corning Costar, Cambridge, MA) in triplicates in 1 mL of serum free medium. The medium was prepared from DMEM-F12 (Invitrogen) containing 1 % methyl cellulose, 60 µg/mL glucose, 1 µM hydrocortisone, 1 µg/mL putrescine, 10 µg/mL transferrin, 3 nM sodium selenite, 2.5 µg/mL insulin, 10 ng/mL β-FGF, 20 ng/µl, EGF 5 U.I./mL, heparin (Sigma-Aldrich), and 0.4 % B27 (Invitrogen). Cells from 24-well plates were fed with fresh media every three days and allowed to grow for 8 days. The number of spheres (> 50 cells/sphere) were then counted from the 24 well plates and expressed as ratio of spheres/1000 plated cells (Sphere Forming Efficiency, SFE).

2.6 Cell cycle analyses

Cell cycle analysis by flow cytometry was used for the quantification of the DNA content using propidium iodide (PI). Cells in G2 phase contain double DNA compared to cells in G1, thus they take up proportionally more dye and will be approximately twice as bright as cells in G1. In most cases, cells must be fixed or permeabilized to allow entry of the dye which is otherwise actively pumped out by living cells. In addition RNase A was included to decrease the background given by PI binding to RNA. The protocol is described below:

One million cells were collected by trypsinization and washed twice with PBS. After centrifugation 5 min at 300 xG, pellets were resuspended and fixed in 70% cold ethanol and stored O/N at 4ºC. Next, cells were centrifuged, washed twice with cold PBS and resuspended in staining solution (1 mM sodium citrate, 15 µg/mL propidium iodide and 300 µg/mL DNAse free RNase A) and incubated 4ºC O/N. Approximately 20,000 cells (counts) were analyzed by flow cytometry with a BD FacsCalibur.

Data were analyzed by FlowJo software using univariate analysis of cellular DNA content that reveals the distribution of cells in three major phases of the cycle (G1 *vs.* S *vs.* G2/M). In more detail, the forward scatter (FSC, X axis) and side scatter (SSC, Y axis) was measured to identify single cells. Cell doublets or clumps were excluded from the analysis by pulsed shape analysis achieved using pulse area vs. pulse width. We combined both gates and apply to the PI histogram plot, plotting FL2-Area (X axis) versus Counts (Y axis). To quantify the percentage of cells in each cell cycle phase the software used an algorithm which attempt to fit Gaussian curves to each phase.

2.7 Polysomal profiling and fraction analysis

During polysome profiling mRNAs are stratified in a linear sucrose gradient by ultracentrifugation on the basis of the number of bound ribosomes, which corresponds to their translational efficiency [214] (**Figure 12**). After ultracentrifugation, the fractionated polysomes can be analyzed using a density gradient fractionation system that allows the recovery of the different fractions containing the free mRNA, monosomes, light and heavy polysomes through the monitorization of absorbance at 254 nm of the nucleic acids (RNAs) with an UV detector (**Figure 12**).

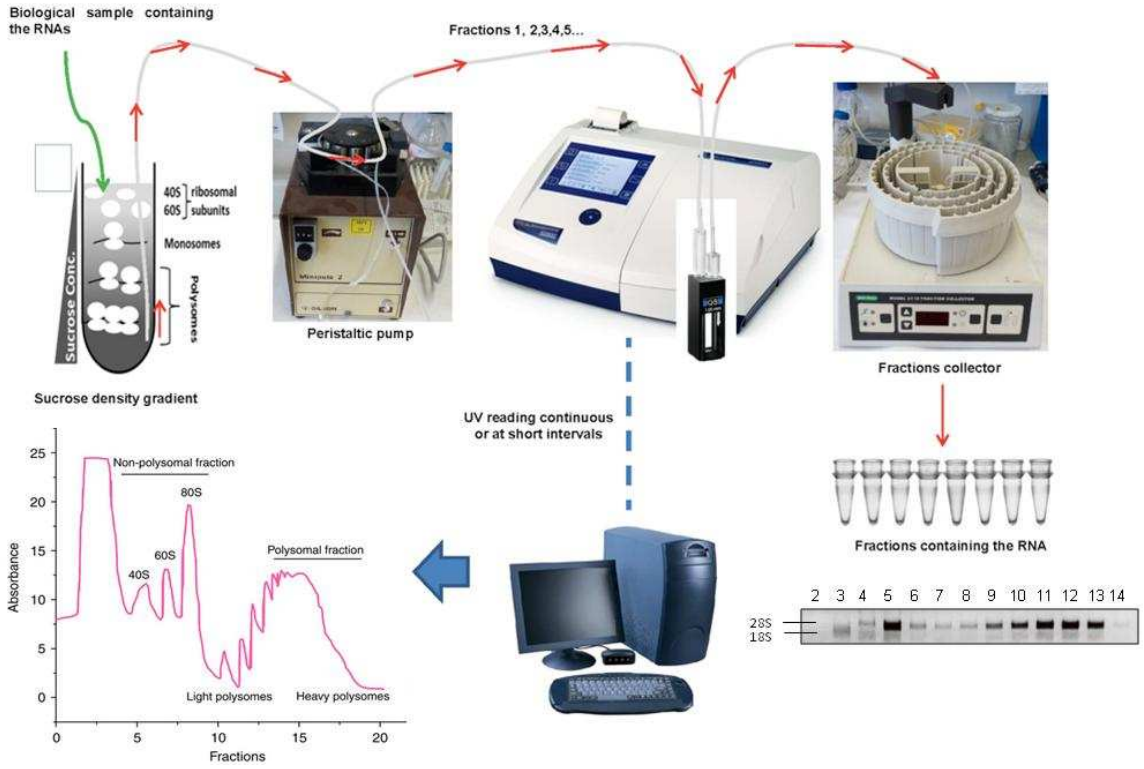

Figure 12. mRNAs are stratified in a linear sucrose gradient by ultracentrifugation. Fractionated polysomes are analyzed by monitorization of absorbance at 245 nm with an UV detector and recovered by a fraction collector. Adapted from Del Prete *et al.* [228].

Briefly, cells grown at 80% confluence were incubated for 5 min at 37 ºC with 100 µg/mL of cycloheximide, CHX (Applichem, Darmstadt, Germany). Twenty million cells were collected per condition, washed in PBS and lysated in polysome buffer (PB) containing 10 mM TRIS-HCL pH 7.4, 100 mM KCL, 10 mM $MgCl_2$, 1% TRITON-X100, 2.5 U/mL Turbo DNAse (Ambion, Carlbad, CA), 2 mM Dithiothreitol, 10 U/mL RNAse inhibitor (Promega) and 100 µg/mL CHX. All buffers were prepared in DEPC-treated water. Equal amount of cytoplasmic extracts were loaded onto a linear 10-50% sucrose gradient prepared in PB using an automated gradient maker (Gradient Master, Biocomp). Polysomes were separated by 2.5 h centrifugation at 37,000 rpm using a Beckmann SW41Ti rotor. Gradients loaded on a BR-188 Density Gradient Fractionation System (Brandel) were monitored by following absorbance at 254 nm with the software TracerDaq with a flow of 1.5 mL/min and a scan rate of 10 Hz. Fourteen fractions of 800 µL were collected using a fraction collector (BioRad). Samples were immediately frozen in dry ice. RNA was extracted from each fraction as described in RNA manipulation part.

2.8 Immunofluorescence

Cells (2 x 10^5) were seeded in sterilized glass coverslips in 24 wells plates. The day after, cells were washed twice with phosphate-buffered saline (PBS) and fixed with 4% paraformaldehyde for 30 minutes. Cells were incubated for 30 min with blocking buffer consisting of 3% BSA-PBS and 0.1% saponine to permeabilize cells. Cells were washed twice with PBS and incubated 1.5 h in a humidified dark chamber with 5 µg/ml of PTOV1 antibody prepared in blocking buffer. Cells were washed three times with PBS and incubated 1 h in a humidified dark chamber with 4 µg/mL of fluorophore-conjugated secondary antibody Alexa Fluor 488 (Invitrogen). Negative control was prepared in parallel without adding the primary antibody. Each coverslip was placed on the mounting medium ProLong Diamond Antifade Mountant with DAPI (ThermoFisher) with the cell-side face down.

3. RNA manipulation

3.1 Total RNA extraction

Total RNA was extracted with the RNeasy mini kit (QIAGEN, Valencia, CA) following instructions supplied by manufacturer protocol. This procedure is designed to isolate total RNA (longer than 200 bases) from small quantities of starting material from animal cells and/or tissues. This method is based on selective binding properties of the silica-gel-based membrane. A specialized high-salt buffer system allows up to 100 µg of RNA longer than 200 bases to bind to the RNeasy silica-gel membrane. Biological samples are first lysed and homogenized in the presence of a highly denaturing guanidine isothiocyanate-containing buffer which immediately inactivates RNases to ensure isolation of intact RNA. Ethanol is added to provide appropriate binding conditions and the sample is then applied to a mini spin column where the total RNA binds to the membrane and contaminants are efficiently washed away. High-quality RNA is then eluted in 50 µL of water.

3.2 Extraction of polysomal-bound mRNA

The phenol-chloroform based TRIZOL procedure was used to purify polysomal-bound mRNA and total RNA. The procotol used was the following:

A. Phase separation. Fractions containing heavy polysomes (≥3) were pooled in a 15 mL tube and supernatant was distributed in aliquots of 400 µL each in eppendorf tubes. One

mL TRIZOL Reagent (Ambion) was added and incubated 5 min at RT. Then, 0.2 mL of chloroform were added. Samples were vortexed vigorously and incubated at RT for 3 minutes. Samples were centrifuged at 12,000 xG for 15 minutes at 4ºC. Upper aqueous phase was carefully transferred without disturbing the interphase into a fresh tube.

B. RNA precipitation. 0.5 mL of isopropyl alcohol were added to samples to precipitate the RNA from the aqueous phase. Samples were incubated for 10 minutes at RT and centrifuged at 12,000 xG for 10 min at 4ºC.

C. RNA wash. RNA pellet was washed twice with 1 mL 75% ethanol and centrifuged at 7,500 xG for 5 minutes at 4ºC. Leftover ethanol was removed.

D. Redissolving RNA. The RNA pellet was air-dried for 5 minutes. Then, it was dissolved in 40 µL of DEPC-treated water.

3.3 Quantitative real time polymerase chain reaction (qRT-PCR)

qRT-PCR is a very sensitive technique for mRNA detection and quantification of changes in gene expression. In this method, RNA is first transcribed into complementary DNA (cDNA) by reverse transcriptase from total RNA or messenger RNA (mRNA). Then, the cDNA is used as the template for the qPCR. For retrotranscription, the *High Capacity cDNA Reverse Transcription Kit* (Applied Biosystems) was used following the manufacturer's protocol in a final volume of 20 µL. Samples were incubated for 10 min at 25ºC, 2 h at 37ºC and 5 min at 85ºC. cDNA was diluted 1:5 in water and kept at 4ºC until its utilization or at -20ºC, for long storage.

Real time qPCRs were performed using the Universal Probe Library System (Roche, Penzberg, Upper Bavaria, Germany) on a LightCycler 480 RealTime PCR instrument (Roche). Data were analyzed with the LightCycler 480 SW 1.5 software. The Universal Probe Library System is based on only 165 short hydrolysis probes, labeled at the 5' end with fluorescein (FAM) and at the 3' end with a dark quencher dye. The sequences of the 165 UPL probes detect 8- and 9-mer motifs that are highly prevalent in the transcriptomes, ensuring optimal coverage of all transcripts in a given transcriptome. In order to maintain the specificity and melting temperature that hybridizing qPCR probes require, Locked Nucleic Acids (LNA, DNA nucleotide analogues with increased binding strengths compared to standard DNA nucleotides) are incorporated into the

sequence of each UPL probe. Each PCR reaction was performed as follows: 2.5 µL cDNA, 1 µL UPL-probe, 0.1 µL forward primer (20 µM), 0.1 µL reverse primer (20 µM), 5 µL UPL Master Mix and 2.2 µL water.

The thermocycler PCR conditions were:

	Cycles	Temperature	Hold	Ramp rate ºC/s
Preincubation	1	95ºC	5 min	4.4
Amplification	40	95ºC 60ºC 72ºC	10 sec 30 sec 1 sec	4.4 2.2 4.4
Cooling	1	40ºC	10 sec	1.5

Table 6. Cycling conditions for RT-qPCR.

To estimate relative transcript levels we used the comparative Ct method. The Threshold cycle (Ct) is the cycle number at which the fluorescence signal crosses the threshold. It is also called Cp (Cross point cycle) for LightCycler terminology. The Ct value is obtained by comparing the samples of interest with a control, or calibrator, such as a non-treated sample or RNA from normal tissue. The Ct values of both the calibrator and the samples of interest are normalized to an appropriate endogenous housekeeping gene:

$\Delta\Delta Ct = \Delta Ct, sample - \Delta Ct, reference$

where *ΔCt, sample* is the Ct value for any sample normalized to the endogenous housekeeping gene and *ΔCt, reference* is the Ct value for the calibrator also normalized to the endogenous housekeeping gene. To calculate the expression change in fold, it is necessary to calculate the value of $2^{-\Delta\Delta Ct}$.

3.4 Primers

Primers (**Table 7**) were designed using the Universal ProbeLibrary Assay design center (*https://qpcr.probefinder.com/organism.jsp*).

3.5 mRNA-Seq library generation

In order to proceed with massively parallel sequencing of cDNA produced from total RNA and polysomal-bound RNA (RNA-seq) we generated a RNA-seq library. The protocol consists of the following steps:

RNA was extracted with TRIZOL as described above:

1. Purification of mRNA by PolyA Selection. A hundred and fifty µL of oligo-dT DynaBeads were collected and washed twice in 100 µL of 2 times concentrated (2X) binding buffer (20 mM Tris-HCl pH 7.5; 1.0 M LiCl; 6.7 mM EDTA). A hundred µg total RNA were diluted in 50 µL with DEPC-treated water and heated 2 min at 80ºC. One µL SUPERaseIn was added. After removing the binding buffer from the beads, the RNA was added and beads were incubated 5 min at RT in the thermomixer at 400 RPM. Beads were washed twice in 100 µL wash buffer (10 mM Tris-HCl pH 7.5; 0.15 LiCl; 1 mM EDTA) to remove non-specific binding, and resuspended in 40 µL of 10 mM Tris-HCl pH 7.0. The RNA was eluted from the beads by heating 2 min at 80ºC and placing the tube on magnet for 30 seconds. The eluted RNA suspension was transferred to a new non-stick tube on ice.

Gen	UPL probe	Forward primer 5' > 3'	Reverse primer 5' > 3'
ABCB1	#17 (CAGCTCCT)	TGTGGGAAGAAGAGCACAGTGG	TTTATTTCTTTGCCATCAAGCA
ALDH1A1	#34 (AGAGGCAG)	GCTCTCCACGTGGCATCT	GCCCCATAACCAGGAACAAT
CCNG2	#55 (GGAGAGGA)	GGGGGTTGTTTTGATGAAAGT	TTGATCACTGGGAGGAGAGC
CD133	#86 (GCAGTGGA)	GGAAACTAAGAAGTATGGGAGAACA	CGATGCCACTTTCTCACTGAT
CDH-1	#35 (AGAAGAGGA)	CCCGGGACAACGTTTATTAC	GCTGGCTCAAGTCAAAGTCC
CDH-2	#15 (TCCTGCTC)	TGCACAGATGTGGACAGGAT	CCACAAACATCAGCACAAGG
JUN	#19(CTCCAGCC)	CCAAAGGATAGTGCGATGTTT	CTGTCCCTCTCCACTGCAAC
EIF4E	#76 (TGGCTGTG)	TTTTGGGCTCTGTACAACCA	CCCACATAGGCTCAATACCATC
EIF4EBP1	#52 (GGGAGGAG)	GCGCAATAGCCCAGAAGATA	TCATAAGGCCTGGCTGGT
EIF4EBP2	#12 (CTCCTTCC)	TTCTGTGACCCTTTCGCTTT	ACAGCCCCAGGACAGGTAG
EIF4EBP3	#52 (GGGAGGAG)	AACGCCAGGCGGTTACTT	GGCAGCTAGTGGACGTTGA
HMBS	#26 (CAGCCCAG)	TGTGGTGGGAACCAGCTC	TGTTGAGGTTTCCCCGAAT
KLF4	#82 (CAGAGGAG)	GCCGCTCCATTACCAAGA	TCTTCCCCTCTTTGGCTTG
KLF9	#76 (TGGCTGTG)	CTCCGAAAAGAGGCACAAG	CGGGAGAACTTTTTAAGGCAGT
KRT18	#85 (GACCTGGA)	GAGGTTGGAGCTGCTGAGAC	ACCTCCCTCAGGCTGTTCTC
LEF1	#31	TGAATCAGGTACAGGTCCAA	CGTTGGGAATGAGCTTCG
LIN28A	#23 (GGGCTGGG)	GAAGCGCAGATCAAAAGGAG	GCTGATGCTCTGGCAGAAGT
MYC	#34 (AGAGGCAG)	CACCAGCAGCGACTCTGA	GATCCAGACTCTGACCTTTTGC
NANOG	#69 (CTTCCTCC)	ATGCCTCACACGGAGACTGT	AGGGCTGTCCTGAATAAGCA
PDCD4	#10 (CCACCTCC)	TGGAAAGCGTAAAGATAGTGTGTG	AATATTCTTTCAGCAGCATATCAATC
POU5F1	#52 (GGGAGGAG)	GTGCCTGCCCTTCTAGGAAT	GGCACAAACTCCAGGTTTTCT
PTOV1	#9 (CATCACCA)	GCTTCGTCAGTGCCATCC	TGAGTTGACACCACCAGGTC
SNAI1	#11 (CTTCCAGC)	GCTGCAGGACTCTAATCCAGA	ATCTCCGGAGGTGGGATG
SOX2	#19 (CTCCAGCC)	ATGGGGTTCGGTGGTCAAGT	GGAGGAAGAGGTAACACAGG
TBP	#87 (CTGCCACC)	GAACATCATGGATCAGAACAACA	ATAGGGATTCCGGGAGTCAT
TUBB2B	#78 (AGCTGGAG)	TTGACCCCACTGGCAGTTAC	GATGGGCCCGAGGAACATA
TUBB4A	#55 (GGAGAGGA)	GGGGCAGTGACCTGCAA	GGGGACATAATTTCCTCCTGT
TWIST1	#6 (TTCCTCTG)	GGCATCACTATGGACTTTCTCTATT	GGCCAGTTTGATCCCAGTATT
VIMENTIN	#16 (GGAGGCAG)	AAAGTGTGGCTGCCAAGAAC	AGCCTCAGAGAGGTCAGCAA
ZEB1	#3 (CTGCTGGG)	GGGAGGAGCAGTGAAAGAGA	TTTCTTGCCCTTCCTTTCTG
β-ACTIN	#11 (CTTCCAGC)	ATTGGCAATGAGCGGTTC	CGTGGATGCCACAGGACT

Table 7. Primers used in RT-qPCR.

2. mRNA alkaline fragmentation. Forty µL of 2X alkaline fragmentation solution (100 mM NaCO3 pH 9.2; 2 mM EDTA) were added to mRNA and incubated 20 min at 95ºC. Then 0.56 mL stop/precipitation solution (0.3M NaOAc pH 5.5; Glycoblue 50 µg/mL) and 0.75 mL isopropanol were added and mixed well. Samples were frozen O/N at -80ºC. Then samples were spun 30 min at 20,000 xG to pellet nucleic acids and pellet was washed in 0.75 mL 80% ice-cold ethanol. Samples were spun 5 min at 20,000 xG. Ethanol was removed and pellet was resuspended in 10 µL 10 mM Tris-HCl pH 7.0.

In order to test if fragmentation worked, fragmented samples were run on 10% TBE Urea gel (Novex, Invitrogen). Ten µL of fragmented RNA sample plus 10 µL 2X Urea sample loading buffer (Novex, Invitrogen) were denatured 80ºC for 2 minutes and loaded in the gel. Gel was run at 200 V for 50 min. Gel was stained with 6 µL SYBR

Gold in 60 mL 1X TBE for 5 min. Fragments of 30–80 nucleotides in size were quickly visualized under U.V. lamp and excised.

3. mRNA Gel extraction. A 21-gauge needle was used to pierce the bottom of 0.5 mL tubes that were placed inside a non-stick 1.5 mL tube. The gel slices containing the desired RNA fragments were excised, placed into 0.5 mL tubes and spun 3 min at 20,000 xG to force the gel through the needle hole. 500 µL 10 mM Tris pH 7.0 were added to gel pieces and incubated 10 minutes at 70ºC in the thermomixer at 1,400 RPM. Gel mixtures were transferred to Costar Spin-X column (Sigma), centrifuged 3 minutes at 20,000 xG and the eluted mixtures were recovered in a new non-stick tube. Two µL glycoblue plus 65 µL 3M NaOAc were added.

4. mRNA Precipitation. 0.6 mL isopropanol were added, mixed well and samples were store at -80ºC O/N. Samples were then spun 30 min at 20,000 xG at 4ºC to pellet nucleic acids. Pellets were washed twice in 0.75 mL 80% ice-cold ethanol and spun 5 minutes at 20,000 xG at 4ºC. Ethanol was removed and samples were resuspended in 25 µL 10 mM Tris-HCl pH 7.0.

5. T4 Polynucleotide Kinase (PNK) 3’ dephosphorylation. T4 PNK (New England BioLab) catalyzes the removal of 3’ phosphoryl groups from 3’-phosphoryl polynucleotides, deoxynucleoside 3’-monophosphates and deoxynucleoside 3’-diphosphates increasing the efficiency of the subsequent ligation. All 25 µL of gel extracted RNAs were denatured for 2 minutes at 80ºC on thermomixer without shaking. 22.5 µL of PNK reaction mix (5 µL 10X PNK buffer, 1.25 µL SUPERaseIn (20 U/ µL), 16.25 DEPC water) plus 2.5 µL T4 PNK (10 U/ µL, New England BioLab) were added to samples and incubated at 37ºC for 1 h, then at 75ºC for 10 min to inactivate the enzyme. 450 µL DEPC-treated water, 56 µL 3M NaOAc, 2 µL glycoblue were added to reaction tube and mixed. Precipitation step was carried out as previously described in step 4. Pellet was resuspended in 9 µL 10 mM Tris-HCl pH 7.0.

6. Small RNA Bioanalysis. One µL of PNK treated sample plus 4 µL DEPC water were denatured 2 minutes at 75ºC. Bioanalysis was performed following Agilent Small RNA bioanalysis protocol. Peaks should correspond to expected sizes between 30 and 80 bp (ideally 50 nt). Bioanalyzer provides concentration as pg/µL. To calculate concentration of sample in pmol we assume for the average 30 bp fragment a

molecular weight of 9133 g/mL (9133 pg/pmol). Take into account the dilution factor of the sample in water (*5):

pmol/µL= (X pg/µL (what bioanalyzer provides)*5 / 9133 pg/pmol (average molecular weight of 30 bp fragment)

7. Adapter ligation. 10 pmol of dephosphorylated RNA (but not more than 5 µL total volume) was used for ligation. In addition, a fifth to the same amount of dephosphorylated RNA was taken as unligated control sample for further use. The rest of sample was frozen at -80ºC. Samples were denatured for 2 minutes at 80ºC and placed immediately on ice. 8 µL 50% PEG (MW 8.000), 2 µL DMSO, 2 µL 10X RNA ligase buffer, 1 µL SUPERaseIn (20U/ µL), 1 µL Linker-1 1 µg/ µL (**Table 8**), 1 µL Truncated T4 RNA ligase 2 (NEB M0242L) were added and mixed well. Samples were incubated at 37ºC for 2 hours, and precipitated with 450 µL DEPC water, 56 µL 3M NaOAc and 2 µL glycoblue. Pellets were resuspended in 8 µL 10 mM Tris-HCl pH 7.0 and samples were added with 8 µL 2X TBU denaturing buffer. Ligated products and unligated control were loaded in 10% TBE-urea gel and ran at 200 V for 50 minutes. Gel was stained with SYBR gold and the ligated fragments (around 70 nt) were cut out. Gel extraction and precipitation of RNA was performed as previously described. Samples were resuspended in 10 µL 10 mM Tris-HCl pH 7.0.

8. Reverse transcription (RT). 3.28 uL 5X First Strand Buffer, 0.82 µL dNTPS 10 mM each and 0.5 µL of the primer o225-link1 at 20µM (**Table 8**) were added to 10 µL of ligated RNA. Samples were denatured 5 minutes at 65ºC in the thermomixer and placed immediately on ice. 0.5 µL SUPERaseIn (20U/ µL), 0.82 µL 0.1M DTT and 0.82 µL Superscript III were added to samples and incubated 30 minutes at 50ºC. To destroy RNA, 1.8 µL 1M NaOH were added to samples and incubate 20 minutes at 98ºC. Nineteen µL 2X TBU denaturing loading buffer were added to samples. Also the 10bp ladder and o225-link1 was used for loading reference. Denatured samples were loaded on a 10% TBU gel. Each sample was split between two lanes (19 µL each). The gel ran at 200V for 65 minutes and was stained with SYBR gold. The band corresponding to the elongated product was cut out to carefully avoid mixing it with the primer band. Gel extraction and precipitation were carried out as above. Pellets were resuspended in 15 µL of 10 mM Tris-HCl pH 7.0.

9. Circularization. Samples were circularized using CircLigase (Epicentre, Madison, Wisconsin). Two µL 10X Circ buffer, 1 µL 1mM ATP, 1 µL 50 mM $MnCl_2$, 1 µL Circ Ligase (Epicentre) were added to the 15 µL of RT product and mixed well. Samples were incubated at 60ºC for 60 min. As Circ Ligase shows some base bias, preferring to ligate 3' A's and T's over G's and C's, 1 µL Circ Ligase was added again and incubated at 60ºC for 60 min. Then, samples were incubated at 80ºC for 10 minutes to heat inactive the enzyme. Put tube on ice to proceed with rRNA subtraction or store at -20ºC.

10. Subtractive hybridization to remove rRNA-derived fragments. Streptavidin C1 DynaBeads (Invitrogen) were prepared as follows: for each sample, 40 µL of beads were aliquoted into a microcentrifuge tube and washed three times in 1X My One C1 dynabead B&W buffer (5 mM Tris-HCl pH 7.5; 0.5 mM EDTA; 1M NaCl and 0.01 % Tween). Equilibrated beads were resuspended in 20 µL of of 2X My One C1 dynabead B&W buffer (10mM Tris-HCl pH 7.5; 1 mM EDTA; 2 M NaCl and 0.01 % Tween). To 5 µL circularized cDNA the following were added: 2 µL 20x SSC (Ambion), 11 µL nuclease-free water, and 2 µL of a 70 µM mixture of the biotinylated oligonucleotides (**Table 8**). Samples were denatured for 2 minutes at 95ºC and annealed for 20 minutes at RT. 20 µL of equilibrated beads were added to 20 µL hybridized samples. The mixture was incubated 20 min at RT in the thermomixer with shaking (400 RPM). Beads were then separated on a magnetic manifold (Invitrogen) and the supernatant recovered to a new 1.5 mL non-stick tube. cDNA was precipitated by adding 60 µL 10 mM Tris-HCl pH 7.0, 7 µL 5 M NaCl and 2 µL glycoblue, 150 µL isopropanol and incubated O/N at -80ºC. Precipitation was performed as described above. Pellets were resuspended in 10 µL 10 mM Tris pH 7.0.

Oligo	Purpose	Sequence
Linker-1	3' cloning adaptor for RNA fragments	App/CTGTAGGCACCATCAAT/3ddC
o225-link1	Primer for reverse transcription	5'/5phos/GATCGTCGGACTGTAGAACTCTGAACCTGTCGGTGGTCGCCGTATCATT/isp18/ CACTCA/ISP18/CAAGCAGAAGACGGCATACGAATTGATGGTGCCTACAG
oNTI298	Subtractive hybridization of rRNA-derived fragments	/5Biosg/ GGGGGGATGCGTGCATTTATCAGATCA
oNTI299	Subtractive hybridization of rRNA-derived fragments	/5Biosg/ TTGGTGACTCTAGATAACCTCGGGCCGATCGCACG
oNTI300	Subtractive hybridization of rRNA-derived fragments	/5Biosg/GAGCCGCCTGGATACCGCAGCTAGGAATAATGGAAT
oNTI301	Subtractive hybridization of rRNA-derived fragments	/5Biosg/ TCGTGGGGGGCCCAAGTCCTTCTGATCGAGGCCC
oNTI302h	Subtractive hybridization of rRNA-derived fragments	/5Biosg/ GCACTCGCCGAATCCCGGGGCCGAGGGAGCGA
oNTI303m	Subtractive hybridization of rRNA-derived fragments	/5Biosg/ GGGGCCGGGCCGCCCCTCCCACGGCGCG
oNTI303h	Subtractive hybridization of rRNA-derived fragments	/5Biosg/ GGGGCCGGGCCACCCCTCCCACGGCGCG
oNTI304m	Subtractive hybridization of rRNA-derived fragments	/5Biosg/ CCCAGTGCGCCCCGGGCGTCGTCGCGCCGTCGGGTCCCGGG
oNTI305	Subtractive hybridization of rRNA-derived fragments	/5Biosg/ TCCGCCGAGGGCGCACCACCGGCCCGTCTCGCC
oNTI306	Subtractive hybridization of rRNA-derived fragments	/5Biosg/ AGGGGCTCTCGCTTCTGGCGCCAAGCGT
oNTI307m	Subtractive hybridization of rRNA-derived fragments	/5Biosg/ GAGCCTCGGTTGGCCCCGGATAGCCGGGTCCCCGT
oNTI307h	Subtractive hybridization of rRNA-derived fragments	/5Biosg/ GAGCCTCGGTTGGCCTCGGATAGCCGGTCCCCCGC
oNTI308	Subtractive hybridization of rRNA-derived fragments	/5Biosg/ TCGCTGCGATCTATTGAAAGTCAGCCCTCGACACA
oNTI309	Subtractive hybridization of rRNA-derived fragments	/5Biosg/ TCCTCCCGGGGCTACGCCTGTCTGAGCGTCGCT
NG30h	Subtractive hybridization of rRNA-derived fragments	/5Biosg/ CCCAGTGCGCCCCGGGCGGGTCGCGCCGTCGG
NG31h	Subtractive hybridization of rRNA-derived fragments	5Biosg/ CCGCCGGTGAAATACCACTACTCTGATCGTTTTTTC

Table 8. Cloning oligos used in this thesis.

11. PCR reaction. Circularized libraries were amplified by 11 PCR cycles using the reverse primer oNTI231 and any of the indexing primers (**Table 8**) using Phusion High-Fidelity (HF) DNA polymerase (Finnzymes by ThermoScientific). Indexed primers are unique synthetic oligonucleotide index sequences added to forward primer sequence in order to distinguish samples after sequencing. Each sample amplified with a unique set of these indexed primers. PCR master mix (16.7 µL 5X HF buffer; 1.7 µL dNTPs 10 mM each; 0.4 µL oNTI231 primer at 100 µM; 50.6 µL DEPC water and 0.8 µL Phusion polymerase) and 4 µL indexed primer (10 µM) were added to 10 µL circularized subtracted sample (**Table 9**). Samples were mixed and split in 5 PCR tubes, 16.7 µL per tube. PCR was performed as following:

a) 98ºC, 30 sec
b) 98ºC, 10 sec
c) 60ºC, 10 sec
d) 72ºC, 5 sec

e) Repeat b-d 11 cycles

f) 4ºC, ∞

Each PCR tube was added with 3.4 µL 6X loading dye and samples (20 µL per lane) were ran on a 8% TBE gel 60 minutes at 180V. Gel was stained with SYBR gold and amplified products (around 160 pb) were cut out. Gel extraction was performed by adding 400 µL DNA gel extraction buffer (5M NaCl; 1M Tris pH 8.0; 500 mM EDTA). Samples were kept in dry ice for 30 min and shaked O/N at 4ºC. 50 µL of 5M NaCl and 0.1 µL of Glycoblue were added to precipitate samples. Pellet was resuspended in 10 µL 10 mM Tris-HCl pH 7.0.

12. Check library quality by Bioanalyzer. High Sensitivity DNA chip (Agilent) was used for checking DNA quality following manufacturer's protocol. Note that peaks must correspond to the expected size (160 nt), no other bands should be present.

Oligo	Sequence 5'-3'
o231	CAAGCAGAAGACGGCATACGA
oCJ30 (TruSeq Index 1)	AATGATACGGCGACCACCGAGATCGGAAGAGCACACGTCTGAACTCCAGTCAC**ATCACG**CGACAGGTTCAGAGTTC
oCJ31 (TruSeq Index 4)	AATGATACGGCGACCACCGAGATCGGAAGAGCACACGTCTGAACTCCAGTCAC**TGACCA**CGACAGGTTCAGAGTTC
oCJ32 (TruSeq Index 7)	AATGATACGGCGACCACCGAGATCGGAAGAGCACACGTCTGAACTCCAGTCAC**CAGATC**CGACAGGTTCAGAGTTC
oCJ33 (TruSeq Index 6)	AATGATACGGCGACCACCGAGATCGGAAGAGCACACGTCTGAACTCCAGTCAC**GCCAAT**CGACAGGTTCAGAGTTC
oCJ35 (TruSeq Index 5)	AATGATACGGCGACCACCGAGATCGGAAGAGCACACGTCTGAACTCCAGTCAC**ACAGTG**CGACAGGTTCAGAGTTC
oCJ38 (TruSeq Index 8)	AATGATACGGCGACCACCGAGATCGGAAGAGCACACGTCTGAACTCCAGTCAC**ACTTGA**CGACAGGTTCAGAGTTC
oCJ39 (TruSeq Index 9)	AATGATACGGCGACCACCGAGATCGGAAGAGCACACGTCTGAACTCCAGTCAC**GATCAG**CGACAGGTTCAGAGTTC
oCJ40 (TruSeq Index 10)	AATGATACGGCGACCACCGAGATCGGAAGAGCACACGTCTGAACTCCAGTCAC**TAGCTT**CGACAGGTTCAGAGTTC
oCJ41 (TruSeq Index 11)	AATGATACGGCGACCACCGAGATCGGAAGAGCACACGTCTGAACTCCAGTCAC**CGGCTAC**CGACAGGTTCAGAGTTC

Table 9. Indexed primers for PCR amplification.

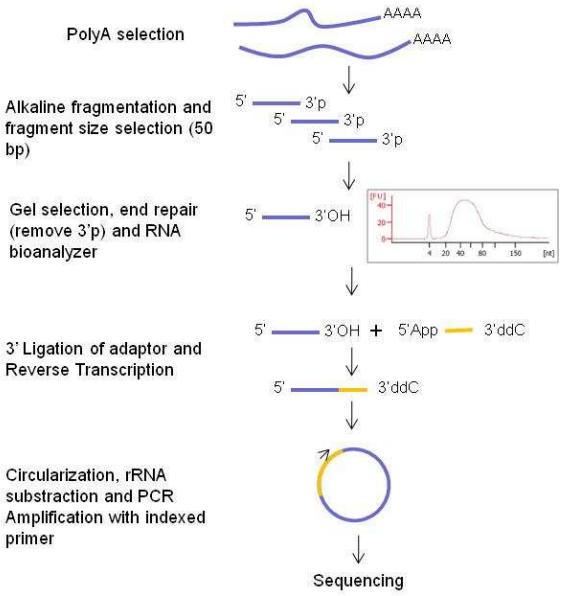

Figure 13. Schematic of mRNA-seq library generation.

3.6 RNA interference to study gene function

The use of RNA interference (RNAi) has emerged as a powerful tool for the study of gene function in mammalian cells. The mechanism is based on the sequence-specific degradation of host mRNA through the cytoplasmic delivery of double-stranded RNA (dsRNA) complementary to the target sequence. Degradation of target gene expression involves the endogenous RNA-induced silencing complex (RISC) with the assistance of Argonaute (Ago) proteins [229].

A form of RNAi involves the use of short hairpin RNAs (shRNAs) synthesized within the cell by DNA vector-mediated production. shRNAs may be transfected as plasmid vectors encoding shRNAs transcribed by RNA Pol III or modified Pol II promoters, but can also be delivered into mammalian cells through infection of the cell with virally produced vectors. shRNAs are capable of DNA integration and consist of two complementary 19–22 bp RNA sequences linked by a short loop of 4–11 nt similar to the hairpin found in naturally occurring miRNA. Following transcription, the shRNA sequence is exported to the cytosol where it is recognized by an endogenous enzyme, Dicer, which processes the shRNA into short interfering RNA (siRNA) duplexes.

Lentiviral vectors carrying short-hairpin RNA to PTOV1 were obtained from Sigma's MISSION shRNA Library (**Table 10**).

shRNA	ID	PTOV1 target sequence
PTOV1	TRCN0000**143**905	CCTGTACTCTTCAGAGAAGAA
PTOV1	TRCN0000**140**104	GTTCCACTTCACCAACAGAGA
PTOV1	TRCN0000**139**737	CCTGTACTCGTCCAAGAAGAA

Table 10. shRNA sequences used for stable knockdown of PTOV1

Tet-on inducible systems provide induced expression of a given sequence (gene, shRNA) in the presence of doxycycline (Dox) by two main components: i) the tetracycline response element (TRE) and ii) the transactivator [230, 231]. The transactivator binds to and activates the TRE promoters in the presence of doxycycline. In this vector the presence of Dox also drives the expression of a Red Fluorescen Protein (RFP) reporter to easily observe expression from the TRE promoter (**Figure 14**).

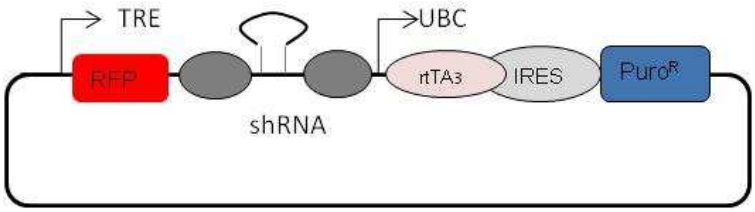

Figure 14. Schematic and features of the pTRIPZ Inducible Lentiviral shRNA vector. TRE, Tetracycline-inducible promoter; tRFP, TurboRFP reporter for visual tracking of transduction and shRNA expression; shRNA, microRNA-adapted shRNA (based on miR-30) for gene knockdown; UBC, Human ubiquitin C promoter for constitutive expression of rtTA3 and puromycin resistance genes; rtTA3, Reverse tetracycline-transactivator 3 for tetracycline-dependent induction of the TRE promoter; PuroR; Puromycin resistance permits antibiotic-selective pressure and propagation of stable integrants; IRES, Internal ribosomal entry site allows expression of rtTA3 and puromycin resistance genes in a single transcript.

pTRIPZ™ Inducible Lentiviral shRNA to inhibit PTOV1 expression were purchased from ThermoScientific (Alcobendas, Madrid, Spain) (**Table 11**).

shRNA	ID	PTOV1 target sequence
PTOV1	V2THS_154353	CTGTACTCTTCAGAGAAGA: sense Mature Antisense: TCTTCTCTGAAGAGTACAG
PTOV1	V3THS_346191	AGAGACTGCGACTCGCTCA:sense Mature Antisense: TGAGCGAGTCGCAGTCTCT
PTOV1	V3THS_346196	GCGTGCACTTTTCCTACAA sense Mature Antisense: TTGTAGGAAAAGTGCACGC

Table 11. pTRIPZ inducible lentiviral shRNA sequences used for inducible knockdown of PTOV1.

4. DNA manipulation

4.1 Chromatin immunoprecipitation

The chromatin immunoprecipitation (ChIP) assay is a powerful method for studying interactions between specific proteins and a genomic DNA region. This assay can be used to determine whether a transcription factor interacts with a candidate target gene sequence. ChIP was performed using EZ ChIP TM Kit (Millipore) following manufacturer's instructions. Briefly, $3x10^6$ cells were seeded on 15 cm diameter plates. Two plates were used for ChIP. The following day, cells were fixed with 1% formaldehyde and incubated 10 minutes at RT to crosslink proteins and DNA. Next, 1

mL of 1.25M Glycine was added to quench unreacted formaldehyde and cells were incubated for 5 min at RT. Cells were washed in PBS and spun at 700 xG for 5 minutes. Cell pellets were resuspended in 1 mL SDS Lysis Buffer (1% SDS, 10 mM EDTA, 50 mM Tris pH 8.1) containing Protease Inhibitor Cocktail II. Supernatant was aliquoted (400 µL) and cross-linked chromatin was sonicated to generate smaller DNA fragments. Twenty µL of protein G magnetics beads (Invitrogen) were used for each immunoprecipitation (IP). Magnetic protein G beads (Invitrogen) were prepared for IP by washing them in dilution buffer and incubation overnight with the desired antibody. For PTOV1 immunoprecipitation the rabbit PTOV1 antibody (4 µg) was used. Positive controls were antibodies to total RNA-Polymerase II (1 µg) and phosphorylated RNA-Polymerase II (1 µg). Negative controls were mouse IgG and rabbit IgG (1 µg each). Extra beads bound to unspecific antibodies (IgG mouse or IgG rabbit) were prepared to prewash cell supernatants before the IP. Supernatants were incubated with IgG mouse/rabbit coated-beads 3 h at 4ºC for prewashing. Then, 1% supernatant was taken as Input and stored at -20ºC for further use. Supernatants were incubated with appropriate antibody-coated beads O/N at 4ºC with rotation. Any DNA sequences associated with the target protein will co-precipitate as part of the cross-linked chromatin complex. After IP, beads were washed twice in each of the following buffers:

- Low salt immune complex wash buffer (0.1% SDS, 1% Triton X-100, 2 mM EDTA, 20 mM Tris-HCl pH 8.1, 150 mM NaCl)
- High salt immune complex wash buffer (0.1% SDS, 1% Triton X-100, 2 mM EDTA, 20 mM Tris-HCl pH 8.1, 500 mM NaCl)
- LiCl immune complex wash buffer (0.25M LiCl, 1% IGEPAL-CA630, 1% deoxycholic acid (sodium salt), 1 mM EDTA, 10 mM Tris-HCl pH 8.1)
- TE buffer (10 mM Tris-HCl, 1 mM EDTA pH 8.0)

To elute Protein/DNA complexes 100 µL of Elution buffer (EB) (10 µL 20% SDS, 20 µL 1M $NaHCO_3$ and 170 µL dH_2O) was added to antibody/beads complex. For input tubes, 200 µL of EB were added. Samples were incubated for 15 min at RT. One hundred µL of EB was added again to antibody/beads complexes and samples were incubated 15 more min. To reverse crosslinking and to free the DNA, samples were added with 8 µL 5M NaCl followed by O/N incubation at 65ºC. Next, all samples were added with 1 µL of RNAse A (10 mg/ml) and incubated for 30 minutes at 37ºC. Then, 4

µL 0.5M EDTA, 8 µL 1M Tris-HCl and 1 µL Proteinase K (10 mg/mL) were added and samples were incubated at 45ºC for 2 hours. Finally, the DNA was purified using Illusta GFX PCR DNA Purification kit and it was eluted in 50 µL of EB and stored at -20ºC for further use. This DNA was used as template for PCR reactions with specific primers (**Table 12**) using the Hot-Start *Taq* polymerase (Platinum PCR master mix, Invitrogen). Reactions were as follows: 25 µL Platinum mix, 1 µL Forward primer (10 µM), 1 µL Reverse primer (10 µM) and 2 µL of desired DNA. The amplification cycles were as follows:

Initial denaturation 94ºC 5 min

Denature 94ºC 20 sec
Anneal 57ºC 30 sec
Extension 72ºC 30 sec
} repeat for 37 cycles

Final extension 72ºC 2 min

Gene	Forward primer 5'>3'	Reverse primer 5'>3'
ABCB1 promoter 1	AAGGTCTTCCCAGTAACCTACCA	GGCAGGCTTGAAAGCACTAAT
ABCB1 promoter 3	CTCTGCCTTCGTGGAGATGC	CGGTCCCCTTCAAGATCCAT
ALDH1A1 promoter	TGGAGCGTGCCGTCCTTTAT	TAACCCAAAACTCCGCTCACC
CCNG2 promoter	GAGCGTGACATTCCCCCAA	AAAGTCCGCCCAAAGTAGCC
LIN28A promoter	GAGGGGGTGTCAAACCTCAA	AAGGCAAAGGGTTGGTTCGG
NANOG promoter	CCATTCCTGTTGAACCATATTCCT	ACTGACCCACCCTTGTGAAT
TUBB2B promoter	CCTCCATCGTTCCCATCCG	CCGGCTGACGTAATGCTCC

Table 12. Primers used for ChIP experiments.

Samples were loaded in an acrylamide gel prepared as follows:

Reagent	Volume (mL)
30% Acrylamide mix	2
TBE buffer	2
ddH_2O	6
APS 10%	0.060
TEMED	0.0075

Table 13. Preparation of acrylamide gel for ChIP assays.

Gel was stained with SYBR SAFE and visualized with a Molecular Imager Gel Doc^{TM} XR system (BioRad).

4.2 Vectors and constructions

All plasmid vectors employed in this thesis are listed below:

HA-PTOV1

Full length human PTOV1 cDNA was obtained from clone IMAGE ID 5928807 and subcloned into EcoRI and XhoI sites of pCMV-HA (Clontech Laboratories, Mountainview, CA) to generate pHA-PTOV1[101].

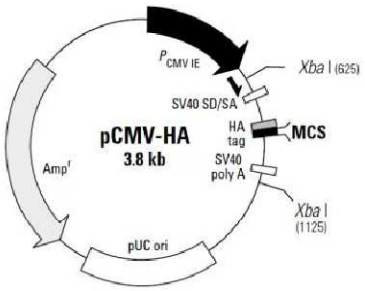

GFP-PTOV1

Constructs for the expression of chimeric GFP-PTOV1 were generated in pEGFP-N1 (Clontech) by placing the full-length PTOV1 cDNA in frame and downstream with GFP, either at the amino or the carboxyl termini of PTOV1 [73] .

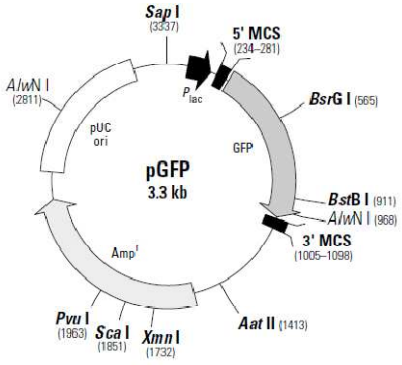

pLucire-HA-PTOV1

The lentiviral pHA-PTOV1-IRES-GFP plasmid was generated by replacing the *Luciferase* sequences from pRRL-Luc- IRES-EGFP (a gift from D. Luis Álvarez-Vallina, Hospital Universitario Puerta de Hierro, Madrid, Spain) with the N-terminal HA-tagged human full-length PTOV1[101].

c-Jun-HA

c-Jun full length cDNA placed in frame with HA tag in the p-CMV-HA vector (Clontech), was kindly provided by D. Bohmann, (University of Rochester Medical Center, Rochester, NY).

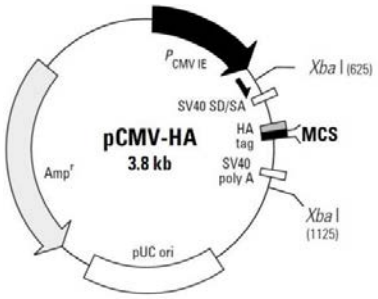

pCMV-TAM67

The mutant c-Jun TAM-67 [232] was cloned as an EcoRI fragment then blunted and ligated into the Not1 site of the pCMV-P expression vector replacing the P-galactosidase gene. The TAM-67 plasmid was kindly provided by D. Landázuri (Instituto de Investigación La Princesa, Madrid, Spain).

pRRL-Luc-IRES-EGFP

Vector was a generous gift of D. Luis Álvarez-Vallina (Unidad de Inmunología Molecular, Hospital Universitario Puerta de Hierro, Madrid, Spain). pRRL-Luc-IRES-EGFP vector drives the expression of luciferase and for its construction, the NheI/XbaI fragment derived from the plasmid pGL3 Basic Vector (Promega, Madison, WI, USA) was ligated into the XbaI digested backbone of plasmid pRRL-IRES-EGFP.

4.3 Preparation of competent bacteria

To increase the DNA transformation efficiency of the bacteria and make them more susceptible to uptake the plasmid DNAs, we generated competent cells. We used a protocol based in the use of the alkali metal halid rubidium chloride (RbCl). *Escherichia coli,* streak DH5α, were treated with a hypotonic solution containing RbCl expand. As a result of this treatment, the expulsion of membrane proteins from the bacteria allows negatively charged DNA to bind. The protocol used is detailed as follows:

Cell strain to be made competent was plated on LB-agar without antibiotics and incubated O/N at 37ºC. A single colony was picked from the plate and inoculated in 30

mL of LB with 300 µL Mg^{++} ($MgCl_2$ 1M + $MgSO_4$ 1M). Flasks were shaken O/N at 37ºC. Eight mL of the O/N culture were inoculated into a flask containing 200 mL of LB plus 2 mL of Mg^{++}. Flask was shaken at 37ºC until an OD_{550} of about 0.45-0.55 (about 2 hours). The culture was collected into four sterile 50 mL conical tubes and chilled rapidly on ice for 15 minutes. Then, cells were pelleted by centrigugation at 2,700 xG for 10 min at 4ºC. The supernatant was discarded and pellets were resuspended gently in 16 mL of Transformation Buffer 1 (100 mM RbCl, 50 mM $MnCl_2{\cdot}4H_2O$, 30 mM KAc pH 7.5, 10 mM $CaCl_2{\cdot}2H_2O$, 15% Glycerol 99% v/v) and incubated on ice for 15 minutes. After a second centrifugation at 2,700 xG, the supernatant was discarded and cells were resuspended in 4 mL of Transformation Buffer 2 (10 mM MOPS, 10 mM RBCl, 75 mM $CaCl_2{\cdot}2H_2O$, 15% Glycerol). Cells were collected into one conical tube and incubated in RF2 on ice for 15 min. Then, cells were aliquoted (100 µL each) into chilled 1.5 mL eppendorf tubes, frozen on dry ice, and stored at -80ºC.

4.4 Bacterial transformation, growth and plasmid DNA isolation

We used a standard heat-shock transformation method of chemically-competent bacteria. The protocol details are below:

One µL of DNA (usually 10 pg to 100 ng) was added to 50 µL of competent bacteria in a microcentrifuge tube, gently mixed and placed on ice for 30 minutes. The tube was placed at 42ºC for 60 seconds and put it back on ice for 37ºC. Two hundred µL of LB media without antibiotic were added and 60 min at 37°C in a shaking incubator. Thirty µL of the transformation were plated onto a 10 cm LB agar plate containing the appropriate antibiotic and plates were incubated O/N at 37°C. A portion of an isolated colony was scraped with a sterile pipette tip, immersed in a sterile culture tube containing LB media (3 mL) supplemented with the appropriate antibiotic (100 µg/mL) and shaked in an orbital shaker at 37ºC for 2 h. For plasmid DNA preparation, 3 mL of culture were placed into a sterile flask (500 mL) containing approximately 100 mL of LB media plus the appropriate antibiotic and shake in an orbital shaker O/N at 37 ºC (no more than 17 h). On the next day, for plasmid DNA isolation we used the *Nucleobond AX PC 100 kit* (Macherey-Nagel Gmbh, Düren, Germany), following the manucfacturer's instructions. Briefly, the bacterial cells were lysed by buffers based on the NaOH/SDS alkaline lysis. After equilibration of the column, the entire lysate was loaded by gravity flow and simultaneously cleared by column filters. The silica resin consists of hydrophilic,

macroporous silica beads functionalized with methyl-amino-ethanol that provides a high overall positive charge density under acidic pH conditions that permits the negatively charged phosphate backbone of plasmid DNA to bind with high specificity. Plasmid DNA was bound to the silica resin and after an efficient washing step with ethanol 70% the DNA was eluted, precipitated with isopropanol, dissolved in water and stored at -20ºC for further use.

5. Protein manipulation

5.1 Protein extraction

Cells and tissues were lysed in a lysis buffer containing 50 mM Tris pH 7.5; 200 mM NaCl; 5 mM EDTA; 0.1% Triton X-100, proteases inhibitors (Proteases Inhibitor Cocktail from Sigma-Aldrich; 1:200) and phosphatases inhibitors (1 mM Sodium Fluoride). The protocol is detailed below:

Cells were washed twice with cold PBS and ice-cold lysis buffer was added (approximately 100 µL per $1x10^6$ cells in 10 cm dish). Adherent cells were collected using a cell scraper, transferred into a pre-cooled microfuge tube, vortexed and kept on ice for 30 min. Lysates were centrifuged 15 min at 12,000 xG at 4ºC. Supernatant was collected in a new tube kept on ice and it was stored at -20ºC for later use.

5.2 Determination of protein concentration

To determine protein concentration we used the Bradford method. Bovine serum albumin (BSA) was used as standard. This method can determine the total protein concentrations in solutions depending on the change in absorbance based of the bound dye Coomassie Blue G-250 to proteins. A set of BSA (Panreac) standards was created from a stock of 2 mg/mL (0, 0.25, 0.5, 0.75, 1, 1.5, 1.75 and 2 mg/mL). Five µL of standards, or sample, were added to a 96 well plate. Then, 200 µL of Bradford solution (Panreac) was added and plate was incubated for 15 min at RT. Absorbance was measured at 595 nm in an Epoch™ Microplate Spectrophotometer (BioTek). The values obtained for the BSA standards were used to construct a standard curve used to compare the samples values to know their concentration.

5.3 Protein analysis by Sodium Dodecyl Sulfate Polyacrylamide Gel Electrophoresis (SDS-PAGE) and Western blotting

Western blotting is a widely used technique used in research to separate and identify proteins. In denaturing SDS-PAGE, a mixture of proteins is separated based on molecular weight, and not by intrinsic electrical charge of the polypeptide, through gel electrophoresis. These results are then transferred to a membrane producing a band for each protein. Later, the membrane is incubated with labels antibodies specific to the protein of interest [233].

Protein samples were denatured in loading buffer (*Laemmli buffer:* 250 mM Tris pH 6.8; 10% SDS; 0.5% Bromophenol blue; 50% Glycerol; 500 nM DTT) and boiled at 95°C for 5 min. The concentrations of all the components of the polyacrylamide gels used in this thesis are shown in **Table 13**. Generally, at least 30 µg of protein lysate was added to sample wells at the top of the gel. One well was loaded with molecular weight markers to help in the identification of the protein sizes and to monitor electrophoretic run. The electrophoresis was run in the running buffer (25 mM Tris base; 190 mM Glycine; 0.1% SDS; pH 8.3) for approximately 1.5 h or until the migration front reached the bottom of the gel.

	Stacking gel 5% (10mL)	**Resolving gel 8% (10 mL)**	**Resolving gel 10% (10 mL)**	**Resolving gel 12% (10 mL)**
ddH_2O	6.8 mL	4.6 mL	4 mL	3.3 mL
Acrylamide: Bisacrylamide (29:1)	1.7 mL	2.7 mL	3.3 mL	4 mL
Tris-HCl 1M	1.25 mL (pH 6.8)	2.5 mL (pH 8.8)	2.5 mL (pH 8.8)	2.5 mL (pH 8.8)
10% SDS	100 µL	100 µL	100 µL	100 µL
10% APS	100 µL	100 µL	100 µL	100 µL
TEMED	10 µL	6 µL	4 µL	4 µL

Table 14. Preparation of acrylamide-bisacrylamide gels for Western blotting.

After the electrophoresis, the separated proteins were transferred onto a solid support matrix. Electrophoretic wet transfer was used to immobilize proteins onto polyvinylidene difluoride (PVDF) membranes. PVDF were previously pre-wetted with methanol prior to submersion in transfer buffer (25 mM Tris-HCl pH 8.3; 192 mM

glycine; 20% (v:v) methanol). The gel and PVDF membrane were submerged under transfer buffer in tanks where they were sandwiched between buffer-wetted filter papers that were in direct contact with flat-plate electrodes. The electric field strength makes negatively-charged proteins travel towards the positively-charged electrode, but the membrane stops them, binds them, and prevents them from continuing on. The electrophoresis conditions for transference were the following:

- For large proteins (>100 kD) the transference was performed slowly O/N at 60 mA/h.
- For small proteins (<100 kD) the transference was run for 2 h at 400 mA/h.

To visualize the transferred proteins, membranes were stained with Ponceau S for 5 min. Specific proteins in the membranes were detected by incubation with antibodies.

Antibody	Origen	Dilution	Reference
Actin I-19	Goat	1/500	Santa Cruz Biotechnology
Annexin II	Mouse	1/500	BD Transduction laboratories
c-Jun (H79)	Rabbit	1/500	Santa Cruz Biotechnology
c-Myc (9E10)	Mouse	1/500	Santa Cruz Biotechnology
Cyclin B1(V152)	Mouse	1/1,000	Abcam
E4-BP1 (53H11)	Rabbit	1/1,000	Cell Signaling Technology
E-cadherin (clone 36)	Mouse	1/8,000	BD Transduction laboratories
eIF4E (C46H6)	Rabbit	1/1,000	Cell Signaling Technology
Fibronectin	Goat	1/500	Sigma-Aldrich, polyclonal
HA.11 (16B12)	Mouse	1/500	Covance
Keratin 18 (CD10)	Mouse	1/500	NeoMarkers
N-cadherin (clone 32)	Mouse	1/500	BD Transduction laboratories
p-AKT (Ser473)	Rabbit	1/500	Cell Signaling Technology
PARP-1(H-250)	Rabbit	1/500	Santa Cruz Biotechnology
PDCD4	Rabbit	1/500	Cell Signaling Technology
phospho-E4-BP1 (Thr37/46)	Rabbit	1/1,000	Cell Signaling Technology
phospho-eIF4E (Ser209)	Rabbit	1/1,000	Cell Signaling Technology
phospho-SAPK/JNK (Thr183/Tyr185)	Mouse	1/500	Cell Signaling Technology
PTOV1	Rabbit	1/500	Made in our laboratory
Puromycin (12D10)	Mouse	1/10,000	Millipore
Ribosomal protein S6 (5G10)	Rabbit	1/1000	Cell Signaling Technology
SAPK/JNK	Rabbit	1/1000	Cell Signaling Technology
Snail1 (Sn9H2)	Rat	1/500	Abcam
Vimentin (VI-10)	Mouse	1/2,000	Abcam
Zeb-1 (H3)	Mouse	1/1,000	Santa Cruz Biotechnology

Table 15. Primary antibodies used in Western blotting assays.

First, membranes were blocked to prevent non-specific binding of the antibodies. Blocking solution was 5% not-fat milk or BSA solution prepared in Tris Buffer Saline Tween (TBST) buffer (50 mM Tris-Cl pH 7.5; 150 mM NaCl; 0.1% Tween) for 30 min incubation. Primary antibodies, prepared in the same solution, were diluted according to the datasheet information (**Table 14**) and incubated O/N at 4ºC. Membranes were washed several times in TBST and incubated with secondary antibodies 1 h at RT. Horseradish peroxidase (HRP)-conjugated secondary antibodies diluted 1:2000 in blocking buffer were used (**Table 15**). Finally, ECL Western Blotting Detection reagent (Amersham, GE Healthcare) was used to reveal the specific proteins on the membranes. This is a light emitting nonradioactive method for detection of immobilized specific antigens with HRP-labelled antibodies.

Antibody	Origen	Dilution	Reference
Anti-goat immunoglobulins/HRP	Goat	1/2000	Dako
Anti-rabbit immunoglobulins/HRP	Rabbit	1/2000	Dako
Anti-mouse immunoglobulins/HRP	Mouse	1/2000	Dako

Table 16. Primary antibodies used in Western blotting assays.

5.4 Analysis of protein stability

In order to determine the half-life of a given protein we utilized the cycloheximide chase assays. This is a popular method employed to compare protein stability in eukaryotic cells based in the action of cycloheximide (CHX) as an inhibitor of protein translational elongation [234]. Briefly, 24 h after seeding cells ($3x10^5$ in 6 well plates), the media was changed to fresh media containing 100 µg/mL CHX. At time t=0, control cells were lysed (50 mM Tris pH 7.5; 200 mM NaCl; 5 mM EDTA; 0.1% Triton X-100 and proteases inhibitors) and stored at -80ºC. Lysates were collected at different time points and protein extraction was as described above.

5.5 Analysis of protein synthesis

5.5.1 ^{35}S Methionine labeling

Metabolic labeling of cells with low-energy beta-emitting radioisotopes such as ^{35}S-Methionine is often used to follow the biosynthesis, maturation and degradation of

proteins *in vivo*. Labeling of methionine-containing proteins in cells relies in the use of methionine-free culture media supplemented with a radiolabeled source of ^{35}S. Then, the neosynthesized protein will be quantified or identified by using a scintillation counter or by separation on two-dimensional SDS-PAGE gel and autoradiography. Cells (3.5 x 10^4 cells/well) in quintuplicates in 6-well plates were incubated for 2 h with Methionine-Cysteine-free medium supplemented with 10% dialysed serum at 37ºC and pulse-labeled (30 min) with 20 µCi/ml [^{35}S]-Methionine (EasyTag Perkin Elmer ^{35}S Express Protein Labeling Mix, NEG772). At the indicated times, cells were lysed in lysis buffer containing 50 mM Tris pH 7.5; 200 mM NaCl; 5 mM EDTA; 0.1% Triton X-100; and proteases inhibitors at 4ºC and proteins were quantified as described above. Equal amounts of proteins per condition (20 µg) were precipitated by adding cold ethanol (9 times the volume of the sample). Tubes were incubated 60 min at -20ºC and centrifugated for 15 min at 13,000 xG. Supernatant was discarded and dried-air pellet was redissolved in 30 µL Tris-HCl 100 nM pH 7.4. Five mL of scintillation fluid was added to samples and the incorporated radioactivity was quantified on a LS6500 Multi-Purpose β-Scintillation Counter (Beckman Coµlter, Brea, CA).

5.5.2 Surface sensing of translation (SUnSET)

SUnSET is a nonradioactive method to monitor protein synthesis [235]. It is based in the use of low amounts of puromycin, a structural analog of aminoacyl tRNAs, which is incorporated into the nascent polypeptide chain preventing elongation. mRNA translation can be analyzed by Western blotting using a monoclonal antibody to puromycin. Briefly, the protocol is:

Cells (3 x 10^5) were seeded in 6 well plates. Twenty-four hours later cells were treated with 10 µg/mL puromycin for 10 minutes. Non treated cells were the negative control. Positive control cells were treated with 10 µg/mL puromycin and 10 µg/mL cycloheximide for 10 minutes. Cell lysates were collected and analyzed by Western blotting. Monoclonal puromycin antibody was prepared 1:10,000 in 5% BSA in TBST.

6. In vivo *tumorigenic assays*

The firefly luciferase gene was integrated into the genome of PC3 cells by lentiviral transduction of pRRL-Luc-IRES-EGFP. PC3 shControl and PC-3 shPTOV1

cells ($3x10^6$) in 100 µL of PBS:Matrigel (1:1) were inoculated subcutaneously in the right flank of 6-week old male SCID-beige mice (n=6 for PC3 shControl; n=4 for PC3 shPTOV1) (Charles River Laboratories, Barcelona, Spain). All animal experimental procedures were approved by the Vall d'Hebron Hospital Animal Experimentation Ethics Committee. Tumor growth was monitored twice a week by calliper measurements (D x $d^2/2$, where D is the major diameter and *d* the minor diameter) and *in vivo* bioluminescence imaging (BLI). BLI intensity was quantified in photons per second (ph/s) using the IVIS Spectrum Imaging System equipped with the Living Image 4.0 software (Caliper Life Sciences, Hopkinton, M). After reaching 1.5 cm in diameter, tumors were excised, weighted and tumor/control (T/C) weight ratio calculated by dividing the median value of the tumor weight of the test tumors with respect to the control group and imaged by *ex vivo* BLI. Mice were monitored for metastatic growth after tumor excision to detect secondary metastases by *in vivo* bioluminescent imaging of the animals using the IVIS Spectrum. Experimental end-point was metastasis detection after which mice were euthanized and selected tissues analyzed by *ex vivo* BLI and then processed for histopathology.

7. Analyses of genetic alterations in human samples

The mRNA expression of several genes was analyzed from published datasets of different human primary prostate tumors (GSE46691, n=545; GSE29079, n=95) and breast tumors (GSE28844, n=61), and gene base survival analysis were performed using the R2 bioinformatics platform (http://r2.amc.nl). The most informative probeset, according to its average present signal (APS) and average value (Avg) was selected in every dataset and the details of probeset genome location was verified for each gene. Copy number alterations and mutational profile of a subset of genes in metastatic prostate tumors were analyzed using cBioPortal platform [236, 237]. Additional analyses of microarray data were carried out with GEO's DataSet Analysis Tool, GEO2R.

8. Statistics

Results are expressed as the average + standard deviation of the mean. IC_{50} values for docetaxel treatments were determined by non-linear regression. For statistical analysis, depending on whether data were sampled from a Gaussian distribution or not, the unpaired t-test or Mann-Whitney U test were used to compare two groups. For

multiple comparisons, ANOVA followed by the Dunnett method or the alternative non-parametric method (Kruskal-Wallis followed by Dunn method) were employed. To quantify the association between two quantitative variables, the Spearman correlation was used for statistical analysis. The Fisher's exact test was employed to determine whether a non-random association of co-occurrence between two categorical variables was significant. A p value ≤ 0.05 was taken as the level of significance. These analyses were performed using GraphPad Prism 5 software.

Chapter 5:

PTOV1 AS AN INDUCTOR OF THE EPITHELIAL-MESENCHYMAL TRANSITION AND A PROMOTER OF TUMORIGENESIS IN PROSTATE CANCER

Part of these results was included in this publication:

Regulation of protein translation and c-Jun expression by prostate tumor overexpressed . N. Marqués*, M. Sesé*, **V. Cánovas**, F. Valente, R. Bermudo, I. de Torres, Y. Fernández, I. Abasolo, P.L Fernández, H. Contrera, E. Castellón, T. Celià-Terrassa, R. Méndez, S. Ramón y Cajal, T.M. Thomson and R. Paciucci. Oncogene, 2014. **33**(9): p. 1124-34.*Equal contribution

***Puente de los Peligros**-Murcia (Literally, Brigde of Dangers)*

One of the most emblematic structures of Murcia the Puente de los Peligros, also known as Puente Viejo (Old Bridge), which has been one of main ways to cross the River Segura since it was completed in 1740 by Toribio Martínez. To build it, a part of the old Church of los Peligros was removed. Thus, as a reminder of the existence of the sacred place, the Virgen of Los Peligros was kept in its niche close to Brigde for centuries (right picture).

1. PTOV1 induces a partial epithelial-mesenchymal transition through the upregulation of c-Jun, snail1 and vimentin in prostate cancer cells

In prior studies of our group PTOV1 was shown to be associated with more advanced stages of several types of cancer [104] and promoted motility and invasive properties of prostate cancer cells [101]. Its overexpression activated the expression of the oncogene c-Jun at translation levels but not at mRNA levels. Given this association, we studied whether the increased motility and invasion induced by PTOV1 was mediated by an epithelial-mesenchymal transition (EMT) through c-Jun expression. Thus, we analyzed PC3 cells overexpressing PTOV1, Jun-HA or PTOV1 plus Tam67 (T), a truncated form of c-Jun that blocks its activity, for the expression of genes involved in EMT (**Figure 15A**).

The overexpression of PTOV1 or c-Jun caused a significant upregulation of Snail1, Vimentin , N-cadherin and Annexin A2 proteins (**Figure 15B**), well-characterized effectors of epithelial-mesenchymal transition and involved in migration and metastasis [64-66, 238]. However, no significant modulation of other EMT transcription factors such as Fibronectin, or the cell-cell adhesion protein E-cadherin, known target of Snail1 were observed in PC3 cells [66].Co-transfection with Tam67, abrogated Snail1, Vimentin and Annexin II upregulation observed by PTOV1 overexpression, indicating that PTOV1-promoted EMT requires c-Jun (**Figure 15A** and **B**).

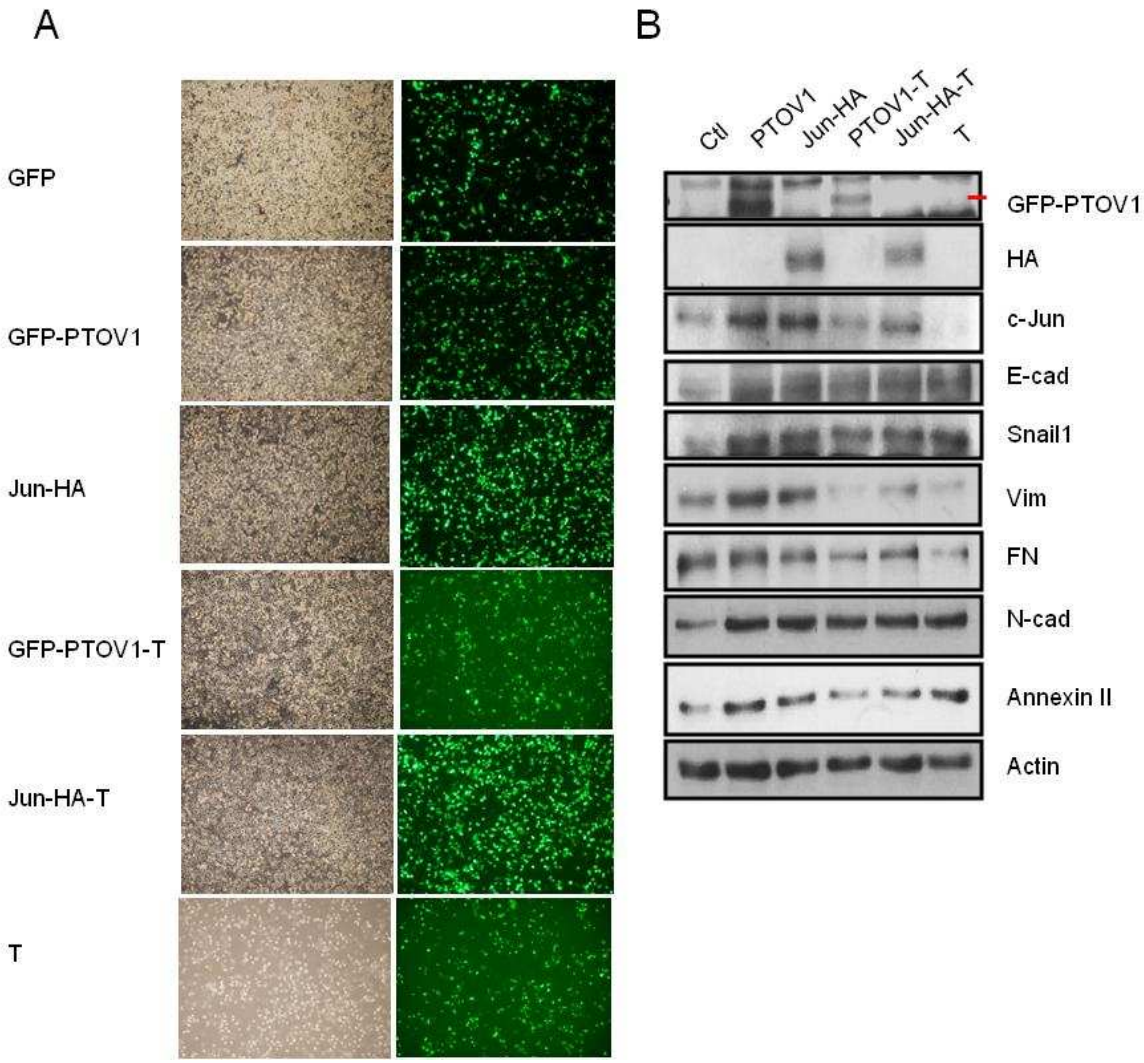

Figure 15. Expression of PTOV1 induce a partial epithelial-mesenchymal transition through the upregulation of c-Jun, Snail1 and Vimentin in PC3 cells. **(A)** Microscopic images of PC3 cells transfected with GFP-PTOV1, Jun-HA, GFP-PTOV1 plus Tam67 (PTOV1-T), Jun-HA plus Tam67 (Jun-HA-T) or Tam67 alone (T). Fluorescence microscope images were acquired at 4X with an inverted microscope (BX61, Olympus). **(B)** Cells transfected as in (a) were analyzed by Western blotting for expression of: c-Jun, E-Cadherin (E-cad), snail1, vimentin (Vim), fibronectin (FN), N-cadherin (N-Cad), c-Myc, Annexin II and β-catenin (β-cat). Actin signal was used to monitor protein loading.

In epithelial non transformed MDCK cells the overexpression of PTOV1 or Jun-HA provoked similar increased levels of Snail1 and Vimentin (**Figure 16A** and **B**), effects that were abrogated by Tam67 mutant. As observed in PC3 cells, no significant modulation of E-cadherin or fibronectin was observed in MDCK cells (**Figure 16B**). These data suggest that PTOV1 induces a partial epithelial-mesenchymal transition through the upregulation of c-Jun.

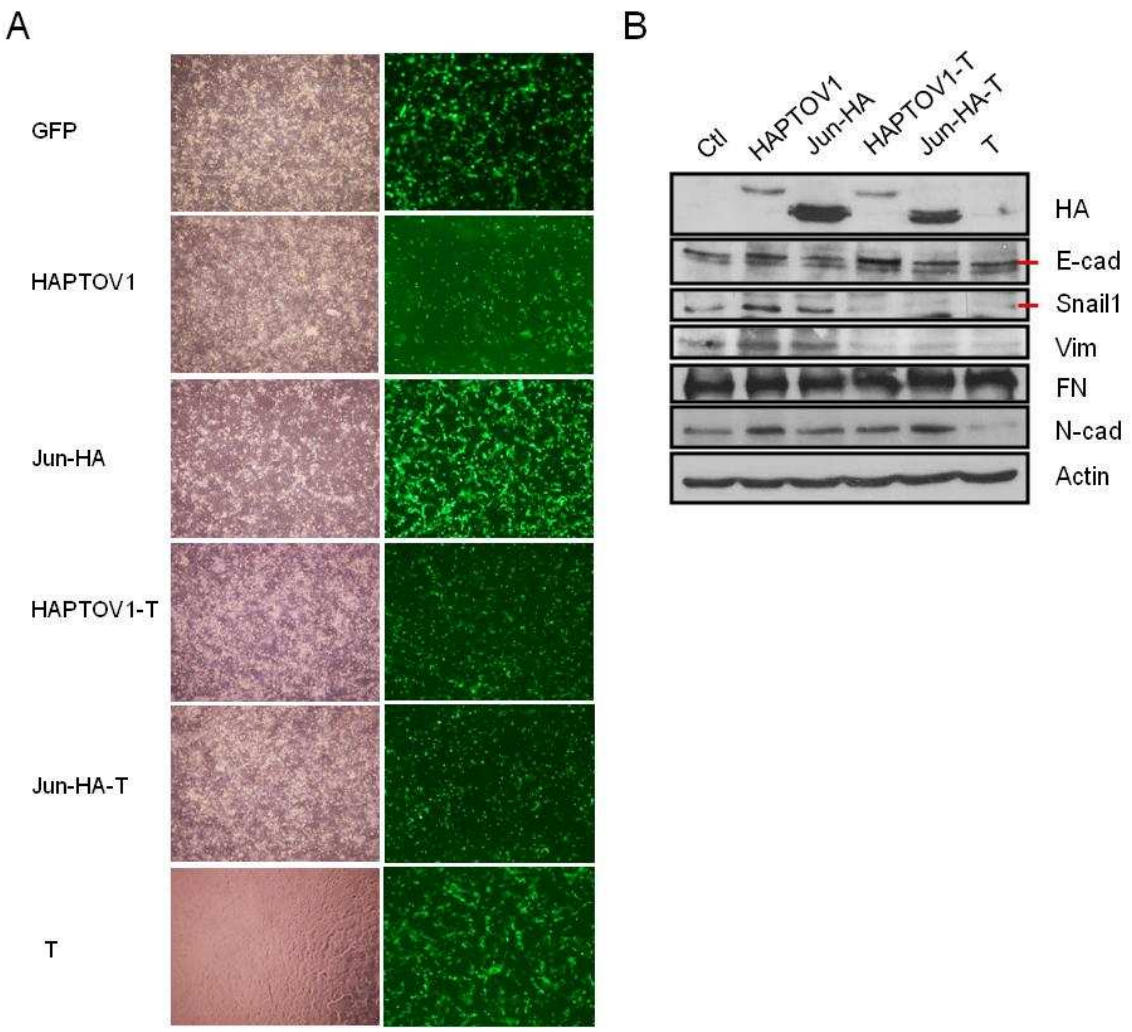

Figure 16. Transfection of PTOV1 or Jun-HA induces an upregulation of Snail1 and Vimentin in MDCK cells. **(A)** Microscopic images of MDCK cells transfected with GFP-PTOV1, Jun-HA, GFP-PTOV1 plus Tam67 (PTOV1-T), Jun-HA plus Tam67 (Jun-HA-T) or Tam67 alone (T). Fluorescence microscope images were acquired at 4X with an inverted microscope (BX61, Olympus) **(B)** MDCK cells transfected as in (a) were analyzed by Western blotting for expression of: E-Cadherin (E-cad), Snail1, vimentin (Vim), fibronectin (FN), N-cadherin (N-Cad). Actin signal was used to monitor protein loading.

To further explore whether PTOV1 was required for transcriptional activity of c-Jun, PC3 cells knockdown for PTOV1 were transfected with the c-Jun responsive *collagenase* promoter or a construct bearing AP1 *response elements* (TRE). We observed a significant decrease in the transcriptional activity of those promoters upon PTOV1 inhibition (**Figure 17**), suggesting that the full transcriptional activity of c-Jun requires the presence of PTOV1.

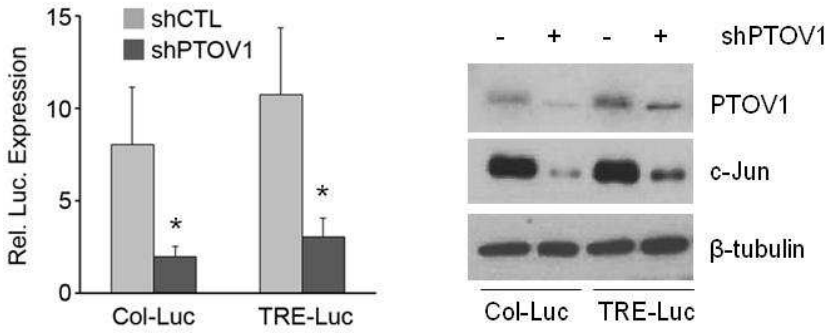

Figure 17. PTOV1 is required for the transcriptional activity of c-Jun. PC-3 cells, cells knocked down for PTOV1 by shRNA or control cells were transfected with the plasmids HA-Jun and CMV-Renilla and either *collagenase*-Luc or AP1 *response element* (*TRE*)-Luc. Forty-eight hours after transfection, transactivation levels (left-panel) were determined as Firefly luciferase activity normalized to Renilla luciferase activity and are indicated as Relative Luciferase expression and (right panel) c-Jun and PTOV1 levels were analyzed by Western blotting.

2. PTOV1 expression correlates with tumor aggressiveness and vimentin expression in primary human prostate tumors

In orden to study the EMT signature in prostate tumors, we analyzed published datasets containing information from PCa tissues (n=545) derived from primary prostatectomies of naïve untreated patients. Patients with a higher Gleason score (GS) have significantly higher levels of *PTOV1* compared to patients with GS≤6 (**Figure 18A**). Regarding transcriptions factors inductors of EMT, no significant differences were found in *JUN*, *SNAI1*, *CDH1*, *TWIST1* or *CDH2* expression in this database (data not shown). However, a significant increase in *vimentin* (VIM) levels was observed in patients with higher GS (**Figure 18A**). Furthermore, *PTOV1* and *VIM* levels are significantly higher in tumors of patients that after radical prostatectomy developed regional or distal metastasis (**Figure 18B**). In addition, a statistically significant correlation (r: 0.63; p<0.0001) exists between the expression of *PTOV1* and *VIM* in tumor samples (**Figure 18C**).

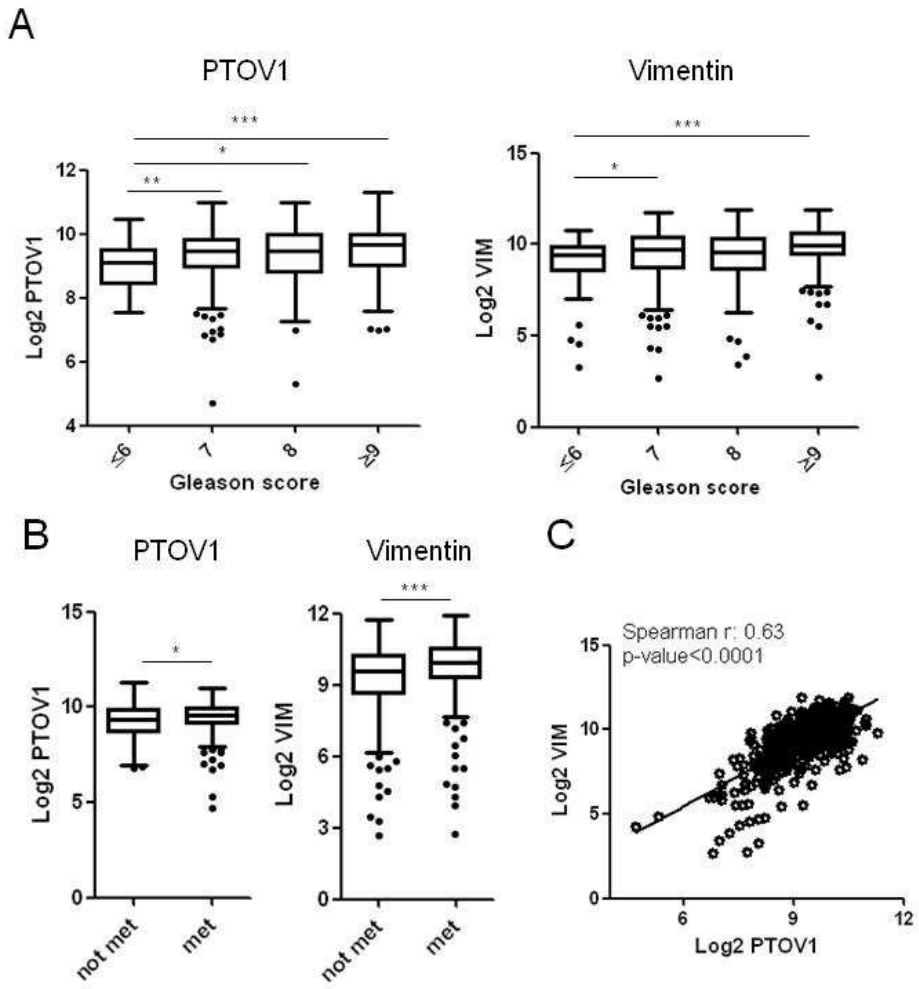

Figure 18. Higher *PTOV1* and *Vimentin* levels correlate with aggressiveness in prostate tumors. **(A)** Box and whisker plots representing *PTOV1* and *Vimentin* expression in tumors with different Gleason obtained from published prostate cancer gene expression profiles (GSE46691; Gleason score (GS) ≤6, n= 63; GS 7, n=271; GS 8, n=68; GS ≥9, n=143). **(B)** Box and whisker plots representing *PTOV1* and *VIM* expression in tumors of patients that did not develop metastasis after radical prostatectomy (not met, n=333) compared to patients that did developed metastasis (met, n=212) (GSE46691).**(C)** Significant statistical correlation between the expression of *PTOV1* and *VIM* in tumors analyzed in (a). p-value: *< 0.05; **< 0.01; *** < 0.005.

PTOV1 expression was previously found to correlate with prostate cancer progression showing faint staining in benign peripheral zone (BPZ) and an increasing intensity from no metastatic primary tumors to metastatic primary tumors and the corresponding matched lymph node metastatic lesions (**Figure 19**) [100, 101].

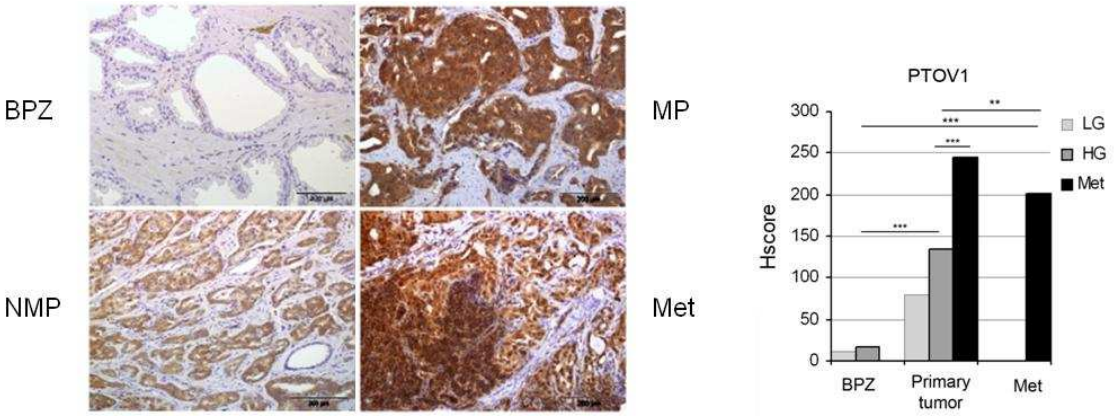

Figure 19. PTOV1 expression correlates with prostate cancer progression. No metastatic prostate adenocarcinomas (NMP), metastatic primary tumors (MP) and lymph node metastasis (Met) were analyzed with antibodies to PTOV1. Expression levels were semiquantitatively analyzed by the Hscore method. For comparison, the expression in the benign peripheral prostate associated to tumors (BPZ) was studied. Adapted from Marqués, Sesé *et al.* 2014 [101].

The expression status of PTOV1 in metastatic tumor specimens from a wide range of metastatic sites including bone, liver, brain, lymph node or lungs, was also analyzed using available datasets from cBioPortal [236, 237]. Metastatic samples were derived from individuals with castration resistant tumors. The transcript levels of PTOV1 are strikingly upregulated in 94% of metastatic samples (**Figure 20A**). At DNA levels PTOV1 is amplified in 19% of metastatic specimens, whereas only 0.3% of primary adenocarcinomas show PTOV1 amplification (**Figure 20B**). Most alterations in metastatic specimens cover the complete amplification of the gene, and include also the amplification of neighboring genes *MED25* and *AKT1S1* (**Figure 20C**). Of those metastatic samples with mRNA data (n=49), 69.4% of samples present elevated levels of both PTOV1 and VIM, although analysis of co-ocurrence alteration does not reach statistical significancy (**Figure 20D**). All together, these data support a role of PTOV1 as a promoter of a partial EMT state and suggest the expression of *PTOV1* is associated to the metastatic phenotype in prostate cancer.

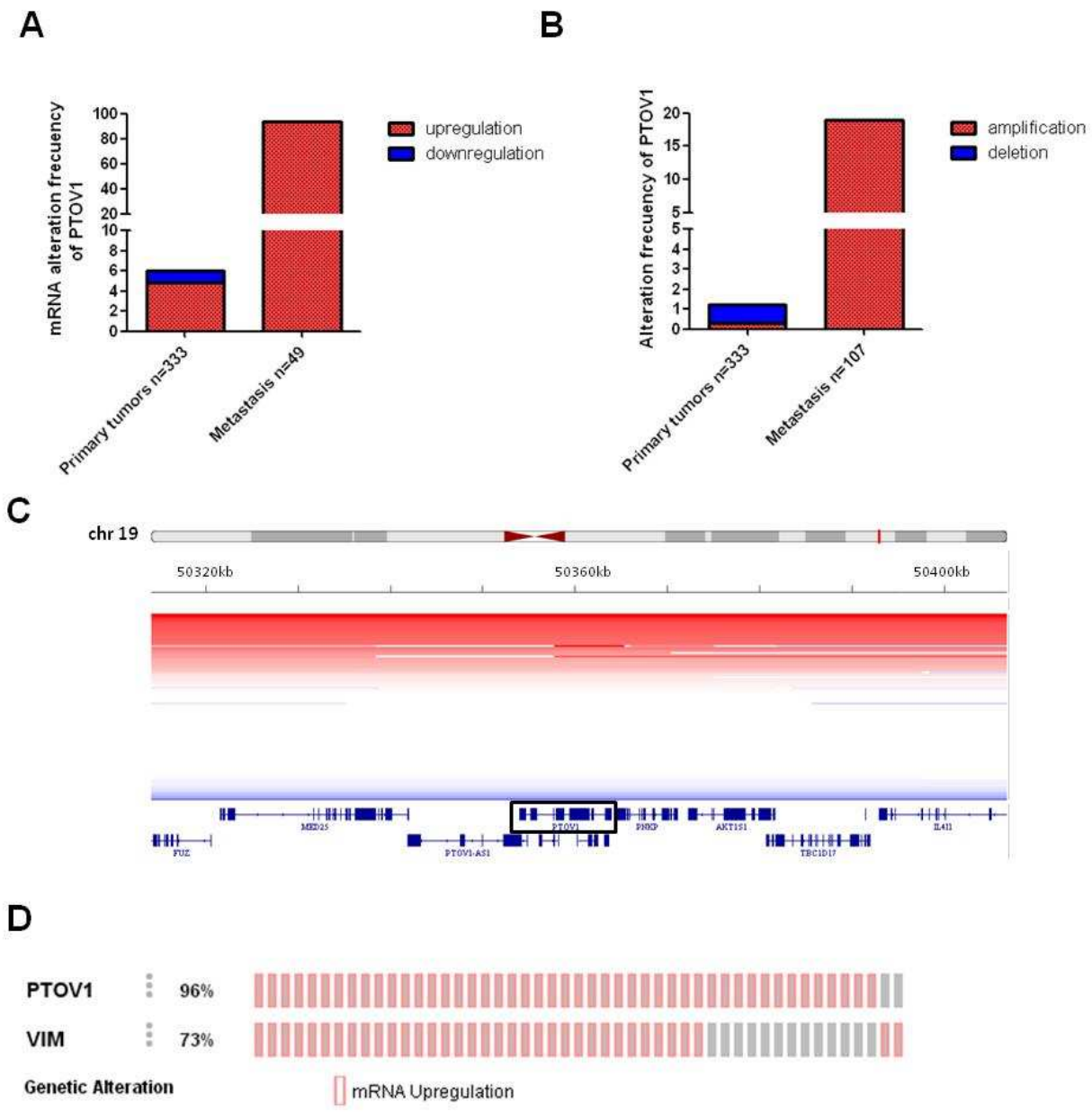

Figure 20. PTOV1 is amplified and overexpressed in metastatic prostate cancer. **(A)** mRNA alteration frecuency of PTOV1 (z-score threshold ±1.8) in primary [239] and metastatic tumors [240]. **(B)** DNA alteration frequency (amplifications and deletions) of PTOV1 in primary tumors and metastatic tumors. **(C)** Copy number status of PTOV1 locus. Color intensity and location are indicative of level and focality of amplification. **(D)** mRNA alteration frecuency of PTOV1 and VIM (z-score threshold ±2.0) in metastatic tumors [240].

3. PTOV1 expression correlates with poor prognosis and high risk of relapse in different tumor types

Our group previously described the overexpression of PTOV1 in tumor types including colon, breast, kidney, bladder and cerebral gliomas, and its association with high-malignant tumors [104]. In order to know whether PTOV1 expression in tumors correlates with overall survival and risk of relapse, we analyzed different genomic microarray database containing patients survival data. No available data from survival was obtained for prostate cancer. However, **Figure 21** shows that high expression of PTOV1 significantly correlates with lower overall survival in pancreas, lung and neuroblastoma tumors. In addition, we observed that high levels of PTOV1 are associated to low relapse-free survival probability in colon and breast tumors (**Figure 21**), suggesting that PTOV1 overexpression may be indicative of risk for relapse.

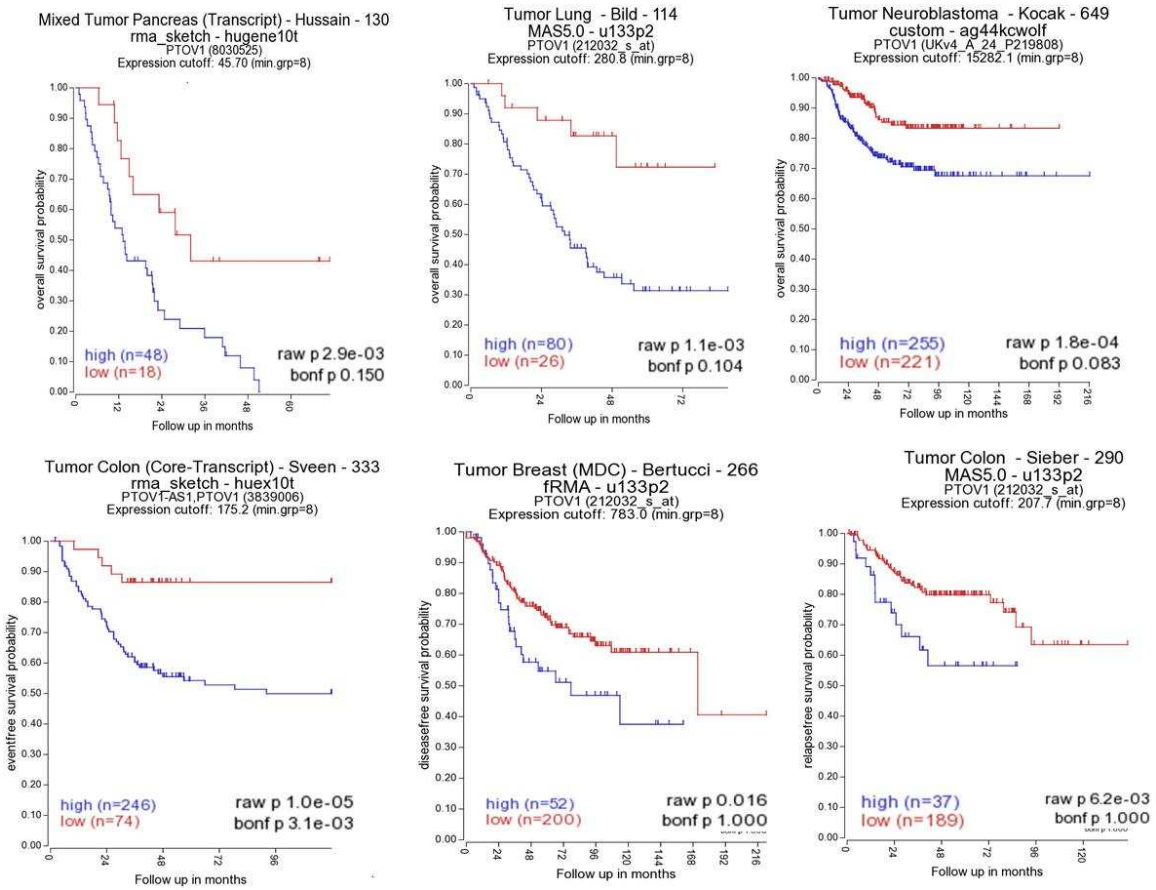

Figure 21. PTOV1 expression correlates with poor overall survival in different types of cancer. Public datasets (GSE62452; GSE3141; GSE45547; GSE24551; GSE21653; GSE14333) containing information of survival rates in patients with different types of cancer were analyzed using R2 platform (http://r2.amc.nl).

4. PTOV1 is required for tumorigenesis and metastasis of PC3 prostate cancer cells

To determine the relevance of PTOV1 in tumorigenesis and prostate cancer progression, we obtained a Tet-On inducible system to silence PTOV1. Due to the inhibitory effects of doxycycline in prostate cancer cells proliferation and c-Jun expression, we did not use this inducible system to knockdown PTOV1 (see Chapter 6). Therefore, PC3-Fluc cells were stably knocked down for PTOV1 by shRNA (sh1397) and inoculated subcutaneously in SCID-beige mice (**Figure 22A**). As illustrated in **Figure 22B** and **C**, the knockdown of PTOV1 significantly inhibited tumor growth compared to control cells.

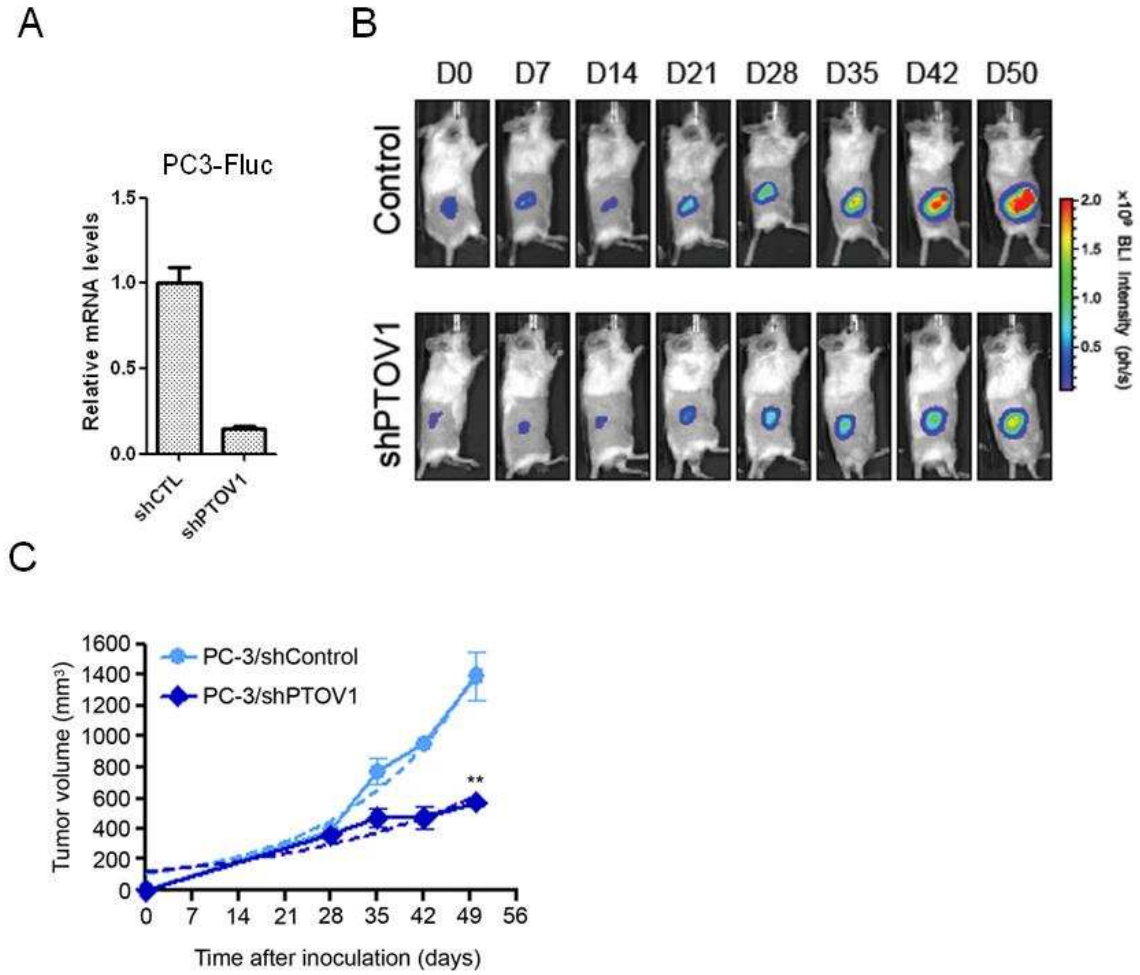

Figure 22. Knockdown of PTOV1 in prostate cancer cells inhibits tumor growth in immunodeficient mice. **(A)** The expression of PTOV1 by qRT-PCR in PC3 cells knocked by a shRNA sequence (sh1397) and a control shRNA (shCTL). (**B**) PC-3 cells (3×10^3) knocked down for PTOV1 (n = 4) or control cells (n = 6) were implanted subcutaneously into the right flank of SCID-beige male mice. **(C)** Graph shows the growth curves of implanted tumors, monitored by a caliper twice a week. Mean values + SEM are displayed.

Statistically significant differences in the growth of knockdown vs. control cells were observed (** $p < 0.005$).

These differences were clearly reflected based on the post-excision treated/control (T/C) weight ratio, which was 16% for tumors grown from shPTOV1 cells, significantly lower ($p = 0.0095$) than control (**Figure 23A** and **B**). PC3 shPTOV1 cells disseminated to distant sites (axillary lymph nodes and lungs) with a significant delay ($p = 0.001$) as compared to control cells (**Figure 23C**).

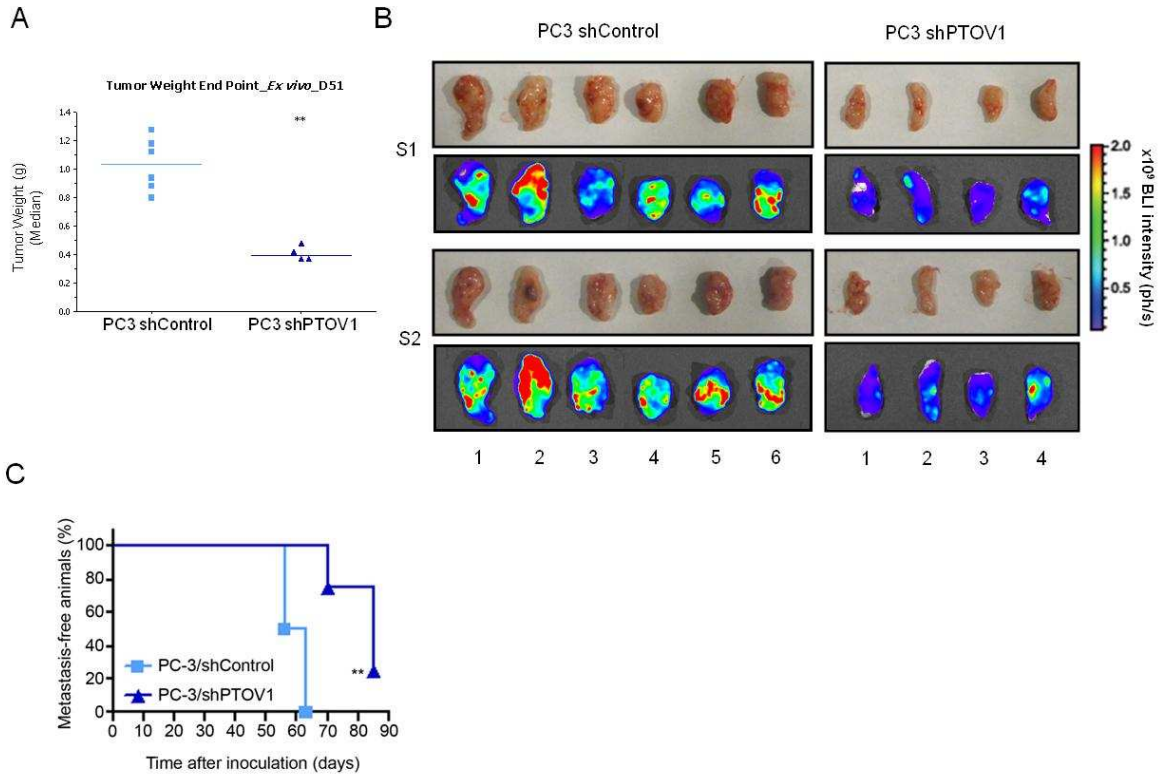

Figure 23. Knockdown of PTOV1 in prostate cancer cells metastasizes at later times than control cells. **(A)** Graph shows the tumor weight at end point (day 51) of implanted tumors. **(B)** Photograph of tumor bioluminiscence after tumor excision (day 51). **(C)** Kaplain-Maier representation of metastasis-free animals after tumor excision as monitored by *in vivo* bioluminescent imaging. Metastases formed by PC-3/shPTOV1-tumors appeared at significantly later time compared to control cells (** $p = 0.001$).

Although the appearance of metastasis in the shPTOV1 tumors was significantly delayed compared to shCTL tumors, similar sites of distant metastatic growth were observed such as in diaphragm, salivary glands and lungs (**Figure 24**). These results provide evidence that PTOV1 is required for the full tumorigenic and metastatic capacities of PC3 cancer cells *in vivo*.

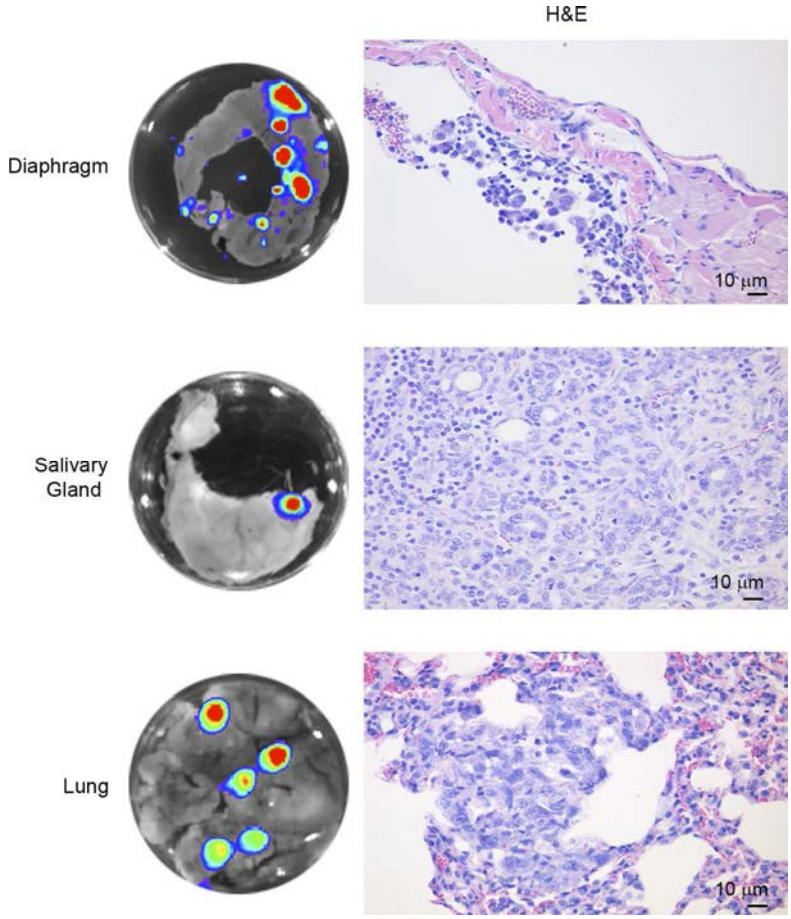

Figure 24. Tumors formed by shCTL and shPTOV1 PC3 cells metastasize at distant organs. Mice were subcutaneously injected with shCTL or shPTOV1 PC3 cells (3 x 10^6). After reaching 1.5 cm in diameter, tumors were excised and mice further maintained and screened for metastatic dissemination by *in vivo* bioluminescent imaging. Bioluminiscent images of the explanted organs reveal the presence of metastatic cells, confirmed by hematoxylin and eosin staining (H&E).

Figure 25 shows that tumors developed from shPTOV1 cells have a marked reduction in PTOV1 protein levels as well as a strong decrease in the levels of total and active c-Jun, as compared to control tumors. These results provide evidence that PTOV1 and c-Jun are required for the full tumorigenic and metastatic capacities of PC3 cancer cells *in vivo*.

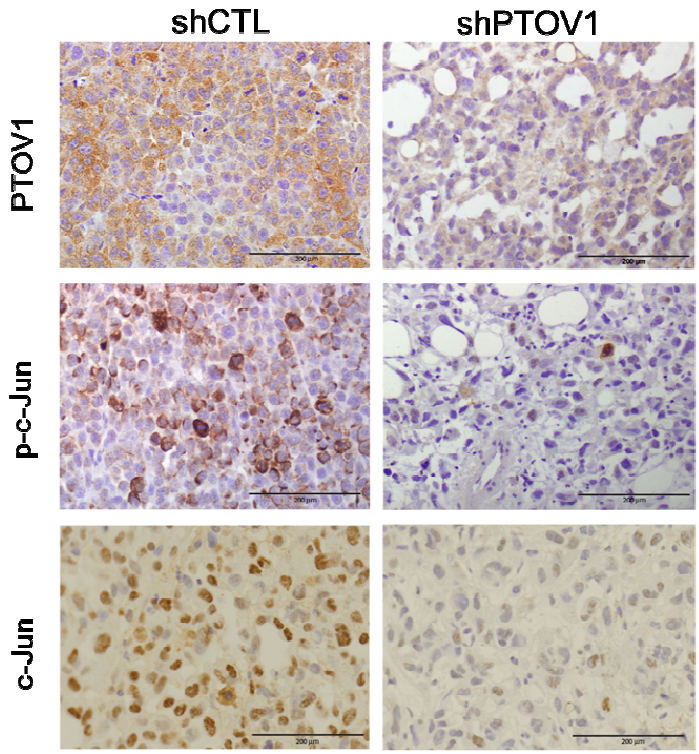

Figure 25. Immunohistochemistry of explanted tumors. A strongly decreased expression of PTOV1, total c-Jun and phosphorylated c-Jun is detected in tumors formed by shPTOV1 cells vs shCTL derived tumors. Size bar: 200 µm

5. PTOV1 expression in normal tissues

Most functions of PTOV1 have been surmised in pathological conditions, such as cancerous cells and tissues [72, 100, 101, 133, 150]. However, its expression has also been detected in normal tissues at low levels (human brain, heart, skeletal muscle, kidney, liver, ovary, aorta and salivary gland), although little has been described about its function at those sites [73, 87, 95, 96]. In order to know the expression levels of PTOV1 in other normal tissues, we analyzed an extensive number of samples (n=2,921) from different normal tissues using published database generated by the Genotype-Tissue Expression (GTEx) project using *R2: Genomics Analysis and Visualization Platform.* We observed a diverse range of PTOV1 expression among different tissues (**Figure 26**), with high PTOV1 expression in several brain tissues (pituitary, cerebellar hemisphere, and cerebellum), adrenal glands, ovary, prostate and testis.

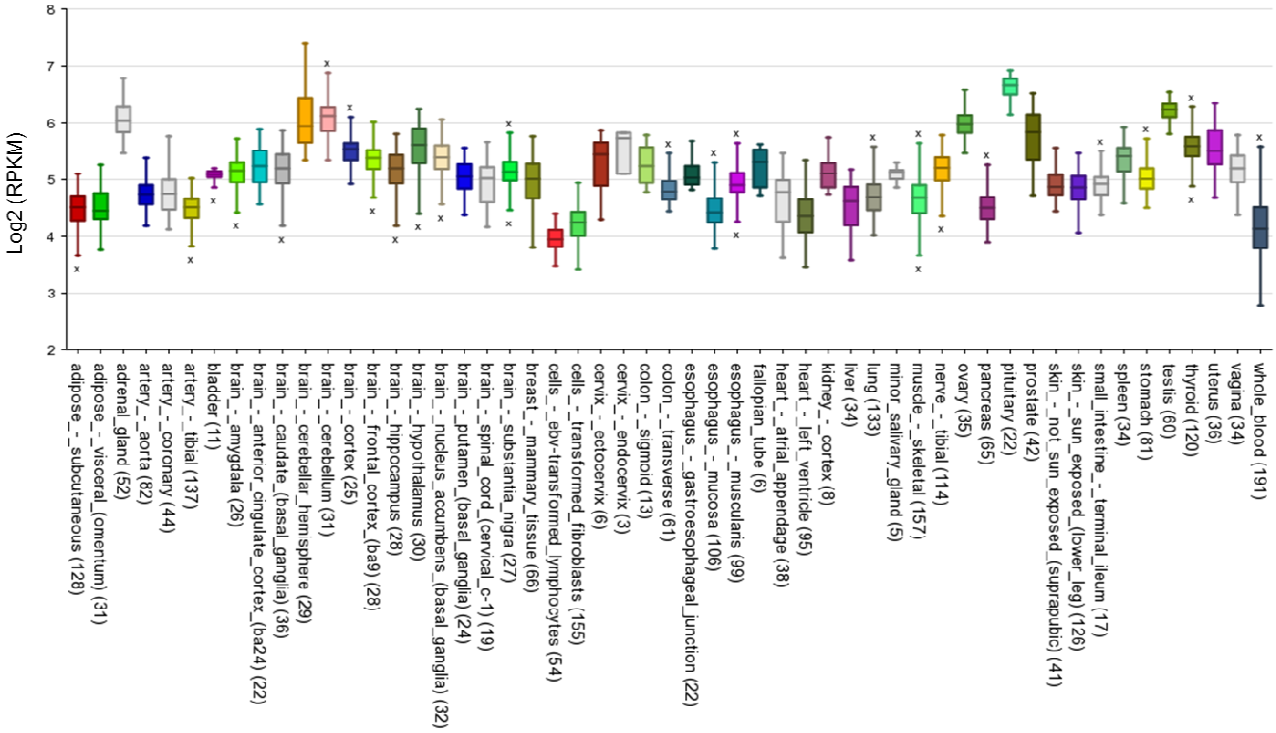

Figure 26. mRNA PTOV1 expression in normal tissues.

To study the function of PTOV1 in non-tumorigenic prostate cells, we knockdown its expression in RWPE-1 cells, derived from the peripheral zone of a histologically normal human prostate immortalized by human papilloma virus 18 (HPV-18) encoding the oncogenic E7 proteins. Downregulation of PTOV1 in these cells inhibits cell proliferation and colony formation capacities (**Figure 27 A, B** and **C**). These data suggest that PTOV1 is required for the function of non-tumorigenic prostatic cells.

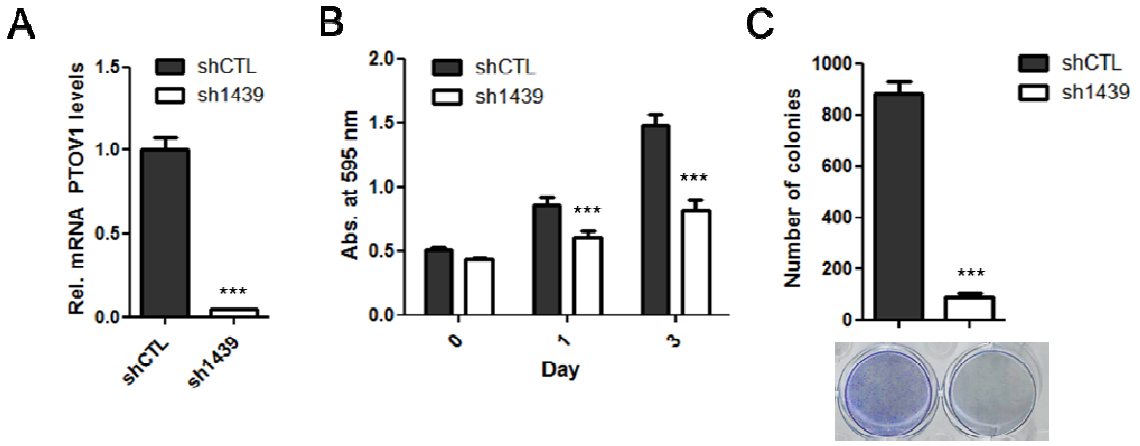

Figure 27. Knockdown of PTOV1 decreases cell proliferation and colony formation abilities in non-tumorigenic prostate cells. **(A)** The expression of PTOV1 by qRT-PCR in RWPE1 cells knocked by a shRNA sequence (sh1439) and a control shRNA (shCTL). **(B)** Histogram representing the proliferation of

RPWE1 cells knockdown for PTOV1 as in (a). Proliferating cells were determined by crystal violet staining and absorbance at 595 nm after 96h from lentiviral transduction. **(C)** Colony formation abilities by RWPE1 cells knockdown for PTOV1 as in (a).

6. Discussion

The epithelial-mesenchymal transition process is required for normal embryonic development, and it has also been described in several pathological conditions, including fibrosis and cancer. During this process epithelial cells lose cell-to-cell adhesion structures and polarity and develop features of mesenchymal cells with higher motility and invasiveness [241]. Master regulators of the process include the EMT-inducing transcriptions factors Snail, Slug, Twist, Zeb1/2 and Vimentin [64, 242]. The activation of different combinations of these transcription factors confers migratory and invasive capacity to carcinoma cells. The acquisition of mesenchymal cell traits by epithelial carcinoma cells is associated with carcinogenesis, invasion, metastasis and an increased risk of cancer recurrence among patients with different solid tumor types [242-244].

We have shown that overexpression of PTOV1 in prostate cancer PC3 and non-neoplastic MDCK cells induces the expression of Snail1 and Vimentin, well known effectors of the EMT [245, 246] through the upregulation of c-Jun, a member of AP1 transcription factors. Additionally, increased expression of Annexin A2, a key regulator of the EGF-induced EMT and migration was observed in PC3 cells upon PTOV1 overexpression [238, 247]. c-Jun, but not PTOV1, was shown to bind to the *SNAI1* promoter inducing motility and invasion of prostate cancer cells [101]. These results are supported by concomitant studies from other groups that show TGFβ-TRAF6 upregulation and activation of c-Jun and its binding to the *SNAI1* promoter [248]. In addition, we showed that in prostate tumor samples the expression of PTOV1 positively correlates with *vimentin* levels and high tumor grade. Vimentin, an intermediate filament, is overexpressed in several tumor types and its expression correlates with cancer progression, invasion and poor prognosis [249]. Very recently, cell-surface Vimentin has been validated as a marker for detecting mesenchymal circulating tumor cells (CTCs) from sarcoma, breast and colon cancer [250]. A significant higher number of CTCs were isolated in castration resistant prostate cancer patients compared to hormone sensitive ones based on detection of cell-surface vimentin [250].

The EMT program can be manifested in cells as a plastic program in various degrees, leading to the term "partial-EMT" state, where epithelial features can be retained alongside with the acquisition of mesenchymal ones [64]. AP1 transcription complexes are known to enhance migration and invasiveness [223], even with limited downregulation of cell-to-cell adhesion molecules such as E-cadherin [251]. This is relevant to our previous observations that increased invasiveness of prostate epithelial cells induced by PTOV1 or c-Jun overexpression [101] occurs without significant effects on E-cadherin. The concept of "partial-EMT" may present a metastatic advantage, in which mesenchymal features are initially acquired to enable migration from the primary tumour site, survival in the circulation and arrival at a secondary site, and at the same time, this mixed epithelial/mesenchymal state may be essential for metastatic colonization [64]. Accordingly, disseminated carcinoma cells with loss of all epithelial traits and phenotypic plasticity, have been found to be ineffective in seeding metastatic colonies [252, 253].

Interaction of PTOV1 with some proteins as described in the Introduction, may contribute to promote its motility and invasion properties [100, 101]. For instance, we described PTOV1 interaction with RACK1 [101], a scaffold protein found in the 40S ribosomal subunit [165, 254]. After growth factor stimulation, PTOV1, RACK1, and ribosomal protein S6 (RPS6) co-localized at membrane ruffles suggesting that the protein synthesis machinery is recruited to membranes structures, presumably to facilitate the local synthesis of proteins involved in migration and invasion [101, 255, 256]. In addition, the interaction with cytoplasmic HDAC6 [141], a deacetylase that regulates microtubule stability, chemotaxis and cell migration [142, 143, 257], may contribute in promoting the pro-oncogenic role of PTOV1: by interacting with HDAC6, PTOV1 might more directly act on the cytoskeleton and cell motility. Reported interactions of PTOV1 with other cytoskeletal proteins such as actin filament associated protein 1 like 1 (AFAP1L1), Spectrin1 or Dematin [258], proteins that bundles actin filaments and are involved in the organization of intracellular organelles and cell morphology may contribute to PTOV1 increased cell motility and invasion, as reported in other tumors [259-262]. However, further investigation is required to ascertain the contribution of these proteins to the oncogenic capacities of PTOV1.

We showed that PTOV1 is required for optimal tumorigenesis and metastatic spread of prostate cancer cells *in vivo*. The JNK/c-Jun pathway has been widely reported to promote cancer progression [263]. Analyses of explanted tumors formed by prostate cancer cells knockdown for PTOV1 revealed low PTOV1 and c-Jun expression levels supporting the important role of both proteins in tumorigenesis. Furthermore, recently Cui *et al*. [133] demonstrated that PTOV1 overexpression enhances the tumorigenic potential of breast cancer cells *in vivo*. In contrast, the knockdown of PTOV1 dramatically inhibited the tumor-initiating ability of breast cancer cells. These data suggest that PTOV1 is important for tumorigenesis in different types of cancer. In human prostate tumors, the expression levels of PTOV1 and phosphorylated c-Jun compared to non-metastatic adenocarcinomas, were significantly correlated and increased in metastatic tumors and lymph node metastases. [101]. Similar findings reported elevated JNK activity and overexpression of c-Jun in correlation with unfavorable clinical outcome in other types of tumors including prostate cancer [264-266].

Little is known about the function of PTOV1 protein in normal tissues. The analysis of PTOV1 expression in normal tissues using published database revealed a variable expression between tissues. Among tissues expressing higher mRNA PTOV1 levels we can clearly distinguish two main subsets: i) nervous tissues such as pituitary, cerebellum and cerebellar hemisphere and ii) testosterone producer organs such as testis, adrenal gland, prostate and ovaries. According to these results, it has been previously reported in normal prostate epithelium that few sporadic luminal cells in isolated glands display intense PTOV1 staining, mostly cytoplasmic. These PTOV1-positive cells also stain for chromogranin A, suggesting their neuroendocrine origin [72] (**Figure 28**). The promoter region of PTOV1 contains a putative Androgen Responder Element (ARE) and PTOV1 expression has been shown to be androgen-responsive [73, 87]. In spite of most of testosterone being synthetized in testis, other organs can also contribute to its levels such as adrenal glands and ovaries [267]. Thus, the higher expression of PTOV1 in these organs can be the result of a regulation by androgens.

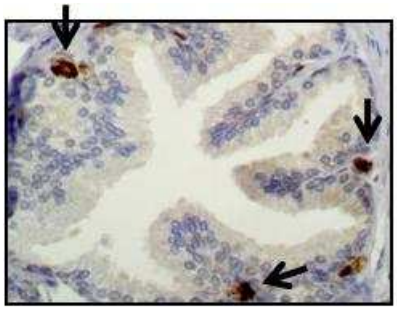

Figure 28. PTOV1 expression in neuroendocrine cells of prostatic normal glands.

PTOV1 was firstly identified as overexpressed in prostate tumors by our group [73]. More recently, numerous reports have described its overexpression in different types of tumors such as breast, pancreas, liver, colon, kidney, bladder, laryngeal, cerebral gliomas and ovary [96, 99, 102-105, 268]. The association between its overexpression and high grade of malignancy correlated with the clinic-pathological characteristics and tumor aggressiveness of primary hepatocellular carcinoma, ovarian cancer, breast cancer, and clear cell renal carcinomas [70, 96, 102, 103, 105]. In breast cancer, 99.4% of the cancer samples analyzed expressed PTOV1, of which 49.1% showed high expression. In esophageal squamous cell carcinoma (ESCC) high PTOV1 expression was found to increase with progressing clinical stage, and the IHC staining score was higher in the lesions associated to lymph node metastasis [269]. As part of the work of this thesis, we demonstrated that high PTOV1 expression is associated with poor overall survival and poor relapse-free survival in different tumors including breast, colon, pancreas and glioblastoma. Accordingly, Lei *et al.* 2014 [102], reported that the median survival of breast cancer patients with high PTOV1 levels was 78 months *versus* 115 months in patients with low PTOV1 expression. In laryngeal squamous cell carcinoma and ESCC, PTOV1 expression correlates with advanced clinical stage and it was an independent predictor of overall survival and progression-free survival [269, 270]. In ESCC, patients with high PTOV1 expression were ~6.3 times likelier to die of ESCC than patients with low PTOV1 expression, with a median survival time of 33 months vs 60 months [269]. Similarly, the disease free survival (DFS) in high PTOV1 expression patients was shorter than in ESCC patients with low PTOV1 expression (43 months vs >60 months). The human papillomavirus (HPV) -positive head and neck cancers show better prognosis than HPV-negative cancers [271, 272]. In this context, the levels of expression of PTOV1 in combination with the infection status with HPV could predict outcome in early-stage

laryngeal squamous cell carcinoma [270]. Patients' subgroup with HPV-positive/PTOV1-negative was associated to a better outcome, in contrast to the HPV-negative/PTOV1-positive subgroup that showed the worst outcome. Altogether, data point to a pro-oncogenic role of PTOV1 in different tumors and indicate that it is a candidate gene for patient prognosis.

Chapter 6:

DOXYCYCLINE INHIBITS C-JUN EXPRESSION AND DECREASES PROSTATE CANCER CELL VIABILITY

El Cristo de Monteagudo- Monteagudo (Murcia)

We are not in Rio of Janeiro. The name of Monteagudo is given by the existence of the mountain that rises majestically dominating the whole valley. Given its strategic location Monteagudo's head was occupied from very early times as evidenced by the remains of an argaric necropolis (1700-1200 BC), as well as prehistoric Bronze Age utensils. Upon Muslims arrival, the place acquired great importance and became one of the sets of fortresses constituting a defensive line to protect Murcia and the different roads connecting Murcia with Orihuela….. We can not fail to mention a singular construction that from the beginning of this Century characterizes this district: the image of the Sacred Heart of Jesus…..”

1. Establishment of an inducible lentiviral shRNA to knockdown PTOV1.

To determine the relevance of PTOV1 in tumorigenesis and prostate cancer progression, we obtained a Tet-On inducible system to silence PTOV1. Du145 prostate cancer cells were transduced with three different inducible lentiviral short hairpin RNA (shRNA) vectors (sh6191, sh6196 and sh4353) to knockdown PTOV1 expression. Cells were treated for 48 h with doxycycline 1 µg/mL (Dox) or with vehicle (control). The transduction efficiency was high for the three lentiviral vectors, as it is shown by the expression of the RFP reporter (**Figure 29A**). Nevertheless, analysis of the mRNA levels of PTOV1 revealed that only one shRNA vector (sh6191) significantly decreases the expression of the gene (**Figure 29B**). Surprisingly, doxycycline treatment significantly decreased the expression of *JUN* and this effect was regardless the levels of expression of PTOV1 (**Figure 29C**).

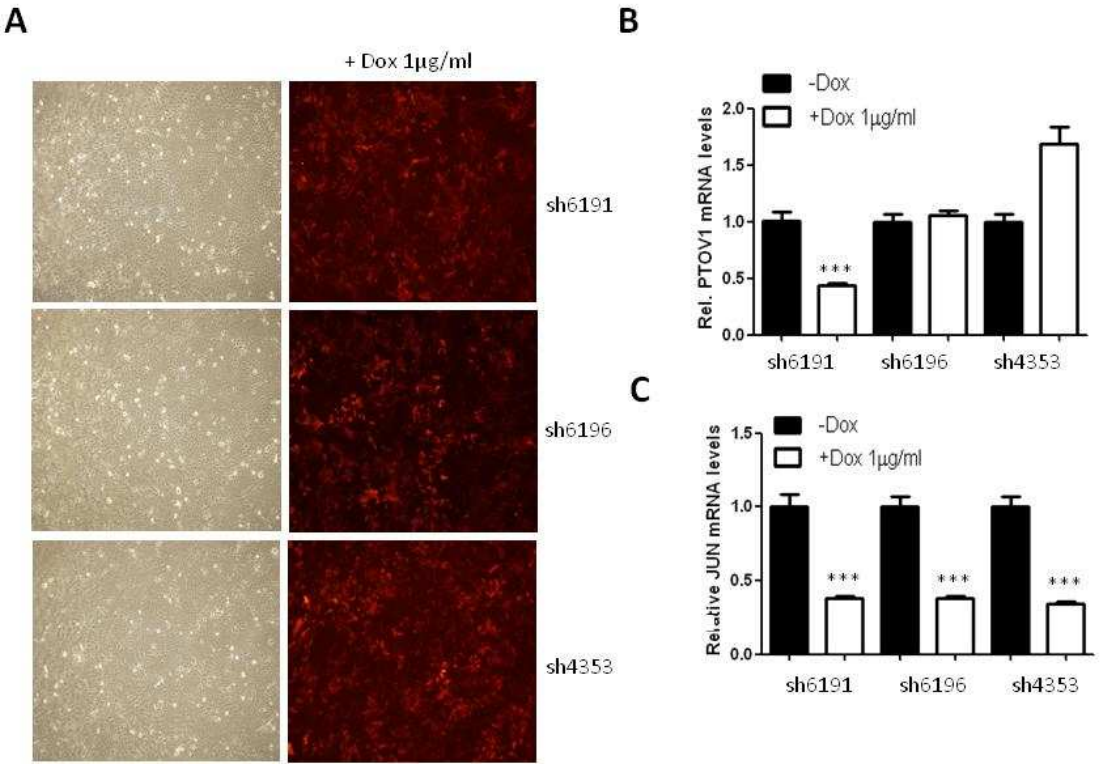

Figure 29. Doxycycline transcriptionally represses c-Jun expression in Du145 prostate cells. **(A)** Microscopic images of Du145 cells transduced with three inducible lentiviral shRNA silencing PTOV1 expression (sh4353, sh6191 and sh6196) and treated with doxycycline. Fluorescence microscope images were acquired with an inverted microscope (BX61, Olympus). Relative *PTOV1* mRNA levels **(B)** and *JUN* mRNA levels **(C)** by qRT-PCR of cells transduced as in (a).

2. Doxycycline decreases JNK1 phosphorylation and inhibits the expression of JUN.

To confirm that doxycycline treatment affects the expression of the oncogene *JUN* independently of the lentiviral transduction, Du145 and PC3 prostate cancer cells were treated with doxycycline for 24 h with a dose commonly used in inducible lentiviral systems (1 µg/ml) and checked the expression of c-Jun at protein and mRNA levels. **Figure 30A** and **B** show a striking significant decrease in c-Jun expression after 24 h of cell exposure to the drug. To determine whether doxycycline affects c-Jun expression at early times, we performed a time-course assay treating Du145 and PC3 cells with doxycycline for different lengths of time. A significant inhibition of c-Jun expression is detected in both cell lines (**Figure 30C and D**). While Du145 cells showed an initial increase in c-Jun protein and mRNA levels at short time treatments (0.5-1 h) and a statistically significant decrease after exposure to doxycycline for longer times (**Figure 30C** and **D**), PC3 cells showed significant decrease of protein and RNA levels starting at 0.5 h. However, because tetracyclines were described to decrease the phosphorylation and activity of the c-Jun N-terminal Kinase 1(JNK1) in corneal epithelial cells [273], we explored the effects of doxycycline on this signaling pathway upstream to c-Jun. **Figure 30C** shows that phosphorylated JNK1 but not total JNK1 expression was significantly inhibited by doxycycline exposure. To explore whether doxyxycline treatment also affects JNK signaling in additional cancer cells, breast cancer cells (BT-549) and metastatic pharyngeal cancer cells (CCL-138) were treated with increasing doses of doxycycline (**Figure 30E**). Doxycycline strongly repressed c-Jun expression in breast and pharyngeal cancer cells. These data suggest that doxycycline decreases JNK1 phosphorylation and activity and inhibits the expression of the downstream transcription factor c-Jun in cancer cells.

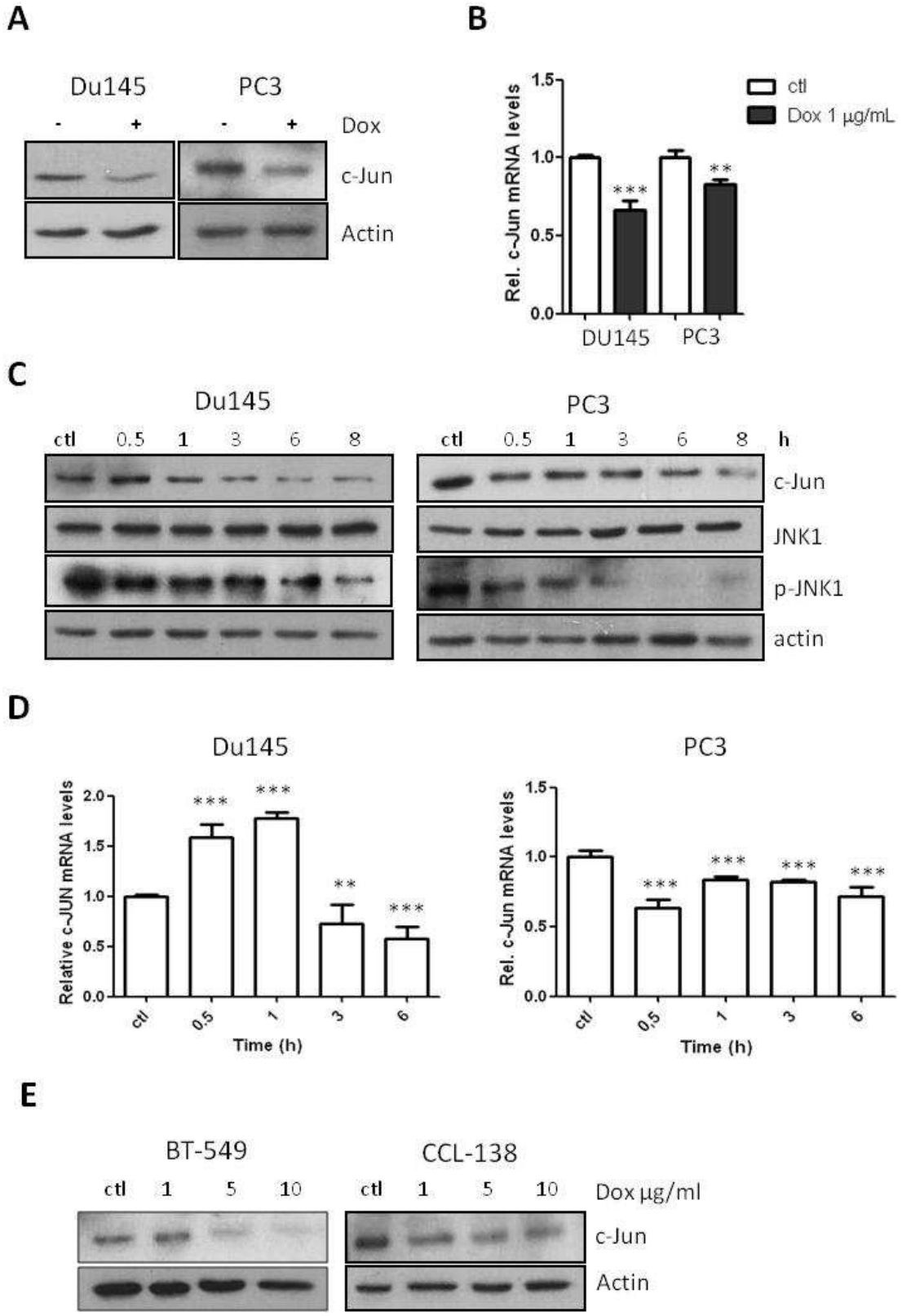

Figure 30. Doxycycline inhibits c-Jun expression in cancer cells. Immunoblots **(A)** and quantitative qRT-PCR **(B)** showing c-Jun levels in Du145 and PC3 prostate cancer cells after 24 h of exposure to 1 µg/mL doxycycline. **(C)** Immunoblots showing several MAPK signaling proteins in Du145 –left panel- and PC3 –right panel- prostate cancer cells after exposure to 1 µg/ml Doxycycline at different times. Antibodies used are shown on the right. **(D)** Relative c-Jun mRNA levels in Du145 and PC3 cells treated as in (c). **(E)**

Immunoblots showing c-Jun expression in breast (BT-549) and pharyngeal (CCL-138) cancer cells treated with increasing doses of doxycycline. p-value: *< 0.05; **< 0.01; *** < 0.005.

3. Doxycycline decreases cell viability in prostate cancer cells

Because the JNK pathway was shown to be important in cell proliferation and viability [274, 275], we studied doxycycline effects on cell viability of prostate cancer cells. Doxycycline exposure provokes a significant dose dependent decrease in proliferation of Du145 and PC3 (**Figure 31A**). These findings are in line with previous observations showing that doxycycline decreased the proliferation of different types of cells [276, 277]. As expected, the treatment with a specific JNK1/2 inhibitor (JNK inhibitor II) also impairs cell viability/proliferation (**Figure 31B**), indicating the critical role of JNK signaling in this process [274, 275].

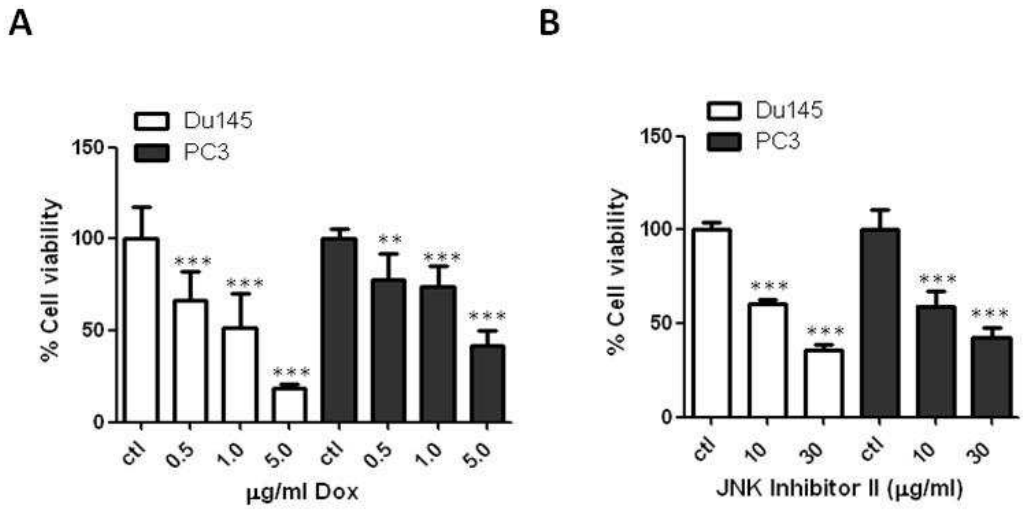

Figure 31. Doxycycline inhibits cell proliferation of prostate cancer cells. Du145 and PC3 cells were treated with increasing doses of doxycycline **(A)** or JNK inhibitor II **(B)** for 72h and cell viability was analyzed by crystal violet.

4. Tetracyclines analogs inhibit c-jun and reduce viability of prostate cancer cells

To avoid doxycycline off-target effects found on the expression of *JUN*, we next explored the use of doxycycline analogs minocycline (Mino) and methacycline (Metha) as alternative inductors in Tet-On system (**Figure 32A**). For these experiments, Du145 cells were transducted with sh6191 vector and treated for 48 h with each analog. As it is shown in **Figure 32B**, Mino (3 µg/mL) barely induces the expression of the RFP reporter,

whereas Metha (1 µg/mL) is able to induce well its expression. Disregarding the efficiency of induction of the transgene by these doxycycline analogs, we confirmed that the treatment of parental untransduced Du145 and PC3 with Metha or Mino also decreased c-Jun levels (**Figure 32C**) as result of inhibition of JNK1 phosphorylation (**Figure 32D**). As expected, minocycline and methacycline also impaired the viability of prostate cancer cells (**Figure 32E** and **F).**

Our data strongly support that doxycycline, minocycline and methacycline analogs decrease the activity of the JNK pathway, inhibit the transcription factor c-Jun and decrease the number of viable cells.

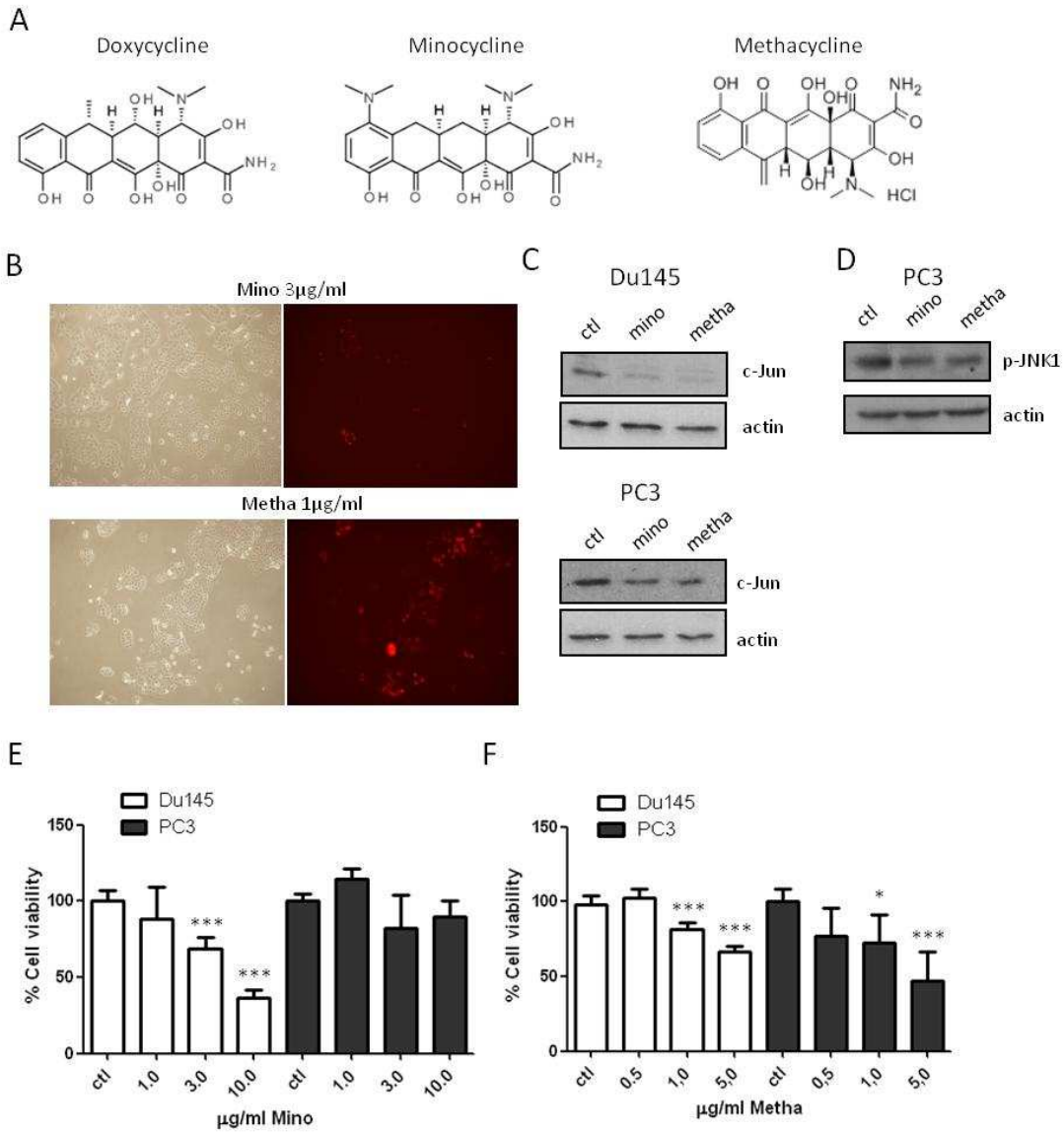

Figure 32. Doxycycline analogs minocycline and methacycline inhibits c-Jun expression and proliferation of prostate cancer cells. **(A)** Molecular structure of tetracyclines analogues **(B)** Microscopic images of Du145 cells transduced with a inducible lentiviral shRNA silencing PTOV1 expression (sh6191) and and treated with minocycline or methacycline. Fluorescence microscope images were acquired with an inverted

microscope (BX61, Olympus). **(C)** and **(D)** Western blooting analysis of prostate cancer cells treated with minocycline (3 µg/mL) or methacycline (1 µg/mL). Antibodies used are shown on the right. Du145 and PC3 cells were treated with increasing doses of minocycline **(E)** and methacycline **(F)** for 72h and cell viability was analyzed by crystal violet.

5. Discussion

Doxycycline based inducible systems have been widely employed over the course of the last fifteen years to analyze the biological effects of the modulation of expression of genes *in vitro* and *in vivo* [231, 278, 279]. An increasing body of evidence supports the effects of tetracyclines in animal cells including the impairment of mitochondrial metabolism and energetics [276, 280-282]. Here, we presented evidences showing that doxycycline, minocycline and methacycline treatment of Du145 and PC3 prostate cancer cells significantly inhibit JNK activity and the expression of the oncogene c-Jun provoking a decrease of prostate cancer cells viability. These effects were detected at doses of antibiotic frequently used in inducible systems and alert that caution must be taken when using these systems for studying genes involved in cell proliferation.

Previous studies and current ongoing clinical trials have reported the use of doxycycline in cancer treatment for its inhibitory effect on proliferation [283-286]. However, in those studies significantly higher doses of antibiotic were used compared to those required for inducible systems. c-Jun was found overexpressed in a number of tumors and its action on transcription has been associated to the activation of proliferation, *EMT* and metastasis in cancer cells [101, 251, 287]. Therefore, the inhibition of this signaling pathway in cancer is critical to avoid progression to metastasis. Interestingly, although Doxycycline was shown to inhibit the activity of methaloproteinases (MMPs) [273, 280, 284, 288-293], little is known about its link with the repression of the oncogene c-Jun. Doxycycline inhibited the MMPs activation by TGF-β1 through repression of JNK1/2, ERK1/2 and p38 in epithelial corneal cells [273]. Similarly, methacycline and doxycycline, block EMT process in part through inhibition of the TGF-β1-induced JNK, p38 and AKT in lung cancer cells [294]. Our observations provide a direct link between the known tetracyclines effects on cancer cell proliferation and the inhibition of expression of the oncogene c-Jun and contribute to shed light into the mechanisms implicated in the known anticancer effects of these antibiotics that are currently under study in pre-clinical and clinical trials in aggressive, metastatic and recurrent tumors [286, 295-301].

As we previously reported, PTOV1 acts as a regulator of c-Jun expression and most of the oncogenic functions of PTOV1, such as promoting invasion and tumor growth are mediated through the upregulation of c-Jun in prostate cancer cells [101]. In addition, the overexpression of PTOV1 in prostate cancer cells was found to activate the expression of uPA, uPAR, and induce MMP2 activity, known targets of c-Jun [101]. Therefore, the transcriptional repression of c-Jun caused by doxycycline strongly interferes with the functions of PTOV1 and the use of similar inducible systems was disregarded.

Finally, our results highlight the importance of a stringent experimental design when doxycycline is used in inducible expression systems and underscore the importance of further investigation to completely understand the mechanisms of action and the effects of these antibiotics in human cells.

Chapter 7:

PTOV1 PROMOTES DOCETAXEL RESISTANCE AND SURVIVAL OF CASTRATION RESISTANT PROSTATE CANCER CELLS

Part of these data was published as:

Cánovas V, Puñal Y, Maggio V, Redondo E, M Marín, Mellado B, Olivan M, Lleonart M**,** Planas J, Morote J, Paciucci R**. Prostate Tumor Overexpressed-1 (PTOV1) promotes docetaxel-resistance and survival of castration resistant prostate cancer cells.** Oncotarget. July 22, 2017

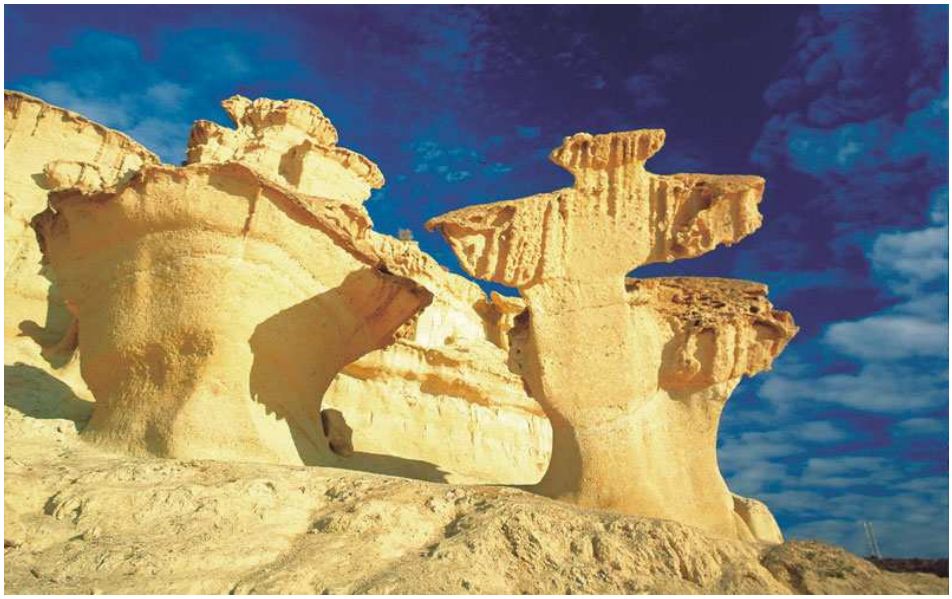

Las Gredas de Bolnuevo-*Mazarrón (Murcia)*

Las Gredas de Bolnuevo, also known as Ciudad Encantada de Bolnuevo (Enchanted city), are heavily eroded sandstone formations along the beach of Bolnuevo. The sandstone shapes are the results of the erosion caused by water and wind over thousands of years which resulted in mushroom and almost vertical shapes defying the laws of the gravity. The clay consisted of microfossils that date from the Pliocene period, about 4.5 million years ago.

1. *PTOV1 is overexpressed in docetaxel resistant CRPC cells*

Because previous results suggested an active participation of PTOV1 in cancer progression and its overexpression correlates with poor survival, we investigated whether its overexpression is associated to the acquisition of resistance to a therapeutic stress. Thus, PTOV1 expression was analyzed in Du145 and PC3 prostate cancer cells rendered resistant to docetaxel *in vitro* as representative models of CRPC progression to a docetaxel resistant (DR) stage [302]. DR Du145 and DR PC3 cells show an evident mesenchymal phenotype (**Figure 33A**) [62, 302], with a very significant decrease in epithelial markers and overexpression of genes implicated in the acquisition of drug resistance [62, 302-306] (**Figure 33B, C** and **D**).

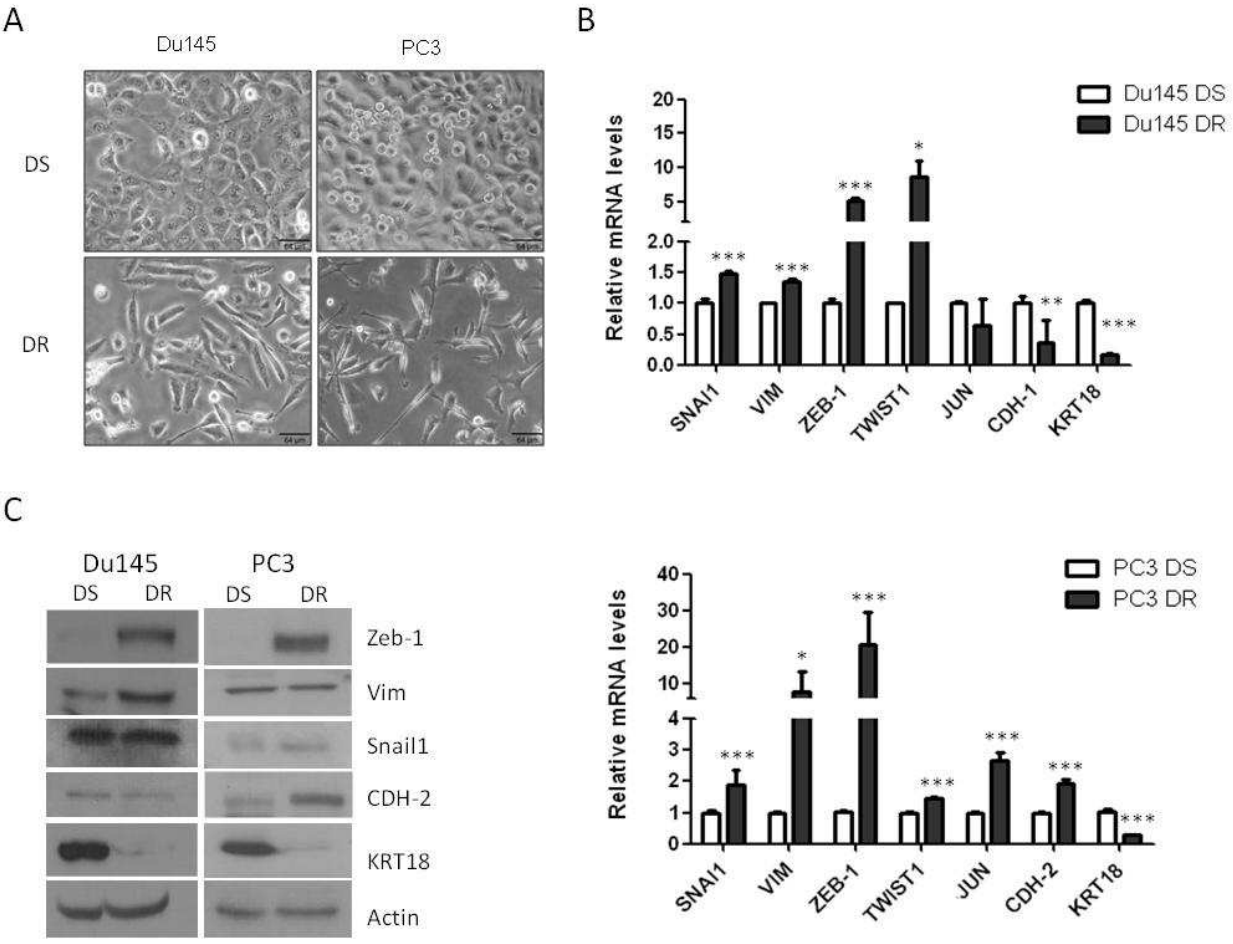

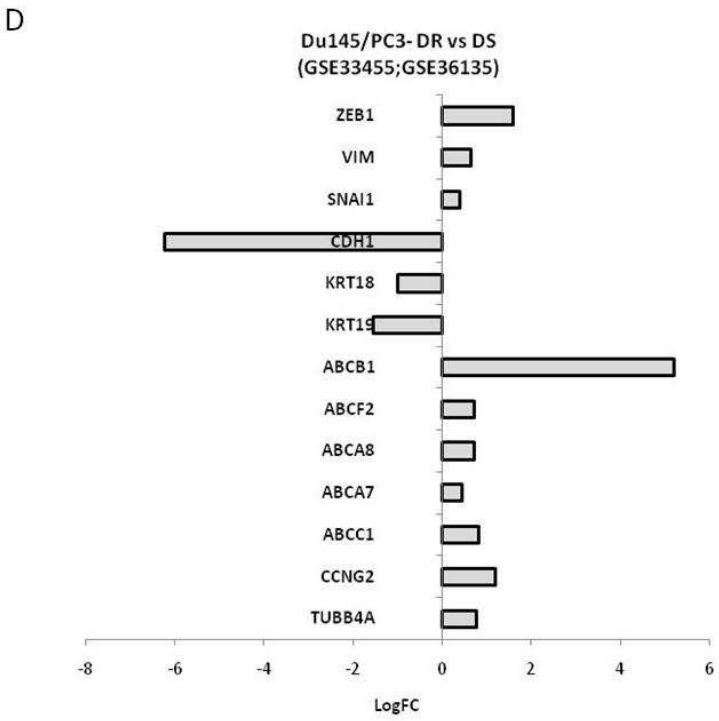

Figure 33. Docetaxel resistant cells show a mesenchymal phenotype. **(A)** Phase contrast images of docetaxel sensitive (DS) and resistant (DR) Du145 and PC3 cells in culture. Size bar, 64 µm. Images were acquired with an inverted microscope (BX61, Olympus). **(B)** Endogenous mRNA levels of indicated genes determined by real-time qRT-PCR in DS and DR Du145 and PC3 cells. Data represent the average of two independent experiments (mean ± S.D.). **(C)** Representative immunoblots showing endogenous levels of Zeb-1, Vimentin, Snail1, CDH-2, KRT18 in same cells as in (a). Actin signal was used as to monitor protein loading. **(D)** Histogram representing the RNA expression of several genes (logarithm of fold change, logFC) of the analysis of published RNA array data of Du145 and PC3 docetaxel resistant cells.

Analyses of public datasets of MDA-MB-231 breast cancer cells resistant to paclitaxel and docetaxel (GSE28784) also showed a decrease in epithelial markers and overexpression of genes implicated in the acquisition of drug resistance, such as *ALDH1A1*, *CCNG2* and *ABCB1* as reported in taxanes resistant prostate cancer cells (**Figure 34**).

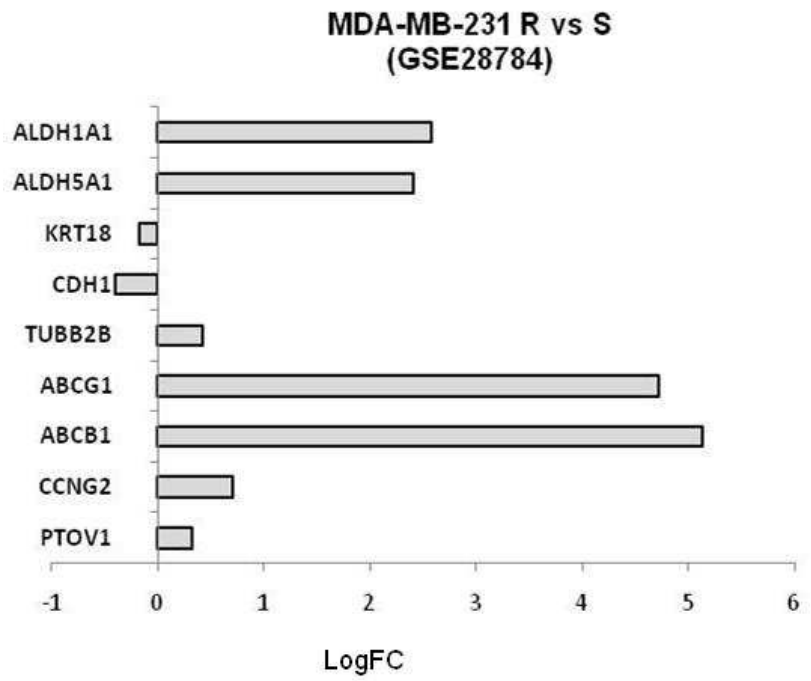

Figure 34. Docetaxel-breast cancer cells show downregulation of epithelial markers and upregulation of ABC transporters. Histogram representing the RNA expression of several genes (logarithm of fold change, logFC) of the analysis of published RNA array data of docetaxel and paclitaxel resistant breast cancer cells.

In contrast to its low levels in benign prostate derived RWPE1 cells, PTOV1 is strongly expressed in most prostate carcinoma cells lines (**Figure 35A**). Both DR-Du145 and DR-PC3 cell variants have a consistently increased PTOV1 protein levels compared with parental docetaxel sensitive (DS) cells (**Figure 35B**), and a significant increase in RNA levels is observed in DR-Du145 but not in DR-PC3 cells (**Figure 35C**). Of note, proteins and RNA were extracted in the absence of docetaxel in the culture medium.

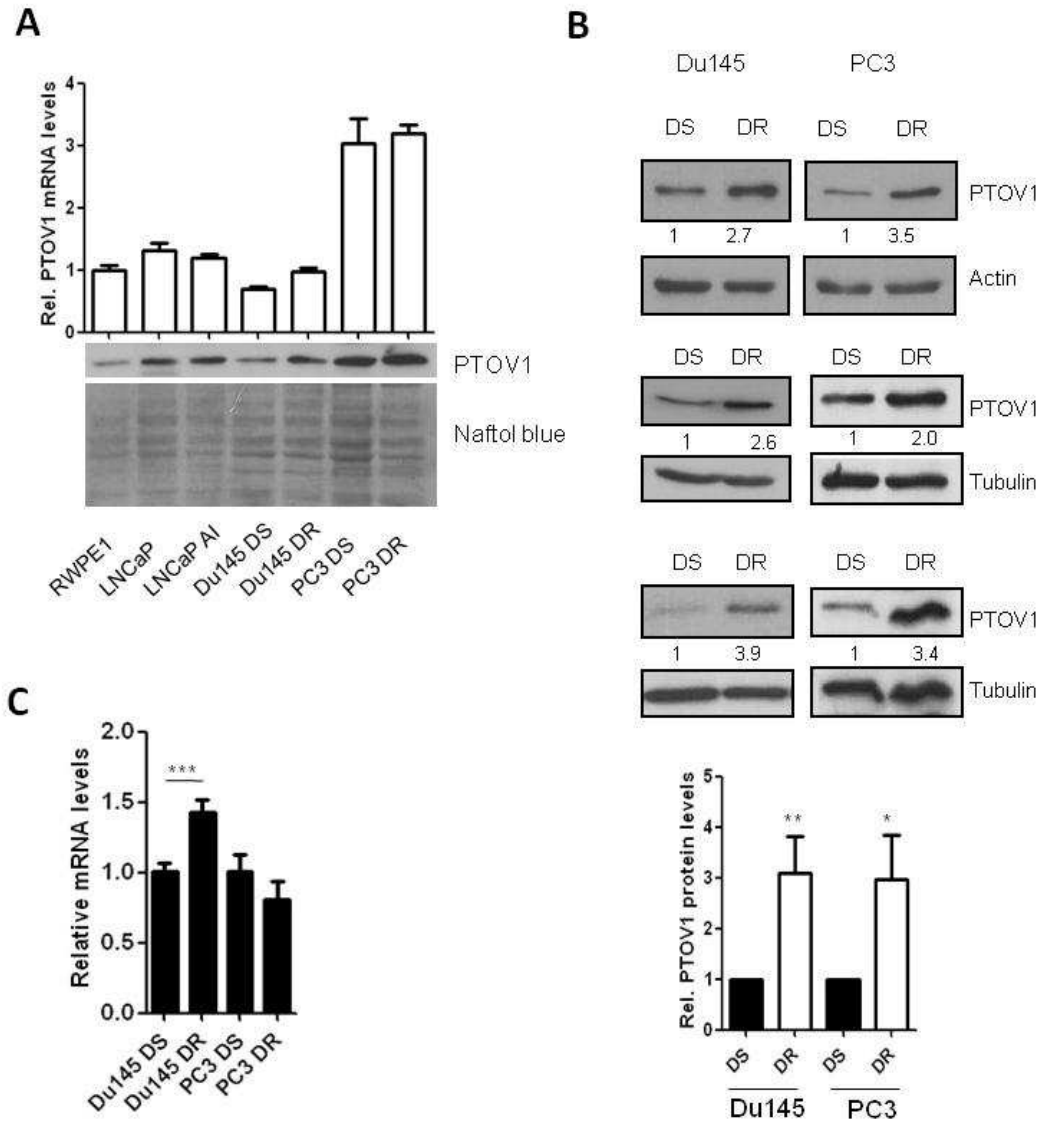

Figure 35. PTOV1 is overexpressed in docetaxel resistant CRPC cell lines. **(A)** PTOV1 mRNA and protein levels are shown by qRT-PCR and Western blotting in normal prostate cells (RWPE1), androgen sensitive (LNCaP) and castration resistant (LNCaP AI, Du145 and PC3) prostate cancer cells. Naftol blue blot was used for normalization. **(B)** Representative immunoblots showing expression of endogenous PTOV1 in Du145 and PC3 cells -up panel- and relative quantification of immunoblots using Image J software – bottom panel-. **(C)** Endogenous mRNA levels of PTOV1 (mean ± S.D.) by qRT-PCR.

To address whether translation rates may contribute to increase PTOV1 protein levels in DR cells, especially in PC3 cells, we analyzed the levels of PTOV1 transcripts more actively translated by studying the amount of mRNA loaded on polysomes (**Figure 36A**). No significant differences are found comparing the total (DR-T) and polysomes-associated mRNA levels (DR-P) in docetaxel resistant cells compared to control DS cells, suggesting that the higher protein expression observed in DR cells is not contributed by an enhanced protein synthesis. Next, we analyzed whether protein stability played a role

in PTOV1 protein levels. Although a significant increase in PTOV1 protein stability is detected in cycloheximide (CHX)-treated DR-Du145 cells, no significant differences were detected in DR-PC3 cells (**Figure 36B**), suggesting that the mechanisms underlying the higher PTOV1 protein expression in DR cells need to be explored further.

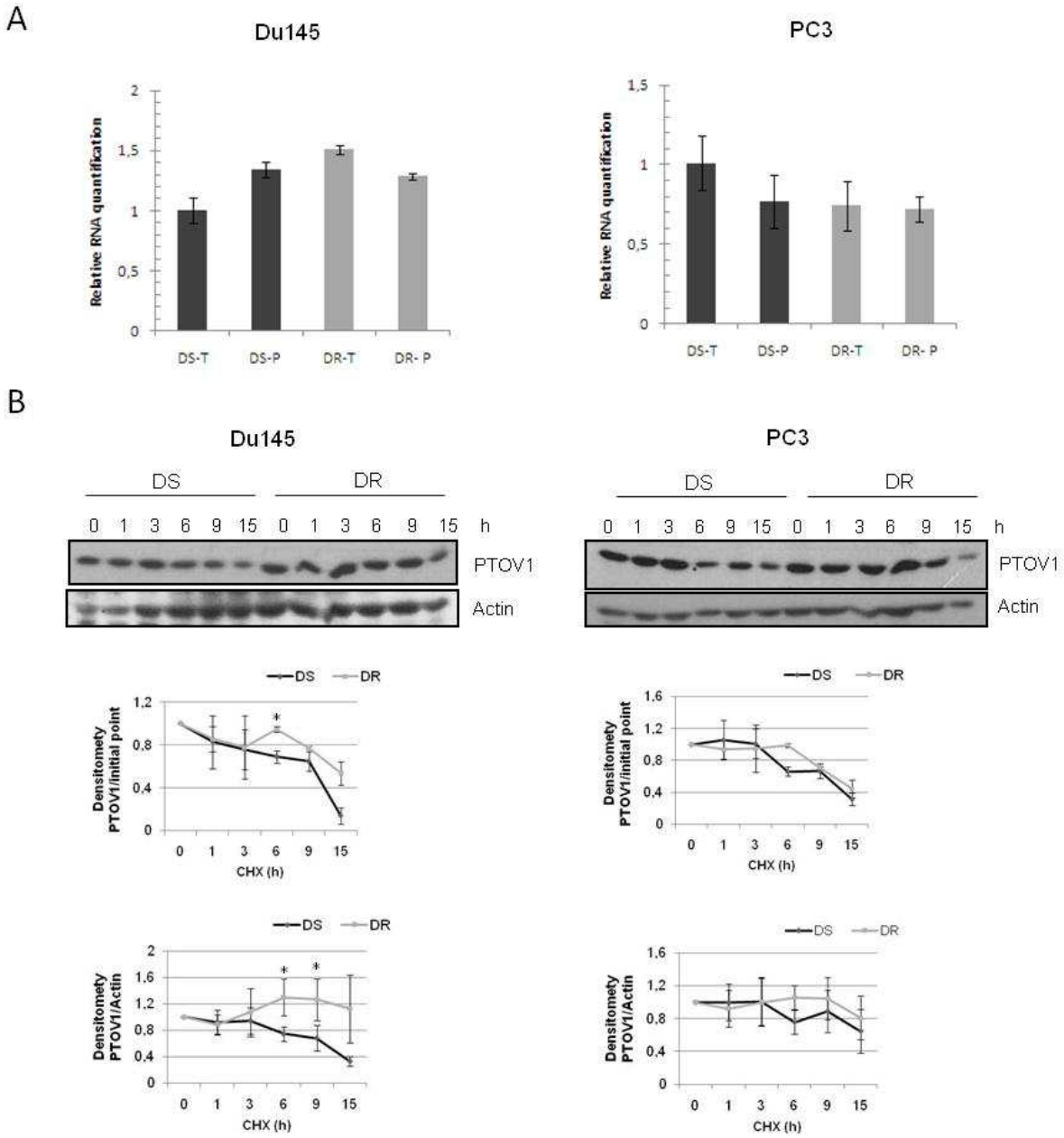

Figure 36. Translational levels and stability of PTOV1 in docetaxel resistant prostate cancer cells. **(A)** Representative histogram of PTOV1 Total RNA levels (T) and Polysome-bound mRNA (P) levels in DS and DR Du145 and PC3 cells, show the PTOV1 mRNA levels in active translation. **(B)** Analysis of the stability of the protein PTOV1 in cancer cells. Du145 and PC3 cells were treated with cycloheximide (CHX, 100 μg/mL) for the indicated time points. Upper panels show Western blotting; middle panels show graphs with densitometry scanning of PTOV1 signals normalized to control initial point 0 (untreated cells); and bottom panels show graphs with densitometry scanning of PTOV1 signals normalized to a control protein (actin) and to the control point 0. Densitometries were obtained by ImageJ software.

2. PTOV1 promotes docetaxel resistance in CRPC cells

To establish if the increased PTOV1 expression in DR cells has a role in the acquisition of resistance to docetaxel, parental sensitive cells were transduced with a lentivirus encoding HAPTOV1 (HAPTOV1-ires-GFP), or the control lentivirus encoding the GFP gene (**Figure 37A, B** and **C**).

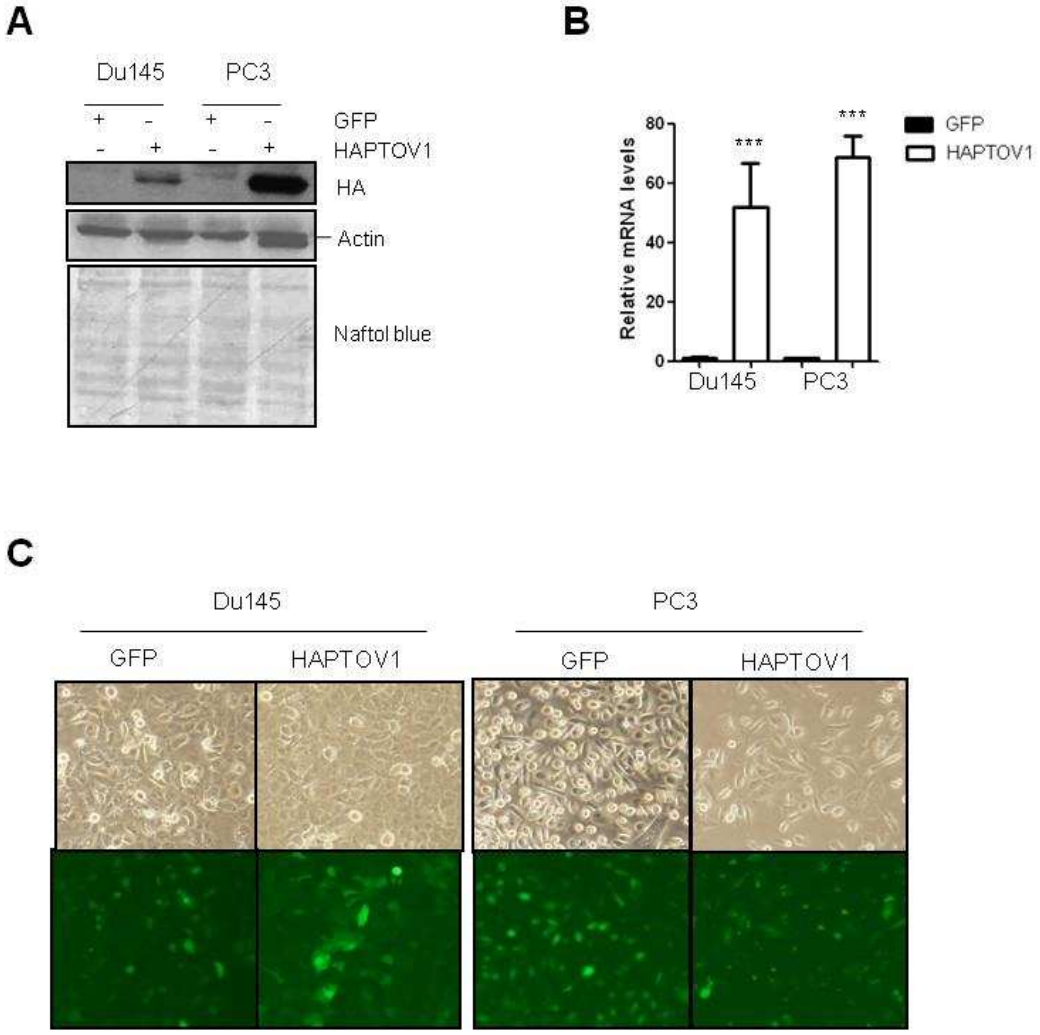

Figure 37. The ectopic expression of PTOV1 in DS Du145 and PC3 cell lines . **(A)** DS-Du145 or DS-PC3 cells transduced with a lentivirus encoding the fusion protein HA-PTOV1 or a control lentivirus encoding the GFP protein, were analyzed by western blotting using first antibodies to Hemoagglutinin (HA) to detect PTOV1, then antibodies to actin. The double bands in the HAPTOV1 lanes visible in the second panel (actin), are the signal left from the anti-HA antibody. **(B)** Relative mRNA PTOV1 levels by quantitative RT-PCR in DS-Du145 or DS-PC3 cells transduced as in (a). **(C)** Phase contrast images and fluorescence images of DS-Du145 or DS-PC3 transduced as in (a). Images were acquired with an inverted microscope (BX61, Olympus).

Transduced cells were treated with increasing doses of docetaxel for 48 h (Du145) and 72 h (PC3). The expression of PTOV1 was associated to a significantly augmented

IC_{50} to docetaxel in both cell lines, compared to control DS-GFP cells (**Figure 38A**). The IC_{50} for docetaxel in resistant Du145 and PC3 cells transduced with control lentivirus are also shown for comparison. To elucidate the molecular mechanisms implicated in this PTOV1-mediated chemoresistance, a battery of genes previously implicated in docetaxel resistance were analyzed in PTOV1-overexpressing cells [69, 302, 304, 307]. **Figure 38B** shows that PTOV1 significantly induces the expression of *CCNG2, ABCB1, TUBB4A* and *TUBB2B* genes, supporting its action in promoting the resistance to docetaxel.

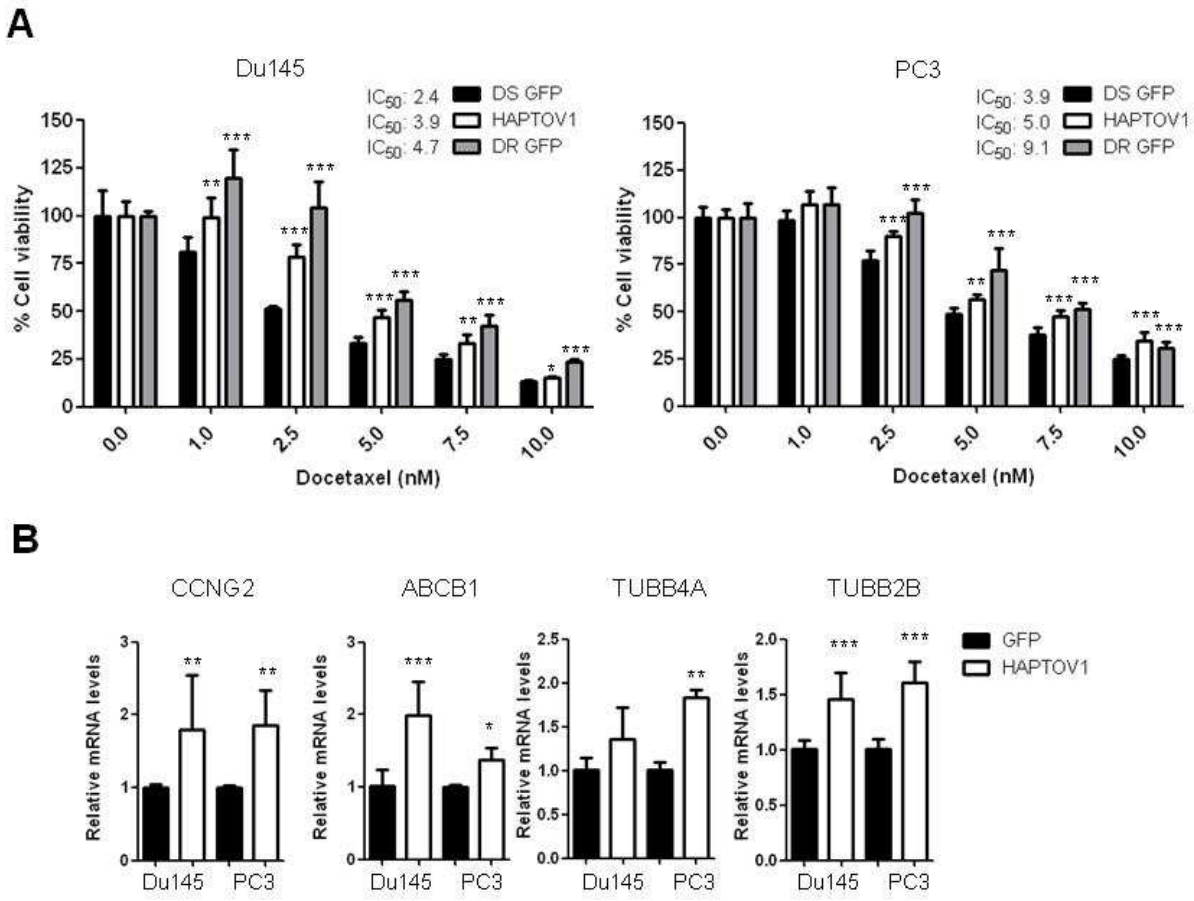

Figure 38. The ectopic expression of PTOV1 in DS Du145 and PC3 cell lines promotes docetaxel resistance. **(A)** Transduced cells were treated with increasing doses of docetaxel for 48 h (Du145) or 72 h (PC3) and cell viability was analyzed by crystal violet. Control docetaxel resistant GFP cells (DR GFP) are shown for reference. A representative experiment of three performed is shown. **(B)** Real-time RT-PCR of the genes indicated analyzed in DS-HAPTOV1 cells compared to controls (DS-GFP). Results are the mean of three independent experiments performed in triplicates and are shown as the mean ± S.D; p-value: *< 0.05; **< 0.01; *** < 0.005. nM, nanomolar.

Upregulation of *ABCB1* and *TUBB2B* were also observed when PTOV1 was overexpressed in the AR-positive LNCaP cells (**Figure 39A**), suggesting that the PTOV1-induced upregulation of these genes may be AR independent. The expression of PTOV1 significantly associated with the levels of the multidrug transporter *ABCB1*

(Spearman r: 0.64; $p = 0.0014$), suggesting a specific action of PTOV1 on the expression of this gene (**Figure 39B**).

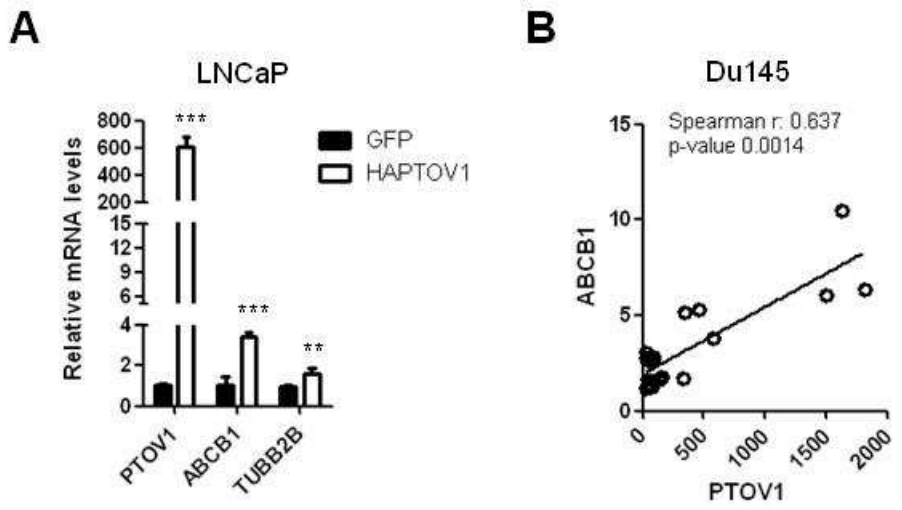

Figure 39. The ectopic expression of PTOV1 in docetaxel sensitive prostate cancer cells induces changes in their gene expression profiles. **(A)** The expression of *ABCB1* and *TUBB2B* genes was analyzed by qRT-PCR in LNCaP cells transduced with HAPTOV1 or a control (GFP) (mean ± S.D.). **(B)** The histogram represents the distribution and correlation between *PTOV1* and *ABCB1* mRNA levels in Du145 cells expressing increased amounts of HAPTOV1 (3, 7.5, 15 and 30 µg).

We next explored the potential role of PTOV1 in the acquisition of resistance to other taxanes, such as cabazitaxel, a second generation of taxanes synthesized to overcome the resistance to docetaxel [308]. Ectopic PTOV1 in DS-Du145 and DS-PC3 cells exposed to cabazitaxel did not produce significant changes in the cells sensitivity to this drug, indicating the specificity of PTOV1 in promoting resistance to docetaxel in CRPC cells (**Figure 40**). Results also suggest that the induction of *ABCB1* expression might be a relevant part of the mechanism by which PTOV1 confers cells with resistance to docetaxel.

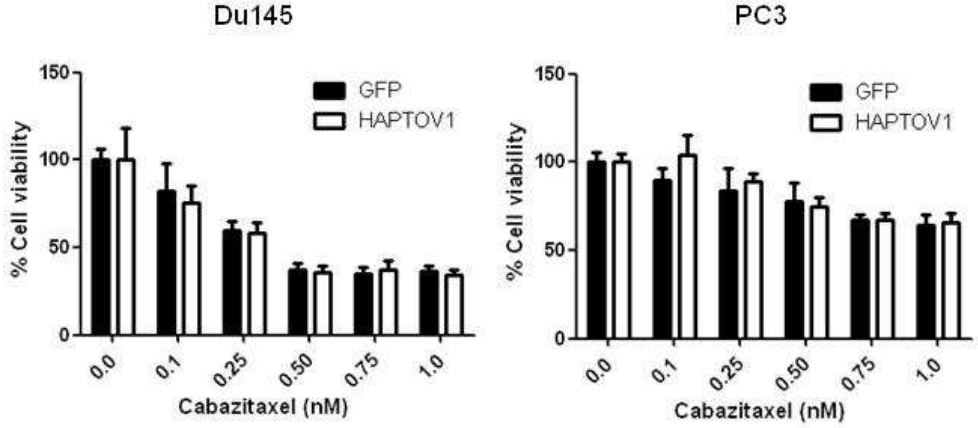

Figure 40. PTOV1 does not promote resistance to cabazitaxel. DS-Du145 and DS-PC3 cells transduced with HAPTOV1 or a control (GFP) were treated with increasing doses of cabazitaxel for 48 h. Cell viability was analyzed by crystal violet.

3. PTOV1 promotes the acquisition of self-renewing properties of CRPC cells

The significant association between PTOV1 and ABCB1 transporter expression, a protein also implicated in the modulation of the stemness phenotype in cancer cells [309], is in agreement with previous data showing PTOV1 as a promoter of self-renewal properties of prostate and breast cancer cells [100, 133]. The use of sphere-forming assays provides a widely recognized *in vitro* method for the identification and characterization of tumor initiating cells (TICs) [310]. Thus, we investigated whether the role of PTOV1 in the resistance to docetaxel is associated to the activation of self-renewing characteristics in prostate cancer cells by analyzing the effects of the overexpression and knockdown of PTOV1 in the prostatospheres forming capacities of docetaxel-sensitive cells. **Figure 41A** and **B** shows that DS-HAPTOV1 cells have a significant increase in the sphere-forming efficiency in comparison to DS-GFP control cells.

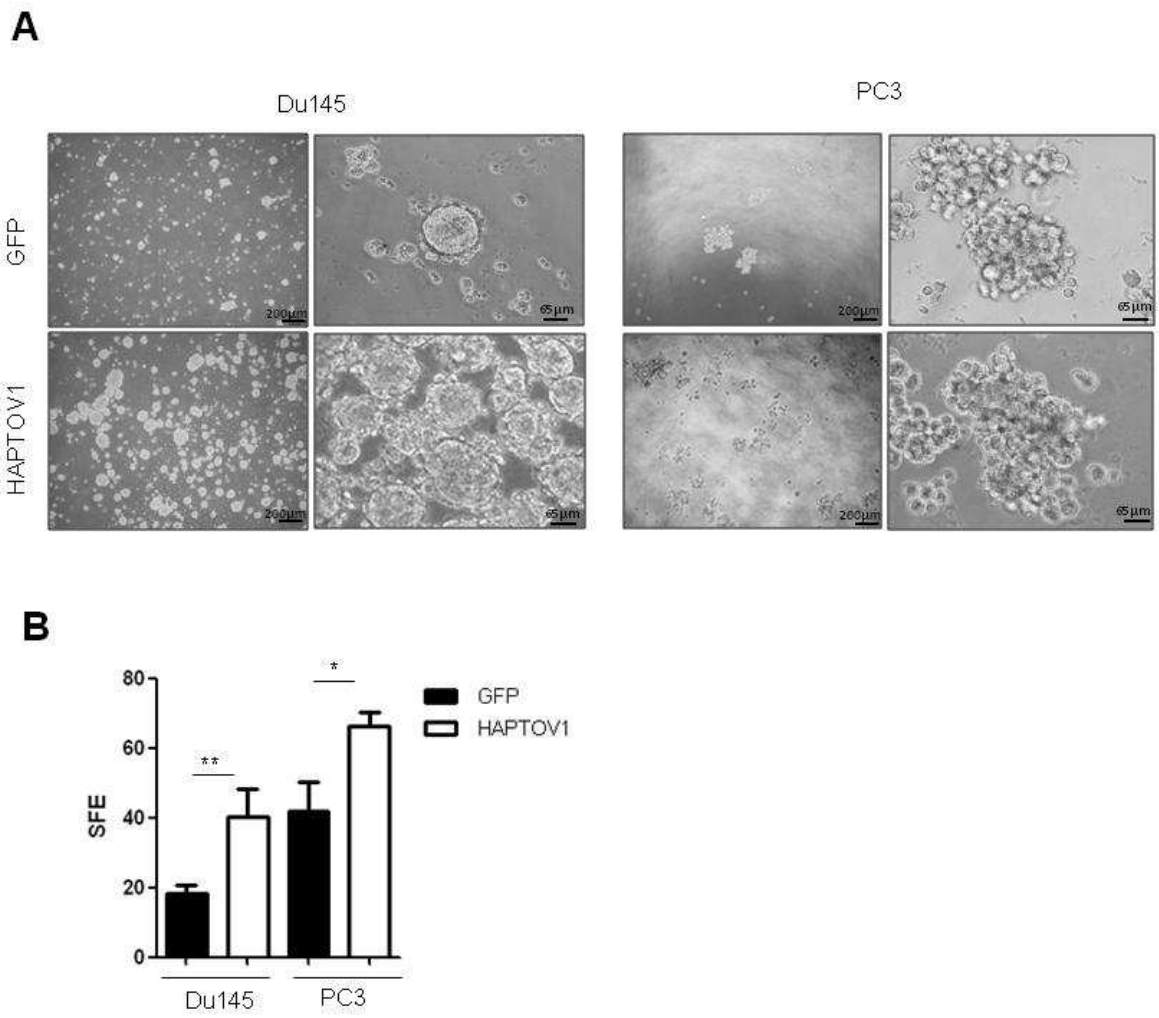

Figure 41. PTOV1 increases the tumorigenic capacity of Du145 and PC3 cells *in vitro*. **(A)** Phase contrast images and **(B)** quantification of prostatospheres from cells transduced with lentiviruses encoding HAPTOV1 or GFP. Images in A and B were acquired with an inverted microscope (BX61, Olympus). SFE: Sphere Forming Efficiency (number of spheres formed /1,000 cells). Results are shown as the mean ± S.D; p-value: *< 0.05; **< 0.01; *** < 0.005.

To confirm that the observed generation of spheres (G1) is not the result of cell aggregation, prostatospheres from Du145 DS-GFP and DS-HAPTOV1 were dissociated and an equal number of single cells were seeded in non-adherent conditions and allowed to grow for 8 days (Generation 2, G2). As previously observed, Du145 DS-HAPTOV1 prostatospheres in G2 show a significant increase in the sphere-forming efficiency compared to control GFP cells (**Figure 42**).

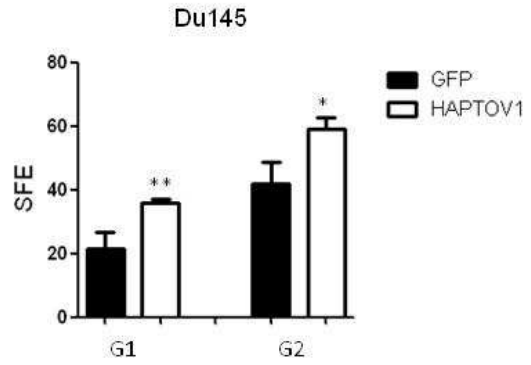

Figure 42. PTOV1 increases the tumorigenic capacity of Du145 cells. Quantification of prostatospheres of generation 1 (G1) and generation 2 (G2) from Du145 cells transduced with lentiviruses encoding HAPTOV1 or GFP. SFE: Sphere Forming Efficiency (number of spheres formed /1,000 cells). Results are shown as the mean ± S.D; p-value: *< 0.05; **< 0.01; *** < 0.005.

The analysis of mRNA of DS-Du145 HAPTOV1 and DS-PC3 HAPTOV1 cells growing in adherent conditions revealed an increased expression of pluripotency factors compared to parental cells. In Du145 cells, the overexpression of HAPTOV1 in adherent cells also associated to significantly increased levels of stemness genes *LIN28A, ALDH1A1*, *MYC* and *CD133* whereas in PC3 cells it is associated to a significant expression of *LIN28A, MYC, NANOG* and *POU5F1* genes (**Figure 43**), in agreement with reports in breast cancer cells [133].

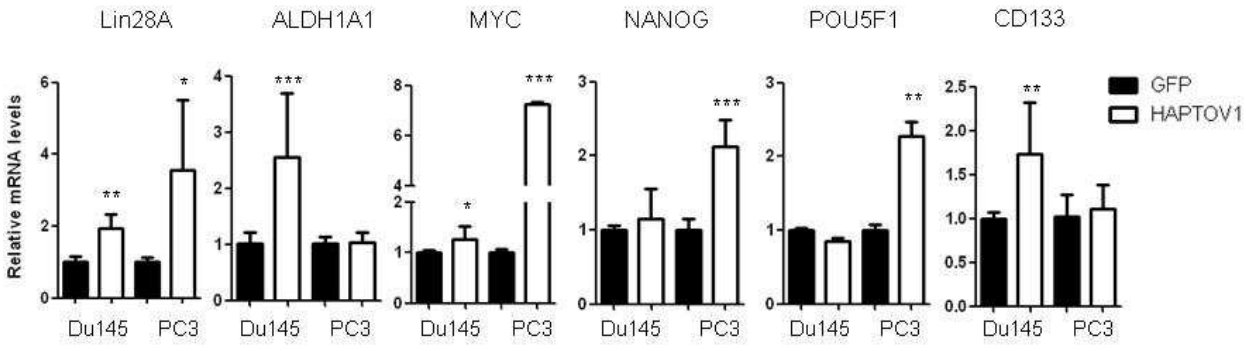

Figure 43. PTOV1 induces the expression of self-renewal genes in prostate cancer cells. Relative mRNA levels by qRT-PCR of the genes associated to self-renewal in DS-HAPTOV1 and DS-GFP cells. Results represent the average of three independent experiments (mean ± S.D). p-value: *< 0.05; **< 0.01; *** < 0.005.

Significantly increased levels of *LIN28A*, *MYC* and *NANOG* were also observed in adherent LNCaP cells overexpressing HAPTOV1 (**Figure 44A**). Of note, the expression of *PTOV1* is significantly associated with the levels of *LIN28A* (Spearman r: 0.71; $p < 0.0001$) (**Figure 44B**) in Du145 cells, again indicating its ability to induce a stemness phenotype and confirming previous observations [100, 133].

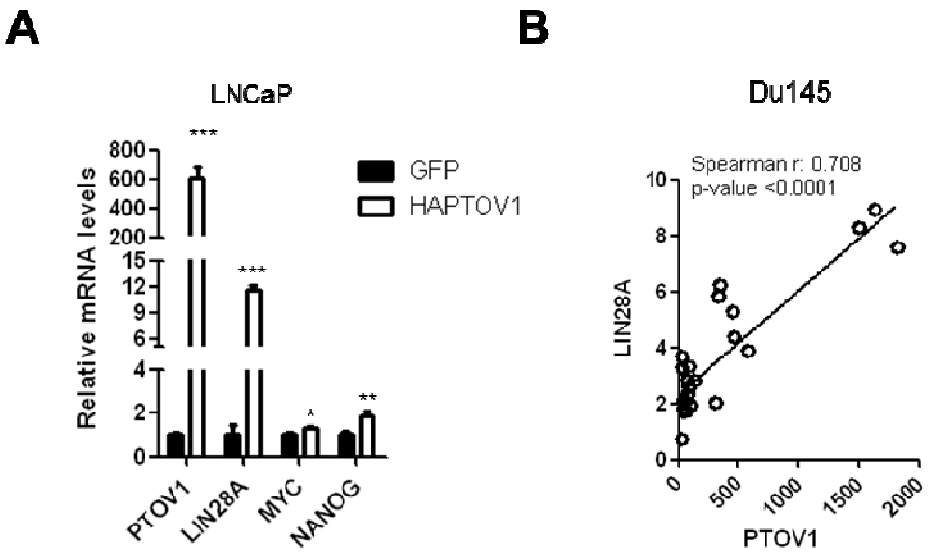

Figure 44. PTOV1 induces the expression of self-renewal genes in androgen dependent LNCaP cells. **(A)** Expression of *LIN28A*, *MYC* and *NANOG* by qRT-PCR in LNCaP cells transduced with HAPTOV1 or a control lentivirus (GFP) (mean ± S.D.) **(B)** Histogram representing the distribution and correlation between *PTOV1* and *LIN28A* expression in Du145 cells expressing increased amounts of HAPTOV1 (3, 7.5, 15 and 30 μg).

Mechanistically, PTOV1 actions were previously described to be mediated in part through the activation of c-Jun protein synthesis [101] and Wnt/β-catenin signaling [133]. In Du145 cells the inhibition of JNK signaling significantly decreases *ABCB1* expression, as previously described [311], and *CCNG2* expression (**Figure 45A**). We studied whether the PTOV1 promoted activation of genes involved in docetaxel resistance is mediated by JNK or Wnt signaling. As it is shown in **Figure 45A**, the strong JNK inhibitor II, very significantly inhibits the expression of *JUN*, as expected, and also of *ABCB1* and *CCNG2*, indicating that these genes, but not *ALDH1A1* and *LIN28A*, are regulated by c-Jun expression. Regarding Wnt/ β-catenin signaling, prostate cancer cells require Wnt3a conditioned medium (Wnt3a-CM) for its activation (**Figure 45B**). Cells added with Wnt3a-CM medium upregulate the expression of *ABCB1, ALDH1A1* and the known Wnt-target genes *LEF1* and *JUN* [312-315]. These effects are counteracted by the iCRT14 Wnt inhibitor, as previously observed (**Figure 45B**). Of notice, the activation of Wnt/β-catenin signaling also increases the expression of *CCNG2* (**Figure 45B**). The overexpression of PTOV1 significantly increased *ABCB1* expression and, reversibly, this is significantly abolished by Wnt and JNK inhibitors, suggesting that PTOV1 action on this gene is mediated at least in part by these signaling pathways (**Figure 43C**). However, no inhibition of *ALDH1A1, CCNG2* or *LIN28A* expression is observed in the presence of

these inhibitors in PTOV1-overexpressing cells, suggesting that the action of PTOV1 on promoting their expression is independent of Wnt and JNK signaling (**Figure 45C**).

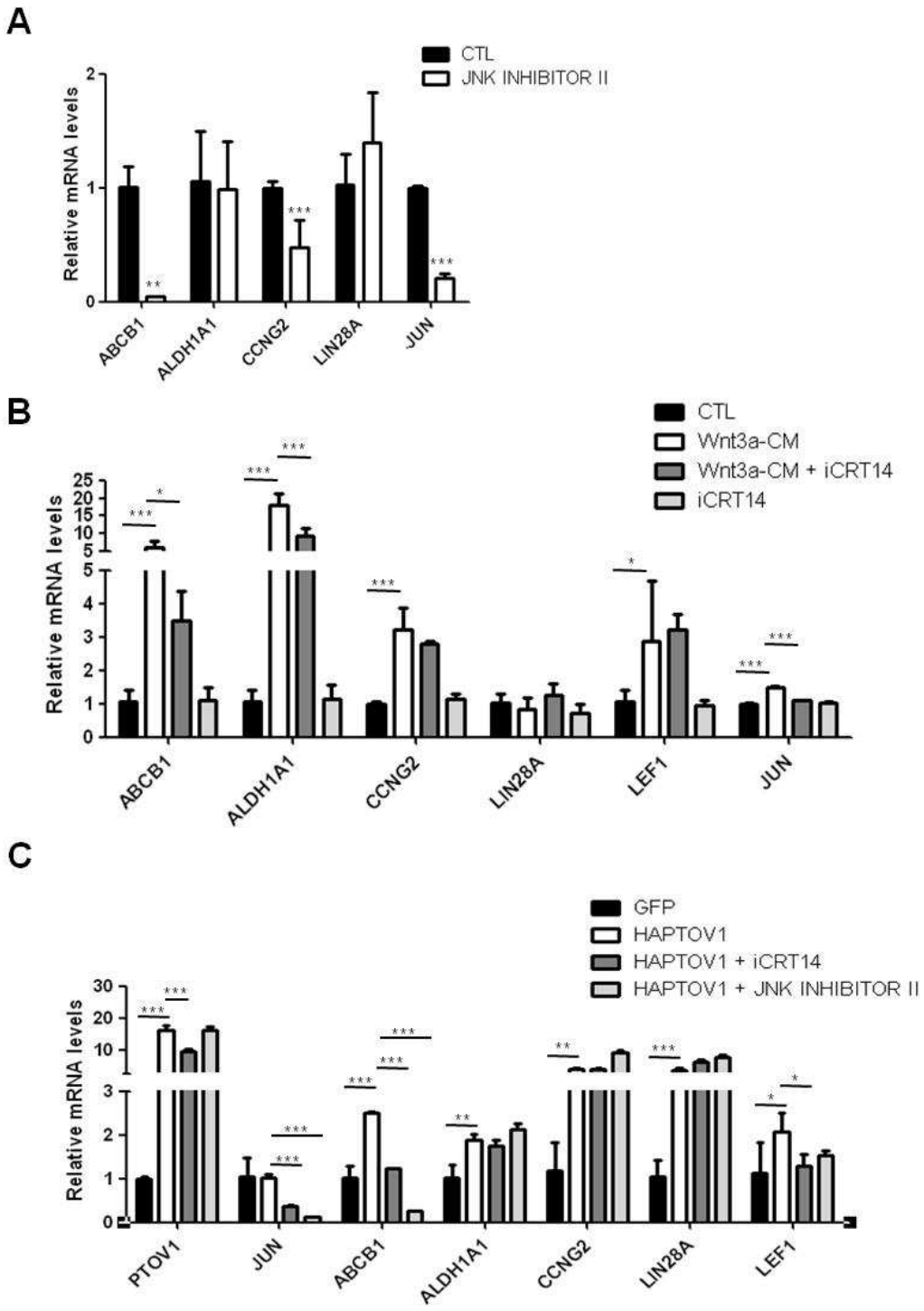

Figure 45. The Jun and Wnt pathways are implicated in the transcriptional activity of PTOV1. **(A)** Gene expression was determined by qRT-PCR in DS-Du145 cells after 24 h of treatment with the JNK inhibitor II. **(B)** Gene expression in DS-Du145 cells analyzed after the addition of conditioned medium with Wnt3a (Wnt3a-CM), without and with a Wnt/β-catenin inhibitor (iCRT14), or control cells treated only with iCRT14. LEF1 expression levels indicate the activity of the Wnt pathway. **(C)** Gene expression was

determined by qRT-PCR in HAPTOV1 transfected DS-Du145 cells treated with Wnt/β-catenin inhibitor (iCRT14) or JNK inhibitor II. These results are the average of two independent experiments.

Interestingly, PTOV1 expression is also significantly inhibited by the Wnt inhibitor iCRT14 in PTOV1-overexpressing cells (**Figura 46A**), suggesting that this pathway regulates PTOV1 expression. As it is demonstrated in **Figure 46B**, the activation of Wnt signaling increases the endogenous PTOV1 mRNA levels, whereas inhibition of Wnt/β-catenin signaling decreases PTOV1 expression.

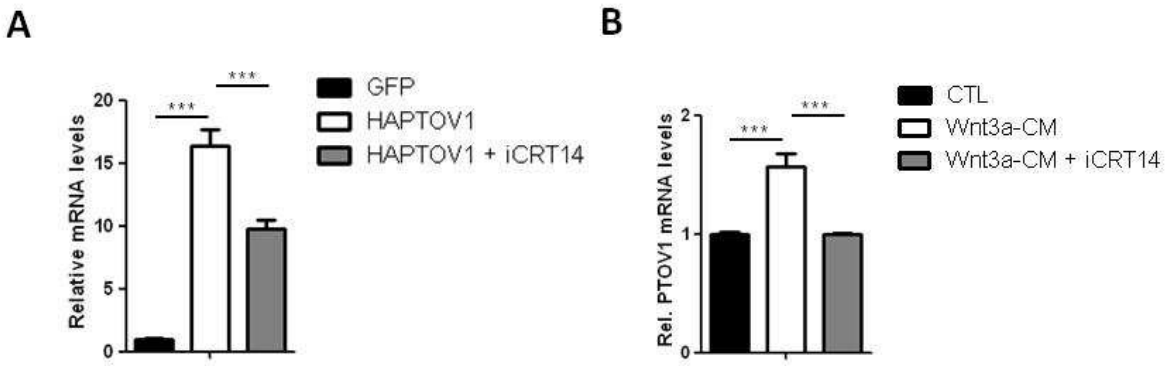

Figure 46. Wnt/β-catenin signaling pathway regulates PTOV1 expression. **(A)** PTOV1 expression was determined by qRT-PCR in DS-Du145 HAPTOV1 cells after 24 h of treatment with iCRT14 Wnt inhibitor. **(B)** PTOV1 expression was determined by qRT-PCR in parental Du145 cells after the addition of conditioned medium with Wnt3a (Wnt3a-CM), without and with a Wnt/β-catenin inhibitor (iCRT14).

To further explore a direct role of PTOV1 in the regulation of some of these genes, we performed chromatin immunoprecipitation (ChIP) assays in LNCaP cells with overexpression of HAPTOV1. **Figure 47** shows that PTOV1 binds to *CCNG2*, *TUBB2B* and *ALDH1A1* promoters. However, we did not observed a proper binding to *ABCB1*, *LIN28A* or *NANOG* promoter region. Unlike previously observed repressive action on the *HES1, HEY1* and *DKK1* promoters, PTOV1 binding to the *CCNG2*, *TUBB2B* and *ALDH1A1* promoters activates their transcription. These findings indicate that PTOV1 might be a transcription factor with activating roles.

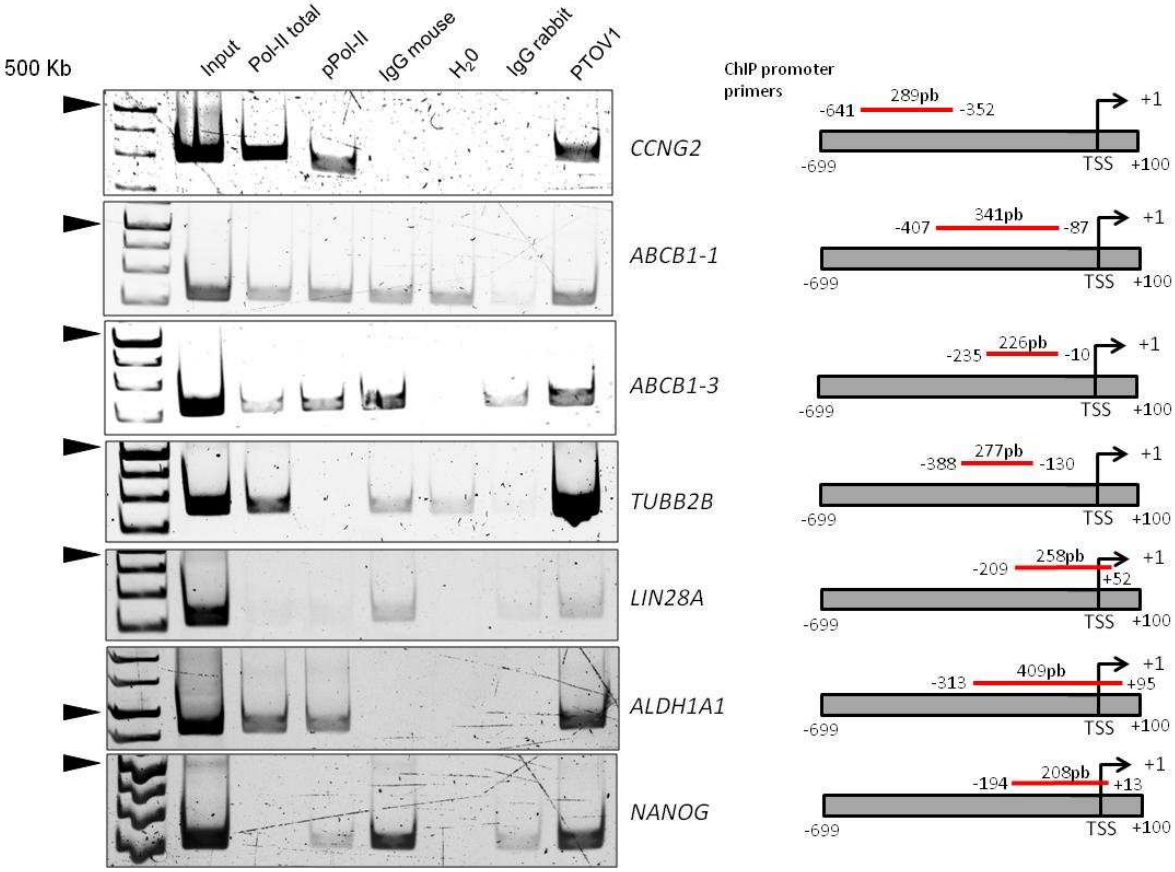

Figure 47. PTOV1 binds to *CCNG2*, *TUBB2B* and *ALDH1A1* endogenous promoters. Sheered chromatin from LNCaP cells transduced with a lentivirus encoding the fusion protein HAPTOV1 was immunoprecipitated with antibodies to PTOV1, total and phosphorylated polymerase II, and same specie-IgGs. Associated DNA fragments were analyzed by PCR with primers specific for *CCNG2*, *TUBB2B* and *ALDH1A1* promoter regions. ChIP promoter primers location and length of amplified promoter regions are indicated on the right panel. TSS: transcription start site

4. The knockdown of PTOV1 induces G2/M cell cycle arrest and apoptosis of CRPC cells

The knockdown of PTOV1 by different short hairpin RNAs (sh1439, sh1401) (**Figure 48A**) provokes a striking and significant repressive effect of the sphere-forming efficiency (SFE) of the cells in comparison to control cells bearing an unrelated shRNA sequence (shCTL) (**Figure 48B** and **C**). These findings indicate a promoting action of PTOV1 in the proliferation and/or survival of prostate cancer cells.

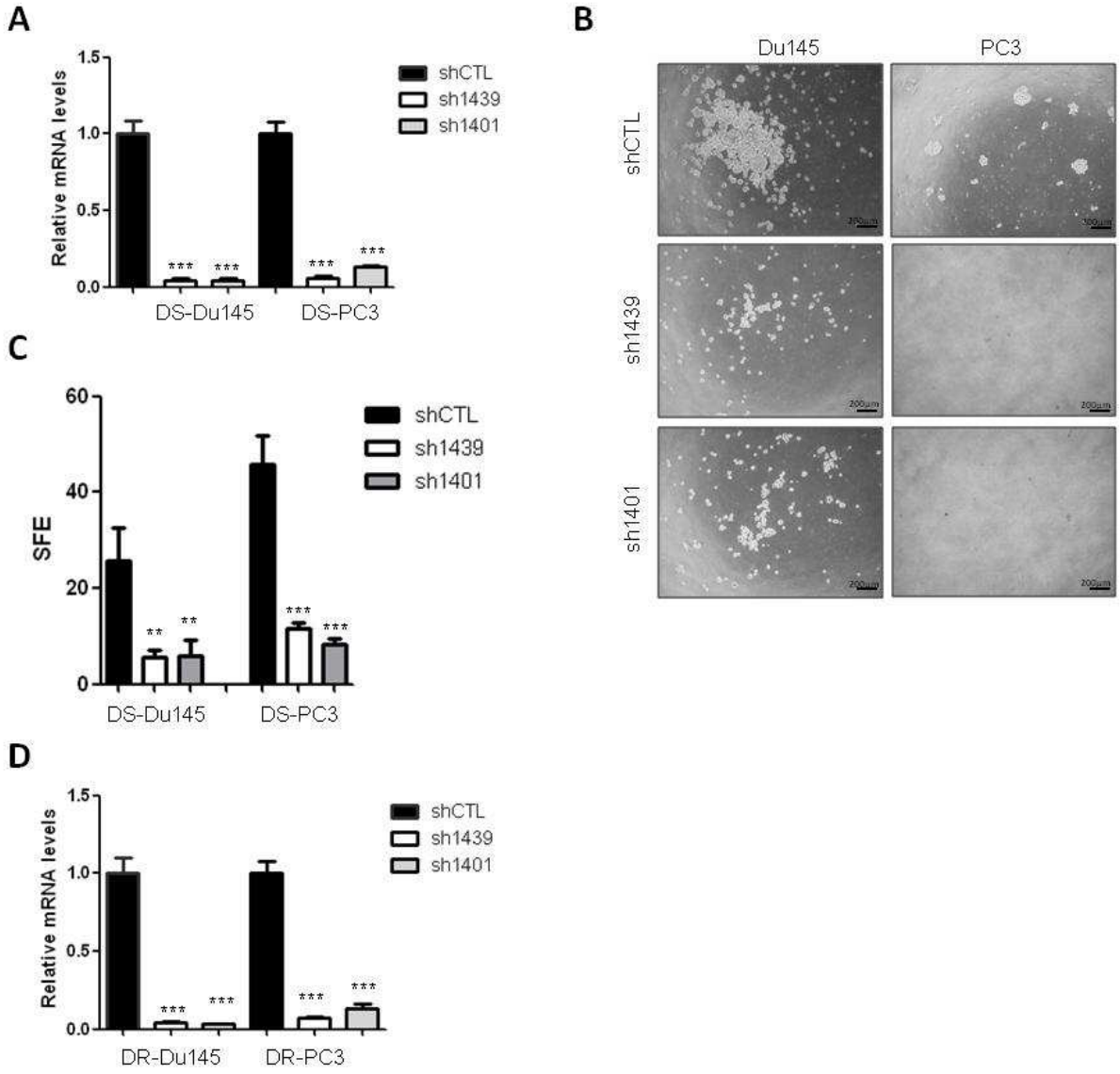

Figure 48. PTOV1 decreases the tumorigenic capacity of Du145 and PC3 cells *in vitro*. **(A)** The expression of PTOV1 by qRT-PCR in DS Du145 and PC3 cells knocked by two different shRNA sequences (sh1439 and sh1401) and a control shRNA (shCTL). Phase contrast images 4X **(B)** and quantification of prostatospheres **(C)** from cells transduced with lentiviruses carrying non-specific sequences (shCTL). Images in A were acquired with an inverted microscope (BX61, Olympus). SFE: Sphere Forming Efficiency (number of spheres formed/1,000 cells). **(D)** The expression of PTOV1 by qRT-PCR in docetaxel resistant Du145 and PC3 cells knocked by two different shRNA sequences (sh1439 and sh1401) and a control shRNA (shCTL). Size bar: 200 µm. Results are shown as the mean ± S.D; p-value: *< 0.05; **< 0.01; *** < 0.005.

Because docetaxel resistant prostate cancer cells show an increased expression of PTOV1 (**Figure 35B**), we determined the effects of its knockdown in both docetaxel sensitive and resistant cells (**Figure 49A** and **D**). The downregulation of the protein is observed in both the nucleus and cytoplasm of knockdown cells as it is shown by immunofluorescence assays (**Figure 49**).

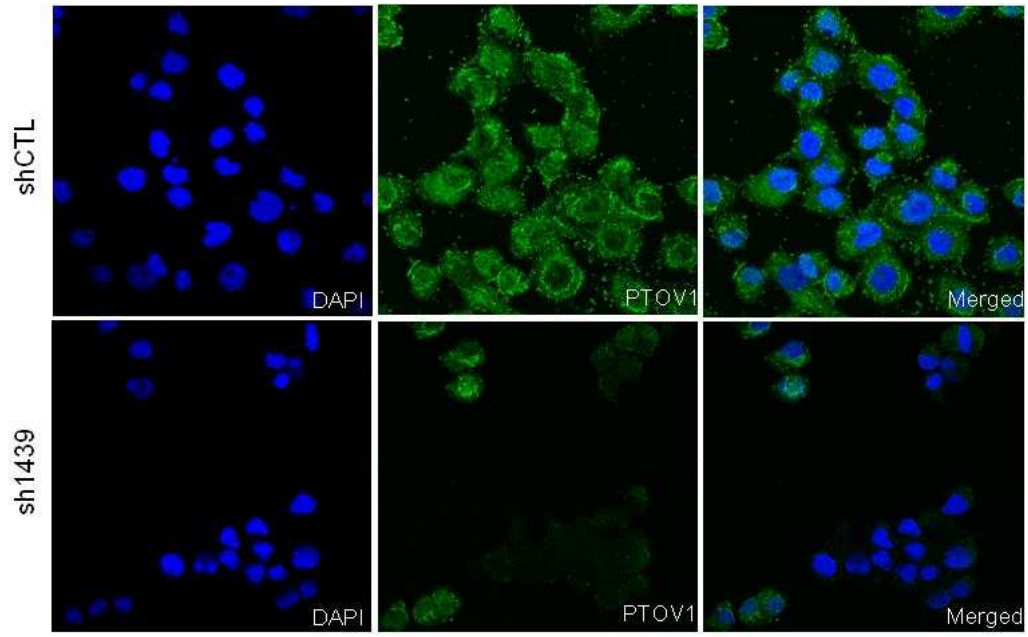

Figure 49. The knockdown of PTOV1 in docetaxel sensitive (DS) Du145 cells efficiently decreases its endogenous gene expression**.** Immunocytochemical localization of PTOV1 in DS-Du145 knockdown for PTOV1 by a shRNA sequence (sh1439).

As also previously demonstrated [72, 150], cell proliferation requires the expression of PTOV1 (**Figure 50A**). This impair in proliferation is translated in a significant increase in cell mortality as it is shown by the Trypan blue exclusion assay (**Figure 50B**). These effects are enhanced in DR cells compared to DS cells, suggesting that resistant cells are more dependent on the expression of PTOV1.

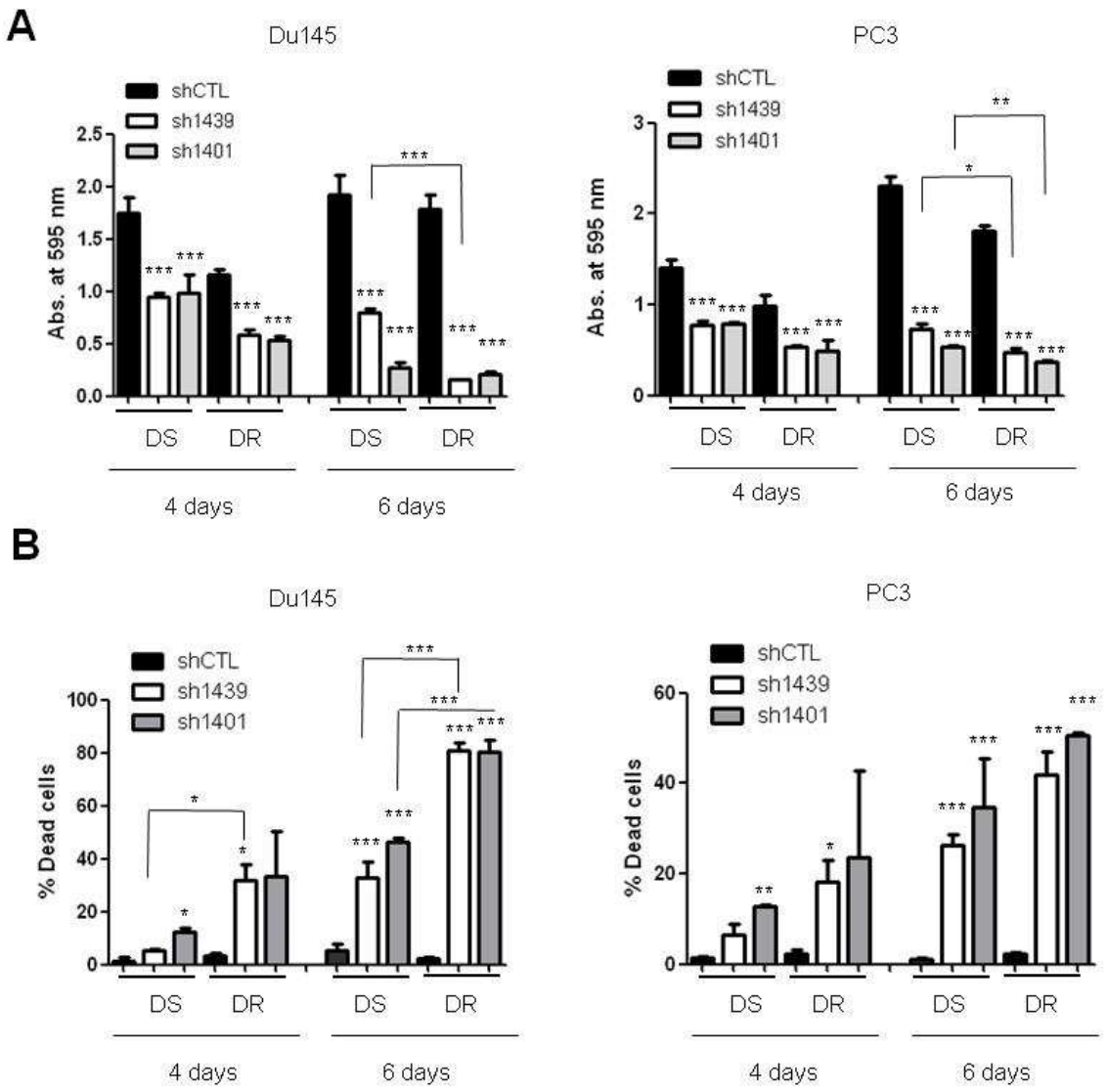

Figure 50. Downregulation of PTOV1 reduces proliferation and promotes cell death in CRPC cells. **(A)** Histogram representing the proliferation of DS- and DR-Du145 (left panel) and DS- and DR-PC3 (right panel) cells knockdown for PTOV1 compared to a control shRNA (shCTL), as in Figure 52. Proliferation was determined by crystal violet staining and absorbance at 595 nm after 4 or 6 days from lentiviral transduction. **(B)** Histogram representing the dead cells as assessed by the Trypan blue exclusion in knockdown cells after 4 or 6 days from lentiviral transduction.

Additional experiments with a different shRNA (sh1397) corroborate that PTOV1 inhibition significantly affects cell proliferation and viability of prostate cancer cells (**Figure 51A, B** and **C**).

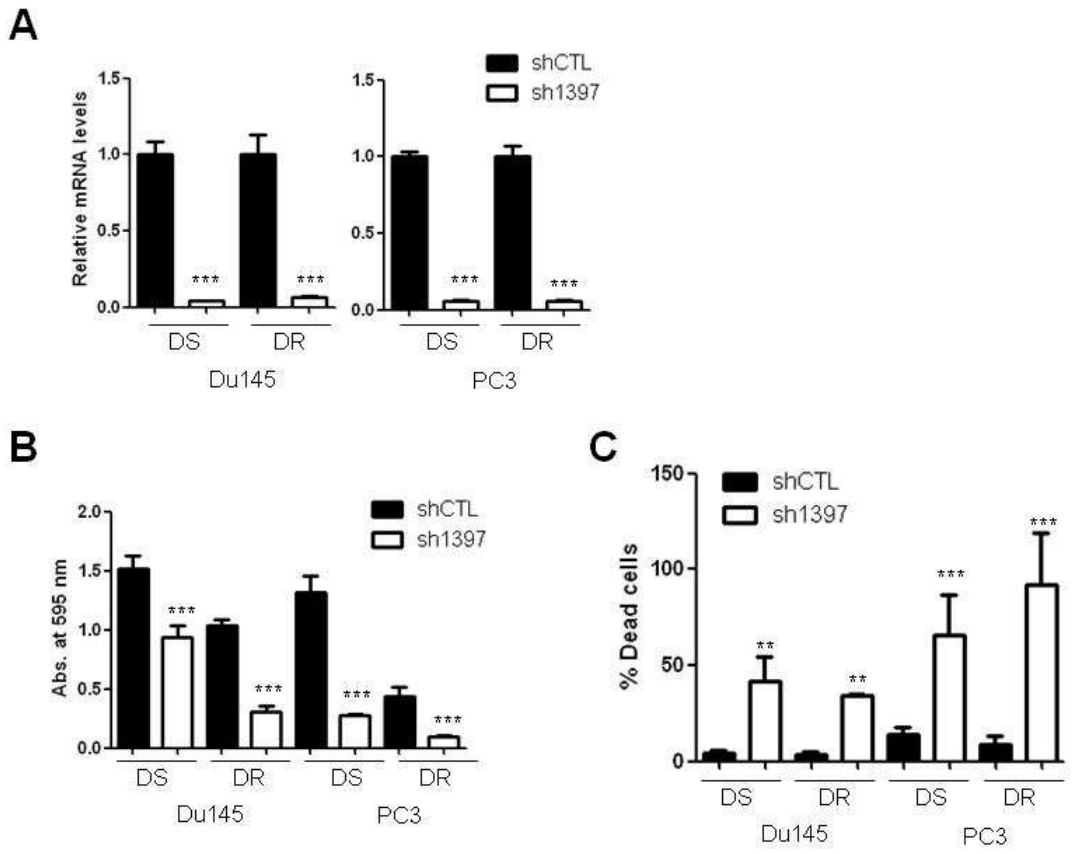

Figure 51. Downregulation of PTOV1 reduces proliferation and promotes cell death in CRPC cells. **(A)** The expression of PTOV1 by qRT-PCR in DS and DR Du145 and PC3 cells knocked by a shRNA sequences (sh1397) and a control shRNA (shCTL). **(B)** Histogram representing the proliferation of DS and DR Du145 and PC3 cells knockdown for PTOV1 as in (a). Proliferating cells were determined by crystal violet staining and absorbance at 595 nm after 96h from lentiviral transduction. **(C)** Histogram representing the number of dead cells assessed by the Trypan blue exclusion in knockdown cells as in (a) after 96h from lentiviral transduction.

Clonogenic assays show the loss of reproductive integrity and inability to proliferate indefinitely upon PTOV1 inhibition (**Figure 52A** and **B**). Large and small colonies referred to high-proliferative-potential or low-proliferative potential colony-forming cells, respectively. Of note, docetaxel resistant cells are more enriched with low-proliferative cells compared to sensitive cells, as it is evident from the more abundant formation of smaller colonies.

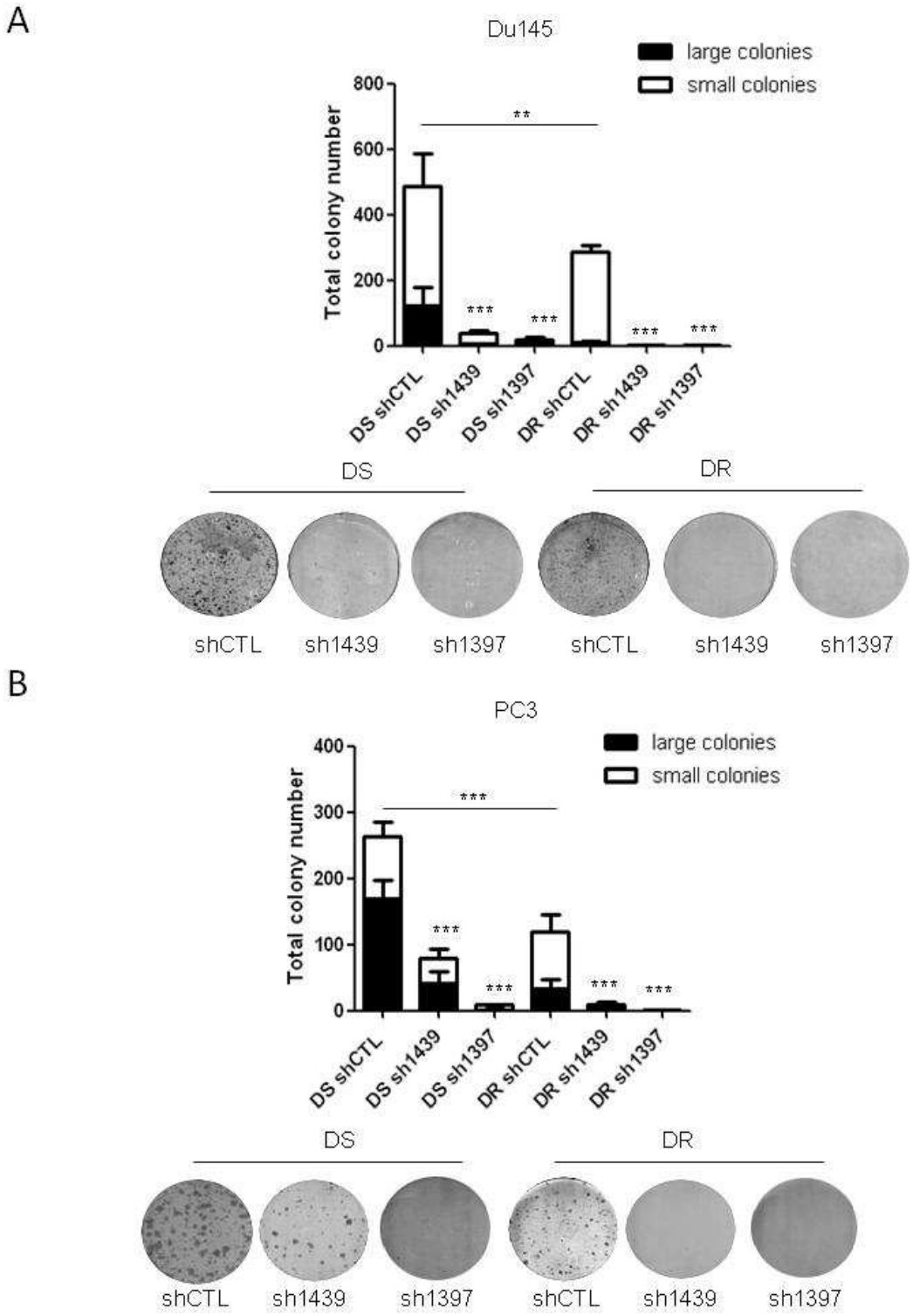

Figure 52. Colony forming abilities of prostate cancer cells knockdown for PTOV1. Colonies formation abilities by DS and DR Du145 cells **(A)** and DS and DR PC3 cells **(B)** after the knockdown of PTOV1 (sh1439; sh1397), and a control shRNA (shCTL). After seven days, cells were stained with 0.5% of crystal violet. The upper graphs show the quantification of the number of colonies, including large colonies (> 1mm Ø) and small colonies (< 1mm Ø). At the bottom, macroscopic images of the culture dishes are shown.

Microscopic images of the colonies show that sensitive cells generate confluent and tightly packed colonies, whereas resistant cells-derived colonies are smaller and cells appeared more isolated within the colony, in agreement with a more mesenchymal phenotype (**Figure 53**). PTOV1 is required for maintaining cell proliferative potential both in sensitive and resistant cells.

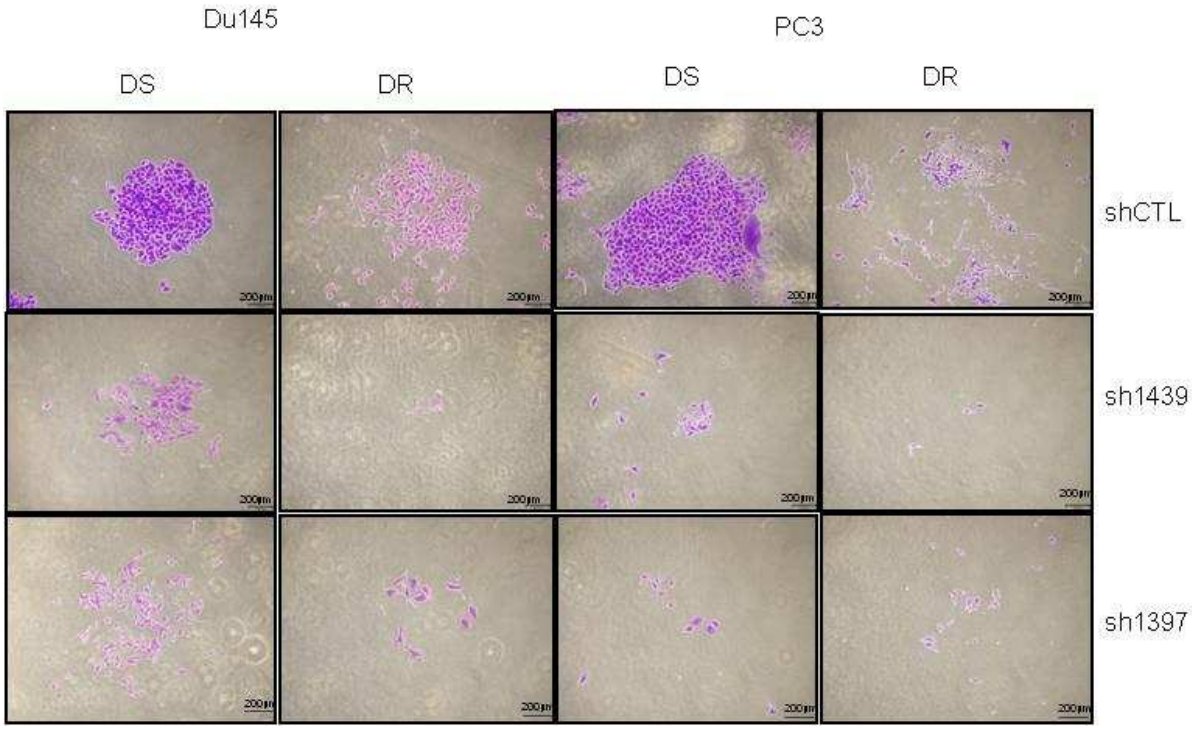

Figure 53. Microscopic images of colonies of prostate cancer cells knockdown for PTOV1. Microscopic images of colonies formed by DS- and DR-Du145 cells and DS- and DR- PC3 cells after the knockdown of PTOV1 (sh1439; sh1397), and a control shRNA (shCTL). Size bar: 200 µm.

Additional experiments in AR-positive LNCaP cells confirm that the downregulation of PTOV1 significantly impairs cell proliferation and decreases cell viability (**Figure 54**).

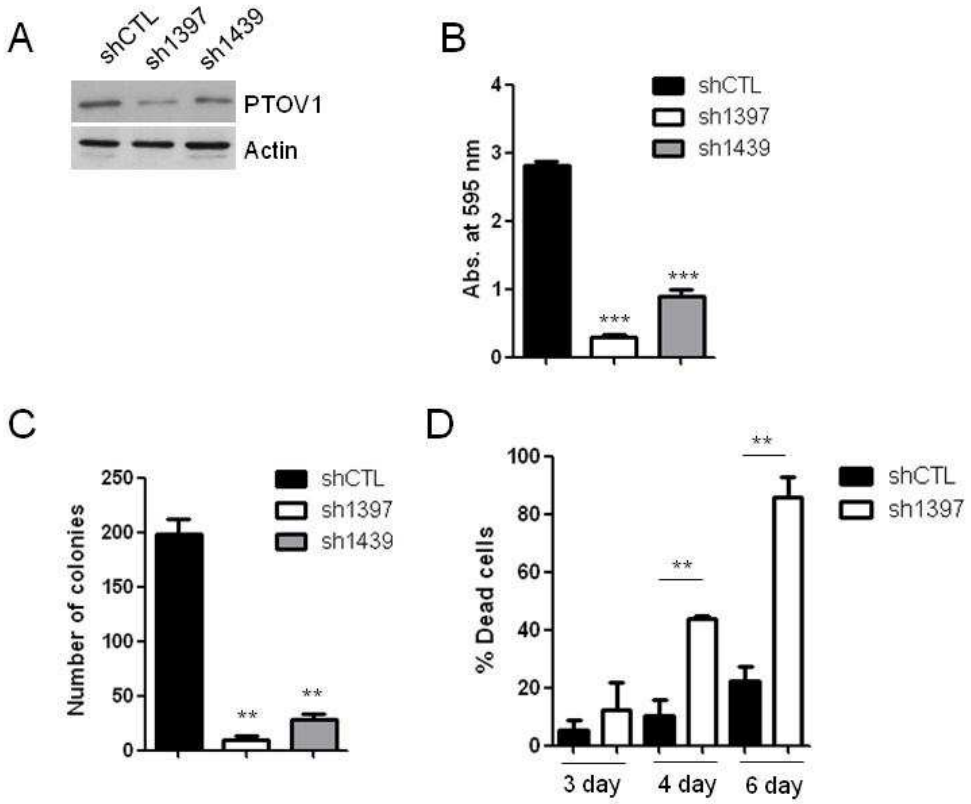

Figure 54. PTOV1 downregulation in AR-positive LNCaP induces impair cell proliferation and cell death **(A)** Immunoblots showing the expression of PTOV1 in LNCaP cells knocked for PTOV1 by a shRNA sequences (sh1397; sh1439) and a control shRNA (shCTL). **(B)** Histogram representing the proliferation of LNCaP cells knockdown for PTOV1 as in (a). Proliferating cells were determined by crystal violet staining and absorbance at 595 nm after 96 h from lentiviral transduction. (C) Colony formation abilities by LNCaP cells knockdown for PTOV1 as in (a). **(D)** Histogram representing the number of dead cells assessed by the trypan blue exclusion in LNCaP knockdown for PTOV1 (sh1397) after 96 h from lentiviral transduction.

To investigate into the mechanisms of the requirement for PTOV1 in proliferation and/or survival, cells were analyzed by flow cytometry using propidium iodide. **Figure 55A** and **B** show that cells knockdown for PTOV1 significantly accumulate in the G2/M phase in concomitance to a significant increase in the proportion of cells in the sub-G1 peak (**Figure 56A** and **B**). In agreement with our previous observations, the accumulation of cells in the G2/M phase and the increase in the sub-G1 peak are more pronounced in DR cells.

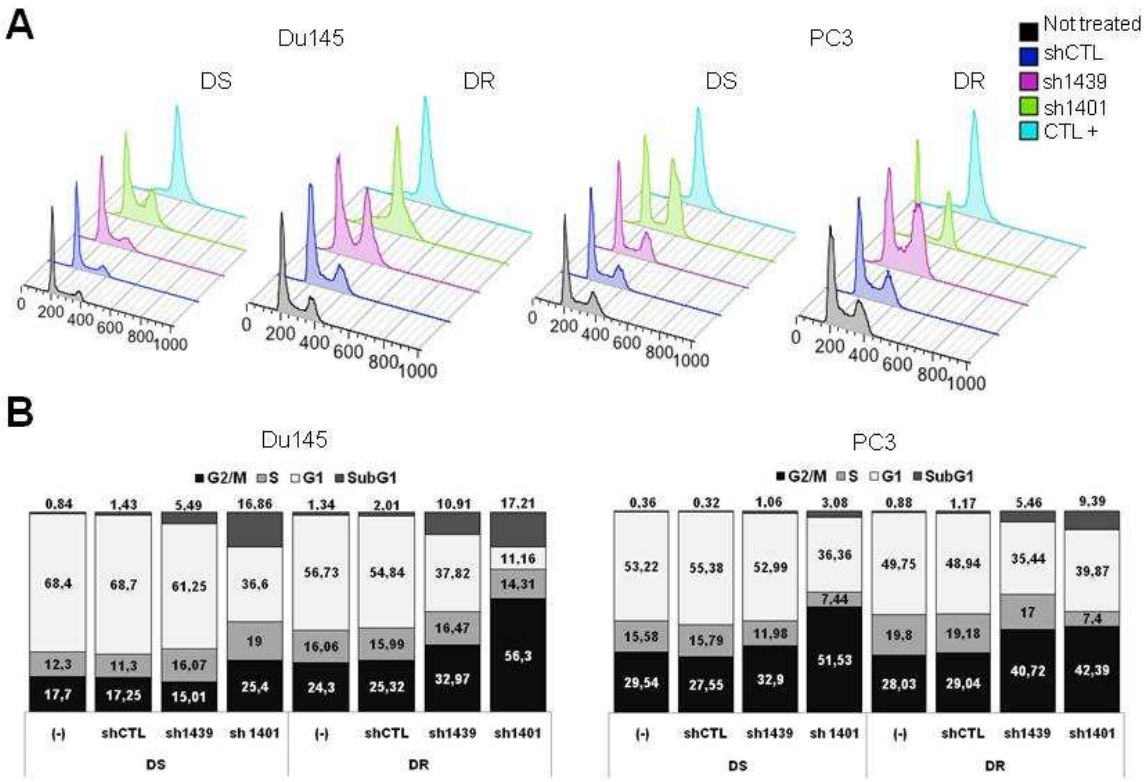

Figure 55. Downregulation of PTOV1 promotes G2/M cell cycle arrest **(A)** Docetaxel sensitive and resistant Du145 and PC3 knockdown cells as in Figure 48 and control cells were analyzed at 96 h after PTOV1 knockdown by flow cytometry using propidium iodide. DS-Du145 cells treated with docetaxel at high concentration (1 μM) for 24h were used as a control for G2/M arrest (CTL+). A representative experiment of three independently performed is shown. **(B)** Histograms representing the percentage of knockdown cells and controls found in each phase of the cell cycle from the experiment shown in (a).

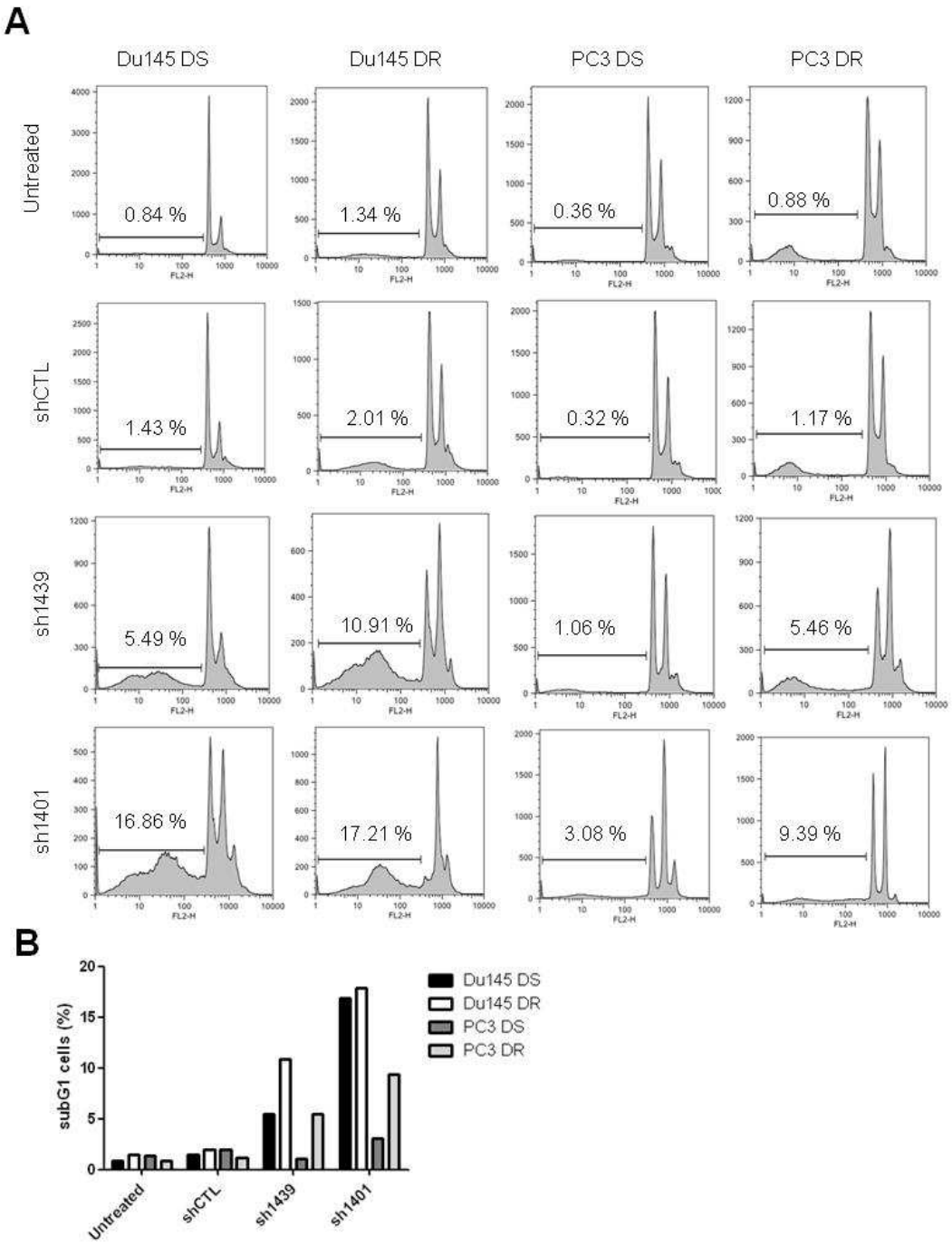

Figure 56. Prostate cancer cells knockdown for PTOV1 accumulate in the sub-G1 peak of the cell cycle. **(A)** Histograms and **(B)** graph represent the cell cycle analysis by cytometry of total cells (viable and not viable cells) in DS and DR prostate cancer cells knockdown for PTOV1. Percentages shown in each histogram represent the proportion of cells in sub-G1 peak and reflect the proportion of dead cells.

The expression of cyclin B1 and the appearance of a cleaved PARP1 fragment in the knockdown cells, confirm the accumulation of cells in G2/M phase and the boost of apoptosis observed by cell cycle analyses (**Figure 57**).

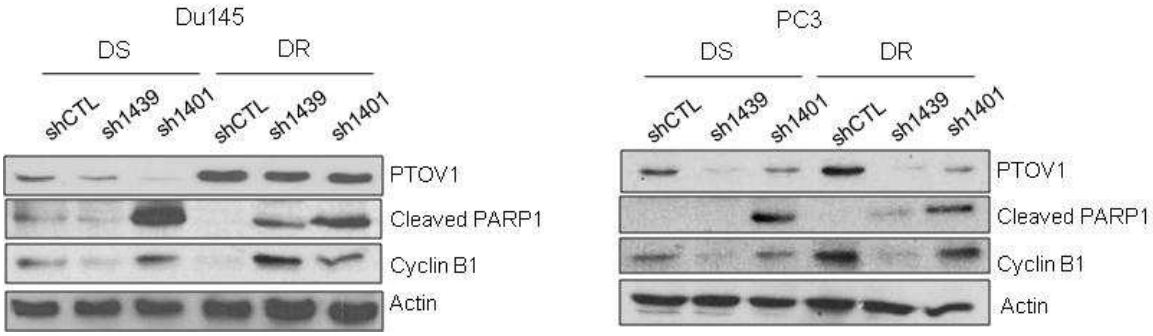

Figure 57. Downregulation of PTOV1 activates the cleavage of PARP1. **(A)** Immunoblots with the indicated antibodies showing the apoptosis caused by the knockdown of PTOV1 compared to controls.

In addition, staining with Hoechst 33342 of DS- and DR- Du145 cells 72 h after PTOV1 inhibition demonstrates nuclear condensation and fragmentation in cells undergoing apoptosis (**Figure 58**). All together, these results support a requirement of the onco-protein PTOV1 for the survival of Du145 and PC3 prostate cancer cells.

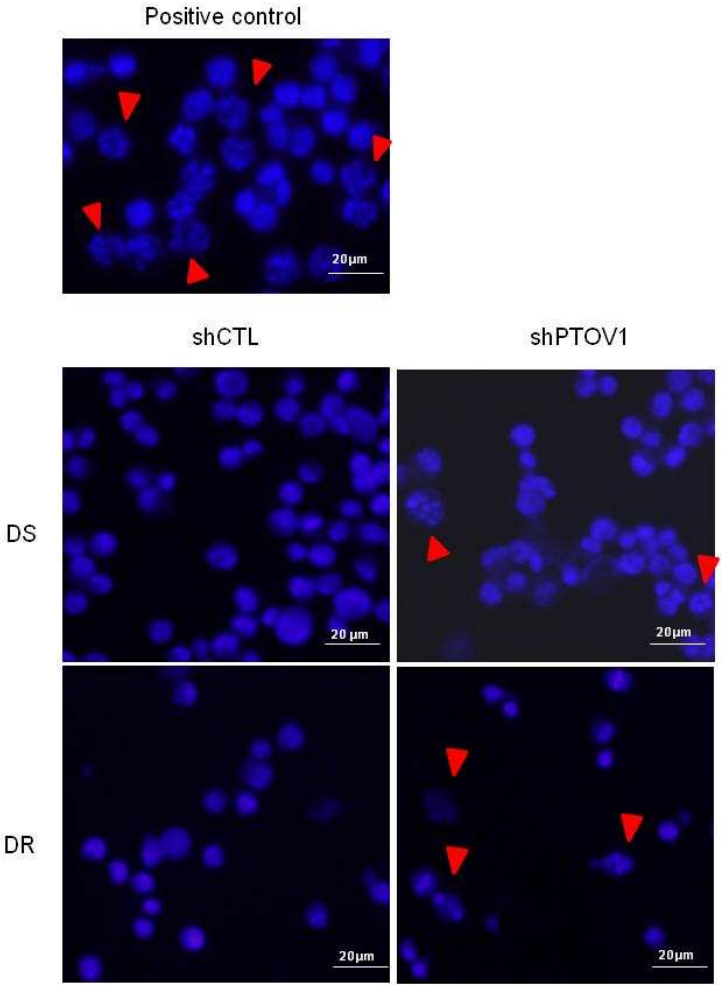

Figure 58. Inhibition of PTOV1 induces nuclear fragmentation in prostate cancer cells. Upper panel-microscopic images of Du145 cells staining with Hoechst 33342 after exposure to 1µM Docetaxel for 24 h

(positive control). Bottom panel- knockdown for PTOV1 with a shRNA sequence (sh1397) or a control shRNA (shCTL). Arrows point to nuclear fragmentated cells. Images were acquired with an inverted microscope (BX61, Olympus).

5. PTOV1 expression is induced in response to DNA damage

The G2/M checkpoint prevents the initiation of mitosis until DNA replication is completed before completion of S phase. Progression through the cell cycle is also arrested at the G2 checkpoint in response to DNA damage [316]. This arrest allows the cells more time to repair the damage. Inhibition of RNA protein synthesis or exposure of cells to certain drugs such as taxanes arrest cells in G2. **Figure 55** and **56** show that the depletion of PTOV1 and cell cycle arrest in G2/M phase is followed by cell death by apoptosis, indicating a role of PTOV1 in this checkpoint. Therefore, to explore whether PTOV1 is implicated in the DNA damage response, DS-Du145 and DR-Du145 cells were treated for 24 h with docetaxel to induce DNA damage. As it shown in **Figure 59A**, docetaxel exposure increases PTOV1 protein levels in both sensitive and resistant cells. As previously shown, in the absence of docetaxel resistant cells exhibit higher levels of PTOV1 protein (see **Figure 35B**). To further explore whether PTOV1 is induced after treatment with other DNA-damaging agents (DDAs) we treated sensitive Du145 cells with different drugs. Treatment with docetaxel, cisplatin or etoposide strongly induces PTOV1 expression (**Figure 59B**). Double-strand breaks (DSBs) are deleterious DNA lesions which, if left unrepaired, may lead to genomic instability and cell death. Amongst the different markers of double-strand breaks (DSBs), a well characterized marker is the phosphorylation of the histone H2AX (γ-H2AX) [317]. As it is shown in **Figure 59C**, PTOV1 overexpression mediated by DDAs is associated to activation of γ-H2AX in both DS- and DR-Du145 cells.

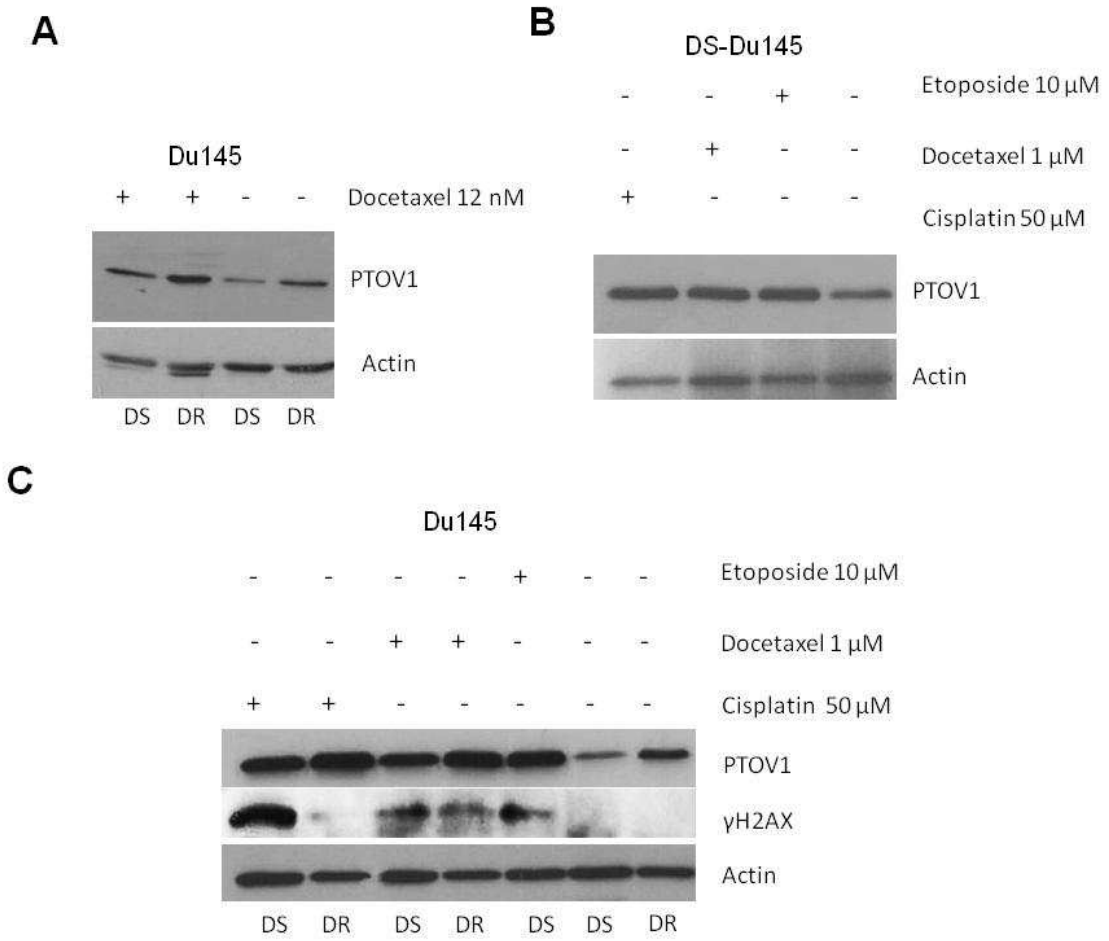

Figure 59. PTOV1 is overexpressed in response to DNA damage agents. **(A)** Western blotting of DS and DR Du145 cells treated for 24 h with the indicated concentration of docetaxel. Western blotting of DS Du145 **(B)** or both DS and DR Du145 cells **(C)** treated with different DNA damaging agents.

The presence of γ-H2AX foci indicates the presence of a DSB. **Figure 60** shows that 48 h after the knockdown of PTOV1 the accumulation of DNA damage can be detected by the increase in the number of Du145 cells with positive γ-H2AX foci. Of notice, the nuclear fragmentation with Hoechst 33342 staining is not detected at 48 h, as it occurred when cells were knockdown for PTOV1 for 72 h (see Figure 56). This indicates that the appearance of γ-H2AX foci in response to PTOV1 depletion occurs earlier than the nuclear fragmentation, suggesting that the lack of PTOV1 is the cause, rather than the consequence, of apoptosis. All together, these findings suggest that PTOV1 may contribute to the DNA damage response signaling and repair and may be required for the proper functioning of mitotic checkpoints.

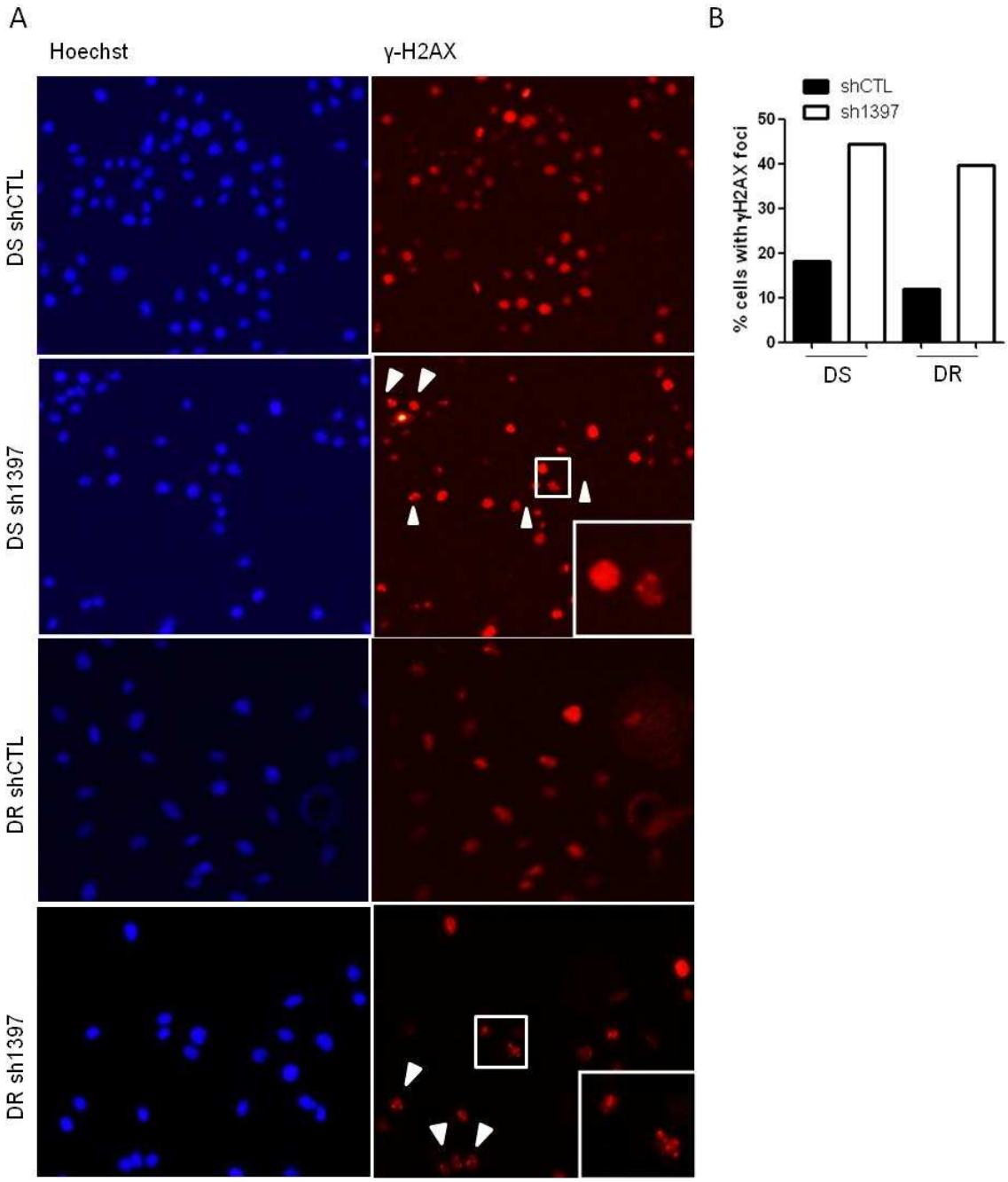

Figure 60. PTOV1 depletion activates the DNA damage response (DDR). (**A**) Fluorescent microscopic images of Du145 cells depleted for PTOV1 with the sh1397 sequence or control shRNA (shCTL) 48 h after lentiviral transduction. Cells were stained with Hoechst and antibodies to phosphorylated H2AX (γ-H2AX). White arrows indicate cells with γ-H2AX foci. (**B**) Nuclei positive for γ-H2AX foci were counted in each condition under the microscope. The percentage of cells with γ-H2AX foci was calculated with respect to the control (shCTL).

6. Correlation of PTOV1 with ALDH1A1 and CCNG2 expression in metastatic prostate tumors

We examined the clinical significance of the upregulation of *ALDH1A1, CCNG2* and *MYC* genes, previously reported in aggressive prostate tumors [304, 318-321], and their association with PTOV1 using publicly available database containing expression data clinical and pathological information from prostate tumors of not-treated patients. These analyses reveal that the higher expression of *PTOV1* in primary prostate tumors is significantly correlated to *CCNG2* and *MYC* also overexpressed compared to benign tissue (**Figure 61A** and **B**). In this set of tumors, the expression of *PTOV1*, *ALDH1A1* and *CCNG2* significantly correlates with prostate tumor aggressiveness (**Figure 61C**), in agreement with previous reports [318, 320]. In addition, a statistically significant correlation exists between the expression of *PTOV1* with *ALDH1A1* and *CCNG2* (**Figure 61D**). However, according to this dataset the expression of *MYC* appears more significantly associated to the presence of carcinoma compared to benign tissue, than to the aggressiveness of the tumors. *ALDH1A1, PTOV1* and *CCNG2* transcripts levels are also significantly higher in primary prostatic adenocarcinomas of patients who after radical prostatectomy developed regional or distal metastasis (**Figure 61E**), again supporting their relationship with the metastatic progression of prostate tumors.

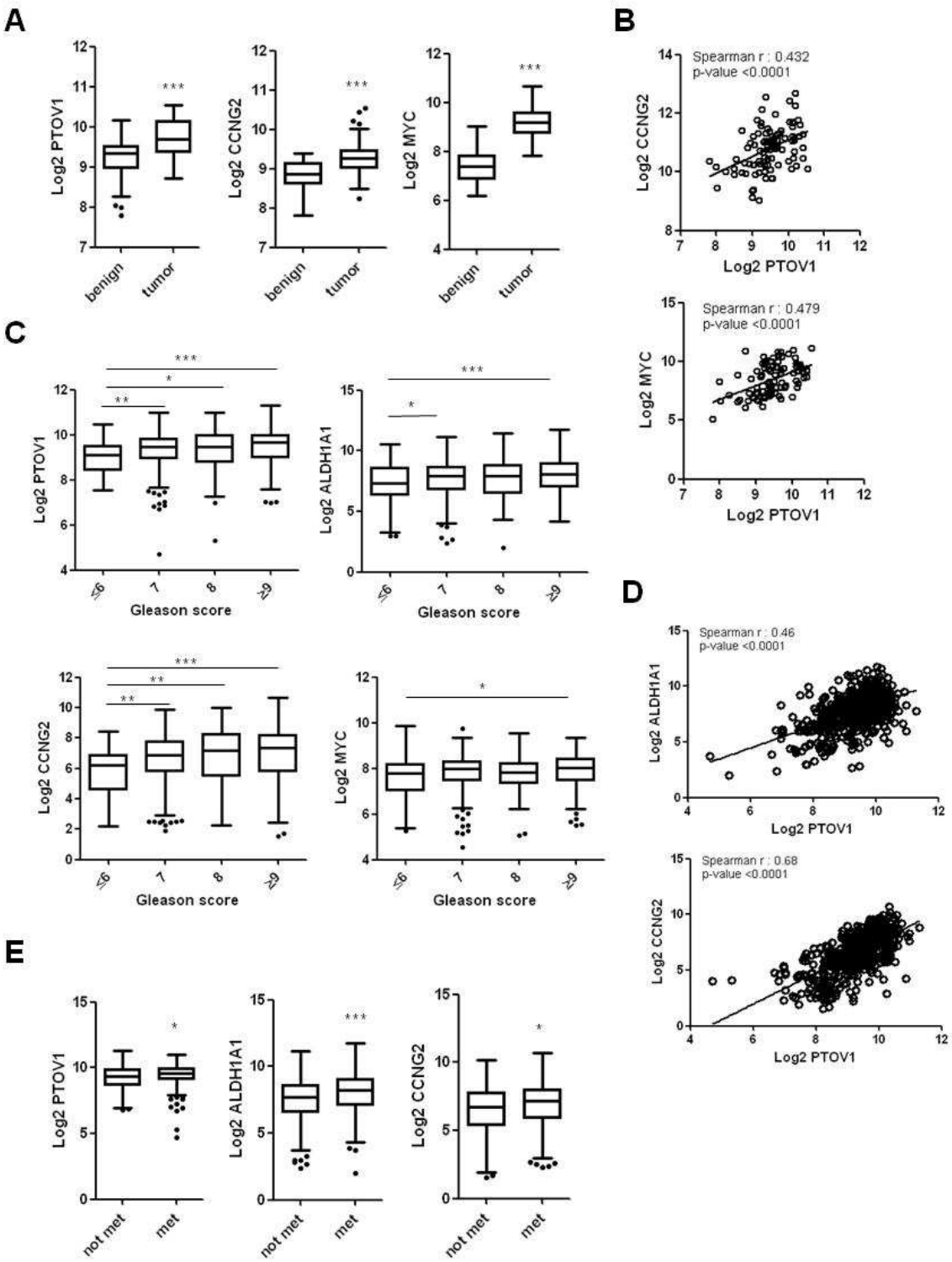

Figure 61. The expression of *PTOV1, ALDH1A1, CCNG2* and *MYC* is significantly increased in human prostate tumors. **(A)** Box and whisker plots represent *PTOV1, CCNG2* and *MYC* expression levels in prostate cancer compared to benign tissues from publicly available database (GSE29079; benign n=48; tumor n=47). **(B)** Significant statistical correlations between the expression of *PTOV1* with *CCNG2* and *MYC* in tumors analyzed in (a). **(C)** Box and whisker plots representing *PTOV1, ALDH1A1, CCNG2* and *MYC* expression in tumors with different Gleason as obtained from published prostate cancer gene expression profiles (GSE46691; Gleason score (GS) ≤6, n=63; GS 7, n=271; GS 8, n=68; GS ≥9, n=143).

(D) Significant statistical correlations between the expression of *PTOV1* with *ALDH1A1* and *CCNG2* in tumors analyzed in C. **(E)** Box and whisker plots representing *PTOV1, ALDH1A1* and *CCNG2* expression in tumors of patients that did not develop metastasis after radical prostatectomy (not met, n=333) compared to patients that did developed metastasis (met, n=212) (GSE46691). p-value: *< 0.05; **< 0.01; *** < 0.005.

7. Correlation of PTOV1 with chemotherapy resistance and poor survival in breast cancer and ovarian cancer

The correlation of the overexpression of PTOV1 with tumor progression and poor survival was previously confirmed in breast cancer [102, 133, 322]. We analyzed dataset from breast cancer tissues derived from patients treated with taxanes plus anthracyclines [322] and found a significant increase of *PTOV1* and *CCNG2* mRNA levels in patients with lower Miller and Payne grade, corresponding to bad responders to that chemotherapy (**Figure 62**), reinforcing a potential role of PTOV1 and CCNG2 in conferring resistance to chemotherapy with taxanes.

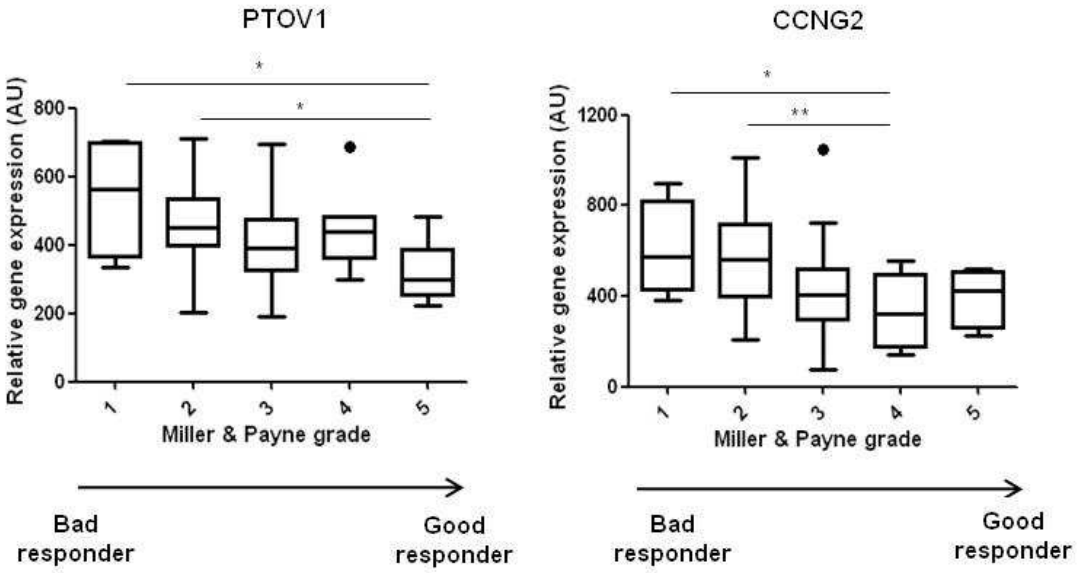

Figure 62. The expression of *PTOV1* and *CCNG2* is significantly increased in breast tumors of patients with lower Miller and Payne grade (the group of bad responders to chemotherapy). Box and whisker plots representing *PTOV1* and *CCNG2* expression was obtained from published breast cancer gene expression profiles (GSE28844; grade 1 n=4; grade 2 n=24; grade 3 n=20; grade 4 n=7; grade 5 n=6). Patients with breast cancer were given neoadjuvant chemotherapy treatment based on anthracyclines and taxanes, and tumor samples were obtained before and after chemotherapy.

In addition, integration of different datasets of breast cancer patients treated with chemotherapy or following surgery plus chemotherapy, show that high PTOV1 levels significantly correlates with a lower relapse-free survival (RFS) and distant-metastasis

free survival (DMFS) probability [323], suggesting that PTOV1 expression may be predictive of bad response to chemotherapy (**Figure 63**). Of note, chemotherapy in this cohort of patients consists mainly in the use of anthracyclines, a DNA intercalating agent, suggesting that PTOV1 may contribute to resistance to other types of chemotherapies.

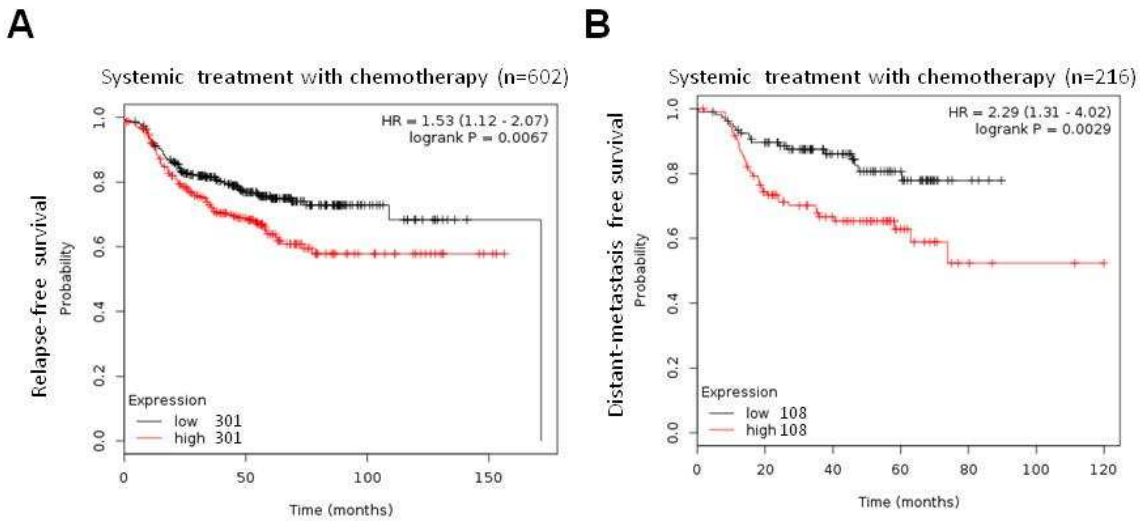

Figure 63. Survival analyses associated PTOV1 expression in breast cancer patients treated with chemotherapy. **(A)** Relapse-free survival analysis associated PTOV1 expression in breast cancer patients integrating gene expression data (GSE1456; GSE16446; GSE19615; GSE21653; GSE31519; GSE3494; GSE37946; GSE45255; GSE4611; GSE5327). **(B)** Distant-metastasis free survival analysis of breast cancer patients integrating gene expression data (GSE16446; GSE17907; GSE19615; GSE3494; GSE45255). Data were analyzed using the Kaplan-Meier plotter tool (http://kmplot.com/analysis/). Patients were split by median.

In ovarian cancer patients treated with a taxol-base chemotherapy, low levels of PTOV1 are associated with better overall survival although data do not reach statistical significance (p=0.07) (**Figure 64A**). In ovarian cancer patients treated with a platinum-based chemotherapy or a combined chemotherapy based in taxol plus platinum, high PTOV1 levels are significantly associated with poorer overall survival (**Figure 64B** and **C**).

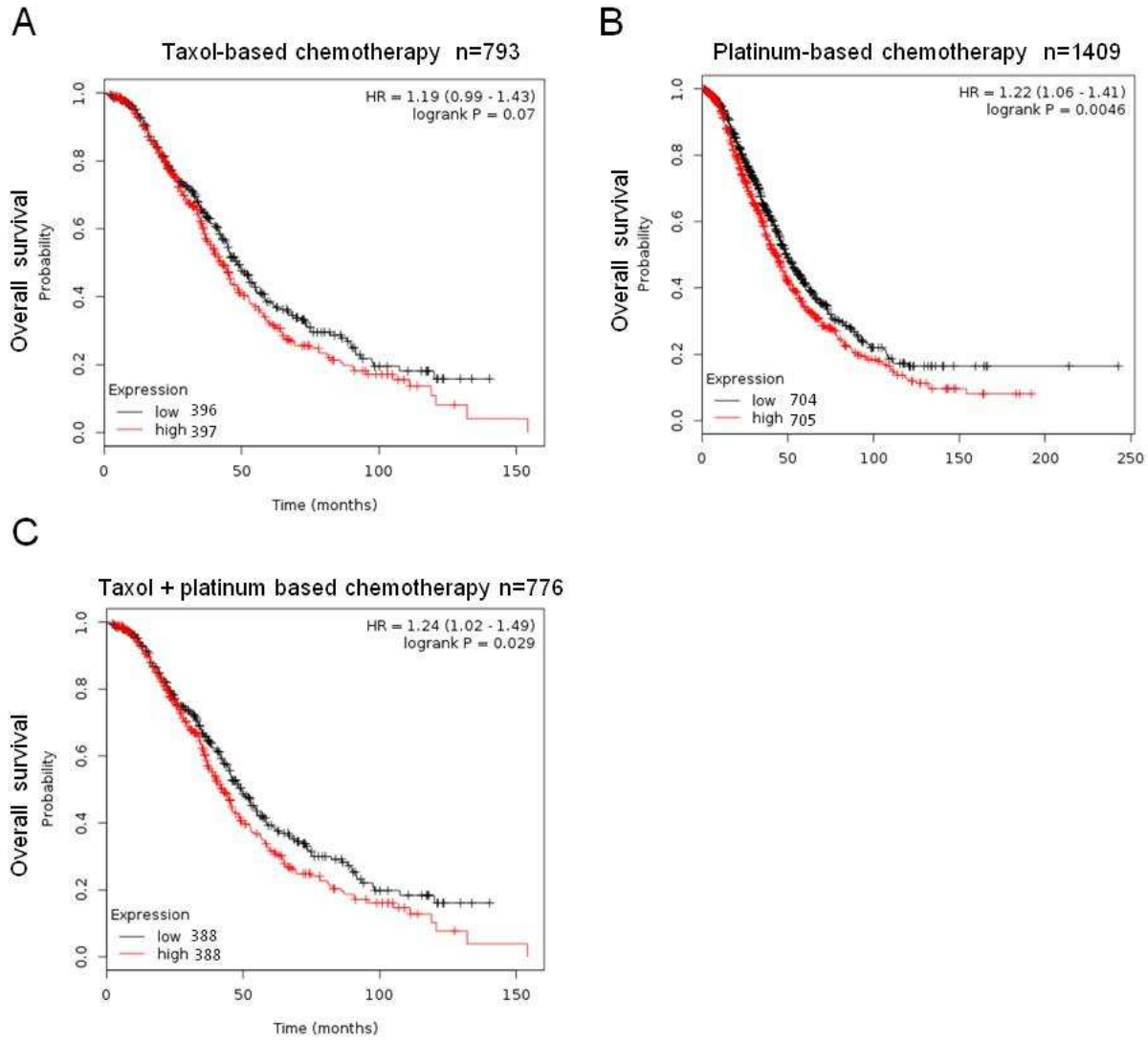

Figure 64. Overall survival analyses associated PTOV1 expression in ovarian cancer patients treated with chemotherapy **(A)**, platinum-based chemotherapy **(B)** or taxol plus platinum **(C)**. Data were analyzed using the Kaplan-Meier plotter tool (http://kmplot.com/analysis/) integrating data from GSE14764; GSE15622; GSE26193; GSE32062; GSE63885; GSE9891; GSE26712; GSE51373; TCGA). Patients were split by median.

8. Analyses of RNA expression and DNA mutation events from metastasis of castration resistant tumors

To study whether the associations of PTOV1 with self-renewal and docetaxel resistant genes found here are detectable in metastasis, we interrogated database containing information from metastatic lesions of prostate cancer patients [236, 237, 240]. Forty-nine metastatic lesions from 114 metastatic specimens had available data for RNA expression. Significantly, 96-100% of those lesions show concurrent increased expression of *PTOV1, CCNG2*, and *MYC* genes (**Figure 65A**). Similarly, concurrent expression is also found for *ALDH1A1* gene in 33% of lesions. Frequent amplifications of

PTOV1, *MYC*, *ALDH1A1* and *CCNG2* genes are found (**Figure 65B**). In addition, very significant co-occurrence of alterations in DNA events is found among *PTOV1*, *ALDH1A1,* and *MYC* (**Table 16**).

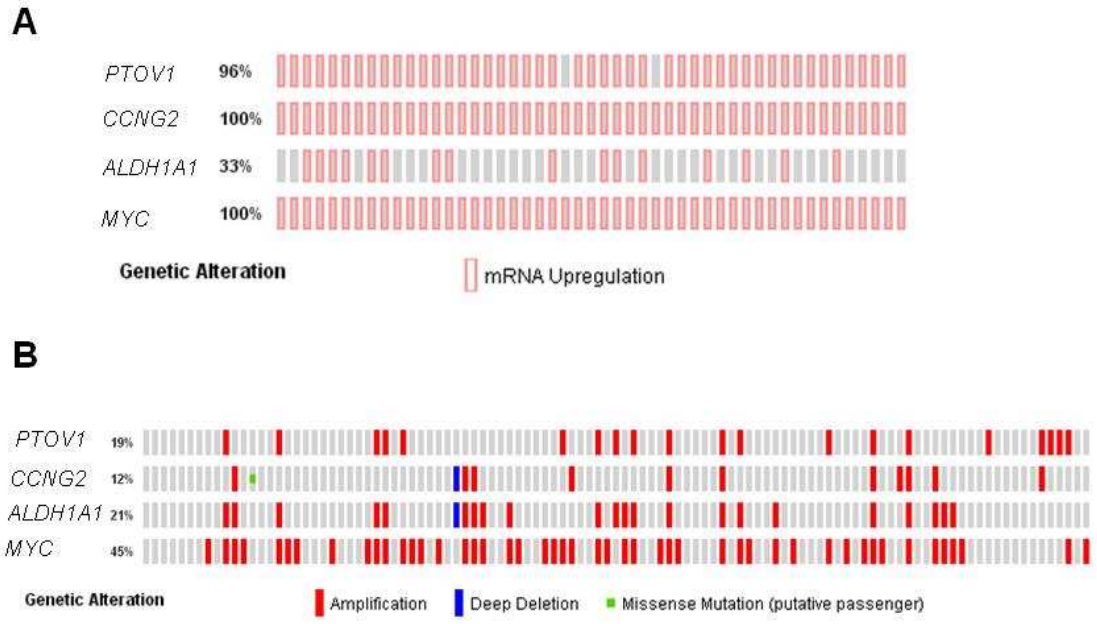

Figure 65. Expression status and mutational profile of PTOV1 and related genes in metastatic lesions from CRPC patients. **(A)** Alteration of gene expression in 49 metastatic specimens from 35 CRPC patients (Beltran *et al*. [240]). **(B)** Copy number alteration and mutations in a cohort of 107 metastatic specimens from 77 patients from Beltran *et al.* [240]. Each bar represents one individual. Vertically aligned bars positions correspond to the same specimen.

Altogether, our findings indicate that the overexpression of PTOV1 in prostate cancer is significantly associated to the acquisition of resistance to chemotherapy with docetaxel, and probably to other chemotherapeutic agents, and to an increase in self-renewal properties of the resistant cells. In addition, the significant concurrent increased expression of *PTOV1, ALDH1A1* and *CCNG2* in primary prostate tumors of patients that develop metastasis is also found in a cohort of metastasic lesions. These findings reveal that the above genes may be predictors of metastasis and bad prognosis.

Gene A	Gene B	p-value	Log Odds ratio
PTOV1	*ALDH1A1*	**<0.001**	2.338
CCNG2	*ALDH1A1*	**<0.001**	2.554
ALDH1A1	*MYC*	**<0.001**	>3
PTOV1	*MYC*	**0.003**	1.591
CCNG2	*MYC*	0.056	1.155
PTOV1	*CCNG2*	0.065	1.191

Table 17. Co-occurrence of DNA alterations in metastatic CRPC. The table shows the quantification (Log Odds ratio) of how strongly the presence of an alteration in gene A is associated with an alteration in the gene B analyzed from published datasets from Beltran *et al.* [240]. Log odds>0: association towards co-occurrence. *p*-value <0.05.

9. Discussion

9.1 PTOV1 promotes docetaxel resistance in prostate cancer cells

In this work we provide evidences supporting a role of PTOV1 in promoting the resistance to docetaxel and self-renewal abilities of prostate cancer cells. We further show that the expression of *PTOV1* and the downstream activated genes *ALDH1A1* and *CCNG2* in primary tumors may be predictive of metastasis and bad prognosis.

We have shown that both DR-Du145 and DR-PC3 cell lines endogenously overexpress PTOV1 at protein levels, however little increase or no increase is observed at transcript levels. This is of relevance because previous microarrays analyses did not reveal significant overexpression of *PTOV1* in DR cells and underscore the importance of post-transcriptional regulatory mechanisms in these phenotypes [69, 302, 304]. Thus, although it is commonly accepted that changes in mRNA abundance are reflected by changes in protein synthesis, numerous exceptions are known [324-326]. Protein stabilization is a common event in the progression of diseases, including cancer [327, 328]. Our own previous data demonstrated that in PC3 cells PTOV1 interacts with RACK1 and ribosomes, promoting global protein synthesis, including the translation of

JUN mRNA without affecting JUN steady-state mRNA levels [101]. Thus, to obtain a clear view of protein expression in specific cell conditions it is crucial to consider both the transcriptome and the proteome. We attempt here to discern the basis of this discordant expression between PTOV1 protein and mRNA levels in prostate cancer cell models, however the experiments performed do not allow us to conclude the cause of this higher increase in PTOV1 protein levels. Western blot analysis of cycloheximide-treated cells has some limitations. For instance, if PTOV1 higher levels in resistant cells are dependent on the specific expression of another protein with shorter half-life, differences in PTOV1 protein stability would not be detected. Perhaps, other methods are more suitable to study the precise measurement of protein stability, for instance pulse-chase and immunoprecipitation assay or measurement of fluorescence of tryptophan [329, 330]. However it is important to remark that differences in PTOV1 mRNA levels are normally observed in tumor tissues compared to benign areas, suggesting that this discordant expression between mRNA and protein levels may be a particular event observed in a particular cell line.

Our data show that not only PTOV1 is associated to more aggressive, potentially resistant stages [72, 73, 100, 101, 104], but also that docetaxel resistant prostate cancer cells express increased levels of this protein concomitantly with genes associated to resistance [302-306]. Significantly, its ectopic expression in docetaxel sensitive cells, significantly increased their IC_{50} to this drug and activated the expression of *ABCB1, TUBB4A*, *TUBB2B, MYC,* and *CCNG2* genes, demonstrating PTOV1 as a relevant factor to overcome toxicity to docetaxel.

The significant increase of *ABCB1* expression, a drug transporter with high affinity for docetaxel but low affinity for cabazitaxel [308, 331], might explain its specific action in inducing cell resistance to docetaxel but not to cabazitaxel. The upregulation of *ABCB1* might be a major mechanism of taxane resistance in an initial response to docetaxel in several advanced tumors, and in Du145, 22Rv1 and C4-2B prostate cancer cell lines [69, 306, 307, 332]. However, the protein ABCB1, not its RNA levels, was shown to correlate with the Gleason score in prostate tumors, possibly explained by a lower efficiency of RNA evaluation in those samples [333]. Here, we demonstrated that increased *ABCB1* levels induced by PTOV1 overexpression are mediated, at least in part, by the JNK pathway and Wnt/β-catenin signaling. Recently, PTOV1 was shown to increase the number of spheres, the proportion of $CD24^-/CD44^+$ cells and the side population (SP) through the activation of Wnt/β-catenin signaling in breast cancer [133].

Several studies described SP cells as populations of cells with stemness features, upregulation of ABCB1 and a taxol-resistant phenotype [334-336]. These observations support our findings and suggest that PTOV1 promotes the acquisition stemness features and the resistance to docetaxel partly through the expression of ABCB1 and Wnt and JNK activation. However, several lines of evidence suggest that PTOV1 has a direct role in the activation of other genes implicated in taxanes resistance, such as *CCNG2*, *TUBB2B* and *ALDH1A1* [304, 337], as observed in ChIP experiments where PTOV1 was detected in the promoter regions of these genes. The expression of specific β-tubulin isotypes including βIVa-tubulin and βIII-tubulin, have often been reported associated to tumor aggressiveness and survival to chemotherapy with taxanes in cancer cell lines and tumors [337-340]. In addition, the activation of Snail1 expression and EMT program by PTOV1 [101] might link to its action in the development to resistance to docetaxel [67, 341].

We showed that higher PTOV1 levels correlates with higher levels of the RNA-binding protein and the key embryonic stem cell factor Lin28A in prostate cancer cells. Lin28A and other members of the family, such as Lin28B, was shown to be frequently overexpressed in human cancers, associates with poor clinical prognosis and its ectopic expression in pancreatic cancer cells increases the ability to form spheres [342-345]. Activation of the Lin28/let-7 axis is critical for cell transformation and promotes a stem-like phenotype by regulating tumor-initiating and self-renewal properties of TICs in human cancers, including prostate cancer [346, 347]. Lin28 was shown to promote the development of resistant to abiraterone and enzalutamide by enhancing the expression of AR splice variants such as ARV7, linking the expression of this protein with the therapeutic stress [348].

The concurrent overexpression of *CCNG2* and *ALDH1A1* found in the cell lines with the ectopic HAPTOV1 is confirmed in primary tumors of patients that developed metastasis and in metastatic lesions of CRPC patients, revealing their participation in the metastatic process. While *ALDH1A1* and *MYC* genes were reported in metastasis of several tumor types and associated with poor prognosis [310, 318, 320, 349, 350], for *CCNG2*, an unconventional cell cycle checkpoint, the association to stemness is not clear. It was described to have tumor suppressor functions in different neoplasias [351, 352], although, supporting our observations, CCNG2 was positively associated with aggressiveness and prostate cancer recurrence after radical prostatectomy [319]. Unpublished data from our group, confirmed a significant increase of *CCNG2* mRNA

expression in prostatospheres derived from prostate cancer cell lines and human prostate tumors along with an increase in other stem cell markers such as *NANOG*, *SOX2* and *ALDH1A1*, suggesting that the expression of CCNG2 may be linked to stemness features. Supporting its oncogenic role, CCNG2 was shown to promote hypoxia-driven local invasion in glioblastoma by controlling cytoskeletal dynamics [353]. Tumor hypoxic microenvironment affects the biology of tumors including apoptosis repression by alteration of pro-survival gene expression, genomic instability, induces invasiveness, neovasculation of tumors, resistance to therapy and contributes to poor prognosis [354, 355]. In primary glioblastoma, CCNG2 is highly expressed in severely hypoxic regions, mainly consisting of actively migrating glioma cells. CCNG2 interacts with actin filaments at membrane ruffles through regulation of the actin-binding proteins cortactin and dynamin 2, and this interaction is required for the motility of glioblastoma cells. CCNG2 is a negative regulator of the cell cycle upregulated in response to DNA damage and was shown to induce microtubule bundling and stability [304, 356-358]. We speculate that additional time in S or G2 phase of the cell cycle coupled with increased DNA repair protein activity may afford a survival advantage over the bulk of cells and contributes to resistance to chemotherapy presumably by facilitating a delay in the cell cycle that may allow reorganization of microtubules and chromatin repairs after drug exposure [304, 356-358].

The development of CRPC was described to lead to increased resistance to docetaxel also in chemotherapy-naïve patients, suggesting that intrinsic chemoresistance may be present in tumors even before drug exposure [359-361]. Chemotherapy effectively induces death of the bulk of proliferating tumor cells and concomitantly results in the enrichment of cell populations characterized by a higher intrinsic resistance, such as TICs, considered major responsible for the poor prognosis of patients with cancer [338, 359, 362]. In line with this possibility, our findings suggest that aggressive tumor cells with increased expression of *PTOV1*, *ALDH1A1*, and *CCNG2* might correspond to populations of cells with stemness features and with great capacity to metastasize and higher resistance to docetaxel.

The analyses of public datasets containing data from untreated patients, do not confirm the statistically significant correlation of *PTOV1* with *ABCB1, TUBB4A, TUBB2B, NANOG, POU5F1,* and *LIN28A* found in the cell line models. This lack of correlation might be related to the metastatic origin of the cell lines from CRPC patients,

a more advanced tumor stage compared to those (untreated) included in the data base [302, 363]. In addition, the known heterogeneous genetic profiles of prostate tumors may not allow to discern those alterations found in isolated cells, that may be present in specific subsets of tumors but become undetectable in a large heterogeneous cohort [122, 333].

Here, we show that breast cancer tumors with no response to taxanes treatment express significantly higher levels of PTOV1 and CCNG2 than tumors with good response to chemotherapy, indicated that the high expression of these proteins may be a predictor of chemotherapy response. In addition, in breast and ovarian cancer patients following different chemotherapies, including taxols, platinums and anthracyclines, higher PTOV1 expression is significantly associated with poor overall survival and shorter times of disease-relapse suggesting a role of PTOV1 in the resistance to other chemotherapeutic agents. Accordingly, PTOV1 has been described as overexpressed in breast cancer tumors in correlation with tumor progression and poor prognosis, and its expression was associated with an increased side population and enrichment of $CD24^{-}$ $CD44^{+}$ breast cancer cells [102, 133].

All together, our findings indicate that *PTOV1* confers prostate cancer cells the advantages to survive docetaxel toxicity, through upregulation of *ABCB1,* and genes involved in docetaxel resistance and pluripotency factors. Of notice, our study identifies *PTOV1, ALDH1A1* and *CCNG2* as potential markers of metastasis and bad prognosis when detected in primary prostate tumors. Our data also suggest that chemotherapy elicits a selective pressure that activates the expression of adaptive capabilities in selected populations of cells within the bulk of a tumor whose proportion may vary depending on their molecular characteristics. Although further validations are required in additional models, our data reveal that PTOV1 might be a marker of chemotherapy response to taxanes and other drugs and a valid future option to prevent the development of resistance to docetaxel in CRPC.

9.2 PTOV1 is required for cell survival and cell cycle progression

We reported here that PTOV1 inhibition causes an accumulation of cells in G2/M phase of the cell cycle followed by cell death. G2/M checkpoint is a cell cycle regulatory point that prevents the initiation of mitosis until DNA replication is completed before completion of S phase and cell cycle is also arrested at the G2 checkpoint in response to

DNA damage [364]. This arrest allows time for the damage to be repaired. Inhibition of RNA, protein synthesis or exposure of cells to certain drugs such as taxanes arrest cells in G2. PTOV1 action was previously found associated to cell cycle progression of prostate cancer cells, with nuclear concentration of the protein at the beginning of S phase and peaking in mitosis [72]. High levels of PTOV1 significantly associated with high expression of Ki67, indicating an association with active proliferation status [72]. Thus, our present observations indicate that PTOV1 is an activator of protein synthesis which function might be critical in the G2 phase before mitosis when there is a need for a rapid synthesis of proteins required for cell division and DNA damage needs to be repaired [101].

On the other hand, we also found that cells treatment with DNA damaging agents also induces the expression of PTOV1. DNA damage response (DDR) mechanisms include both arrest of cells at specific checkpoints of the cell cycle and recruitment of the DNA repair machinery. Cells have different DNA repair pathways that are specific for each set of DNA lesions and involve a complex array of proteins. Increasing evidence support that preferential activation of the DNA damage checkpoint response and overexpression of proteins involved in DNA damage repair, such as ERCC1, Rad51, PARP-1 or Ku70/Ku80, have predictive and prognostic values for various tumor types treated with radiotherapy or chemotherapy [365-372]. Several examples are available: (i) Ku80 overexpression is an independent predictor factor of regional failure and mortality following radiotherapy in head and neck cancer, especially in HPV-negative head and neck squamous cell carcinoma [366]. (ii) In invasive breast carcinoma, nuclear Ku70/Ku80 expression was correlated with features of poor prognosis including lymphovascular invasion, negative estrogen receptor expression, basal-like phenotype and higher histological grade [373]. (iii) A benefit from cisplatin-based adjuvant chemotherapy is associated with the absence of ERCC1 in lung cancer and locally advanced head and neck squamous cell carcinoma [365, 367]. (iv) Interestingly, enhanced expression of DNA polymerase eta (Pol η), characterized by low fidelity and the ability to replicate across certain types of damaged sites in template DNA, contributes to cisplatin resistance of ovarian cancer stem cells [374]. The cisplatin-induced DNA cross-links are bypassed during replication through translesion DNA synthesis. (v) The activation of DNA response and DNA repair capacity have been identified as a mechanism of glioma CSCs that contributes to radioresistance [372]. Finally,

interestingly some oncogenes have been involved in DNA damage repair and their downregulation causes similar effects as those observed upon PTOV1 downregulation [375, 376], including cell cycle arrest, accumulation of γ-H2AX foci and death by apoptosis.

In contrast to what occurs in normal cells, cancer cells have lost one or more DDR pathways, such as genetic alterations and mutations in TP53, BRCA, and Rad51, increased genomic instability that lead cells to a greater dependency on the remaining DDR pathways [364]. The loss of some elements of one DNA repair pathway may be compensated for by the increased activity of other elements or pathways. For instance, Ku70/Ku80 expression was associated with BRCA1 deficient or negative tumors in both hereditary and sporadic breast cancers [373]. In addition, colon cancer cells upregulated the homologous recombination DNA repair pathway to compensate for the loss of base excision repair as a mechanism to overcome resistance to PARP-1 and PARP-2 inhibitors, critical enzymes for DNA damage repair [377]. Because the upregulated DNA repair pathways can cause resistance to DNA-damaging chemotherapy and radiotherapy [367, 373, 374], inhibitors of these pathways can be used as a strategy to sensitize cells to those therapies.

The above findings are interesting in the contest of the structural similarity between the PTOV domain (of MED25) and the β-barrel domains of Ku70/Ku80 heterodimer [88-90] (**Figure 66**). This is one of the first complex binding to the DNA end in the "classical" non-homologous end joining (C-NHEJ) pathway, and is very important in DNA double-strand break (DSB) repair [378]. Ku70/80 binds double-stranded DNA ends and serves as the scaffold to assemble the entire DNA repair complex. In addition, Ku also associates with telomere ends protecting them from being recognized as DSBs and preventing their recombination and degradation.

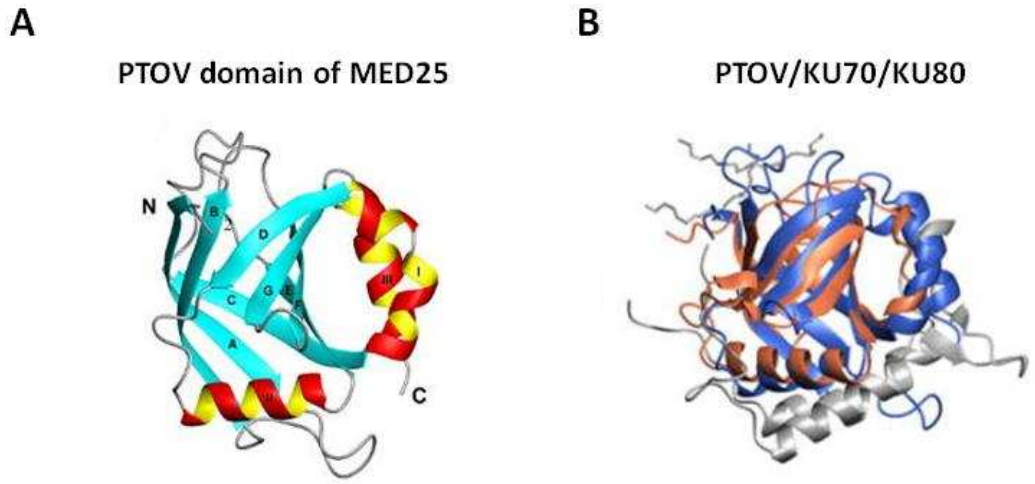

Figure 66. Structural similarity between PTOV domain in MED25 and Ku70/Ku80 heterodimer. **(A)** Ribbon diagram of the lowest-energy conformer of MED25(391–543): α-helices I, II and III are shown in *red* and *yellow*, β-strands A to G are shown in *cyan*, and other polypeptide segments are shown in *gray*. **(B)** Ribbon diagrams of MED25 (391–543) in *blue* and the β-barrel domain of Ku70 subunit (1JEY) in *orange* with the extended loop of residues 276–340 interacting with DNA being omitted for clarity after superposition of C^{α} atoms identified by DALI Regions of Ku80 subunit and DNA backbone interacting with the β-barrel domain are shown in *grey*. Figure adapted from Eletsky, Ruyechan *et al.* [89].

More recently, an extended (e)AT-hook motif was identified in PTOV1 [92]. In addition, very recent data from another member of our group indicate the presence of a new previously unknown canonical AT-hook motif in the A domain of PTOV1, shown by gel electrophoresis mobility shift assay (EMSA), suggesting a function for PTOV1 as DNA binding protein (experiments not shown). Strong support to this *in vitro* observation is provided by the detection of PTOV1 by immunohistochemistry in the nucleus of mitotic cells associated to the compacted chromosomes in colon tumors (**Figure 67**). Additionally, we observed that protein is present both in the cytoplasm and in the nucleus, accordingly to previous data [72]. The subcellular distribution of PTOV1 in breast cancer and nasopharyngeal carcinomas was also detected both in the nucleus and cytoplasm of carcinomatous cells [72, 102, 105]. In urothelial carcinoma PTOV1 nuclear staining was significantly more frequent compared to benign tissue and a reduced cytoplasmic expression significantly correlated with higher pathological stage and grade, suggesting a functional shift for PTOV1 from the cytoplasm to the nucleus in the progression of these tumors [379]. These observations are in line with previous reports showing that intense nuclear PTOV1 expression was able to distinguish in a significant manner high-grade urothelial carcinoma [104]. Very recently, in ESCC the frequence of nuclear PTOV1 staining was significantly higher in metastatic cancer cells [269].Thus, the nuclear presence of PTOV1 might be critical for proliferation and tumor progression,

suggesting that its transcription regulating abilities and potentially its direct binding to DNA, might be relevant for its oncogenic functions.

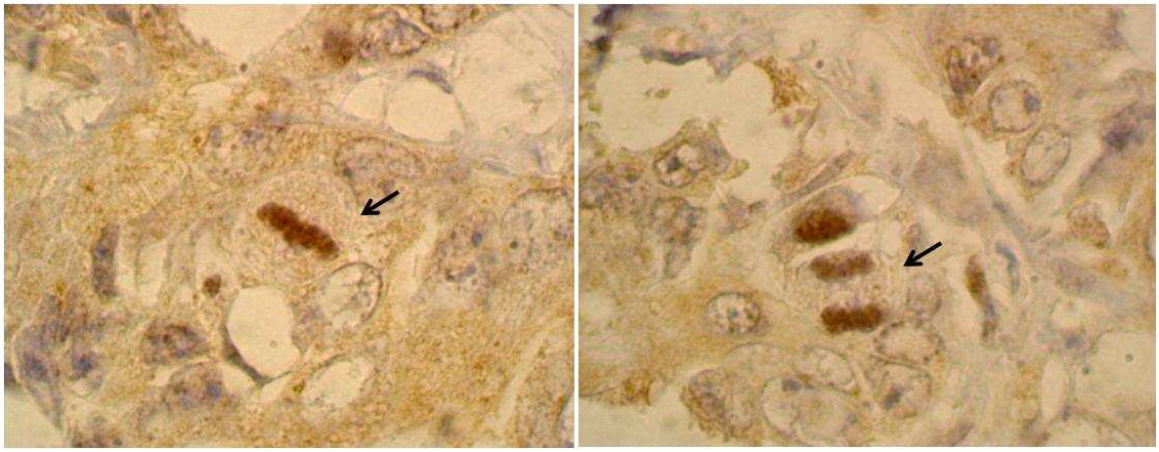

Figure 67. PTOV1 expression in the nucleus of mitotic cells in colon cancer. Arrows indicated mitotic cells.

Altogether, several lines of evidence suggest a critical role of PTOV1 for a proper function of cell cycle progression and point to a possible role in the DNA damage response: i) The protein is overexpressed shortly after treatments with different DNA damage agents, ii) cells knockdown for PTOV1 are unable to progress in the cell cycle, accumulate at the G2/M phase and show an increase in γ-H2AX foci formation and cell death, iii) the resemblance of PTOV domain with secondary structure of Ku70/Ku80, a complex involved in DNA DSB repair, iv) the ability of PTOV1 to bind DNA through its AT-hook domain and (e)AT-hook domain, and v) the association of PTOV1 with poor prognosis in patients treated with DNA damaging agents such as taxols or platinum [92].

These results supports that cells arrested at the end of the G2 phase in PTOV1 knockdowns are unable to bypass the DNA damage checkpoint and enter a programmed cell death suggesting a role of PTOV1 in cell cycle progression and maintenance of DNA integrity. We speculate that in prostate cancer cells with genetic alterations in several DDR pathways, such as mutations in p53 highly reported in prostate cancer tumors [21], cancer cells may increase the expression of proteins involved in alternative DNA repair pathways, including PTOV1 overexpression. Thus, PTOV1 depletion together with mutations in other DDR pathway may lead to cell death. However, further investigation such as studies of colocalization of PTOV1 with other DNA damage response proteins recruited to DSB sites is required to clarify whether PTOV1 has a direct role in the DNA damage response and if so, in which DNA repair pathway could be implicated.

Chapter 8:

TRANSLATIONAL LANDSCAPE OF PROSTATE CANCER CELLS RESISTANT TO ADT AND DOCETAXEL

La feria de Septiembre *(September Fair)*

"This fair is held in the first fortnight of September, granted by King Alfonso X the Wise, and takes in a wide range of celebrations. These include the fun fair, the cattle fair, the Moors and Christians fiesta and the Pilgrimage to La Fuensanta. The September Pilgrimage commemorates the solemn coronation of the Virgin and pilgrimages accompany the city's patron saint, the Virgin of La Fuensanta, to her sanctuary. The Moors and Christians commemorates the founding of Murcia by the Moors and the conquest of the city by Alfonso X the Wise. They parade with their "armies" through the centre of the city. Their eye-catching clothing together with the gun powder and the music, add a touch of historical colour to the September Feria".

A growing body of evidence, including data from our group [101], supports that translational control play an important role in cancer development and progression [380-383]. Changes in different components of the translational machinery can lead to more general changes affecting both global control of protein synthesis and selective translation of specific mRNAs. Therefore, it is of utmost importance to understand the role of mRNA translation and protein synthesis in human cancer. We studied here alterations in translational control associated to the resistance to conventional therapies in prostate cancer.

1. Docetaxel resistant prostate cancer cells have a deacrease in PI3K/AKT/mTOR signaling pathway that affects global protein synthesis rates

We observed a significant decreased cell proliferation in both Du145 and PC3 docetaxel-resistant cells compared to sensitive cells (**Figure 68A**). Because the PI3K/AKT/mTOR pathway is a major regulator of cell proliferation and protein synthesis, we explored whether resistant cells presented alterations in the PI3K/AKT/mTOR pathway. We observed increase protein levels of total eIF4E-BP1 (4E-BP1) and PDCD4 in both DR-Du145 and DR-PC3 cells, well known inhibitors of protein synthesis [178, 384] and a decrease of phosphorylated (p)-AKT (**Figure 68B**). We also observed less phosphorylated eIF4E-BP1 in DR-Du145 cells. Addionally, DR-PC3 but not DR-Du145 cells have a decrease in phosphorylated (p)-eIF4E protein. At RNA level, a significant increase in 4E-BP1, 4E-BP2 and PDCD4 was observed in DR-PC3 cells, in agreement with observations at protein levels (**Figure 68C**). Similarly, DR-Du145 cells show significant increase in 4E-BP1 and PDCD4 and a decrease in (p)-AKT and (p)-eIF4E-BP1 proteins (**Figure 68B**). However, no changes in 4E-BPs at RNA levels were detected, suggesting a post-transcriptional regulation of these factors (**Figure 68C**). These data suggest that the observed decrease in cell proliferation may be due to a significant downregulation of the PI3K/AKT/mTOR signaling activity.

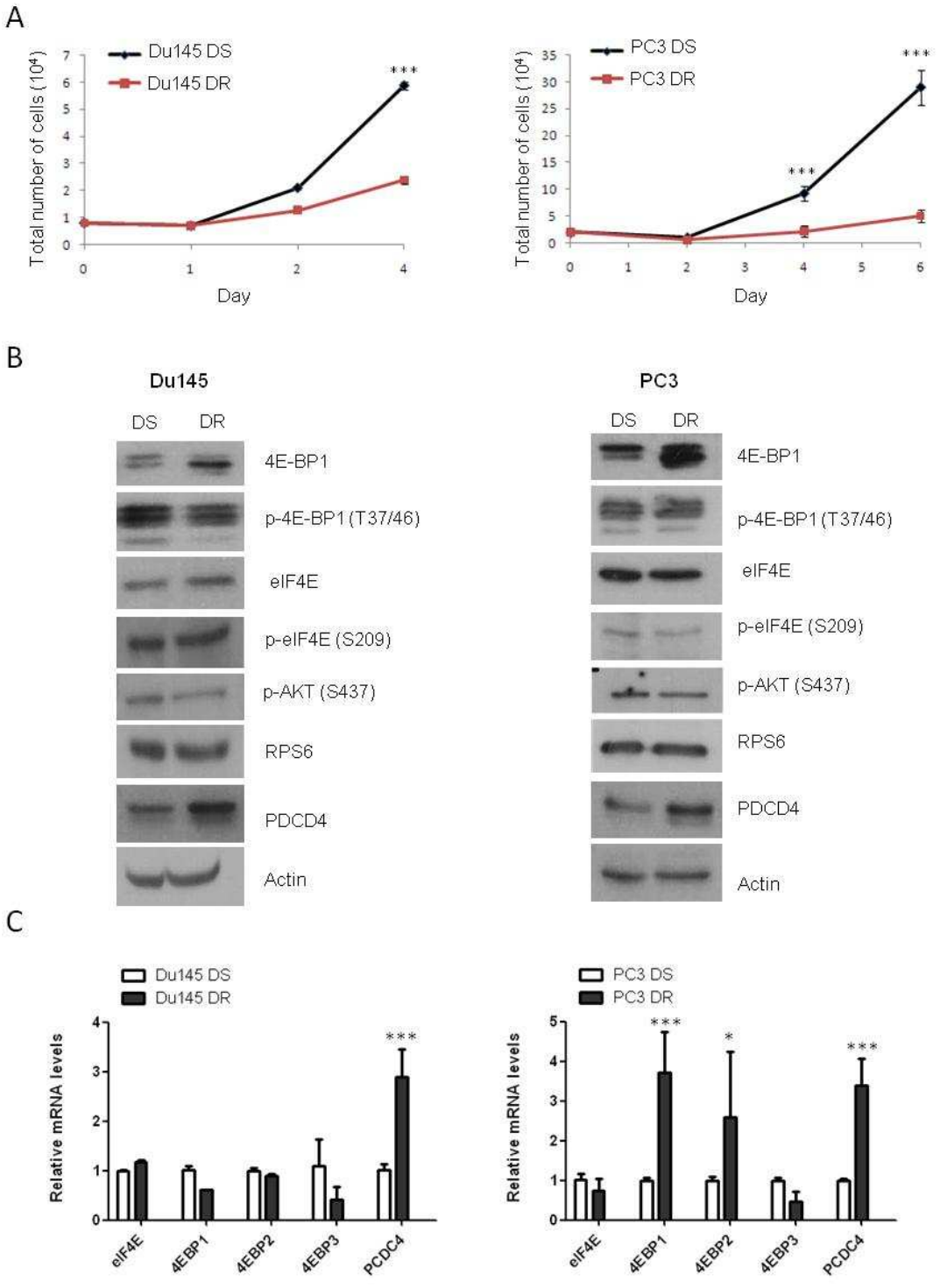

Figure 68. Docetaxel resistant prostate cancer cells have a decrease in cell proliferation and a deregulation of PI3K/AKT/mTOR pathway. **(A)** Growth curve of DS- and DR-Du145 cells and DS-and DR-PC3 cells. **(B)** Immunoblots with the indicated antibodies showing the expression of several components of the PI3K/AKT/mTOR pathway in same cells as (a). **(C)** Endogenous mRNA levels of several components of the PI3K/AKT/mTOR pathway by qRT-PCR in same cells.

Supporting our findings, analyses of published microarray data of docetaxel resistant prostate cancer cells revealed a cluster of genes involved in ribonucleoprotein

complexes formation and protein biosynthesis that are predominantly downregulated in DR prostate cells (**Figure 69**).

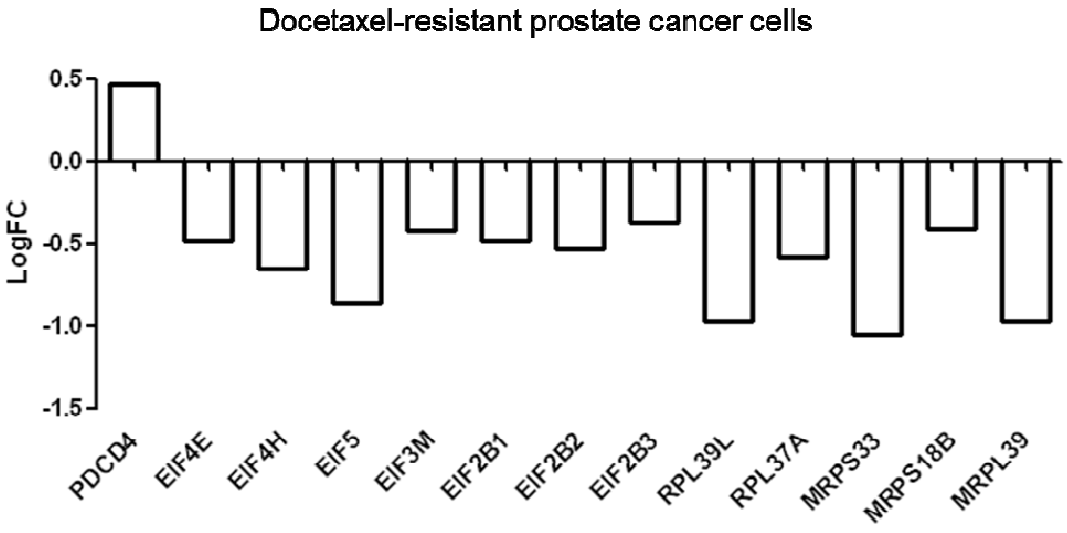

Figure 69. Genes involved in ribonucloprotein complexes formation and protein biosynthesis are downregulated in docetaxel resistant prostate cancer cells. Histogram representing the RNA expression of several genes involved in protein biosynthesis and ribonucleoprotein complexes (logarithm of fold change, logFC) of the analysis of published RNA array data (GSE33455) of Du145 and PC3 docetaxel resistant cells.

We further analyzed whether the rate of protein synthesis in docetaxel resistant prostate cancer cells was affected. As it is shown in **Figure 70A**, using the incorporation of ^{35}S-methionine, the global rate of protein synthesis in DR-PC3 compared to control cells is significantly decreased. However, a small non significant decrease in protein synthesis rate was also observed in DR-Du145 cells. The nonradioactive SUnSET method was additionally employed to monitor mRNA translation in resistant cells [235]. As a positive control for inhibition of protein synthesis, we treated Du145 cells with increasing doses of the protein synthesis inhibitor cycloheximide (**Figure 70B**). These cells exhibit a dramatic decrease in protein synthesis as observed with the SUnSET method. **Figure 70C** shows that DR-PC3 cells have a decrease in the rate of mRNA translation compared to DS cells, as previously observed by the incorporatarion of ^{35}S-methionine. However, no changes in protein synthesis rates were observed in DR-Du145 cells.

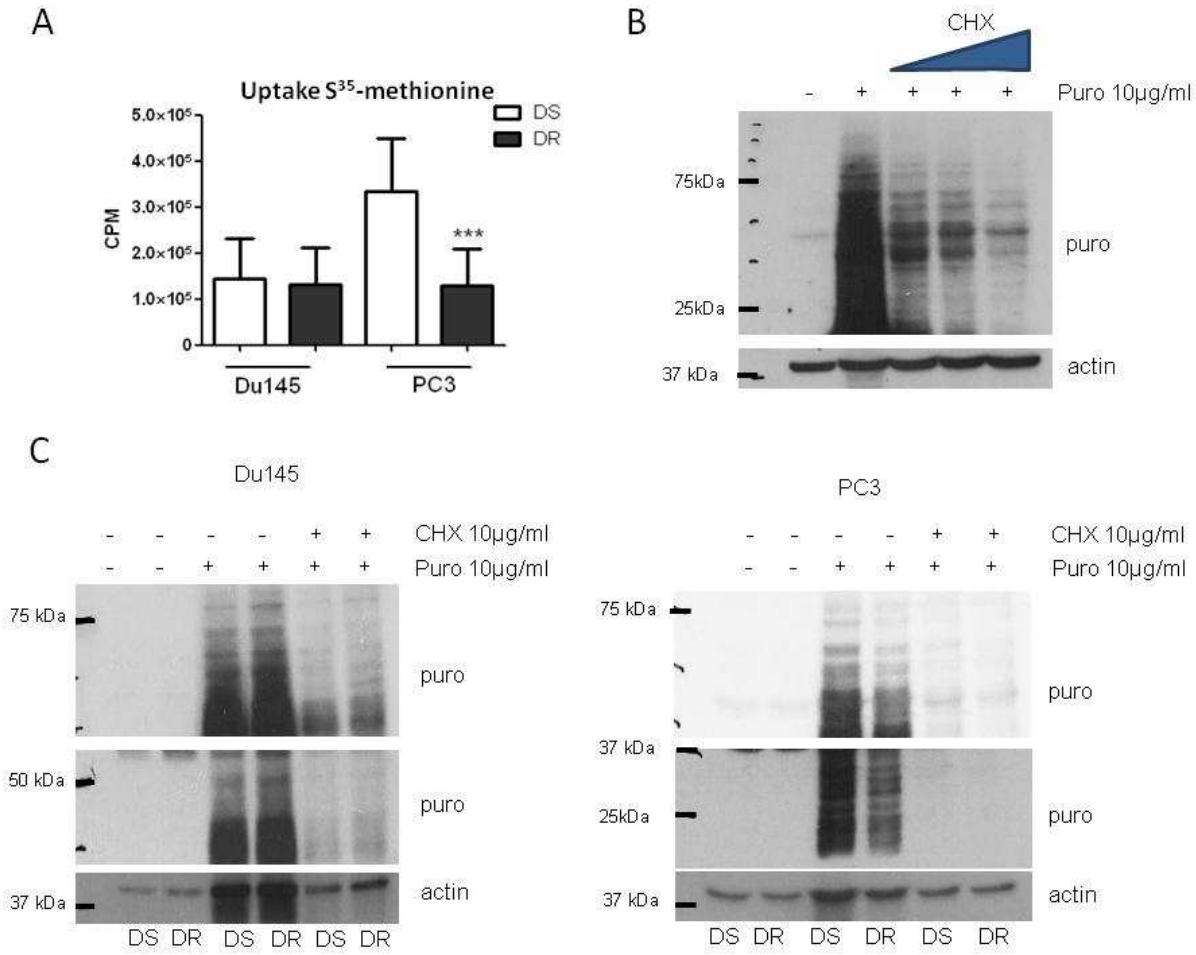

Figure 70. Protein synthesis is inhibited in docetaxel resistant PC3 cells compared to parental cells. **(A)** Histogram representing incorporation of ^{35}S methionine in DS and DR prostate cancer cells. CPM: counts per minute. **(B)** Western blotting showing protein synthesis by SUnSET method in Du145 cells treated with increasing doses (1; 10 and 100 µg/mL) of protein synthesis inhibitor cycloheximide (CHX). Western blotting showing protein synthesis by SUnSET method in DS and DR Du145 **(C)** and DS and DR PC3 cells **(D)**.

The androgen deprivation therapy (ADT) is the standard first-line therapy for patients with early metastatic PCa based on the fact that all prostate cells depend on androgen for their survival [40]. The great majority of these patients initially respond to ADT, however the disease progresses despite of androgen depletion, developing a castration resistant PCa status. Thus, we explored whether the resistance to this therapy also affected proliferation and PI3K/AKT/mTOR pathway. The *in vitro* derived androgen-independent LNCaP cells (LNCaP AI) [385] exhibit a significant impairs in cell proliferation (**Figure 71A**) and a significant increase in several protein synthesis inhibitors such as 4E-BP1, 4E-BP2, 4E-BP3 and PCDC4 (**Figure 71B**). These data, together with previous findings in docetaxel resistant cells suggest that both androgen

deprivation therapy and chemotherapy might select populations of cells with slow-cycling abilities.

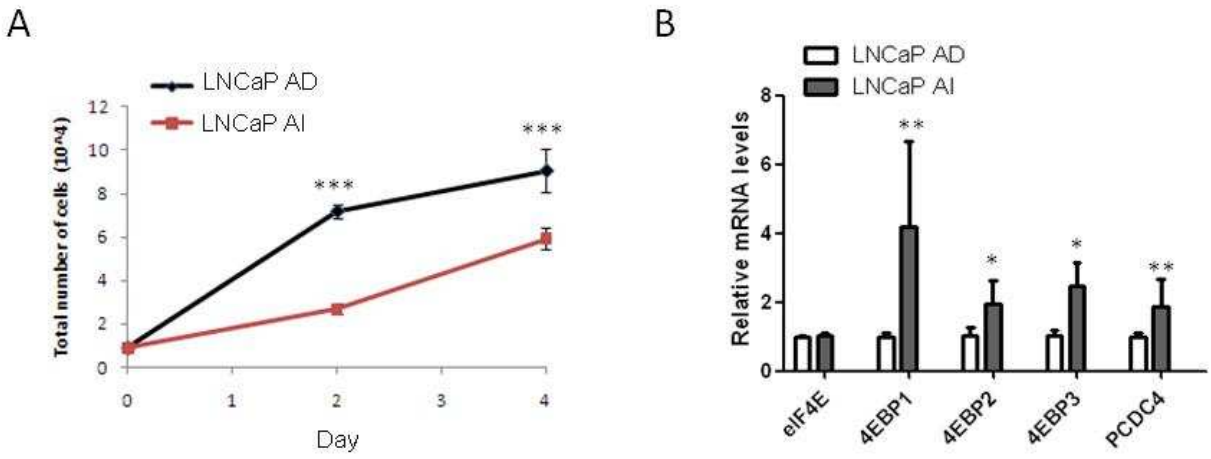

Figure 71. Androgen independent prostate cancer cells have a decrease in cell proliferation and a deregulation of PI3K/AKT/mTOR pathway. **(A)** Growth curve of androgen dependent (AD) and androgen independent (AI) LNCaP cells. **(B)** Endogenous mRNA levels of several components of the PI3K/AKT/mTOR pathway by qRT-PCR in same cells.

Slow-cycling cells have been previously linked to increased tumorigenic capacity [386]. Therefore, we evaluated the tumorigenic capacity of resistant cells *in vitro* by the sphere-formation assay. Analyses of tumorigenic capacity *in vitro* showed an increased number of prostatospheres in androgen independent and docetaxel resistant prostate cancer cells compared to parental cells (**Figure 72A**). We analyzed a stemness gene signature to discern whether these populations of prostate cancer cells that become resistant to conventional therapies, with low proliferation and increased tumorigenic capacity, share expression of some stemness-associated genes. Increased expression of the stemness markers *SOX2*, *NANOG*, *POU5F1*, *CD133* and *CD44* was observed in androgen-independent LNCaP cells (**Figure 72B**), whereas in docetaxel resistant Du145 cells we only observed high expression of *POU5F1* and *LIN28A* (**Figure 72C**). These data suggest that therapies are selecting populations of cells with stemness-like features.

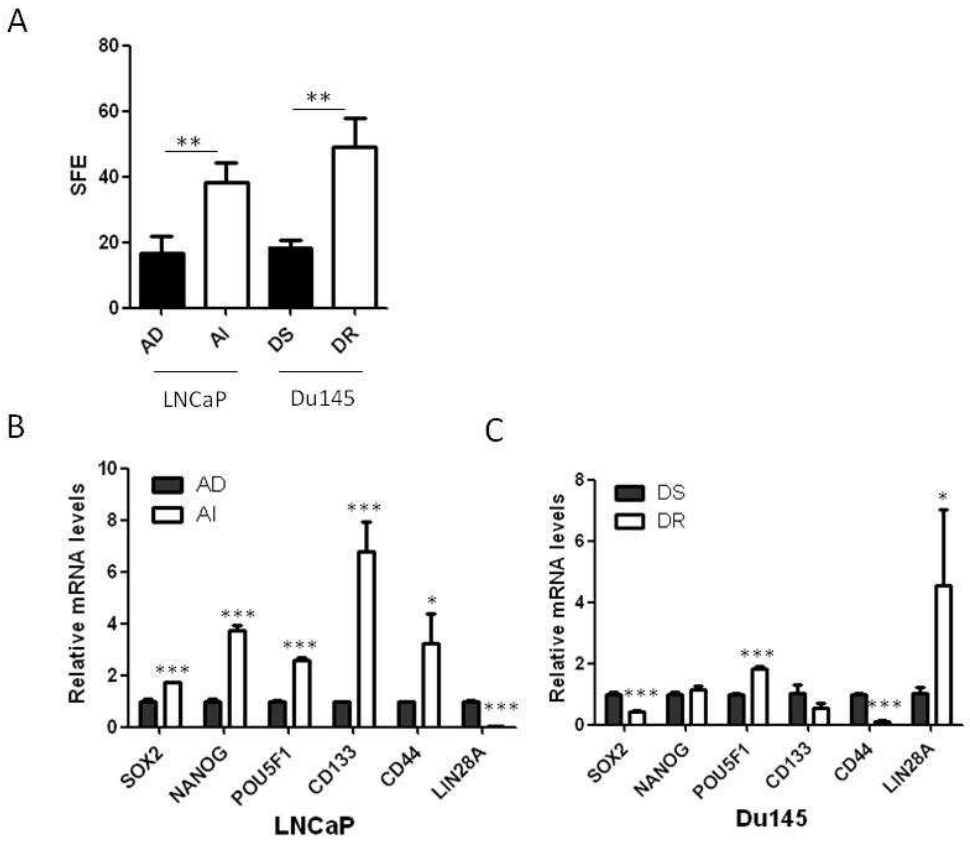

Figure 72. Prostate cancer cells resistant to conventional therapies have increased tumorigenic capacity. **(A)** Quantification of prostatospheres derived from AD and AI LNCaP cells and DS and DR Du145 cells. **(B)** Relative mRNA levels by qRT-PCR of prostatospheres from same cells.

2. Polysome profiling to study mRNA translational efficiency

The distribution of transcripts in polyribosomes reflects the rate of synthesis of their corresponding proteins [214]. The analyses of the polysomal profiles of the cell models LNCaP, Du145 and PC3 reveal that cells resistant to docetaxel or to androgen deprivation have a decrease in polysomal fractions and, especially docetaxel resistant cells tend to accumulate non-actively translating ribosomes (80S fraction), corresponding to cells with a decrease in the mRNA translation rate (**Figure 73**).

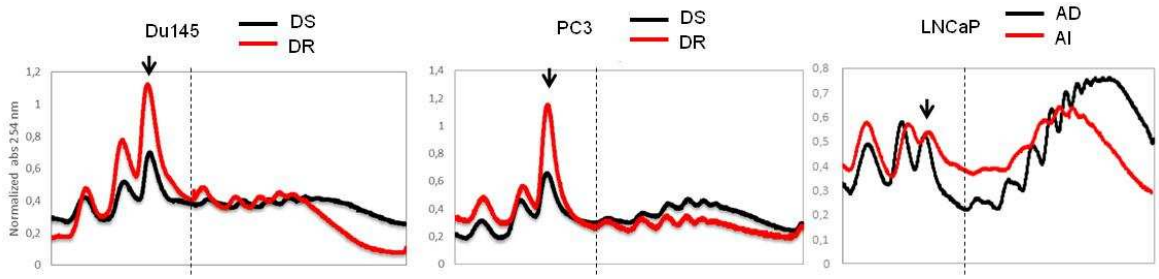

Figure 73. Polysome profiling of resistant prostate cancer cells. For each polysome profile, the first three peak detected before the dashed vertical line represented translationally inactive ribosomes (40S, 60S and 80S), whereas the subsequent series of peaks after the vertical line represented the polysomes with increasing numbers of ribosomes attached to the mRNA. Arrows locate 80S peak.

Isolated RNA molecules from the fractionated polysomes can be coupled to NGS for gene expression screenings at the translational level. Thus, combining sucrose gradient centrifugation with differential screening using NGS enables simultaneous analysis of both transcriptional (total RNA) and translational regulation (polysome-bounded RNA). Since a growing body of evidence indicate that mRNA levels do not necessarily reflect protein levels in cells [325, 326, 387, 388], we decided to explore whether a de-regulation in translation occurs during prostate cancer progression in the acquired resistance to ADT and chemotherapy using this methodology coupled to NGS. For these studies we are collaborating with Prof. Sonenberg's group at the Goodman Cancer Research Centre, McGill University, Montreal (Canada). We performed polysome profiling analyses of resistant and sensitive LNCaP, Du145 and PC3 cells. We isolated total RNA and polysomal-bounded mRNA from polysome fractions and generated mRNA library for RNA sequencing, as illustrates **Figure 74** (more detailed in Material and Methods). The sequencing data are now under analysis. This wide genome approach will allow us to elucidate the mechanisms operating in the control of RNA translational in prostate cancer progression.

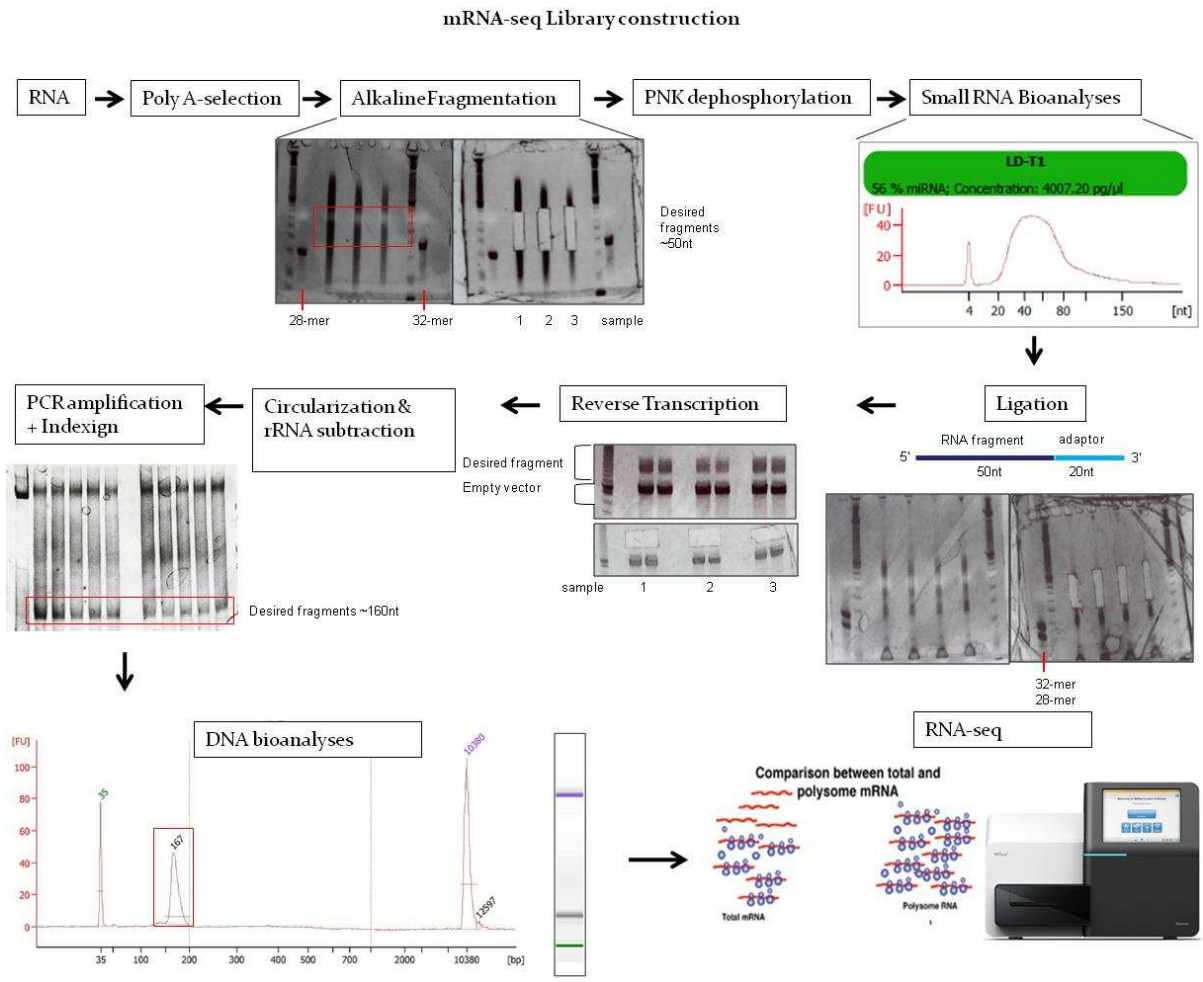

Figure 74. Representative scheme of the mRNA-seq library construction.

3. Discussion

Docetaxel resistant prostate cancer Du145 and PC3 cells show a mesenchymal phenotype with low expression of epithelial markers, *e.g.* downregulation of KRT18 and overexpression of mesenchymal transcription factors including ZEB1, VIM and SNAI1 (see Figure 33), widely reported in docetaxel-resistant cells. Moreover, we showed that both docetaxel resistant and androgen independent prostate cancer cells display a striking decrease in cell proliferation, possess higher *in vitro* tumorigenic capacity and an increased expression of stem-cell like markers compared to parental cells [62, 63]. Supporting our observations, Domingo-Domenech *et al*. [69] demonstrated that KRT18 and KRT19-negative docetaxel-resistant prostate cancer cells and primary metastatic cancer tissue samples exhibit active chemorresistant abilities. *In vivo* experiments demonstrated that docetaxel resistant PCa cells had higher tumor-initiating capacity than

their parental sensitive cells when injected into NOD/SCID IL-2 receptor gamma chain null (NSG) mice [69].

The PI3K/AKT/mTOR signaling pathway, a major regulator of protein synthesis and cell growth [389, 390], has been linked to cell survival, proliferation, growth, differentiation, migration, angiogenesis and cancer progression [102, 391-394]. Docetaxel resistant and androgen independent cells show a downregulation of proteins that trigger PI3K/AKT/mTOR signaling activation (p-AKT, eIF4E) whereas they overexpressed proteins that negatively regulate this pathway such as 4E-BPs and PDCD4. Additionally, the polysome profiles of resistant cells revealed a shift in the proportion of polysomes toward monosomes, with a clear increase of the 80S peak, which are similar to cells with lower protein synthesis rates and inhibition of mTOR pathway [395, 396]. According with our *in vitro* observations, gene expression analyses of androgen-independent, or castration resistant prostate tumors from the primary site of patients who progressed to develop metastasis, revealed downregulation of a main cluster of genes involved in protein biosynthesis and ribonucleoprotein complexes formation [397]. In addition, Puhr *et al*. [63] reported that docetaxel-resistant prostate cancer cells display an increased $CD24^{low}$-$CD44^{high}$ subpopulation compared with their parental counterparts, according to cells with a stemness cell-like phenotype. Here, we reported an increase in self-renewal gene expression (*NANOG*, *POU5F1*, *SOX2*, *CD44* and *CD133)* in androgen independent LNCaP cells, whereas docetaxel resistant cells are enriched in *POU5F1* and *LIN28A*. However, we did not observe an increase in $CD44^{high}$ subpopulation as previously reported in DR-Du145 [63].These observations support the hypothesis that conventional cancer therapies indirectly select for populations of slow cycling cells with stem-cell like features.

Tumors have developed different strategies to satisfy their rapid proliferation and growth requirements, including the deregulation of the initial step of mRNA translation to obtain increased rates of protein synthesis and eventually tumor progression [174-176]. Numerous studies have shown that aggressive tumors possess higher expression and activity of the protein synthesis machinery [380, 383, 398, 399]. However, tumor cell heterogeneity has been widely reported and it is difficult to predict how protein translation is regulated in distinct cell populations that include slow cycling cells. Normal stem cells have a slow-cycling nature as demonstrated by studies employing pulse/chase methodology. These cells undergo few divisions and retain detectable quantities of tritiated thymidine (-TdR) for much longer periods of time that rapidly dividing transit

amplifying (TA) cells [400]. By polysome profiling and gene expression analysis, mouse embryonic stem cells (ESCs) display a striking downregulation of bulk mRNA translation and protein accumulation compared to their differentiated progeny (embryoid bodies) [401]. Differentiation of mESC induces an increase in global transcript levels and leads to more efficient loading of mRNAs into polysomes, increasing protein synthesis and total protein content.

TICs, are expected to share characteristics commonly found in stem cells populations such as the potential to proliferate indefinitely, slow-cycling growth, differential metabolic activity and specific signaling activity, albeit with aberrant regulation [402]. For instance, most early-stage PCa tissues are mainly composed of highly proliferative positive-PSA and -AR cells, whereas advanced PCa mainly comprise poorly differentiated cells, largely negative for PSA and AR expression (PSA-/low) are quiescent or slow cycling cells [403]. These PSA-/low PCa cells undergo asymmetric cell division to generate PSA positive cells, are resistant to chemotherapy and androgen deprivation therapy (ADT) and can initiate tumor development [403]. Additionally, a transcriptome analyses revealed the overexpression of genes involved in anti-stress responses, hypoxia-responsive genes and DNA damage repair genes suggesting that PSA -/low cells may be resistant not only to ADT and chemotherapeutic agents but also to other stresses. This internally slow cycling rate is believed to provide inherent defense against chemotherapeutic agents, which affect mainly fast dividing cells [403]. Accordingly, slow-cycling cells, isolated by label retention technique with the lipophilic labeling dye DiI from pancreas adenocarcinoma cells, were shown to be more resistant to chemotherapeutic treatment than fast-cycling cells and were able to recreate the initial heterogeneous tumor cell population [404]. This population of slow-cycling cells exhibited a more mesenchymal phenotype, with increased invasive and tumorigenic potential *in vivo* [404].

Using mouse skin stem cells, Blanco *et al*. [405] demonstrated that activation of stress response pathways leads both a global reduction of protein synthesis and altered translational programs that together promote stem cell functions and tumorigenesis. Forced reduction of protein synthesis by genetic deletion of the RNA-methyltransferase NSun2, that modulates global translation by protecting tRNAs from cleavage, enriches for tumour-initiating cells [405]. NSun2 ablation reduces protein synthesis in tumors and knockout NSun2 mice develop tumours with increased undifferentiated populations.

Hsieh *et al.* [406] found in a preclinical trial that tumors that are resistant to inhibition of the PI3K-AKT-mTOR pathway presented an enrichment of a specific population of tumor-forming luminal prostate epithelial cells with high levels of 4EBP1 and low protein synthesis rates [406]. These findings suggest that different thresholds of protein synthesis rates can prime cells for drug resistance. In addition, human samples from a phase 2 clinical trial with a PI3K inhibitor (BKM120) showed higher amount of 4EBP1 after treatment with this PI3K inhibitor [406].

Our above findings suggest that conventional cancer treatments, including androgen suppression and chemotherapies, target and kill rapidly proliferating cells in heterogeneous tumor populations, while quiescent and slow cycling cells survive. These cells would have the ability to produce rapidly dividing progenitor cells that can re-establish the tumor.

Most attempts to determine the mRNA profile of androgen independent cells and chemoresistant cells have made use of total RNA for gene expression analysis [69, 302, 304, 397]. However, as it has been explained earlier, several lines of evidence suggest that translational control is a central regulator of gene expression in cancer [182, 207]. Besides being global translation rates commonly enhanced in cancer cells, it is known that oncogenic signaling also induces transcript-specific changes in translation. Many cellular mechanisms, such as self-renewal, differentiation and inflammation are also dependent on the control of protein synthesis by posttranscriptional mechanisms and thus, using mRNA levels as a read out of protein abundance is not always accurate [216, 401, 407-410]. The use of the polysome profiling method coupled to RNA sequencing is useful for analysis of the translation state of many different RNAs in the cell and provides information on the UTR sequences. For instance, RNA-seq analysis comparing both total mRNA fraction and the subpopulation of mRNAs associated with translating ribosomes showed that there is a percentage of mRNAs regulated at translational level or at the level of transcript stability which is directly related to the length of their UTRs [217]. In particular, these genes encode proteins involved in the oxidative stress response which contributes to a protective response against the oxidative stress that may occur during adipogenic differentiation or lipid metabolism. Additionally, Wong *et al.* [409] separated mRNAs based on their ribosomal load and identified a significant proportion of variant mRNAs in ESCs and ESC derived Neural Precursor cells (NPCs) with differential translation rates. These differences in translation rates correlated with processing events

that affect 5' and 3' UTR sequences, with 5'UTR sequences having a predominant role suggesting that mRNA variants containing alternate UTRs are under different post-transcriptional controls. Moreover, LIN28, widely known for its negative regulation of let-7 microRNA expression, was shown to exhibit let-7 independent functions [407, 411]. LIN28 preferentially associates with a small subset of cellular mRNAs in human ESCs (hESCs) encoding RNP proteins, ribosomal proteins, proteins participating in translation and involved in cellular metabolism and embryonic development [407]. Polysome profiling suggests that LIN28, through its interaction with RNA helicase A (RHA), stimulates the translation of many targets such as *POU5F1, HMGA1, RPS13* and *EEF1G*, important for the growth and survival of hESCs. LIN28 most likely exerts its biological effects by binding to its RNA targets and LIN28 -responsive elements (LREs) have been found in coding regions of target genes.

Additional evidences of the importance of addressing translational control in cancer comes from Hsieh *et al.* [207] and Jechlinger *et al.* [412] studies, in which they provide genome-wide characterization of translationally controlled mRNAs involved in epithelial plasticity, invasion and metastasis, downstream of oncogenic mTOR signaling. This repertoire of mRNAs contains new specific sequences of response to mTOR, known as pyrimidine-rich translational element (PRTE), shown to be crucial for expression of a subset of mRNAs involved in invasion, cell proliferation and metastasis. This group includes *YB1* (Y-box binding protein 1), vimentin, *MTA1* (metastasis associated 1) and *CD44* [207]. Taken together these data indicate that translation can be controlled on a global level, through regulation of eIFs factors, or on specific mRNAs regulation, and therefore it demonstrates the importance of addressing the study of translation regulation in cancer initiation and progression through methods that allow the genome-scale profiling of mRNA translation.

Polysome Profiling *versus* Ribosome Profiling: advantages and limitations

To obtain the translatome profiling of androgen and docetaxel resistant prostate cancer cells we employed the polysome profiling approach. The main difference between the RiboPro and the PolyPro lies on the possibility to obtain position-specific information regarding the location of ribosomes on mRNA transcripts. The importance of this information relies in identification of physiological situations where ribosomes stall on an

mRNA transcript without producing a protein and do not translate the main open reading frame (ORF) but translate upstream open reading frames (uORFs) [219-221] (**Figure 75A**). However, the analyses of the immense amount of data from the ribosome profiling could entail a challenge because it depends on precise mapping of small fragments (short ribosome-protected fragments of about 30 nucleotides) on the genome. Moreover, because ribosome profiling is focused on the footprint of individual ribosomes rather than on entire transcripts and utilizes nuclease digestion for that purpose, some important information, e.g. coming from the 5' and 3' UTRs, can be lost. Nonetheless, this limitation can be complemented by polysome profile that is useful for study transcripts variants differing in their 5' and/or 3' UTRs [413, 414]. One important limitation of the RiboPro is the impossibility to discern among distinct mRNA subpopulations translated at different levels and therefore constituted by different numbers of ribosomes (**Figure 75B**). In contrast, PolyPro allows to distinguish between a uniform decrease in the number of ribosomes on all copies of a transcript and a complete repression of a sub-population of mRNAs [401]. For instance, recent efforts to identify mTOR-sensitive mRNAs have resulted in conflicting results [415]. Whereas PolyPro suggested that mTOR regulates translation of both 5'-terminal oligopyrimidine (TOP) mRNAs and non-TOP mRNAs identifying them as mTOR sensitive, the RiboPro showed limited efficiency and only allowed the identification of TOP mRNAs. Profiling 5'UTRs of non-TOP mRNAs revealed two different subsets of mTOR-sensitive mRNAs encoding proteins with different biologic functions and that require different translation initiation factors [415]. It is certain that PolyPro approach presents some technical difficulties in resolving the exact number of ribosomes bound to highly ribosome-loaded transcripts and to cleanly resolve more than five ribosomes per transcript it requires a skilled investigator. Analytical and technical biases should be taken into consideration when performing transcriptome-wide analysis of translational regulation. Nonetheless, both approaches are commonly applied, thereby indicating the lack of a consensus regarding optimal data analysis.

In this study, by using the polysome profiling approach we aim to discern selective regulation of a subset of mRNAs among resistant cells that might help us to elucidate the mechanisms operating in the control of RNA translational in prostate cancer progression, especially in the development of resistance to current therapies.

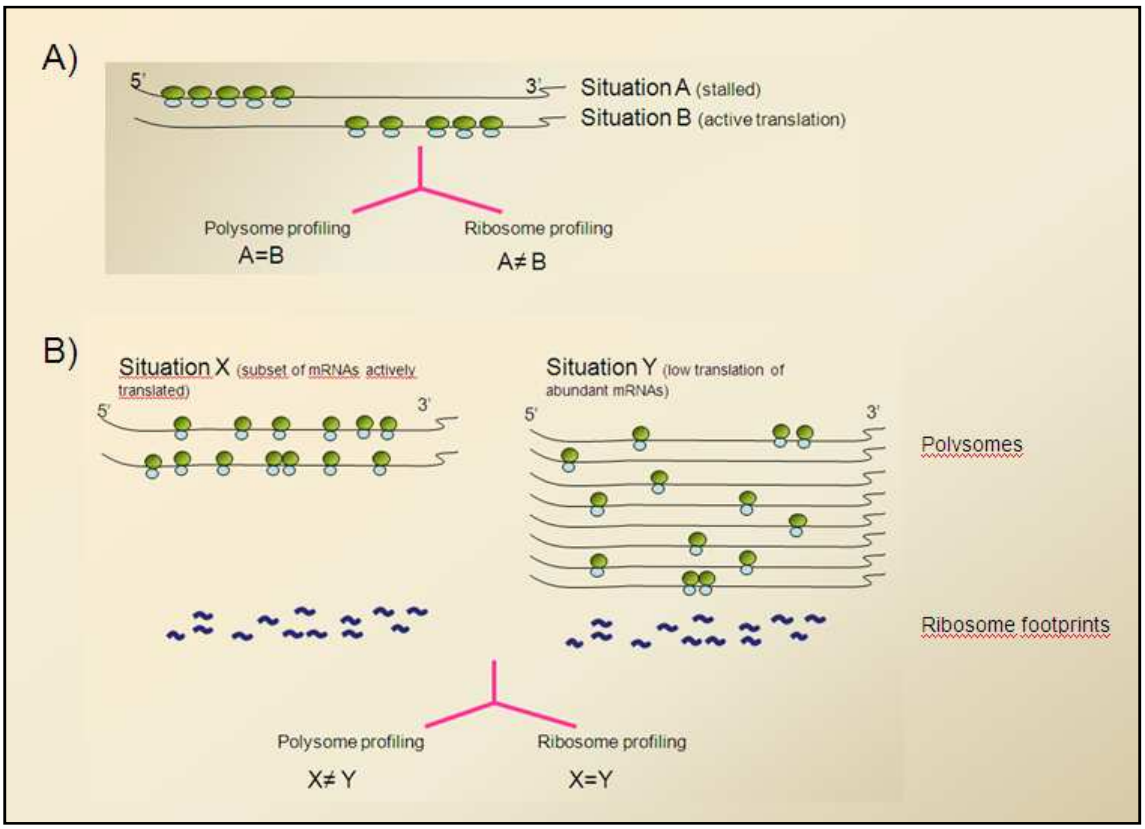

Figure 75. Polysome profiling vs Ribosome profiling: two perspectives from the same translational situation.

Chapter 9:

DISCUSSION

Regional Natural Parks. Las Salinas de San Pedro del Pinatar (left) and Calblanque beach (right)

"The San Pedro salt marshes Regional Park (left picture), situated in the northem part of the Mar Menor, lies on the Mediterranean coastal fringes and it is about 6 kilometres long. Due to his high natural value, this wetland was declared in 1998 a Special Protection Bird Area, being part of the European Natura 2000 network. Calblanque (right picture) is a protected natural beach of high landscape value. This beach is located within the regional park Parque Regional de Calblanque, one of the best preserved unspoilt natural landscapes on the coast. Its enormous natural wealth is based on its arid mountains, its long, ochre and golden-coloured beaches as well as its lonely coves, the formation of its fossil dunes, its white salt lakes and its mountain massifs, which contrast with the blue sea."

A model for PTOV1 actions

One main objective of this present thesis was the study of the functions of PTOV1 in prostate cancer progression and the development and maintenance of resistance to chemotherapy with taxanes. The peculiar structure of PTOV1 protein with one tandem duplicated domain, together with its little resemblance with any other protein motif, makes difficult the study of PTOV1 function based on examination of its sequence. By integration of previous data with the most recently described actions of PTOV1, mostly based in its interactions with other proteins, we proposed a mechanistic model (**Figure 76**). PTOV1, as a nucleocytoplasmic shuttling protein, may have dual functions in the regulation of gene expression at transcriptional and translational levels.

In the nucleus, by direct or indirect association to specific promoters, PTOV1 can activate or repress transcription of a number of genes related to cell proliferation, survival, EMT, and chemoresistance. The protein is found associated with the regulatory regions of at least three genes where it recruits deacetylases and other DNA modifying enzymes to modulate transcription. The association with transcriptional repressor complexes, including HDACs and NCoR, has been reported for the repression of a few genes (*HES1, HEY1*, and *DKK1*) [100, 133]. Transcriptional repression by PTOV1 might also occur through an association with activators, such CBP in the *RARβ2* gene. In this case, the complex PTOV1-CBP is not bound to chromatin, but the protein competes with MED25 sequestering the activator away from the Polymerase II complex [110]. Conceivably, the association CBP-PTOV1 could also act promoting transcription in different genes. Here, we reported for the first time that the association of PTOV1 with promoter regions of several genes (*CCNG2*, *TUBB2B*, and *ALDH1A1*) is able to activate their transcription. However, the upregulation of ABCB1 expression by PTOV1 seems to be mediated by the activation of JNK and Wnt/β-catenin pathway. In the cytoplasm, PTOV1 regulates protein synthesis by direct association with RACK1 and 40S ribosomes in translation pre-initiation complexes [101]. In PTOV1 overexpressing cells, significantly more JUN mRNA levels were loaded on polysomes compared to actin, but PTOV1 is not found in polysomal fractions, suggesting that its action is directed to translation initiation, possibly mediating the recruitment of specific mRNA-protein complexes to ribosomes.

Significant for these dual functions that we described for PTOV1 is the very recent identification of the N-terminal (e)AT-hook motif, that binds with higher affinity to RNA [92], and the canonical AT-hook motif that we found in the A domain that allow the protein to bind directly to DNA (V Maggio, V Canovas, C Ciudad and R Paciucci, unpublished observations). Nucleic acids binding through the (e)AT-hook and canonical AT-hook would feasibly allow simultaneous interactions of PTOV1 with different factors binding the A and B domains. For example, PTOV1 may interact with DNA and protein complexes in promoters, or with ribonucleoprotein complexes charged with specific mRNAs to be translated. Interestingly, the nuclear subcellular localization of the specific interactions mediated by the A domain with HDAC1 and RBP-jκ, are coupled to actions in the regulation of transcription [100]. In contrast, the interactions with cytoplasmic RACK1 and Flotillin-1, exclusively engaging the B domain are linked to activities more closely related to protein synthesis [100, 150]. All together these evidences indicate that PTOV1 might be a new moonlighting protein able to perform different activities in the cell [416], and may utilize separate protein surfaces for its multiple actions [417]. Examples of moonlighting or multitasking proteins have been described in many species including animals [418]. For instance, the ATF2 transcription factor has a role in the DNA damage response that is uncoupled from its transcriptional activity [419]. Also, STAT3 represents a genuine moonlighting protein acting as a transcription factor that translocates to the nucleus to regulate gene expression and independently with a mitochondrial function in the cellular respiration [420].The overexpression of a single protein with multiple actions that converge in activation of proliferation, survival and drug-resistance is energetically convenient for a tumor cell, and might contribute to the acquisition of stemness features. Many questions remain to be solved to understand what is the biological role of PTOV1 in normal tissues, or how does the protein promote tumor progression. The evidences so far suggest that the potential therapeutic effects of its specific targeting in aggressive cancer cells is worthy of being studied.

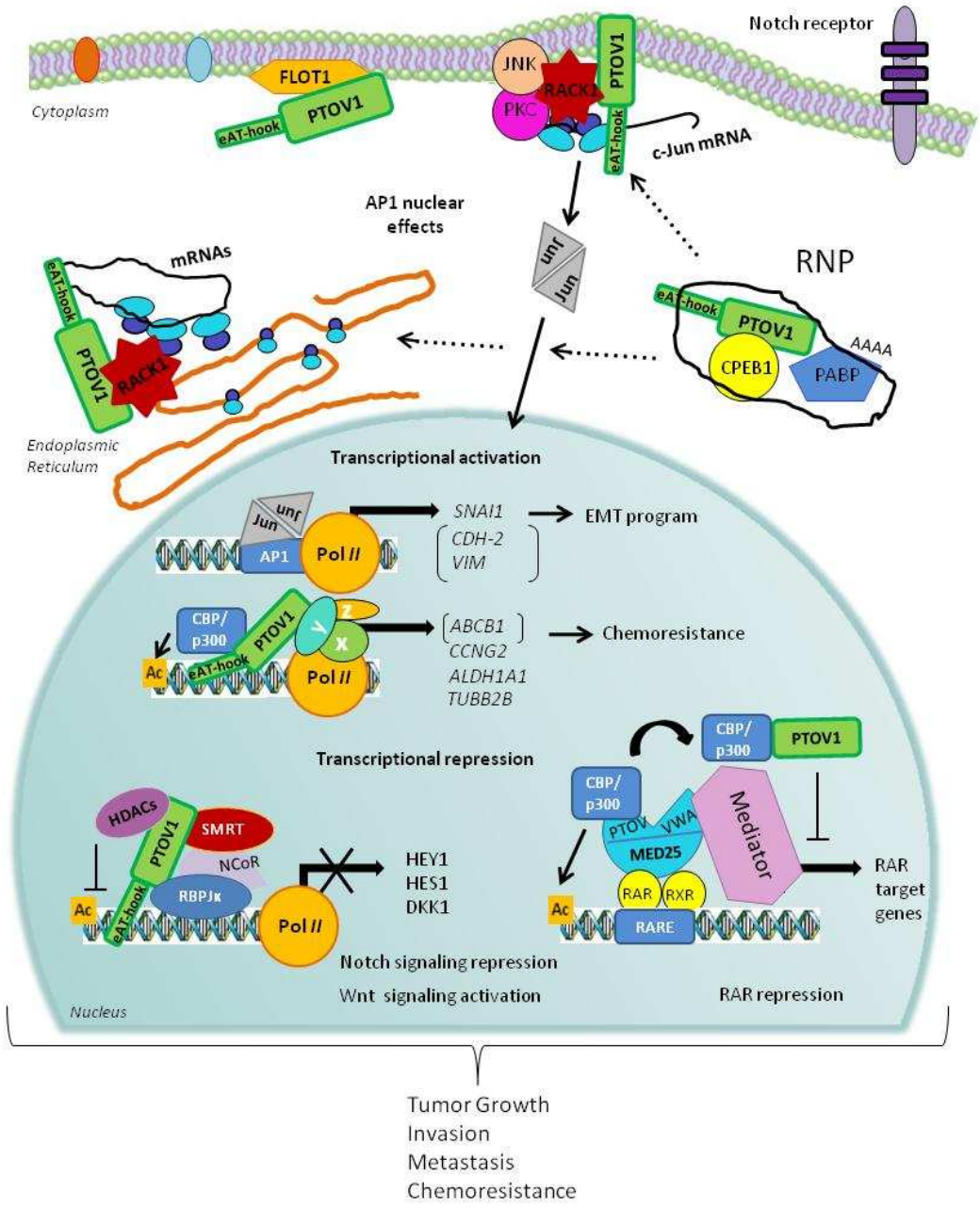

Figure 76. A mechanistic model for PTOV1 actions in cancer progression. PTOV1 can shuttle from the cytoplasm to the nucleus during the progression of the cell cycle. In the cytoplasm, PTOV1 is found at perinuclear and submembranes regions associated to Flotillin-1 and also RACK1 and ribosomes. The latter, likely occur in RNA-protein complexes (RNP) that modulate mRNA translation, including the synthesis of the oncogene c-Jun. In the nucleus, PTOV1 can regulate the expression of a number of genes related to cell proliferation, survival, EMT, and chemoresistance, by direct or indirect (genes shown in parenthesis) association to specific promoters to activate or repress transcription. In turn, c-Jun/AP1 may directly or indirectly contribute to the action of PTOV1 as a transcription factor. PTOV1 is a repressor for the regulation of *HES1, HEY1* and *DKK1*. These effects negative regulate Notch signaling in PCa and Wnt/β-catenin signaling in breast cancer. In both tumors, these effects culminate with increased tumor growth, invasion, metastasis, and chemoresistance. PTOV1 as a transcriptional repressor requires the presence of HDACs, suggesting that it is an epigenetic regulator. An additional mechanism for transcriptional repression was suggested for the *RAR* promoter, where PTOV1 sequesters the activator CBP from MED25, and suppresses transcription of RAR targets. The action of PTOV1 of sequestering activators from MED25 might be associated to

inhibition of other MED25 targets. The recent identification of the nucleic acid-binding motif (e)AT-hook, at the N-terminal region of PTOV1 gives support to its role in regulation of gene expression by direct DNA or RNA binding.

Chapter 10:

CONCLUSIONS

Traditional food. Pastel de carne (left) and Paparajotes (right)

The Murcian meat pie -left image- is a puff pastry pie stuffed mainly with veal, sausage, egg and spices. It is one of the great history dishes of the city and has important Arab roots. It is still made today with the same recipe as was laid down in the 1695 Ordananza. A penalty of two years of exile and a sanction of three thousand maravedis was imposed on anyone who employed goat or sheep meat and lower quality flour for its elaboration. On the right, the "paparajote", also ligated to Arab tradition, is a typical Murcian dessert made with lemon leaves covered with a mass made basically with flour and egg that are fried and sprinkled with sugar and cinnamon.

1. PTOV1 induces a partial epithelial-mesenchymal transition by promoting *JUN* mRNA translation, c-Jun protein increase and activation of *SNAI1* and *VIM* transcription in prostate cancer cells.
2. PTOV1 and c-Jun are required for the full tumorigenic and metastatic abilities of prostate cancer cells. The knockdown of PTOV1 inhibited the expression and activity of c-Jun and decreased cell proliferation *in vitro* and tumor growth *in vivo*.
3. PTOV1 is overexpressed in docetaxel resistant CRPC cells and increases docetaxel resistance of non-resistant prostate cancer cells. This action is associated to the upregulation of *ABCB1* and *LIN28A* transcript levels and to the binding of PTOV1 to the chromatin of promoters of *CCNG2*, *TUBB2B* and *ALDH1A1*.
4. PTOV1 contributes to increase prostate cancer cells tumorigenic abilities *in vitro,* by inducing the expression of self-renewal genes *ALDH1A1*, *LIN28A*, *MYC*, *NANOG*, *POU5F1*.
5. PTOV1 is critical for survival of prostate cancer cells. The knockdown of PTOV1 induces G2/M cell cycle arrest and apoptosis of castration resistant prostate cells.
6. The mRNA expression of *PTOV1*, *ALDH1A1,* and *CCNG2* significantly correlates with prostate tumor aggressiveness and higher Gleason scores. *PTOV1, ALDH1A1,* and *CCNG2* transcripts levels are significantly higher in primary prostatic adenocarcinomas of patients that after radical prostatectomy developed regional or distal metastasis, and metastatic lesions have high expression of these genes, supporting their relationship in the metastatic process.
7. PTOV1 expression correlates with poor prognosis and high risk of relapse in colon, lung, pancreas and breast cancer. Increased levels of *PTOV1* were found in bad responders to chemotherapy with taxanes and correlates with lower relapse-free survival and distant-metastasis free survival probability in breast cancer patients.
8. Prostate cancer cells resistant to androgen suppression and/or to docetaxel have a decreased cell proliferation, PI3K/AKT/mTOR signaling, and a lower rate of mRNA translation. These resistant populations of slow-growing cells overexpress different pluripotency genes and have increased tumorigenic potential *in vitro*.

Chapter 11:

BIBLIOGRAPHY

Real Casino de Murcia (Murcia's Royal Casino)

"Murcia's Royal Casino is an extravagant architectural relic from the late 19th century, and features quite an eclectic mixture of design styles, from Modernist to Neonazari.It is located on Traperia Street, not far from the cathedral. Its construction started in 1847. It was completely restored between 2006 and 2009 thus given the title 'Royal' from H.M. King Juan Carlos I of Spain. Though a private social club, the recently restored building is open for tourist visits and events. While there, you can explore its many rooms and halls, including the Arabic patio, noted for its iron and glass dome; the lavish dance hall complete with paintings, gilt detailing, and giant, sparkling chandeliers; and the main gallery, a covered passageway illuminated by light that pours in from the windowed ceiling. More rooms and opulent corners abound, from the luxurious ladies' room to the glamorous, wooden-shelved library".

1. Selman SH. The McNeal prostate: a review. Urology. 2011; 78(6):1224-1228.
2. Lee JJ, Thomas IC, Nolley R, Ferrari M, Brooks JD and Leppert JT. Biologic differences between peripheral and transition zone prostate cancer. Prostate. 2015; 75(2):183-190.
3. Taylor RA, Toivanen R and Risbridger GP. Stem cells in prostate cancer: treating the root of the problem. Endocr Relat Cancer. 2010; 17(4):R273-285.
4. Verze P, Cai T and Lorenzetti S. The role of the prostate in male fertility, health and disease. Nat Rev Urol. 2016; 13(7):379-386.
5. Wilson JD. The critical role of androgens in prostate development. Endocrinol Metab Clin North Am. 2011; 40(3):577-590, ix.
6. Heinlein CA and Chang C. Androgen receptor in prostate cancer. Endocr Rev. 2004; 25(2):276-308.
7. Siegel RL, Miller KD and Jemal A. Cancer statistics, 2016. CA Cancer J Clin. 2016; 66(1):7-30.
8. Mottet N, Bellmunt J, Bolla M, Briers E, Cumberbatch MG, De Santis M, Fossati N, Gross T, Henry AM, Joniau S, Lam TB, Mason MD, Matveev VB, Moldovan PC, van den Bergh RC, Van den Broeck T, et al. EAU-ESTRO-SIOG Guidelines on Prostate Cancer. Part 1: Screening, Diagnosis, and Local Treatment with Curative Intent. Eur Urol. 2017; 71(4):618-629.
9. Chang JM, Lee HJ, Lee SE, Byun SS, Choe GY, Kim SH, Seong CK and Kim SH. Pictorial review: Unusual tumours involving the prostate: radiological-pathological findings. Br J Radiol. 2008; 81(971):907-915.
10. Board PDQCGE. (2002). Genetics of Prostate Cancer (PDQ(R)): Health Professional Version. PDQ Cancer Information Summaries. (Bethesda (MD): National Cancer Institute (US)).
11. Wu CP and Gu FL. The prostate in eunuchs. Prog Clin Biol Res. 1991; 370:249-255.
12. Ross RK, Pike MC, Coetzee GA, Reichardt JK, Yu MC, Feigelson H, Stanczyk FZ, Kolonel LN and Henderson BE. Androgen metabolism and prostate cancer: establishing a model of genetic susceptibility. Cancer Res. 1998; 58(20):4497-4504.
13. Chrisofos M, Papatsoris AG, Lazaris A and Deliveliotis C. Precursor lesions of prostate cancer. Crit Rev Clin Lab Sci. 2007; 44(3):243-270.
14. Liu W, Laitinen S, Khan S, Vihinen M, Kowalski J, Yu G, Chen L, Ewing CM, Eisenberger MA, Carducci MA, Nelson WG, Yegnasubramanian S, Luo J, Wang Y, Xu J, Isaacs WB, et al. Copy number analysis indicates monoclonal origin of lethal metastatic prostate cancer. Nat Med. 2009; 15(5):559-565.
15. Mehra R, Han B, Tomlins SA, Wang L, Menon A, Wasco MJ, Shen R, Montie JE, Chinnaiyan AM and Shah RB. Heterogeneity of TMPRSS2 gene rearrangements in multifocal prostate adenocarcinoma: molecular evidence for an independent group of diseases. Cancer Res. 2007; 67(17):7991-7995.
16. Greene DR, Wheeler TM, Egawa S, Dunn JK and Scardino PT. A comparison of the morphological features of cancer arising in the transition zone and in the peripheral zone of the prostate. J Urol. 1991; 146(4):1069-1076.
17. Shen MM and Abate-Shen C. Molecular genetics of prostate cancer: new prospects for old challenges. Genes Dev. 2010; 24(18):1967-2000.
18. Kaffenberger SD and Barbieri CE. Molecular subtyping of prostate cancer. Curr Opin Urol. 2016; 26(3):213-218.
19. Barbieri CE, Demichelis F and Rubin MA. Molecular genetics of prostate cancer: emerging appreciation of genetic complexity. Histopathology. 2012; 60(1):187-198.
20. Barbieri CE, Bangma CH, Bjartell A, Catto JW, Culig Z, Gronberg H, Luo J, Visakorpi T and Rubin MA. The mutational landscape of prostate cancer. Eur Urol. 2013; 64(4):567-576.
21. Barbieri CE and Tomlins SA. The prostate cancer genome: perspectives and potential. Urol Oncol. 2014; 32(1):53.e15-22.

22. Nelson WG, Yegnasubramanian S, Agoston AT, Bastian PJ, Lee BH, Nakayama M and De Marzo AM. Abnormal DNA methylation, epigenetics, and prostate cancer. Front Biosci. 2007; 12:4254-4266.
23. Samaratunga H, Delahunt B, Yaxley J, Srigley JR and Egevad L. From Gleason to International Society of Urological Pathology (ISUP) grading of prostate cancer. Scand J Urol. 2016:1-5.
24. Cheng L, Montironi R, Bostwick DG, Lopez-Beltran A and Berney DM. Staging of prostate cancer. Histopathology. 2012; 60(1):87-117.
25. Schalken J, Dijkstra S, Baskin-Bey E and van Oort I. Potential utility of cancer-specific biomarkers for assessing response to hormonal treatments in metastatic prostate cancer. Ther Adv Urol. 2014; 6(6):245-252.
26. Leapman MS, Nguyen HG and Cooperberg MR. Clinical Utility of Biomarkers in Localized Prostate Cancer. Curr Oncol Rep. 2016; 18(5):30.
27. Loeb S, Sanda MG, Broyles DL, Shin SS, Bangma CH, Wei JT, Partin AW, Klee GG, Slawin KM, Marks LS, van Schaik RH, Chan DW, Sokoll LJ, Cruz AB, Mizrahi IA and Catalona WJ. The prostate health index selectively identifies clinically significant prostate cancer. J Urol. 2015; 193(4):1163-1169.
28. Makarov DV, Loeb S, Getzenberg RH and Partin AW. Biomarkers for prostate cancer. Annu Rev Med. 2009; 60:139-151.
29. Luo J, Zha S, Gage WR, Dunn TA, Hicks JL, Bennett CJ, Ewing CM, Platz EA, Ferdinandusse S, Wanders RJ, Trent JM, Isaacs WB and De Marzo AM. Alpha-methylacyl-CoA racemase: a new molecular marker for prostate cancer. Cancer Res. 2002; 62(8):2220-2226.
30. Harden SV, Guo Z, Epstein JI and Sidransky D. Quantitative GSTP1 methylation clearly distinguishes benign prostatic tissue and limited prostate adenocarcinoma. J Urol. 2003; 169(3):1138-1142.
31. Knezevic D, Goddard AD, Natraj N, Cherbavaz DB, Clark-Langone KM, Snable J, Watson D, Falzarano SM, Magi-Galluzzi C, Klein EA and Quale C. Analytical validation of the Oncotype DX prostate cancer assay - a clinical RT-PCR assay optimized for prostate needle biopsies. BMC Genomics. 2013; 14:690.
32. Narayan VM, Konety BR and Warlick C. Novel biomarkers for prostate cancer: An evidence-based review for use in clinical practice. Int J Urol. 2017; 24(5):352-360.
33. Armstrong AJ, Eisenberger MA, Halabi S, Oudard S, Nanus DM, Petrylak DP, Sartor AO and Scher HI. Biomarkers in the management and treatment of men with metastatic castration-resistant prostate cancer. Eur Urol. 2012; 61(3):549-559.
34. Heidegger I, Heidenreich A and Pfister D. New Biomarkers for Selecting the Best Therapy Regimens in Metastatic Castration-Resistant Prostate Cancer. Target Oncol. 2017; 12(1):37-45.
35. Cooperberg MR, Broering JM, Litwin MS, Lubeck DP, Mehta SS, Henning JM, Carroll PR and Ca PI. The contemporary management of prostate cancer in the United States: lessons from the cancer of the prostate strategic urologic research endeavor (CapSURE), a national disease registry. J Urol. 2004; 171(4):1393-1401.
36. Crawford ED, Petrylak D and Sartor O. Navigating the evolving therapeutic landscape in advanced prostate cancer. Urol Oncol. 2017; (35S):S1:S13.
37. Dinh JA, Baker D and Chahal M. Therapy Update for Metastatic Castration-Resistant Prostate Cancer. Consult Pharm. 2016; 31(10):581-592.
38. Rini BI and Small EJ. Hormone-refractory Prostate Cancer. Curr Treat Options Oncol. 2002; 3(5):437-446.
39. Chandrasekar T, Yang JC, Gao AC and Evans CP. Mechanisms of resistance in castration-resistant prostate cancer (CRPC). Transl Androl Urol. 2015; 4(3):365-380.
40. Cornford P, Bellmunt J, Bolla M, Briers E, De Santis M, Gross T, Henry AM, Joniau S, Lam TB, Mason MD, van der Poel HG, van der Kwast TH, Rouviere O, Wiegel T and Mottet N. EAU-ESTRO-SIOG Guidelines on Prostate Cancer. Part II: Treatment of Relapsing, Metastatic, and Castration-Resistant Prostate Cancer. Eur Urol. 2017; 71(4):630-642.

41. Kirby M, Hirst C and Crawford ED. Characterising the castration-resistant prostate cancer population: a systematic review. Int J Clin Pract. 2011; 65(11):1180-1192.
42. Tannock IF, Osoba D, Stockler MR, Ernst DS, Neville AJ, Moore MJ, Armitage GR, Wilson JJ, Venner PM, Coppin CM and Murphy KC. Chemotherapy with mitoxantrone plus prednisone or prednisone alone for symptomatic hormone-resistant prostate cancer: a Canadian randomized trial with palliative end points. J Clin Oncol. 1996; 14(6):1756-1764.
43. Bates D and Eastman A. Microtubule destabilising agents: far more than just antimitotic anticancer drugs. Br J Clin Pharmacol. 2017; 83(2):255-268.
44. James ND, Sydes MR, Clarke NW, Mason MD, Dearnaley DP, Spears MR, Ritchie AW, Parker CC, Russell JM, Attard G, de Bono J, Cross W, Jones RJ, Thalmann G, Amos C, Matheson D, et al. Addition of docetaxel, zoledronic acid, or both to first-line long-term hormone therapy in prostate cancer (STAMPEDE): survival results from an adaptive, multiarm, multistage, platform randomised controlled trial. Lancet. 2016; 387(10024):1163-1177.
45. Tassinari D, Tamburini E, Gianni L, Drudi F, Fantini M, Santelmo C, Stocchi L, Montanari F and Sartori S. Early Docetaxel and Androgen Deprivation in the Treatment of Metastatic, Hormone-Sensitive Prostate Cancer. Rev Recent Clin Trials. 2016; 11(4):317-323.
46. Gravis G, Boher JM, Joly F, Soulie M, Albiges L, Priou F, Latorzeff I, Delva R, Krakowski I, Laguerre B, Rolland F, Theodore C, Deplanque G, Ferrero JM, Culine S, Mourey L, et al. Androgen Deprivation Therapy (ADT) Plus Docetaxel Versus ADT Alone in Metastatic Non castrate Prostate Cancer: Impact of Metastatic Burden and Long-term Survival Analysis of the Randomized Phase 3 GETUG-AFU15 Trial. Eur Urol. 2016; 70(2):256-262.
47. Nakazawa M, Paller C and Kyprianou N. Mechanisms of Therapeutic Resistance in Prostate Cancer. Curr Oncol Rep. 2017; 19(2):13.
48. Sun Y, Zou Q, Sun Z, Li C, Du C, Chen Z, Shan Y, Huang Y, Jin J, Ye ZQ, Xie L, Lin G, Feng Y, De Porre P, Liu W and Ye D. Abiraterone acetate for metastatic castration-resistant prostate cancer after docetaxel failure: A randomized, double-blind, placebo-controlled phase 3 bridging study. Int J Urol. 2016; 23(5):404-411.
49. Shameem R, Hamid MS, Xu KY and Wu S. Comparative analysis of the effectiveness of abiraterone before and after docetaxel in patients with metastatic castration-resistant prostate cancer. World J Clin Oncol. 2015; 6(4):64-72.
50. Sanford M. Enzalutamide: a review of its use in metastatic, castration-resistant prostate cancer. Drugs. 2013; 73(15):1723-1732.
51. Rathkopf DE, Antonarakis ES, Shore ND, Tutrone RF, Alumkal JJ, Ryan CJ, Saleh M, Hauke RJ, Bandekar R, Chow Maneval E, de Boer CJ, Yu MK and Scher HI. Safety and Antitumor Activity of Apalutamide (ARN-509) in Metastatic Castration-Resistant Prostate Cancer with and without Prior Abiraterone Acetate and Prednisone. Clin Cancer Res. 2017.
52. Imamura Y and Sadar MD. Androgen receptor targeted therapies in castration-resistant prostate cancer: Bench to clinic. Int J Urol. 2016; 23(8):654-665.
53. Schweizer MT and Antonarakis ES. Chemotherapy and its evolving role in the management of advanced prostate cancer. Asian J Androl. 2014; 16(3):334-340.
54. Yap TA, Smith AD, Ferraldeschi R, Al-Lazikani B, Workman P and de Bono JS. Drug discovery in advanced prostate cancer: translating biology into therapy. Nat Rev Drug Discov. 2016; 15(10):699-718.
55. Thadani-Mulero M, Portella L, Sun S, Sung M, Matov A, Vessella RL, Corey E, Nanus DM, Plymate SR and Giannakakou P. Androgen receptor splice variants determine taxane sensitivity in prostate cancer. Cancer Res. 2014; 74(8):2270-2282.
56. Darshan MS, Loftus MS, Thadani-Mulero M, Levy BP, Escuin D, Zhou XK, Gjyrezi A, Chanel-Vos C, Shen R, Tagawa ST, Bander NH, Nanus DM and Giannakakou P. Taxane-induced blockade to nuclear accumulation of the androgen receptor predicts clinical responses in metastatic prostate cancer. Cancer Res. 2011; 71(18):6019-6029.

57. Zhu ML, Horbinski CM, Garzotto M, Qian DZ, Beer TM and Kyprianou N. Tubulin-targeting chemotherapy impairs androgen receptor activity in prostate cancer. Cancer Res. 2010; 70(20):7992-8002.
58. Shalli K, Brown I, Heys SD and Schofield AC. Alterations of beta-tubulin isotypes in breast cancer cells resistant to docetaxel. FASEB J. 2005; 19(10):1299-1301.
59. Fojo T and Menefee M. Mechanisms of multidrug resistance: the potential role of microtubule-stabilizing agents. Ann Oncol. 2007; 18 Suppl 5:v3-8.
60. Antonarakis ES, Keizman D, Zhang Z, Gurel B, Lotan TL, Hicks JL, Fedor HL, Carducci MA, De Marzo AM and Eisenberger MA. An immunohistochemical signature comprising PTEN, MYC, and Ki67 predicts progression in prostate cancer patients receiving adjuvant docetaxel after prostatectomy. Cancer. 2012; 118(24):6063-6071.
61. Hanrahan K, O'Neill A, Prencipe M, Bugler J, Murphy L, Fabre A, Puhr M, Culig Z, Murphy K and Watson RW. The role of epithelial-mesenchymal transition drivers ZEB1 and ZEB2 in mediating docetaxel-resistant prostate cancer. Mol Oncol. 2017; 11(3):251-265.
62. Marin-Aguilera M, Codony-Servat J, Reig O, Lozano JJ, Fernandez PL, Pereira MV, Jimenez N, Donovan M, Puig P, Mengual L, Bermudo R, Font A, Gallardo E, Ribal MJ, Alcaraz A, Gascon P, et al. Epithelial-to-mesenchymal transition mediates docetaxel resistance and high risk of relapse in prostate cancer. Mol Cancer Ther. 2014; 13(5):1270-1284.
63. Puhr M, Hoefer J, Schafer G, Erb HH, Oh SJ, Klocker H, Heidegger I, Neuwirt H and Culig Z. Epithelial-to-mesenchymal transition leads to docetaxel resistance in prostate cancer and is mediated by reduced expression of miR-200c and miR-205. Am J Pathol. 2012; 181(6):2188-2201.
64. Chaffer CL, San Juan BP, Lim E and Weinberg RA. EMT, cell plasticity and metastasis. Cancer Metastasis Rev. 2016; 35(4):645-654.
65. Kalluri R and Weinberg RA. The basics of epithelial-mesenchymal transition. J Clin Invest. 2009; 119(6):1420-1428.
66. Batlle E, Sancho E, Franci C, Dominguez D, Monfar M, Baulida J and Garcia De Herreros A. The transcription factor snail is a repressor of E-cadherin gene expression in epithelial tumour cells. Nat Cell Biol. 2000; 2(2):84-89.
67. Kurrey NK, Jalgaonkar SP, Joglekar AV, Ghanate AD, Chaskar PD, Doiphode RY and Bapat SA. Snail and slug mediate radioresistance and chemoresistance by antagonizing p53-mediated apoptosis and acquiring a stem-like phenotype in ovarian cancer cells. Stem Cells. 2009; 27(9):2059-2068.
68. Seruga B, Ocana A and Tannock IF. Drug resistance in metastatic castration-resistant prostate cancer. Nat Rev Clin Oncol. 2011; 8(1):12-23.
69. Domingo-Domenech J, Vidal SJ, Rodriguez-Bravo V, Castillo-Martin M, Quinn SA, Rodriguez-Barrueco R, Bonal DM, Charytonowicz E, Gladoun N, de la Iglesia-Vicente J, Petrylak DP, Benson MC, Silva JM and Cordon-Cardo C. Suppression of acquired docetaxel resistance in prostate cancer through depletion of notch- and hedgehog-dependent tumor-initiating cells. Cancer Cell. 2012; 22(3):373-388.
70. Fernandez S, Mosquera JL, Alana L, Sanchez-Pla A, Morote J, Ramon YCS, Reventos J, de Torres I and Paciucci R. PTOV1 is overexpressed in human high-grade malignant tumors. Virchows Arch. 2011; 458(3):323-330.
71. Morote J, Fernandez S, Alana L, Iglesias C, Planas J, Reventos J, Ramon Y Cajal S, Paciucci R and de Torres IM. PTOV1 expression predicts prostate cancer in men with isolated high-grade prostatic intraepithelial neoplasia in needle biopsy. Clinical cancer research : an official journal of the American Association for Cancer Research. 2008; 14(9):2617-2622.
72. Santamaria A, Fernandez PL, Farre X, Benedit P, Reventos J, Morote J, Paciucci R and Thomson TM. PTOV-1, a novel protein overexpressed in prostate cancer, shuttles between the cytoplasm and the nucleus and promotes entry into the S phase of the cell division cycle. Am J Pathol. 2003; 162(3):897-905.

73. Benedit P, Paciucci R, Thomson TM, Valeri M, Nadal M, Caceres C, de Torres I, Estivill X, Lozano JJ, Morote J and Reventos J. PTOV1, a novel protein overexpressed in prostate cancer containing a new class of protein homology blocks. Oncogene. 2001; 20(12):1455-1464.
74. Diamandis EP, Yousef GM, Luo LY, Magklara A and Obiezu CV. The new human kallikrein gene family: implications in carcinogenesis. Trends Endocrinol Metab. 2000; 11(2):54-60.
75. Simoes VL, Alves MG, Martins AD, Dias TR, Rato L, Socorro S and Oliveira PF. Regulation of apoptotic signaling pathways by 5alpha-dihydrotestosterone and 17beta-estradiol in immature rat Sertoli cells. J Steroid Biochem Mol Biol. 2013; 135:15-23.
76. Yousef GM, Scorilas A and Diamandis EP. Genomic organization, mapping, tissue expression, and hormonal regulation of trypsin-like serine protease (TLSP PRSS20), a new member of the human kallikrein gene family. Genomics. 2000; 63(1):88-96.
77. Yousef GM, Luo LY, Scherer SW, Sotiropoulou G and Diamandis EP. Molecular characterization of zyme/protease M/neurosin (PRSS9), a hormonally regulated kallikrein-like serine protease. Genomics. 1999; 62(2):251-259.
78. Aken BL, Ayling S, Barrell D, Clarke L, Curwen V, Fairley S, Fernandez Banet J, Billis K, Garcia Giron C, Hourlier T, Howe K, Kahari A, Kokocinski F, Martin FJ, Murphy DN, Nag R, et al. The Ensembl gene annotation system. Database (Oxford). 2016; 2016.
79. Pelechano V and Steinmetz LM. Gene regulation by antisense transcription. Nat Rev Genet. 2013; 14(12):880-893.
80. Shin CH, Ryu S and Kim HH. hnRNPK-regulated PTOV1-AS1 modulates heme oxygenase-1 expression via miR-1207-5p. BMB Rep. 2017; 50(4):220-225.
81. Casamassimi A and Napoli C. Mediator complexes and eukaryotic transcription regulation: an overview. Biochimie. 2007; 89(12):1439-1446.
82. Wang C, McCarty IM, Balazs L, Li Y and Steiner MS. A prostate-derived cDNA that is mapped to human chromosome 19 encodes a novel protein. Biochem Biophys Res Commun. 2002; 296(2):281-287.
83. Tomomori-Sato C, Sato S, Parmely TJ, Banks CA, Sorokina I, Florens L, Zybailov B, Washburn MP, Brower CS, Conaway RC and Conaway JW. A mammalian mediator subunit that shares properties with Saccharomyces cerevisiae mediator subunit Cse2. J Biol Chem. 2004; 279(7):5846-5851.
84. Bourbon HM, Aguilera A, Ansari AZ, Asturias FJ, Berk AJ, Bjorklund S, Blackwell TK, Borggrefe T, Carey M, Carlson M, Conaway JW, Conaway RC, Emmons SW, Fondell JD, Freedman LP, Fukasawa T, et al. A unified nomenclature for protein subunits of mediator complexes linking transcriptional regulators to RNA polymerase II. Mol Cell. 2004; 14(5):553-557.
85. Yang F, DeBeaumont R, Zhou S and Naar AM. The activator-recruited cofactor/Mediator coactivator subunit ARC92 is a functionally important target of the VP16 transcriptional activator. Proc Natl Acad Sci U S A. 2004; 101(8):2339-2344.
86. Schwede T, Kopp J, Guex N and Peitsch MC. SWISS-MODEL: An automated protein homology-modeling server. Nucleic Acids Res. 2003; 31(13):3381-3385.
87. Nakamura Y, Suzuki T, Igarashi K, Kanno J, Furukawa T, Tazawa C, Fujishima F, Miura I, Ando T, Moriyama N, Moriya T, Saito H, Yamada S and Sasano H. PTOV1: a novel testosterone-induced atherogenic gene in human aorta. J Pathol. 2006; 209(4):522-531.
88. Bontems F, Verger A, Dewitte F, Lens Z, Baert JL, Ferreira E, de Launoit Y, Sizun C, Guittet E, Villeret V and Monte D. NMR structure of the human Mediator MED25 ACID domain. J Struct Biol. 2010; 174(1):245-251.
89. Eletsky A, Ruyechan WT, Xiao R, Acton TB, Montelione GT and Szyperski T. Solution NMR structure of MED25(391-543) comprising the activator-interacting domain (ACID) of human mediator subunit 25. J Struct Funct Genomics. 2011; 12(3):159-166.
90. Vojnic E, Mourao A, Seizl M, Simon B, Wenzeck L, Lariviere L, Baumli S, Baumgart K, Meisterernst M, Sattler M and Cramer P. Structure and VP16 binding of the Mediator Med25 activator interaction domain. Nat Struct Mol Biol. 2011; 18(4):404-409.

91. Oswald F, Winkler M, Cao Y, Astrahantseff K, Bourteele S, Knochel W and Borggrefe T. RBP-Jkappa/SHARP recruits CtIP/CtBP corepressors to silence Notch target genes. Mol Cell Biol. 2005; 25(23):10379-10390.
92. Filarsky M, Zillner K, Araya I, Villar-Garea A, Merkl R, Langst G and Nemeth A. The extended AT-hook is a novel RNA binding motif. RNA Biol. 2015; 12(8):864-876.
93. Banks GC, Mohr B and Reeves R. The HMG-I(Y) A.T-hook peptide motif confers DNA-binding specificity to a structured chimeric protein. J Biol Chem. 1999; 274(23):16536-16544.
94. Cairns BR, Schlichter A, Erdjument-Bromage H, Tempst P, Kornberg RD and Winston F. Two functionally distinct forms of the RSC nucleosome-remodeling complex, containing essential AT hook, BAH, and bromodomains. Mol Cell. 1999; 4(5):715-723.
95. Yao YW, Shi Y, Jia ZF, Jiang YH, Gu Z, Wang J, Aljofan M and Sun ZG. PTOV1 is associated with UCH-L1 and in response to estrogen stimuli during the mouse oocyte development. Histochem Cell Biol. 2011; 136(2):205-215.
96. Guo F, Feng L, Hu JL, Wang ML, Luo P, Zhong XM and Deng AM. Increased PTOV1 expression is related to poor prognosis in epithelial ovarian cancer. Tumour Biol. 2015; 36(1):453-458.
97. Scarpelli M, Mazzucchelli R, Barbisan F, Santinelli A, Lopez-Beltran A, Cheng L and Montironi R. Is there a role for prostate tumour overexpressed-1 in the diagnosis of HGPIN and of prostatic adenocarcinoma? A comparison with alpha-methylacyl CoA racemase. Int J Immunopathol Pharmacol. 2012; 25(1):67-74.
98. Mazzucchelli R, Barbisan F, Santinelli A, Lopez-Beltran A, Cheng L, Scarpelli M and Montironi R. Immunohistochemical expression of prostate tumor overexpressed 1 in cystoprostatectomies with incidental and insignificant prostate cancer. Further evidence for field effect in prostatic carcinogenesis. Hum Pathol. 2011; 42(12):1931-1936.
99. Mazzucchelli R, Scarpelli M, Barbisan F, Santinelli A, Lopez-Beltran A, Cheng L and Montironi R. Immunohistochemical expression of prostate tumour overexpressed 1 (PTOV1) in atypical adenomatous hyperplasia (AAH) of the prostate: additional evidence linking (AAH) to adenocarcinoma. Cellular oncology (Dordrecht). 2013; 36(1):37-42.
100. Alana L, Sese M, Canovas V, Punyal Y, Fernandez Y, Abasolo I, de Torres I, Ruiz C, Espinosa L, Bigas A, Y Cajal SR, Fernandez PL, Serras F, Corominas M, Thomson TM and Paciucci R. Prostate tumor OVerexpressed-1 (PTOV1) down-regulates HES1 and HEY1 notch targets genes and promotes prostate cancer progression. Molecular cancer. 2014; 13:74.
101. Marques N, Sese M, Canovas V, Valente F, Bermudo R, de Torres I, Fernandez Y, Abasolo I, Fernandez PL, Contreras H, Castellon E, Celia-Terrassa T, Mendez R, Ramon YCS, Thomson TM and Paciucci R. Regulation of protein translation and c-Jun expression by prostate tumor overexpressed 1. Oncogene. 2014; 33(9):1124-1134.
102. Lei F, Zhang L, Li X, Lin X, Wu S, Li F and Liu J. Overexpression of prostate tumor overexpressed 1 correlates with tumor progression and predicts poor prognosis in breast cancer. BMC cancer. 2014; 14:457.
103. Chen S-P, Zhang L-S, Fu B-S, Zeng X-C, Yi H-M and Jiang N. Prostate tumor overexpressed 1 is a novel prognostic marker for hepatocellular carcinoma progression and overall patient survival. Medicine. 2015; 94(4):e423.
104. Fernandez S, Mosquera JL, Alana L, Sanchez-Pla A, Morote J, Ramon Y Cajal S, Reventos J, de Torres I and Paciucci R. PTOV1 is overexpressed in human high-grade malignant tumors. Virchows Archiv : an international journal of pathology. 2011; 458(3):323-330.
105. Yang Q, Lin H, Wu S, Lei F, Zhu X, Song L, Hong M and Guo L. Prostate Tumor Overexpressed 1 (PTOV1) Is a Novel Prognostic Marker for Nasopharyngeal Carcinoma Progression and Poor Survival Outcomes. PLoS One. 2015; 10(8):e0136448.
106. Lee HK, Park UH, Kim EJ and Um SJ. MED25 is distinct from TRAP220/MED1 in cooperating with CBP for retinoid receptor activation. EMBO J. 2007; 26(15):3545-3557.

107. Verger A, Baert JL, Verreman K, Dewitte F, Ferreira E, Lens Z, de Launoit Y, Villeret V and Monte D. The Mediator complex subunit MED25 is targeted by the N-terminal transactivation domain of the PEA3 group members. Nucleic Acids Res. 2013; 41(9):4847-4859.
108. Han EH, Rha GB and Chi YI. MED25 is a mediator component of HNF4alpha-driven transcription leading to insulin secretion in pancreatic beta-cells. PLoS One. 2012; 7(8):e44007.
109. Sela D, Conkright JJ, Chen L, Gilmore J, Washburn MP, Florens L, Conaway RC and Conaway JW. Role for human mediator subunit MED25 in recruitment of mediator to promoters by endoplasmic reticulum stress-responsive transcription factor ATF6alpha. J Biol Chem. 2013; 288(36):26179-26187.
110. Youn HS, Park UH, Kim EJ and Um SJ. PTOV1 antagonizes MED25 in RAR transcriptional activation. Biochem Biophys Res Commun. 2011; 404(1):239-244.
111. Lee B, Wu CY, Lin YW, Park SW and Wei LN. Synergistic activation of Arg1 gene by retinoic acid and IL-4 involves chromatin remodeling for transcription initiation and elongation coupling. Nucleic Acids Res. 2016; 44(16):7568-7579.
112. Simoni D and Tolomeo M. Retinoids, apoptosis and cancer. Curr Pharm Des. 2001; 7(17):1823-1837.
113. Shilkaitis A, Green A and Christov K. Retinoids induce cellular senescence in breast cancer cells by RAR-beta dependent and independent pathways: Potential clinical implications (Review). Int J Oncol. 2015; 47(1):35-42.
114. Freemantle SJ, Spinella MJ and Dmitrovsky E. Retinoids in cancer therapy and chemoprevention: promise meets resistance. Oncogene. 2003; 22(47):7305-7315.
115. Goodman RH and Smolik S. CBP/p300 in cell growth, transformation, and development. Genes Dev. 2000; 14(13):1553-1577.
116. Youn H, Kim EJ and Um SJ. Zyxin cooperates with PTOV1 to confer retinoic acid resistance by repressing RAR activity. Cancer Lett. 2013.
117. Artavanis-Tsakonas S, Rand MD and Lake RJ. Notch signaling: cell fate control and signal integration in development. Science. 1999; 284(5415):770-776.
118. Brou C, Logeat F, Gupta N, Bessia C, LeBail O, Doedens JR, Cumano A, Roux P, Black RA and Israel A. A novel proteolytic cleavage involved in Notch signaling: the role of the disintegrin-metalloprotease TACE. Mol Cell. 2000; 5(2):207-216.
119. Jarriault S, Brou C, Logeat F, Schroeter EH, Kopan R and Israel A. Signalling downstream of activated mammalian Notch. Nature. 1995; 377(6547):355-358.
120. Lai EC. Keeping a good pathway down: transcriptional repression of Notch pathway target genes by CSL proteins. EMBO Rep. 2002; 3(9):840-845.
121. Klinakis A, Lobry C, Abdel-Wahab O, Oh P, Haeno H, Buonamici S, van De Walle I, Cathelin S, Trimarchi T, Araldi E, Liu C, Ibrahim S, Beran M, Zavadil J, Efstratiadis A, Taghon T, et al. A novel tumour-suppressor function for the Notch pathway in myeloid leukaemia. Nature. 2011; 473(7346):230-233.
122. Arrigoni E, Galimberti S, Petrini M, Danesi R and Di Paolo A. ATP-binding cassette transmembrane transporters and their epigenetic control in cancer: an overview. Expert Opin Drug Metab Toxicol. 2016:1-14.
123. Giachino C, Boulay JL, Ivanek R, Alvarado A, Tostado C, Lugert S, Tchorz J, Coban M, Mariani L, Bettler B, Lathia J, Frank S, Pfister S, Kool M and Taylor V. A Tumor Suppressor Function for Notch Signaling in Forebrain Tumor Subtypes. Cancer Cell. 2015; 28(6):730-742.
124. Wang Z, Li Y, Banerjee S, Kong D, Ahmad A, Nogueira V, Hay N and Sarkar FH. Down-regulation of Notch-1 and Jagged-1 inhibits prostate cancer cell growth, migration and invasion, and induces apoptosis via inactivation of Akt, mTOR, and NF-kappaB signaling pathways. J Cell Biochem. 2010; 109(4):726-736.
125. Whelan JT, Kellogg A, Shewchuk BM, Hewan-Lowe K and Bertrand FE. Notch-1 signaling is lost in prostate adenocarcinoma and promotes PTEN gene expression. J Cell Biochem. 2009; 107(5):992-1001.

126. Liu C, Li Z, Bi L, Li K, Zhou B, Xu C, Huang J and Xu K. NOTCH1 signaling promotes chemoresistance via regulating ABCC1 expression in prostate cancer stem cells. Mol Cell Biochem. 2014; 393(1-2):265-270.
127. Ramos YF, Hestand MS, Verlaan M, Krabbendam E, Ariyurek Y, van Galen M, van Dam H, van Ommen GJ, den Dunnen JT, Zantema A and t Hoen PA. Genome-wide assessment of differential roles for p300 and CBP in transcription regulation. Nucleic Acids Res. 2010; 38(16):5396-5408.
128. Oswald F, Kostezka U, Astrahantseff K, Bourteele S, Dillinger K, Zechner U, Ludwig L, Wilda M, Hameister H, Knochel W, Liptay S and Schmid RM. SHARP is a novel component of the Notch/RBP-Jkappa signalling pathway. EMBO J. 2002; 21(20):5417-5426.
129. Kolev V, Mandinova A, Guinea-Viniegra J, Hu B, Lefort K, Lambertini C, Neel V, Dummer R, Wagner EF and Dotto GP. EGFR signalling as a negative regulator of Notch1 gene transcription and function in proliferating keratinocytes and cancer. Nat Cell Biol. 2008; 10(8):902-911.
130. Nicolas M, Wolfer A, Raj K, Kummer JA, Mill P, van Noort M, Hui CC, Clevers H, Dotto GP and Radtke F. Notch1 functions as a tumor suppressor in mouse skin. Nat Genet. 2003; 33(3):416-421.
131. Hu B, Castillo E, Harewood L, Ostano P, Reymond A, Dummer R, Raffoul W, Hoetzenecker W, Hofbauer GF and Dotto GP. Multifocal epithelial tumors and field cancerization from loss of mesenchymal CSL signaling. Cell. 2012; 149(6):1207-1220.
132. Ai L, Tao Q, Zhong S, Fields CR, Kim WJ, Lee MW, Cui Y, Brown KD and Robertson KD. Inactivation of Wnt inhibitory factor-1 (WIF1) expression by epigenetic silencing is a common event in breast cancer. Carcinogenesis. 2006; 27(7):1341-1348.
133. Cui Y, Ma W, Lei F, Li Q, Su Y, Lin X, Lin C, Zhang X, Ye L, Wu S, Li J, Yuan Z and Song L. Prostate tumour overexpressed-1 promotes tumourigenicity in human breast cancer via activation of Wnt/beta-catenin signalling. J Pathol. 2016; 239(3):297-308.
134. Vilchez V, Turcios L, Marti F and Gedaly R. Targeting Wnt/beta-catenin pathway in hepatocellular carcinoma treatment. World J Gastroenterol. 2016; 22(2):823-832.
135. Na Y, Lee SM, Kim DS and Park JY. Promoter methylation of Wnt antagonist DKK1 gene and prognostic value in Korean patients with non-small cell lung cancers. Cancer Biomark. 2012; 12(2):73-79.
136. Rawson JB, Manno M, Mrkonjic M, Daftary D, Dicks E, Buchanan DD, Younghusband HB, Parfrey PS, Young JP, Pollett A, Green RC, Gallinger S, McLaughlin JR, Knight JA and Bapat B. Promoter methylation of Wnt antagonists DKK1 and SFRP1 is associated with opposing tumor subtypes in two large populations of colorectal cancer patients. Carcinogenesis. 2011; 32(5):741-747.
137. Suzuki H, Toyota M, Carraway H, Gabrielson E, Ohmura T, Fujikane T, Nishikawa N, Sogabe Y, Nojima M, Sonoda T, Mori M, Hirata K, Imai K, Shinomura Y, Baylin SB and Tokino T. Frequent epigenetic inactivation of Wnt antagonist genes in breast cancer. Br J Cancer. 2008; 98(6):1147-1156.
138. Canovas V, Lleonart M, Morote J and Paciucci R. The role of prostate tumor overexpressed 1 in cancer progression. Oncotarget. 2017; 8(7):12451-12471.
139. Bonnet J, Romier C, Tora L and Devys D. Zinc-finger UBPs: regulators of deubiquitylation. Trends Biochem Sci. 2008; 33(8):369-375.
140. Pai MT, Tzeng SR, Kovacs JJ, Keaton MA, Li SS, Yao TP and Zhou P. Solution structure of the Ubp-M BUZ domain, a highly specific protein module that recognizes the C-terminal tail of free ubiquitin. J Mol Biol. 2007; 370(2):290-302.
141. Hard RL, Liu J, Shen J, Zhou P and Pei D. HDAC6 and Ubp-M BUZ domains recognize specific C-terminal sequences of proteins. Biochemistry. 49(50):10737-10746.
142. Hubbert C, Guardiola A, Shao R, Kawaguchi Y, Ito A, Nixon A, Yoshida M, Wang XF and Yao TP. HDAC6 is a microtubule-associated deacetylase. Nature. 2002; 417(6887):455-458.

143. Kanno K, Kanno S, Nitta H, Uesugi N, Sugai T, Masuda T, Wakabayashi G and Maesawa C. Overexpression of histone deacetylase 6 contributes to accelerated migration and invasion activity of hepatocellular carcinoma cells. Oncol Rep. 2012; 28(3):867-873.
144. Bazzaro M, Lin Z, Santillan A, Lee MK, Wang MC, Chan KC, Bristow RE, Mazitschek R, Bradner J and Roden RB. Ubiquitin proteasome system stress underlies synergistic killing of ovarian cancer cells by bortezomib and a novel HDAC6 inhibitor. Clin Cancer Res. 2008; 14(22):7340-7347.
145. Bradbury CA, Khanim FL, Hayden R, Bunce CM, White DA, Drayson MT, Craddock C and Turner BM. Histone deacetylases in acute myeloid leukaemia show a distinctive pattern of expression that changes selectively in response to deacetylase inhibitors. Leukemia. 2005; 19(10):1751-1759.
146. Wang Q, Tan R, Zhu X, Zhang Y, Tan Z, Su B and Li Y. Oncogenic K-ras confers SAHA resistance by up-regulating HDAC6 and c-myc expression. Oncotarget. 2016; 7(9):10064-10072.
147. Woan KV, Lienlaf M, Perez-Villaroel P, Lee C, Cheng F, Knox T, Woods DM, Barrios K, Powers J, Sahakian E, Wang HW, Canales J, Marante D, Smalley KS, Bergman J, Seto E, et al. Targeting histone deacetylase 6 mediates a dual anti-melanoma effect: Enhanced antitumor immunity and impaired cell proliferation. Mol Oncol. 2015; 9(7):1447-1457.
148. Yang CJ, Liu YP, Dai HY, Shiue YL, Tsai CJ, Huang MS and Yeh YT. Nuclear HDAC6 inhibits invasion by suppressing NF-kappaB/MMP2 and is inversely correlated with metastasis of non-small cell lung cancer. Oncotarget. 2015; 6(30):30263-30276.
149. Jung KH, Noh JH, Kim JK, Eun JW, Bae HJ, Chang YG, Kim MG, Park WS, Lee JY, Lee SY, Chu IS and Nam SW. Histone deacetylase 6 functions as a tumor suppressor by activating c-Jun NH2-terminal kinase-mediated beclin 1-dependent autophagic cell death in liver cancer. Hepatology. 2012; 56(2):644-657.
150. Santamaria A, Castellanos E, Gomez V, Benedit P, Renau-Piqueras J, Morote J, Reventos J, Thomson TM and Paciucci R. PTOV1 enables the nuclear translocation and mitogenic activity of flotillin-1, a major protein of lipid rafts. Mol Cell Biol. 2005; 25(5):1900-1911.
151. Simons K and Gerl MJ. Revitalizing membrane rafts: new tools and insights. Nat Rev Mol Cell Biol. 2010; 11(10):688-699.
152. Lang DM, Lommel S, Jung M, Ankerhold R, Petrausch B, Laessing U, Wiechers MF, Plattner H and Stuermer CA. Identification of reggie-1 and reggie-2 as plasmamembrane-associated proteins which cocluster with activated GPI-anchored cell adhesion molecules in non-caveolar micropatches in neurons. J Neurobiol. 1998; 37(4):502-523.
153. Munderloh C, Solis GP, Bodrikov V, Jaeger FA, Wiechers M, Malaga-Trillo E and Stuermer CA. Reggies/flotillins regulate retinal axon regeneration in the zebrafish optic nerve and differentiation of hippocampal and N2a neurons. J Neurosci. 2009; 29(20):6607-6615.
154. Baumann CA, Ribon V, Kanzaki M, Thurmond DC, Mora S, Shigematsu S, Bickel PE, Pessin JE and Saltiel AR. CAP defines a second signalling pathway required for insulin-stimulated glucose transport. Nature. 2000; 407(6801):202-207.
155. Gomez V, Sese M, Santamaria A, Martinez JD, Castellanos E, Soler M, Thomson TM and Paciucci R. Regulation of aurora B kinase by the lipid raft protein flotillin-1. J Biol Chem. 2010; 285(27):20683-20690.
156. Cao S, Cui Y, Xiao H, Mai M, Wang C, Xie S, Yang J, Wu S, Li J, Song L, Guo X and Lin C. Upregulation of flotillin-1 promotes invasion and metastasis by activating TGF-beta signaling in nasopharyngeal carcinoma. Oncotarget. 2016; 7(4):4252-4264.
157. Li Z, Yang Y, Gao Y, Wu X, Yang X, Zhu Y, Yang H, Wu L, Yang C and Song L. Elevated expression of flotillin-1 is associated with lymph node metastasis and poor prognosis in early-stage cervical cancer. Am J Cancer Res. 2016; 6(1):38-50.
158. Koh M, Yong HY, Kim ES, Son H, Jeon YR, Hwang JS, Kim MO, Cha Y, Choi WS, Noh DY, Lee KM, Kim KB, Lee JS, Kim HJ, Kim H, Kim HH, et al. A novel role for flotillin-1 in H-Ras-regulated breast cancer aggressiveness. Int J Cancer. 2016; 138(5):1232-1245.

159. Kang M, Ren MP, Zhao L, Li CP and Deng MM. miR-485-5p acts as a negative regulator in gastric cancer progression by targeting flotillin-1. Am J Transl Res. 2015; 7(11):2212-2222.
160. Ron D, Chen CH, Caldwell J, Jamieson L, Orr E and Mochly-Rosen D. Cloning of an intracellular receptor for protein kinase C: a homolog of the beta subunit of G proteins. Proc Natl Acad Sci U S A. 1994; 91(3):839-843.
161. Mochly-Rosen D, Smith BL, Chen CH, Disatnik MH and Ron D. Interaction of protein kinase C with RACK1, a receptor for activated C-kinase: a role in beta protein kinase C mediated signal transduction. Biochem Soc Trans. 1995; 23(3):596-600.
162. Arimoto K, Fukuda H, Imajoh-Ohmi S, Saito H and Takekawa M. Formation of stress granules inhibits apoptosis by suppressing stress-responsive MAPK pathways. Nat Cell Biol. 2008; 10(11):1324-1332.
163. Kiely PA, Sant A and O'Connor R. RACK1 is an insulin-like growth factor 1 (IGF-1) receptor-interacting protein that can regulate IGF-1-mediated Akt activation and protection from cell death. J Biol Chem. 2002; 277(25):22581-22589.
164. Zhang W, Zong CS, Hermanto U, Lopez-Bergami P, Ronai Z and Wang LH. RACK1 recruits STAT3 specifically to insulin and insulin-like growth factor 1 receptors for activation, which is important for regulating anchorage-independent growth. Mol Cell Biol. 2006; 26(2):413-424.
165. Sengupta J, Nilsson J, Gursky R, Spahn CM, Nissen P and Frank J. Identification of the versatile scaffold protein RACK1 on the eukaryotic ribosome by cryo-EM. Nat Struct Mol Biol. 2004; 11(10):957-962.
166. Sharma G, Pallesen J, Das S, Grassucci R, Langlois R, Hampton CM, Kelly DF, des Georges A and Frank J. Affinity grid-based cryo-EM of PKC binding to RACK1 on the ribosome. J Struct Biol. 2013; 181(2):190-194.
167. Gandin V, Miluzio A, Barbieri AM, Beugnet A, Kiyokawa H, Marchisio PC and Biffo S. Eukaryotic initiation factor 6 is rate-limiting in translation, growth and transformation. Nature. 2008; 455(7213):684-688.
168. Lopez-Bergami P, Habelhah H, Bhoumik A, Zhang W, Wang LH and Ronai Z. RACK1 mediates activation of JNK by protein kinase C [corrected]. Mol Cell. 2005; 19(3):309-320.
169. Gandin V, Gutierrez GJ, Brill LM, Varsano T, Feng Y, Aza-Blanc P, Au Q, McLaughlan S, Ferreira TA, Alain T, Sonenberg N, Topisirovic I and Ronai ZA. Degradation of newly synthesized polypeptides by ribosome-associated RACK1/c-Jun N-terminal kinase/eukaryotic elongation factor 1A2 complex. Mol Cell Biol. 2013; 33(13):2510-2526.
170. Berns H, Humar R, Hengerer B, Kiefer FN and Battegay EJ. RACK1 is up-regulated in angiogenesis and human carcinomas. FASEB J. 2000; 14(15):2549-2558.
171. Cao XX, Xu JD, Liu XL, Xu JW, Wang WJ, Li QQ, Chen Q, Xu ZD and Liu XP. RACK1: A superior independent predictor for poor clinical outcome in breast cancer. Int J Cancer. 2010; 127(5):1172-1179.
172. Nagashio R, Sato Y, Matsumoto T, Kageyama T, Satoh Y, Shinichiro R, Masuda N, Goshima N, Jiang SX and Okayasu I. Expression of RACK1 is a novel biomarker in pulmonary adenocarcinomas. Lung Cancer. 2010; 69(1):54-59.
173. Ruan Y, Sun L, Hao Y, Wang L, Xu J, Zhang W, Xie J, Guo L, Zhou L, Yun X, Zhu H, Shen A and Gu J. Ribosomal RACK1 promotes chemoresistance and growth in human hepatocellular carcinoma. J Clin Invest. 2012; 122(7):2554-2566.
174. Shi Z, Wang B, Chihanga T, Kennedy MA and Weber GF. Energy Metabolism during Anchorage-Independence. Induction by Osteopontin-c. PLoS One. 2014; 9(8):e105675.
175. Kianercy A, Veltri R and Pienta KJ. Critical transitions in a game theoretic model of tumour metabolism. Interface Focus. 2014; 4(4):20140014.
176. Sanita P, Capulli M, Teti A, Galatioto GP, Vicentini C, Chiarugi P, Bologna M and Angelucci A. Tumor-stroma metabolic relationship based on lactate shuttle can sustain prostate cancer progression. BMC Cancer. 2014; 14:154.
177. Dancey J. mTOR signaling and drug development in cancer. Nat Rev Clin Oncol. 2010; 7(4):209-219.

178. Loh PG, Yang HS, Walsh MA, Wang Q, Wang X, Cheng Z, Liu D and Song H. Structural basis for translational inhibition by the tumour suppressor Pdcd4. Embo j. 2009; 28(3):274-285.
179. Rozovsky N, Butterworth AC and Moore MJ. Interactions between eIF4AI and its accessory factors eIF4B and eIF4H. Rna. 2008; 14(10):2136-2148.
180. Merrick WC. Cap-dependent and cap-independent translation in eukaryotic systems. Gene. 2004; 332:1-11.
181. Meric F and Hunt KK. Translation initiation in cancer: a novel target for therapy. Mol Cancer Ther. 2002; 1(11):971-979.
182. Truitt ML and Ruggero D. New frontiers in translational control of the cancer genome. Nat Rev Cancer. 2016; 16(5):288-304.
183. Lazaris-Karatzas A, Montine KS and Sonenberg N. Malignant transformation by a eukaryotic initiation factor subunit that binds to mRNA 5' cap. Nature. 1990; 345(6275):544-547.
184. Horvilleur E, Sbarrato T, Hill K, Spriggs RV, Screen M, Goodrem PJ, Sawicka K, Chaplin LC, Touriol C, Packham G, Potter KN, Dirnhofer S, Tzankov A, Dyer MJ, Bushell M, Macfarlane M, et al. A role for eukaryotic initiation factor 4B overexpression in the pathogenesis of diffuse large B-cell lymphoma. Leukemia. 2014; 28(5):1092-1102.
185. Heikkinen T, Korpela T, Fagerholm R, Khan S, Aittomaki K, Heikkila P, Blomqvist C, Carpen O and Nevanlinna H. Eukaryotic translation initiation factor 4E (eIF4E) expression is associated with breast cancer tumor phenotype and predicts survival after anthracycline chemotherapy treatment. Breast Cancer Res Treat. 2013; 141(1):79-88.
186. Yin X, Kim RH, Sun G, Miller JK and Li BD. Overexpression of eukaryotic initiation factor 4E is correlated with increased risk for systemic dissemination in node-positive breast cancer patients. J Am Coll Surg. 2014; 218(4):663-671.
187. Liang S, Guo R, Zhang Z, Liu D, Xu H, Xu Z, Wang X and Yang L. Upregulation of the eIF4E signaling pathway contributes to the progression of gastric cancer, and targeting eIF4E by perifosine inhibits cell growth. Oncol Rep. 2013; 29(6):2422-2430.
188. Jiang YD, Lu YH, Chen SH, Zhu KE, Zhang XL, Yu Z, Zhong J, Zhang T, Luo GX, Chen J, Pan HY, Li Y, Qin LA and Li YQ. [Overexpression of eIF4E gene in acute myeloid leukemia and its relation with disease progression]. Zhongguo Shi Yan Xue Ye Xue Za Zhi. 2013; 21(2):296-299.
189. Wu M, Liu Y, Di X, Kang H, Zeng H, Zhao Y, Cai K, Pang T, Wang S, Yao Y and Hu X. EIF4E over-expresses and enhances cell proliferation and cell cycle progression in nasopharyngeal carcinoma. Med Oncol. 2013; 30(1):400.
190. Ferrandiz-Pulido C, Masferrer E, Toll A, Hernandez-Losa J, Mojal S, Pujol RM, Ramon y Cajal S, de Torres I and Garcia-Patos V. mTOR signaling pathway in penile squamous cell carcinoma: pmTOR and peIF4E over expression correlate with aggressive tumor behavior. J Urol. 2013; 190(6):2288-2295.
191. Tunca B, Tezcan G, Cecener G, Egeli U, Zorluoglu A, Yilmazlar T, Ak S, Yerci O, Ozturk E, Umut G and Evrensel T. Overexpression of CK20, MAP3K8 and EIF5A correlates with poor prognosis in early-onset colorectal cancer patients. J Cancer Res Clin Oncol. 2013; 139(4):691-702.
192. Wei JH, Cao JZ, Zhang D, Liao B, Zhong WM, Lu J, Zhao HW, Zhang JX, Tong ZT, Fan S, Liang CZ, Liao YB, Pang J, Wu RH, Fang Y, Chen ZH, et al. EIF5A2 predicts outcome in localised invasive bladder cancer and promotes bladder cancer cell aggressiveness in vitro and in vivo. Br J Cancer. 2014; 110(7):1767-1777.
193. Sesen J, Cammas A, Scotland SJ, Elefterion B, Lemarie A, Millevoi S, Mathew LK, Seva C, Toulas C, Moyal EC and Skuli N. Int6/eIF3e is essential for proliferation and survival of human glioblastoma cells. Int J Mol Sci. 2014; 15(2):2172-2190.
194. Qi J, Dong Z, Liu J and Zhang JT. EIF3i promotes colon oncogenesis by regulating COX-2 protein synthesis and beta-catenin activation. Oncogene. 2014; 33(32):4156-4163.
195. Wang YW, Lin KT, Chen SC, Gu DL, Chen CF, Tu PH and Jou YS. Overexpressed-eIF3I interacted and activated oncogenic Akt1 is a theranostic target in human hepatocellular carcinoma. Hepatology. 2013; 58(1):239-250.

196. Song N, Wang Y, Gu XD, Chen ZY and Shi LB. Effect of siRNA-mediated knockdown of eIF3c gene on survival of colon cancer cells. J Zhejiang Univ Sci B. 2013; 14(6):451-459.
197. Karlsson E, Perez-Tenorio G, Amin R, Bostner J, Skoog L, Fornander T, Sgroi DC, Nordenskjold B, Hallbeck AL and Stal O. The mTOR effectors 4EBP1 and S6K2 are frequently coexpressed, and associated with a poor prognosis and endocrine resistance in breast cancer: a retrospective study including patients from the randomised Stockholm tamoxifen trials. Breast Cancer Res. 2013; 15(5):R96.
198. Trigka EA, Levidou G, Saetta AA, Chatziandreou I, Tomos P, Thalassinos N, Anastasiou N, Spartalis E, Kavantzas N, Patsouris E and Korkolopoulou P. A detailed immunohistochemical analysis of the PI3K/AKT/mTOR pathway in lung cancer: correlation with PIK3CA, AKT1, K-RAS or PTEN mutational status and clinicopathological features. Oncol Rep. 2013; 30(2):623-636.
199. Zhang X, Ba Y and Song R. [Expression and correlational research of mTOR and 4EBP1 in laryngeal carcinoma]. Lin Chung Er Bi Yan Hou Tou Jing Wai Ke Za Zhi. 2012; 26(23):1077-1079, 1082.
200. Wong QW, Li J, Ng SR, Lim SG, Yang H and Vardy LA. RPL39L is an example of a recently evolved ribosomal protein paralog that shows highly specific tissue expression patterns and is upregulated in ESCs and HCC tumors. RNA Biol. 2014; 11(1):33-41.
201. Rao S, Lee SY, Gutierrez A, Perrigoue J, Thapa RJ, Tu Z, Jeffers JR, Rhodes M, Anderson S, Oravecz T, Hunger SP, Timakhov RA, Zhang R, Balachandran S, Zambetti GP, Testa JR, et al. Inactivation of ribosomal protein L22 promotes transformation by induction of the stemness factor, Lin28B. Blood. 2012; 120(18):3764-3773.
202. Fernandez-Pol JA. Increased serum level of RPMPS-1/S27 protein in patients with various types of cancer is useful for the early detection, prevention and therapy. Cancer Genomics Proteomics. 2012; 9(4):203-256.
203. Du J, Shi Y, Pan Y, Jin X, Liu C, Liu N, Han Q, Lu Y, Qiao T and Fan D. Regulation of multidrug resistance by ribosomal protein l6 in gastric cancer cells. Cancer Biol Ther. 2005; 4(2):242-247.
204. Beelen K, Hoefnagel LD, Opdam M, Wesseling J, Sanders J, Vincent AD, van Diest PJ and Linn SC. PI3K/AKT/mTOR pathway activation in primary and corresponding metastatic breast tumors after adjuvant endocrine therapy. Int J Cancer. 2014; 135(5):1257-1263.
205. Westin JR. Status of PI3K/Akt/mTOR Pathway Inhibitors in Lymphoma. Clin Lymphoma Myeloma Leuk. 2014.
206. Francipane MG and Lagasse E. mTOR pathway in colorectal cancer: an update. Oncotarget. 2014; 5(1):49-66.
207. Hsieh AC, Liu Y, Edlind MP, Ingolia NT, Janes MR, Sher A, Shi EY, Stumpf CR, Christensen C, Bonham MJ, Wang S, Ren P, Martin M, Jessen K, Feldman ME, Weissman JS, et al. The translational landscape of mTOR signalling steers cancer initiation and metastasis. Nature. 2012; 485(7396):55-61.
208. Liu Q, Thoreen C, Wang J, Sabatini D and Gray NS. mTOR Mediated Anti-Cancer Drug Discovery. Drug Discov Today Ther Strateg. 2009; 6(2):47-55.
209. Gygi SP, Rochon Y, Franza BR and Aebersold R. Correlation between protein and mRNA abundance in yeast. Mol Cell Biol. 1999; 19(3):1720-1730.
210. Chen G. Discordant Protein and mRNA Expression in Lung Adenocarcinomas. Molecular & Cellular Proteomics. 2002; 1(4):304-313.
211. Ingolia NT, Ghaemmaghami S, Newman JR and Weissman JS. Genome-wide analysis in vivo of translation with nucleotide resolution using ribosome profiling. Science. 2009; 324(5924):218-223.
212. Marks PA, Rifkind RA and Demon D. Polyribosomes and protein synthesis during reticulocyte maturation in vitro. . Proc Natl Acad Sci U S A. 1963; 50:336-342.
213. Sadowski PD and Howden JA. Isolation of two distinct classes of polysomes from a nuclear fraction of rat liver. J Cell Biol. 1968; 37(1):163-181.

214. Zong Q, Schummer M, Hood L and Morris DR. Messenger RNA translation state: the second dimension of high-throughput expression screening. Proc Natl Acad Sci U S A. 1999; 96(19):10632-10636.
215. Mikulits W, Pradet-Balade B, Habermann B, Beug H, Garcia-Sanz JA and Mullner EW. Isolation of translationally controlled mRNAs by differential screening. Faseb j. 2000; 14(11):1641-1652.
216. Keene JD. RNA regulons: coordination of post-transcriptional events. Nat Rev Genet. 2007; 8(7):533-543.
217. Spangenberg L, Shigunov P, Abud AP, Cofre AR, Stimamiglio MA, Kuligovski C, Zych J, Schittini AV, Costa AD, Rebelatto CK, Brofman PR, Goldenberg S, Correa A, Naya H and Dallagiovanna B. Polysome profiling shows extensive posttranscriptional regulation during human adipocyte stem cell differentiation into adipocytes. Stem Cell Res. 2013; 11(2):902-912.
218. Steitz JA. Polypeptide chain initiation: nucleotide sequences of the three ribosomal binding sites in bacteriophage R17 RNA. Nature. 1969; 224(5223):957-964.
219. Meijer HA and Thomas AA. Ribosomes stalling on uORF1 in the Xenopus Cx41 5' UTR inhibit downstream translation initiation. Nucleic Acids Res. 2003; 31(12):3174-3184.
220. Capell A, Fellerer K and Haass C. Progranulin transcripts with short and long 5'-untranslated regions (UTR) are differentially expressed via post transcriptional and translational repression. J Biol Chem. 2014.
221. Kwon HS, Lee DK, Lee JJ, Edenberg HJ, Ahn YH and Hur MW. Posttranscriptional regulation of human ADH5/FDH and Myf6 gene expression by upstream AUG codons. Arch Biochem Biophys. 2001; 386(2):163-171.
222. Hatle KM, Neveu W, Dienz O, Rymarchyk S, Barrantes R, Hale S, Farley N, Lounsbury KM, Bond JP, Taatjes D and Rincon M. Methylation-controlled J protein promotes c-Jun degradation to prevent ABCB1 transporter expression. Mol Cell Biol. 2007; 27(8):2952-2966.
223. Sioletic S, Czaplinski J, Hu L, Fletcher JA, Fletcher CD, Wagner AJ, Loda M, Demetri GD, Sicinska ET and Snyder EL. c-Jun promotes cell migration and drives expression of the motility factor ENPP2 in soft tissue sarcomas. J Pathol. 2014; 234(2):190-202.
224. Cunningham D and You Z. In vitro and in vivo model systems used in prostate cancer research. J Biol Methods. 2015; 2(1).
225. Alimirah F, Chen J, Basrawala Z, Xin H and Choubey D. DU-145 and PC-3 human prostate cancer cell lines express androgen receptor: implications for the androgen receptor functions and regulation. FEBS Lett. 2006; 580(9):2294-2300.
226. Kutter C and Svoboda P. miRNA, siRNA, piRNA: Knowns of the unknown. RNA Biol. 2008; 5(4):181-188.
227. Duhagon MA, Hurt EM, Sotelo-Silveira JR, Zhang X and Farrar WL. Genomic profiling of tumor initiating prostatospheres. BMC Genomics. 2010; 11:324.
228. del Prete MJ, Vernal R, Dolznig H, Mullner EW and Garcia-Sanz JA. Isolation of polysome-bound mRNA from solid tissues amenable for RT-PCR and profiling experiments. Rna. 2007; 13(3):414-421.
229. Moore CB, Guthrie EH, Huang MT and Taxman DJ. Short hairpin RNA (shRNA): design, delivery, and assessment of gene knockdown. Methods Mol Biol. 2010; 629:141-158.
230. Das AT, Zhou X, Vink M, Klaver B, Verhoef K, Marzio G and Berkhout B. Viral evolution as a tool to improve the tetracycline-regulated gene expression system. J Biol Chem. 2004; 279(18):18776-18782.
231. Das AT, Tenenbaum L and Berkhout B. Tet-On Systems For Doxycycline-inducible Gene Expression. Curr Gene Ther. 2016; 16(3):156-167.
232. Petrak D, Memon SA, Birrer MJ, Ashwell JD and Zacharchuk CM. Dominant negative mutant of c-Jun inhibits NF-AT transcriptional activity and prevents IL-2 gene transcription. J Immunol. 1994; 153(5):2046-2051.
233. Mahmood T and Yang PC. Western blot: technique, theory, and trouble shooting. N Am J Med Sci. 2012; 4(9):429-434.

234. Schneider-Poetsch T, Ju J, Eyler DE, Dang Y, Bhat S, Merrick WC, Green R, Shen B and Liu JO. Inhibition of eukaryotic translation elongation by cycloheximide and lactimidomycin. Nat Chem Biol. 2010; 6(3):209-217.
235. Schmidt EK, Clavarino G, Ceppi M and Pierre P. SUnSET, a nonradioactive method to monitor protein synthesis. Nat Methods. 2009; 6(4):275-277.
236. Cerami E, Gao J, Dogrusoz U, Gross BE, Sumer SO, Aksoy BA, Jacobsen A, Byrne CJ, Heuer ML, Larsson E, Antipin Y, Reva B, Goldberg AP, Sander C and Schultz N. The cBio cancer genomics portal: an open platform for exploring multidimensional cancer genomics data. Cancer Discov. 2012; 2(5):401-404.
237. Gao J, Aksoy BA, Dogrusoz U, Dresdner G, Gross B, Sumer SO, Sun Y, Jacobsen A, Sinha R, Larsson E, Cerami E, Sander C and Schultz N. Integrative analysis of complex cancer genomics and clinical profiles using the cBioPortal. Sci Signal. 2013; 6(269):pl1.
238. Wang T, Yuan J, Zhang J, Tian R, Ji W, Zhou Y, Yang Y, Song W, Zhang F and Niu R. Anxa2 binds to STAT3 and promotes epithelial to mesenchymal transition in breast cancer cells. Oncotarget. 2015; 6(31):30975-30992.
239. The Molecular Taxonomy of Primary Prostate Cancer. Cell. 2015; 163(4):1011-1025.
240. Beltran H, Prandi D, Mosquera JM, Benelli M, Puca L, Cyrta J, Marotz C, Giannopoulou E, Chakravarthi BV, Varambally S, Tomlins SA, Nanus DM, Tagawa ST, Van Allen EM, Elemento O, Sboner A, et al. Divergent clonal evolution of castration-resistant neuroendocrine prostate cancer. 2016; 22(3):298-305.
241. Son H and Moon A. Epithelial-mesenchymal Transition and Cell Invasion. Toxicol Res. 2010; 26(4):245-252.
242. Baulida J and Garcia de Herreros A. Snail1-driven plasticity of epithelial and mesenchymal cells sustains cancer malignancy. Biochim Biophys Acta. 2015; 1856(1):55-61.
243. Sun H, Liu M, Wu X, Yang C, Zhang Y, Xu Z, Gao K and Wang F. Overexpression of N-cadherin and beta-catenin correlates with poor prognosis in patients with nasopharyngeal carcinoma. Oncol Lett. 2017; 13(3):1725-1730.
244. Krebs AM, Mitschke J, Lasierra Losada M, Schmalhofer O, Boerries M, Busch H, Boettcher M, Mougiakakos D, Reichardt W, Bronsert P, Brunton VG, Pilarsky C, Winkler TH, Brabletz S, Stemmler MP and Brabletz T. The EMT-activator Zeb1 is a key factor for cell plasticity and promotes metastasis in pancreatic cancer. Nat Cell Biol. 2017; 19(5):518-529.
245. Tania M, Khan MA and Fu J. Epithelial to mesenchymal transition inducing transcription factors and metastatic cancer. Tumour Biol. 2014; 35(8):7335-7342.
246. Garcia de Herreros A and Baulida J. Cooperation, amplification, and feed-back in epithelial-mesenchymal transition. Biochim Biophys Acta. 2012; 1825(2):223-228.
247. Cui L, Song J, Wu L, Cheng L, Chen A, Wang Y, Huang Y and Huang L. Role of Annexin A2 in the EGF-induced epithelial-mesenchymal transition in human CaSki cells. Oncol Lett. 2017; 13(1):377-383.
248. Thakur N, Gudey SK, Marcusson A, Fu JY, Bergh A, Heldin CH and Landstrom M. TGFbeta-induced invasion of prostate cancer cells is promoted by c-Jun-dependent transcriptional activation of Snail1. Cell Cycle. 2014; 13(15):2400-2414.
249. Satelli A and Li S. Vimentin in cancer and its potential as a molecular target for cancer therapy. Cell Mol Life Sci. 2011; 68(18):3033-3046.
250. Satelli A, Batth I, Brownlee Z, Mitra A, Zhou S, Noh H, Rojas CR, Li H, Meng QH and Li S. EMT circulating tumor cells detected by cell-surface vimentin are associated with prostate cancer progression. Oncotarget. 2017.
251. Wang J, Kuiatse I, Lee AV, Pan J, Giuliano A and Cui X. Sustained c-Jun-NH2-kinase activity promotes epithelial-mesenchymal transition, invasion, and survival of breast cancer cells by regulating extracellular signal-regulated kinase activation. Mol Cancer Res. 2010; 8(2):266-277.

252. Tsai JH, Donaher JL, Murphy DA, Chau S and Yang J. Spatiotemporal regulation of epithelial-mesenchymal transition is essential for squamous cell carcinoma metastasis. Cancer Cell. 2012; 22(6):725-736.
253. Chaffer CL, Brennan JP, Slavin JL, Blick T, Thompson EW and Williams ED. Mesenchymal-to-epithelial transition facilitates bladder cancer metastasis: role of fibroblast growth factor receptor-2. Cancer Res. 2006; 66(23):11271-11278.
254. Coyle SM, Gilbert WV and Doudna JA. Direct link between RACK1 function and localization at the ribosome in vivo. Mol Cell Biol. 2009; 29(6):1626-1634.
255. Nilsson J, Sengupta J, Frank J and Nissen P. Regulation of eukaryotic translation by the RACK1 protein: a platform for signalling molecules on the ribosome. EMBO Rep. 2004; 5(12):1137-1141.
256. Xu B, Jin X, Min L, Li Q, Deng L, Wu H, Lin G, Chen L, Zhang H, Li C, Wang L, Zhu J, Wang W, Chu F, Shen J, Li H, et al. Chloride channel-3 promotes tumor metastasis by regulating membrane ruffling and is associated with poor survival. Oncotarget. 2015; 6(4):2434-2450.
257. Valenzuela-Fernandez A, Cabrero JR, Serrador JM and Sanchez-Madrid F. HDAC6: a key regulator of cytoskeleton, cell migration and cell-cell interactions. Trends Cell Biol. 2008; 18(6):291-297.
258. Stark C, Breitkreutz BJ, Reguly T, Boucher L, Breitkreutz A and Tyers M. BioGRID: a general repository for interaction datasets. Nucleic Acids Res. 2006; 34(Database issue):D535-539.
259. Stelzl U, Worm U, Lalowski M, Haenig C, Brembeck FH, Goehler H, Stroedicke M, Zenkner M, Schoenherr A, Koeppen S, Timm J, Mintzlaff S, Abraham C, Bock N, Kietzmann S, Goedde A, et al. A human protein-protein interaction network: a resource for annotating the proteome. Cell. 2005; 122(6):957-968.
260. Hinrichsen I, Ernst BP, Nuber F, Passmann S, Schafer D, Steinke V, Friedrichs N, Plotz G, Zeuzem S and Brieger A. Reduced migration of MLH1 deficient colon cancer cells depends on SPTAN1. Mol Cancer. 2014; 13:11.
261. Huttlin EL, Ting L, Bruckner RJ, Gebreab F, Gygi MP, Szpyt J, Tam S, Zarraga G, Colby G, Baltier K, Dong R, Guarani V, Vaites LP, Ordureau A, Rad R, Erickson BK, et al. The BioPlex Network: A Systematic Exploration of the Human Interactome. Cell. 2015; 162(2):425-440.
262. Takahashi R, Nagayama S, Furu M, Kajita Y, Jin Y, Kato T, Imoto S, Sakai Y and Toguchida J. AFAP1L1, a novel associating partner with vinculin, modulates cellular morphology and motility, and promotes the progression of colorectal cancers. Cancer Med. 2014; 3(4):759-774.
263. Wang SY, Gao K, Deng DL, Cai JJ, Xiao ZY, He LQ, Jiao HL, Ye YP, Yang RW, Li TT, Liang L, Liao WT and Ding YQ. TLE4 promotes colorectal cancer progression through activation of JNK/c-Jun signaling pathway. Oncotarget. 2016; 7(3):2878-2888.
264. Sheikh A, Takatori A, Hossain MS, Hasan MK, Tagawa M, Nagase H and Nakagawara A. Unfavorable neuroblastoma prognostic factor NLRR2 inhibits cell differentiation by transcriptional induction through JNK pathway. Cancer Sci. 2016; 107(9):1223-1232.
265. Che JP, Li W, Yan Y, Liu M, Wang GC, Li QY, Yang B, Yao XD and Zheng JH. Expression and clinical significance of the nin one binding protein and p38 MAPK in prostate carcinoma. Int J Clin Exp Pathol. 2013; 6(11):2300-2311.
266. Antonyak MA, Kenyon LC, Godwin AK, James DC, Emlet DR, Okamoto I, Tnani M, Holgado-Madruga M, Moscatello DK and Wong AJ. Elevated JNK activation contributes to the pathogenesis of human brain tumors. Oncogene. 2002; 21(33):5038-5046.
267. Rodriguez-Gutierrez R, Villarreal-Perez JZ, Morales-Martinez FA, Rodriguez-Guajardo R, Gonzalez-Saldivar G, Mancillas-Adame LG, Alvarez-Villalobos NA, Lavalle-Gonzalez FJ and Gonzalez-Gonzalez JG. Ovarian and adrenal androgens and their link to high human chorionic gonadotropin levels: a prospective controlled study. Int J Endocrinol. 2014; 2014:191247.
268. Siegel R, Ma J, Zou Z and Jemal A. Cancer statistics, 2014. CA Cancer J Clin. 2014; 64(1):9-29.

269. Li R, Leng AM, Liu XM, Hu TZ, Zhang LF, Li M, Jiang XX, Zhou YW and Xu CX. Overexpressed PTOV1 associates with tumorigenesis and progression of esophageal squamous cell carcinoma. Tumour Biol. 2017; 39(6):1010428317705013.
270. Yang L, Wang H, Wang Y, He Z, Chen H, Liang S, He S, Wu S, Song L and Chen Y. Prostate tumor overexpressed-1 in conjunction with human papillomavirus status, predicts outcome in early-stage human laryngeal squamous cell carcinoma. Oncotarget. 2016.
271. . !!! INVALID CITATION !!!
272. Sivars L, Landin D, Grun N, Vlastos A, Marklund L, Nordemar S, Ramqvist T, Munck-Wikland E, Nasman A and Dalianis T. Validation of Human Papillomavirus as a Favourable Prognostic Marker and Analysis of CD8+ Tumour-infiltrating Lymphocytes and Other Biomarkers in Cancer of Unknown Primary in the Head and Neck Region. Anticancer Res. 2017; 37(2):665-673.
273. Kim HS, Luo L, Pflugfelder SC and Li DQ. Doxycycline inhibits TGF-beta1-induced MMP-9 via Smad and MAPK pathways in human corneal epithelial cells. Invest Ophthalmol Vis Sci. 2005; 46(3):840-848.
274. Fang Y, Wang Y, Wang Y, Meng Y, Zhu J, Jin H, Li J, Zhang D, Yu Y, Wu XR and Huang C. A new tumour suppression mechanism by p27Kip1: EGFR down-regulation mediated by JNK/c-Jun pathway inhibition. Biochem J. 2014; 463(3):383-392.
275. Grose R. Epithelial migration: open your eyes to c-Jun. Curr Biol. 2003; 13(17):R678-680.
276. Ahler E, Sullivan WJ, Cass A, Braas D, York AG, Bensinger SJ, Graeber TG and Christofk HR. Doxycycline alters metabolism and proliferation of human cell lines. PLoS One. 2013; 8(5):e64561.
277. Bernardino AL, Kaushal D and Philipp MT. The antibiotics doxycycline and minocycline inhibit the inflammatory responses to the Lyme disease spirochete Borrelia burgdorferi. J Infect Dis. 2009; 199(9):1379-1388.
278. Sakemura R, Terakura S, Watanabe K, Julamanee J, Takagi E, Miyao K, Koyama D, Goto T, Hanajiri R, Nishida T, Murata M and Kiyoi H. A Tet-On Inducible System for Controlling CD19-Chimeric Antigen Receptor Expression upon Drug Administration. Cancer Immunol Res. 2016; 4(8):658-668.
279. VanderVeen N, Raja N, Yi E, Appelman H, Ng P, Palmer D, Zamler D, Dzaman M, Lowenstein PR and Castro MG. Preclinical Efficacy and Safety Profile of Allometrically Scaled Doses of Doxycycline Used to Turn "On" Therapeutic Transgene Expression from High-Capacity Adenoviral Vectors in a Glioma Model. Hum Gene Ther Methods. 2016; 27(3):98-111.
280. Hanemaaijer R, Visser H, Koolwijk P, Sorsa T, Salo T, Golub LM and van Hinsbergh VW. Inhibition of MMP synthesis by doxycycline and chemically modified tetracyclines (CMTs) in human endothelial cells. Adv Dent Res. 1998; 12(2):114-118.
281. van den Bogert C, Dontje BH and Kroon AM. The antitumour effect of doxycycline on a T-cell leukaemia in the rat. Leuk Res. 1985; 9(5):617-623.
282. Duewelhenke N, Krut O and Eysel P. Influence on mitochondria and cytotoxicity of different antibiotics administered in high concentrations on primary human osteoblasts and cell lines. Antimicrob Agents Chemother. 2007; 51(1):54-63.
283. Fife RS, Sledge GW, Jr., Roth BJ and Proctor C. Effects of doxycycline on human prostate cancer cells in vitro. Cancer Lett. 1998; 127(1-2):37-41.
284. Antonio RC, Ceron CS, Rizzi E, Coelho EB, Tanus-Santos JE and Gerlach RF. Antioxidant effect of doxycycline decreases MMP activity and blood pressure in SHR. Mol Cell Biochem. 2014; 386(1-2):99-105.
285. Uitto VJ, Firth JD, Nip L and Golub LM. Doxycycline and chemically modified tetracyclines inhibit gelatinase A (MMP-2) gene expression in human skin keratinocytes. Ann N Y Acad Sci. 1994; 732:140-151.
286. Zhao Y, Wang X, Li L and Li C. Doxycycline inhibits proliferation and induces apoptosis of both human papillomavirus positive and negative cervical cancer cell lines. Can J Physiol Pharmacol. 2016; 94(5):526-533.

287. Nasrazadani A and Van Den Berg CL. c-Jun N-terminal Kinase 2 Regulates Multiple Receptor Tyrosine Kinase Pathways in Mouse Mammary Tumor Growth and Metastasis. Genes Cancer. 2011; 2(1):31-45.
288. Nukarinen E, Tervahartiala T, Valkonen M, Hynninen M, Kolho E, Pettila V, Sorsa T, Backman J and Hastbacka J. Targeting matrix metalloproteinases with intravenous doxycycline in severe sepsis--A randomised placebo-controlled pilot trial. Pharmacol Res. 2015; 99:44-51.
289. Kwon GT, Cho HJ, Chung WY, Park KK, Moon A and Park JH. Isoliquiritigenin inhibits migration and invasion of prostate cancer cells: possible mediation by decreased JNK/AP-1 signaling. J Nutr Biochem. 2009; 20(9):663-676.
290. Aroui S, Aouey B, Chtourou Y, Meunier AC, Fetoui H and Kenani A. Naringin suppresses cell metastasis and the expression of matrix metalloproteinases (MMP-2 and MMP-9) via the inhibition of ERK-P38-JNK signaling pathway in human glioblastoma. Chem Biol Interact. 2016; 244:195-203.
291. Ho BY, Wu YM, Chang KJ and Pan TM. Dimerumic acid inhibits SW620 cell invasion by attenuating H(2)O(2)-mediated MMP-7 expression via JNK/C-Jun and ERK/C-Fos activation in an AP-1-dependent manner. Int J Biol Sci. 2011; 7(6):869-880.
292. Lee SJ, Park SS, Lee US, Kim WJ and Moon SK. Signaling pathway for TNF-alpha-induced MMP-9 expression: mediation through p38 MAP kinase, and inhibition by anti-cancer molecule magnolol in human urinary bladder cancer 5637 cells. Int Immunopharmacol. 2008; 8(13-14):1821-1826.
293. Fisher GJ, Talwar HS, Lin J, Lin P, McPhillips F, Wang Z, Li X, Wan Y, Kang S and Voorhees JJ. Retinoic acid inhibits induction of c-Jun protein by ultraviolet radiation that occurs subsequent to activation of mitogen-activated protein kinase pathways in human skin in vivo. J Clin Invest. 1998; 101(6):1432-1440.
294. Xi Y, Tan K, Brumwell AN, Chen SC, Kim YH, Kim TJ, Wei Y and Chapman HA. Inhibition of epithelial-to-mesenchymal transition and pulmonary fibrosis by methacycline. Am J Respir Cell Mol Biol. 2014; 50(1):51-60.
295. Galvan-Salazar HR, Soriano-Hernandez AD, Montes-Galindo DA, Espiritu GC, Guzman-Esquivel J, Rodriguez-Sanchez IP, Newton-Sanchez OA, Martinez-Fierro ML, Gomez XG, Rojas-Martinez A and Delgado-Enciso I. Preclinical trial on the use of doxycycline for the treatment of adenocarcinoma of the duodenum. Mol Clin Oncol. 2016; 5(5):657-659.
296. Duivenvoorden WC, Popovic SV, Lhotak S, Seidlitz E, Hirte HW, Tozer RG and Singh G. Doxycycline decreases tumor burden in a bone metastasis model of human breast cancer. Cancer Res. 2002; 62(6):1588-1591.
297. Lokeshwar BL, Selzer MG, Zhu BQ, Block NL and Golub LM. Inhibition of cell proliferation, invasion, tumor growth and metastasis by an oral non-antimicrobial tetracycline analog (COL-3) in a metastatic prostate cancer model. Int J Cancer. 2002; 98(2):297-309.
298. Rudek MA, New P, Mikkelsen T, Phuphanich S, Alavi JB, Nabors LB, Piantadosi S, Fisher JD and Grossman SA. Phase I and pharmacokinetic study of COL-3 in patients with recurrent high-grade gliomas. J Neurooncol. 2011; 105(2):375-381.
299. Addison CL, Simos D, Wang Z, Pond G, Smith S, Robertson S, Mazzarello S, Singh G, Vandermeer L, Fernandes R, Iyengar A, Verma S and Clemons M. A phase 2 trial exploring the clinical and correlative effects of combining doxycycline with bone-targeted therapy in patients with metastatic breast cancer. J Bone Oncol. 2016; 5(4):173-179.
300. Han JJ, Kim TM, Jeon YK, Kim MK, Khwarg SI, Kim CW, Kim IH and Heo DS. Long-term outcomes of first-line treatment with doxycycline in patients with previously untreated ocular adnexal marginal zone B cell lymphoma. Ann Hematol. 2015; 94(4):575-581.
301. Lokeshwar BL. Chemically modified non-antimicrobial tetracyclines are multifunctional drugs against advanced cancers. Pharmacol Res. 2011; 63(2):146-150.
302. Marin-Aguilera M, Codony-Servat J, Kalko SG, Fernandez PL, Bermudo R, Buxo E, Ribal MJ, Gascon P and Mellado B. Identification of docetaxel resistance genes in castration-resistant prostate cancer. Mol Cancer Ther. 2012; 11(2):329-339.

303. Atjanasuppat K, Lirdprapamongkol K, Jantaree P and Svasti J. Non-adherent culture induces paclitaxel resistance in H460 lung cancer cells via ERK-mediated up-regulation of betaIVa-tubulin. Biochem Biophys Res Commun. 2015; 466(3):493-498.
304. Desarnaud F, Geck P, Parkin C, Carpinito G and Makarovskiy AN. Gene expression profiling of the androgen independent prostate cancer cells demonstrates complex mechanisms mediating resistance to docetaxel. Cancer Biol Ther. 2011; 11(2):204-212.
305. Bernard-Marty C, Treilleux I, Dumontet C, Cardoso F, Fellous A, Gancberg D, Bissery MC, Paesmans M, Larsimont D, Piccart MJ and Di Leo A. Microtubule-associated parameters as predictive markers of docetaxel activity in advanced breast cancer patients: results of a pilot study. Clin Breast Cancer. 2002; 3(5):341-345.
306. Zhu Y, Liu C, Nadiminty N, Lou W, Tummala R, Evans CP and Gao AC. Inhibition of ABCB1 expression overcomes acquired docetaxel resistance in prostate cancer. Mol Cancer Ther. 2013; 12(9):1829-1836.
307. Hansen SN, Westergaard D, Thomsen MB, Vistesen M, Do KN, Fogh L, Belling KC, Wang J, Yang H, Gupta R, Ditzel HJ, Moreira J, Brunner N, Stenvang J and Schrohl AS. Acquisition of docetaxel resistance in breast cancer cells reveals upregulation of ABCB1 expression as a key mediator of resistance accompanied by discrete upregulation of other specific genes and pathways. Tumour Biol. 2015; 36(6):4327-4338.
308. Abidi A. Cabazitaxel: A novel taxane for metastatic castration-resistant prostate cancer-current implications and future prospects. J Pharmacol Pharmacother. 2013; 4(4):230-237.
309. Huang B, Fu SJ, Fan WZ, Wang ZH, Chen ZB, Guo SJ, Chen JX and Qiu SP. PKCepsilon inhibits isolation and stemness of side population cells via the suppression of ABCB1 transporter and PI3K/Akt, MAPK/ERK signaling in renal cell carcinoma cell line 769P. Cancer Lett. 2016; 376(1):148-154.
310. Le Magnen C, Bubendorf L, Rentsch CA, Mengus C, Gsponer J, Zellweger T, Rieken M, Thalmann GN, Cecchini MG, Germann M, Bachmann A, Wyler S, Heberer M and Spagnoli GC. Characterization and clinical relevance of ALDHbright populations in prostate cancer. Clin Cancer Res. 2013; 19(19):5361-5371.
311. Sui H, Fan ZZ and Li Q. Signal transduction pathways and transcriptional mechanisms of ABCB1/Pgp-mediated multiple drug resistance in human cancer cells. J Int Med Res. 2012; 40(2):426-435.
312. Correa S, Binato R, Du Rocher B, Castelo-Branco MT, Pizzatti L and Abdelhay E. Wnt/beta-catenin pathway regulates ABCB1 transcription in chronic myeloid leukemia. BMC Cancer. 2012; 12:303.
313. Condello S, Morgan CA, Nagdas S, Cao L, Turek J, Hurley TD and Matei D. beta-Catenin-regulated ALDH1A1 is a target in ovarian cancer spheroids. Oncogene. 2015; 34(18):2297-2308.
314. Filali M, Cheng N, Abbott D, Leontiev V and Engelhardt JF. Wnt-3A/beta-catenin signaling induces transcription from the LEF-1 promoter. J Biol Chem. 2002; 277(36):33398-33410.
315. Hwang SG, Yu SS, Lee SW and Chun JS. Wnt-3a regulates chondrocyte differentiation via c-Jun/AP-1 pathway. FEBS Lett. 2005; 579(21):4837-4842.
316. Chen T, Stephens PA, Middleton FK and Curtin NJ. Targeting the S and G2 checkpoint to treat cancer. Drug Discov Today. 2012; 17(5-6):194-202.
317. Podhorecka M, Skladanowski A and Bozko P. H2AX Phosphorylation: Its Role in DNA Damage Response and Cancer Therapy. J Nucleic Acids. 2010; 2010.
318. Kalantari E, Saadi FH, Asgari M, Shariftabrizi A, Roudi R and Madjd Z. Increased Expression of ALDH1A1 in Prostate Cancer is Correlated With Tumor Aggressiveness: A Tissue Microarray Study of Iranian Patients. Appl Immunohistochem Mol Morphol. 2016.
319. Long Q, Johnson BA, Osunkoya AO, Lai YH, Zhou W, Abramovitz M, Xia M, Bouzyk MB, Nam RK, Sugar L, Stanimirovic A, Williams DJ, Leyland-Jones BR, Seth AK, Petros JA and Moreno CS. Protein-coding and microRNA biomarkers of recurrence of prostate cancer following radical prostatectomy. Am J Pathol. 2011; 179(1):46-54.

320. Hubbard GK, Mutton LN, Khalili M, McMullin RP, Hicks JL, Bianchi-Frias D, Horn LA, Kulac I, Moubarek MS, Nelson PS, Yegnasubramanian S, De Marzo AM and Bieberich CJ. Combined MYC Activation and Pten Loss Are Sufficient to Create Genomic Instability and Lethal Metastatic Prostate Cancer. Cancer Res. 2016; 76(2):283-292.
321. Ross-Adams H, Lamb AD, Dunning MJ, Halim S, Lindberg J, Massie CM, Egevad LA, Russell R, Ramos-Montoya A, Vowler SL, Sharma NL, Kay J, Whitaker H, Clark J, Hurst R, Gnanapragasam VJ, et al. Integration of copy number and transcriptomics provides risk stratification in prostate cancer: A discovery and validation cohort study. EBioMedicine. 2015; 2(9):1133-1144.
322. Vera-Ramirez L, Sanchez-Rovira P, Ramirez-Tortosa CL, Quiles JL, Ramirez-Tortosa M and Lorente JA. Transcriptional shift identifies a set of genes driving breast cancer chemoresistance. PLoS One. 2013; 8(1):e53983.
323. Gyorffy B, Lanczky A, Eklund AC, Denkert C, Budczies J, Li Q and Szallasi Z. An online survival analysis tool to rapidly assess the effect of 22,277 genes on breast cancer prognosis using microarray data of 1,809 patients. Breast Cancer Res Treat. 2010; 123(3):725-731.
324. Gygi SP, Rochon Y, Franza BR and Aebersold R. Correlation between protein and mRNA abundance in yeast. Molecular and cellular biology. 1999; 19(3):1720-1730.
325. Ingolia NT, Ghaemmaghami S, Newman JRS and Weissman JS. Genome-wide analysis in vivo of translation with nucleotide resolution using ribosome profiling. Science (New York, N Y). 2009; 324(5924):218-223.
326. Lichtinghagen R, Musholt PB, Lein M, Romer A, Rudolph B, Kristiansen G, Hauptmann S, Schnorr D, Loening SA and Jung K. Different mRNA and protein expression of matrix metalloproteinases 2 and 9 and tissue inhibitor of metalloproteinases 1 in benign and malignant prostate tissue. European urology. 2002; 42(4):398-406.
327. Wang H, Fang R, Wang X-F, Zhang F, Chen D-Y, Zhou B, Wang H-S, Cai S-H and Du J. Stabilization of Snail through AKT/GSK-3beta signaling pathway is required for TNF-alpha-induced epithelial-mesenchymal transition in prostate cancer PC3 cells. European journal of pharmacology. 2013; 714(1-3):48-55.
328. Koo KH, Jeong WJ, Cho YH, Park JC, Min DS and Choi KY. K-Ras stabilization by estrogen via PKCdelta is involved in endometrial tumorigenesis. Oncotarget. 2015; 6(25):21328-21340.
329. Monsellier E and Bedouelle H. Quantitative measurement of protein stability from unfolding equilibria monitored with the fluorescence maximum wavelength. Protein Eng Des Sel. 2005; 18(9):445-456.
330. Planchais S, Camborde L and Jupin I. Protocols for Studying Protein Stability in an Arabidopsis Protoplast Transient Expression System. Methods Mol Biol. 2016; 1450:175-194.
331. Duran GE, Wang YC, Francisco EB, Rose JC, Martinez FJ, Coller J, Brassard D, Vrignaud P and Sikic BI. Mechanisms of resistance to cabazitaxel. Mol Cancer Ther. 2015; 14(1):193-201.
332. Karatas OF, Guzel E, Duz MB, Ittmann M and Ozen M. The role of ATP-binding cassette transporter genes in the progression of prostate cancer. Prostate. 2016; 76(5):434-444.
333. Bhangal G, Halford S, Wang J, Roylance R, Shah R and Waxman J. Expression of the multidrug resistance gene in human prostate cancer. Urol Oncol. 2000; 5(3):118-121.
334. Murota Y, Tabu K and Taga T. Requirement of ABC transporter inhibition and Hoechst 33342 dye deprivation for the assessment of side population-defined C6 glioma stem cell metabolism using fluorescent probes. BMC Cancer. 2016; 16(1):847.
335. Eyre R, Harvey I, Stemke-Hale K, Lennard TW, Tyson-Capper A and Meeson AP. Reversing paclitaxel resistance in ovarian cancer cells via inhibition of the ABCB1 expressing side population. Tumour Biol. 2014; 35(10):9879-9892.
336. Wang Y and Teng JS. Increased multi-drug resistance and reduced apoptosis in osteosarcoma side population cells are crucial factors for tumor recurrence. Exp Ther Med. 2016; 12(1):81-86.
337. Kulsum S, H VS, P R, D RR, Siddappa G, R N, Chevour P, Ramachandran B, Sagar M, Jayaprakash A, Mehta A, Kekatpure V, Hedne N, Kuriakose MA and Suresh A. Cancer stem cell

mediated acquired chemoresistance in head and neck cancer can be abrogated by Aldehyde dehydrogenase 1 A1 inhibition. Mol Carcinog. 2016.
338. Wiechert A, Saygin C, Thiagarajan PS, Rao VS, Hale JS, Gupta N, Hitomi M, Nagaraj AB, DiFeo A, Lathia JD and Reizes O. Cisplatin induces stemness in ovarian cancer. Oncotarget. 2016.
339. Saker Z, Tsintsadze O, Jiqia I, Managadze L and Chkhotua A. IMPORTANCE OF APOPTOSIS MARKERS (MDM2, BCL-2 AND Bax) IN BENIGN PROSTATIC HYPERPLASIA AND PROSTATE CANCER. Georgian Med News. 2015; (249):7-14.
340. Ploussard G, Terry S, Maille P, Allory Y, Sirab N, Kheuang L, Soyeux P, Nicolaiew N, Coppolani E, Paule B, Salomon L, Culine S, Buttyan R, Vacherot F and de la Taille A. Class III beta-tubulin expression predicts prostate tumor aggressiveness and patient response to docetaxel-based chemotherapy. Cancer Res. 2010; 70(22):9253-9264.
341. Tinzl M, Chen B, Chen SY, Semenas J, Abrahamsson PA and Dizeyi N. Interaction between c-jun and androgen receptor determines the outcome of taxane therapy in castration resistant prostate cancer. PLoS One. 2013; 8(11):e79573.
342. Viswanathan SR, Powers JT, Einhorn W, Hoshida Y, Ng TL, Toffanin S, O'Sullivan M, Lu J, Phillips LA, Lockhart VL, Shah SP, Tanwar PS, Mermel CH, Beroukhim R, Azam M, Teixeira J, et al. Lin28 promotes transformation and is associated with advanced human malignancies. Nat Genet. 2009; 41(7):843-848.
343. Choi SA, Kim SK, Lee JY, Wang KC, Lee C and Phi JH. LIN28B is highly expressed in atypical teratoid/rhabdoid tumor (AT/RT) and suppressed through the restoration of SMARCB1. Cancer Cell Int. 2016; 16:32.
344. Shen H, Yang Y, Zhao L, Yuan J and Niu Y. Lin28A and androgen receptor expression in ER-/Her2+ breast cancer. Breast Cancer Res Treat. 2016; 156(1):135-147.
345. Xu M, Bian S, Li J, He J, Chen H, Ge L, Jiao Z, Zhang Y, Peng W, Du F, Mo Y and Gong A. MeCP2 suppresses LIN28A expression via binding to its methylated-CpG islands in pancreatic cancer cells. Oncotarget. 2016; 7(12):14476-14485.
346. Albino D, Civenni G, Dallavalle C, Roos M, Jahns H, Curti L, Rossi S, Pinton S, D'Ambrosio G, Sessa F, Hall J, Catapano CV and Carbone GM. Activation of the Lin28/let-7 Axis by Loss of ESE3/EHF Promotes a Tumorigenic and Stem-like Phenotype in Prostate Cancer. Cancer Res. 2016; 76(12):3629-3643.
347. Zhou J, Ng SB and Chng WJ. LIN28/LIN28B: an emerging oncogenic driver in cancer stem cells. Int J Biochem Cell Biol. 2013; 45(5):973-978.
348. Tummala R, Nadiminty N, Lou W, Evans CP and Gao AC. Lin28 induces resistance to anti-androgens via promotion of AR splice variant generation. Prostate. 2016; 76(5):445-455.
349. Li T, Su Y, Mei Y, Leng Q, Leng B, Liu Z, Stass SA and Jiang F. ALDH1A1 is a marker for malignant prostate stem cells and predictor of prostate cancer patients' outcome. Lab Invest. 2010; 90(2):234-244.
350. Nowak DG, Cho H, Herzka T, Watrud K, DeMarco DV, Wang VM, Senturk S, Fellmann C, Ding D, Beinortas T, Kleinman D, Chen M, Sordella R, Wilkinson JE, Castillo-Martin M, Cordon-Cardo C, et al. MYC Drives Pten/Trp53-Deficient Proliferation and Metastasis due to IL6 Secretion and AKT Suppression via PHLPP2. Cancer Discov. 2015; 5(6):636-651.
351. Hasegawa S, Nagano H, Konno M, Eguchi H, Tomokuni A, Tomimaru Y, Wada H, Hama N, Kawamoto K, Kobayashi S, Marubashi S, Nishida N, Koseki J, Gotoh N, Ohno S, Yabuta N, et al. Cyclin G2: A novel independent prognostic marker in pancreatic cancer. Oncol Lett. 2015; 10(5):2986-2990.
352. Sun GG, Zhang J and Hu WN. CCNG2 expression is downregulated in colorectal carcinoma and its clinical significance. Tumour Biol. 2014; 35(4):3339-3346.
353. Fujimura A, Michiue H, Cheng Y, Uneda A, Tani Y, Nishiki T, Ichikawa T, Wei FY, Tomizawa K and Matsui H. Cyclin G2 promotes hypoxia-driven local invasion of glioblastoma by orchestrating cytoskeletal dynamics. Neoplasia. 2013; 15(11):1272-1281.
354. Manoochehri Khoshinani H, Afshar S and Najafi R. Hypoxia: A Double-Edged Sword in Cancer Therapy. Cancer Invest. 2016:1-10.

355. Overgaard J. Hypoxic modification of radiotherapy in squamous cell carcinoma of the head and neck--a systematic review and meta-analysis. Radiother Oncol. 2011; 100(1):22-32.
356. Li Y, Hussain M, Sarkar SH, Eliason J, Li R and Sarkar FH. Gene expression profiling revealed novel mechanism of action of Taxotere and Furtulon in prostate cancer cells. BMC Cancer. 2005; 5:7.
357. Li Y, Hong X, Hussain M, Sarkar SH, Li R and Sarkar FH. Gene expression profiling revealed novel molecular targets of docetaxel and estramustine combination treatment in prostate cancer cells. Mol Cancer Ther. 2005; 4(3):389-398.
358. Arachchige Don AS, Dallapiazza RF, Bennin DA, Brake T, Cowan CE and Horne MC. Cyclin G2 is a centrosome-associated nucleocytoplasmic shuttling protein that influences microtubule stability and induces a p53-dependent cell cycle arrest. Exp Cell Res. 2006; 312(20):4181-4204.
359. Maroto P, Solsona E, Gallardo E, Mellado B, Morote J, Arranz JA, Gomez-Veiga F, Unda M, Climent MA and Alcaraz A. Expert opinion on first-line therapy in the treatment of castration-resistant prostate cancer. Crit Rev Oncol Hematol. 2016; 100:127-136.
360. Rybak AP, He L, Kapoor A, Cutz JC and Tang D. Characterization of sphere-propagating cells with stem-like properties from DU145 prostate cancer cells. Biochim Biophys Acta. 2011; 1813(5):683-694.
361. Vaishampayan U, Shevrin D, Stein M, Heilbrun L, Land S, Stark K, Li J, Dickow B, Heath E, Smith D and Fontana J. Phase II Trial of Carboplatin, Everolimus, and Prednisone in Metastatic Castration-resistant Prostate Cancer Pretreated With Docetaxel Chemotherapy: A Prostate Cancer Clinical Trial Consortium Study. Urology. 2015; 86(6):1206-1211.
362. Lu CS, Shieh GS, Wang CT, Su BH, Su YC, Chen YC, Su WC, Wu P, Yang WH, Shiau AL and Wu CL. Chemotherapeutics-induced Oct4 expression contributes to drug resistance and tumor recurrence in bladder cancer. Oncotarget. 2016.
363. Erho N, Crisan A, Vergara IA, Mitra AP, Ghadessi M, Buerki C, Bergstralh EJ, Kollmeyer T, Fink S, Haddad Z, Zimmermann B, Sierocinski T, Ballman KV, Triche TJ, Black PC, Karnes RJ, et al. Discovery and validation of a prostate cancer genomic classifier that predicts early metastasis following radical prostatectomy. PLoS One. 2013; 8(6):e66855.
364. Jackson SP and Bartek J. The DNA-damage response in human biology and disease. Nature. 2009; 461(7267):1071-1078.
365. Olaussen KA, Dunant A, Fouret P, Brambilla E, Andre F, Haddad V, Taranchon E, Filipits M, Pirker R, Popper HH, Stahel R, Sabatier L, Pignon JP, Tursz T, Le Chevalier T and Soria JC. DNA repair by ERCC1 in non-small-cell lung cancer and cisplatin-based adjuvant chemotherapy. N Engl J Med. 2006; 355(10):983-991.
366. Moeller BJ, Yordy JS, Williams MD, Giri U, Raju U, Molkentine DP, Byers LA, Heymach JV, Story MD, Lee JJ, Sturgis EM, Weber RS, Garden AS, Ang KK and Schwartz DL. DNA repair biomarker profiling of head and neck cancer: Ku80 expression predicts locoregional failure and death following radiotherapy. Clin Cancer Res. 2011; 17(7):2035-2043.
367. Handra-Luca A, Hernandez J, Mountzios G, Taranchon E, Lacau-St-Guily J, Soria JC and Fouret P. Excision repair cross complementation group 1 immunohistochemical expression predicts objective response and cancer-specific survival in patients treated by Cisplatin-based induction chemotherapy for locally advanced head and neck squamous cell carcinoma. Clin Cancer Res. 2007; 13(13):3855-3859.
368. Ye J, Ren Z, Gu Q, Wang L and Wang J. Ku80 is differentially expressed in human lung carcinomas and upregulated in response to irradiation in mice. DNA Cell Biol. 2011; 30(12):987-994.
369. Raderschall E, Stout K, Freier S, Suckow V, Schweiger S and Haaf T. Elevated levels of Rad51 recombination protein in tumor cells. Cancer Res. 2002; 62(1):219-225.
370. Slupianek A, Schmutte C, Tombline G, Nieborowska-Skorska M, Hoser G, Nowicki MO, Pierce AJ, Fishel R and Skorski T. BCR/ABL regulates mammalian RecA homologs, resulting in drug resistance. Mol Cell. 2001; 8(4):795-806.

371. Rojo F, Garcia-Parra J, Zazo S, Tusquets I, Ferrer-Lozano J, Menendez S, Eroles P, Chamizo C, Servitja S, Ramirez-Merino N, Lobo F, Bellosillo B, Corominas JM, Yelamos J, Serrano S, Lluch A, et al. Nuclear PARP-1 protein overexpression is associated with poor overall survival in early breast cancer. Ann Oncol. 2012; 23(5):1156-1164.
372. Bao S, Wu Q, McLendon RE, Hao Y, Shi Q, Hjelmeland AB, Dewhirst MW, Bigner DD and Rich JN. Glioma stem cells promote radioresistance by preferential activation of the DNA damage response. Nature. 2006; 444(7120):756-760.
373. Alshareeda AT, Negm OH, Albarakati N, Green AR, Nolan C, Sultana R, Madhusudan S, Benhasouna A, Tighe P, Ellis IO and Rakha EA. Clinicopathological significance of KU70/KU80, a key DNA damage repair protein in breast cancer. Breast Cancer Res Treat. 2013; 139(2):301-310.
374. Srivastava AK, Han C, Zhao R, Cui T, Dai Y, Mao C, Zhao W, Zhang X, Yu J and Wang QE. Enhanced expression of DNA polymerase eta contributes to cisplatin resistance of ovarian cancer stem cells. Proc Natl Acad Sci U S A. 2015; 112(14):4411-4416.
375. Greer YE, Gao B, Yang Y, Nussenzweig A and Rubin JS. Lack of Casein Kinase 1 Delta Promotes Genomic Instability - The Accumulation of DNA Damage and Down-Regulation of Checkpoint Kinase 1. PLoS One. 2017; 12(1):e0170903.
376. Kavanaugh GM, Wise-Draper TM, Morreale RJ, Morrison MA, Gole B, Schwemberger S, Tichy ED, Lu L, Babcock GF, Wells JM, Drissi R, Bissler JJ, Stambrook PJ, Andreassen PR, Wiesmuller L and Wells SI. The human DEK oncogene regulates DNA damage response signaling and repair. Nucleic Acids Res. 2011; 39(17):7465-7476.
377. Liu X, Han EK, Anderson M, Shi Y, Semizarov D, Wang G, McGonigal T, Roberts L, Lasko L, Palma J, Zhu GD, Penning T, Rosenberg S, Giranda VL, Luo Y, Leverson J, et al. Acquired resistance to combination treatment with temozolomide and ABT-888 is mediated by both base excision repair and homologous recombination DNA repair pathways. Mol Cancer Res. 2009; 7(10):1686-1692.
378. Fell VL and Schild-Poulter C. The Ku heterodimer: function in DNA repair and beyond. Mutat Res Rev Mutat Res. 2015; 763:15-29.
379. Rausch S, Hennenlotter J, Scharpf M, Teepe K, Kuhs U, Aufderklamm S, Bier S, Mischinger J, Gakis G, Stenzl A, Schwentner C and Todenhofer T. Prostate tumor overexpressed 1 expression in invasive urothelial carcinoma. J Cancer Res Clin Oncol. 2016; 142(5):937-947.
380. Dong Z and Zhang JT. Initiation factor eIF3 and regulation of mRNA translation, cell growth, and cancer. Crit Rev Oncol Hematol. 2006; 59(3):169-180.
381. Evdokimova V, Tognon C, Ng T, Ruzanov P, Melnyk N, Fink D, Sorokin A, Ovchinnikov LP, Davicioni E, Triche TJ and Sorensen PH. Translational activation of snail1 and other developmentally regulated transcription factors by YB-1 promotes an epithelial-mesenchymal transition. Cancer Cell. 2009; 15(5):402-415.
382. Coleman LJ, Peter MB, Teall TJ, Brannan RA, Hanby AM, Honarpisheh H, Shaaban AM, Smith L, Speirs V, Verghese ET, McElwaine JN and Hughes TA. Combined analysis of eIF4E and 4E-binding protein expression predicts breast cancer survival and estimates eIF4E activity. Br J Cancer. 2009; 100(9):1393-1399.
383. Fan S, Ramalingam SS, Kauh J, Xu Z, Khuri FR and Sun SY. Phosphorylated eukaryotic translation initiation factor 4 (eIF4E) is elevated in human cancer tissues. Cancer Biol Ther. 2009; 8(15):1463-1469.
384. Jackson RJ, Hellen CU and Pestova TV. The mechanism of eukaryotic translation initiation and principles of its regulation. Nat Rev Mol Cell Biol. 2010; 11(2):113-127.
385. Gao M, Ossowski L and Ferrari AC. Activation of Rb and decline in androgen receptor protein precede retinoic acid-induced apoptosis in androgen-dependent LNCaP cells and their androgen-independent derivative. J Cell Physiol. 1999; 179(3):336-346.
386. Richichi C, Brescia P, Alberizzi V, Fornasari L and Pelicci G. Marker-independent method for isolating slow-dividing cancer stem cells in human glioblastoma. Neoplasia. 2013; 15(7):840-847.

387. Tang M, Yang Y, Yu J, Wu N, Chen P, Xu L, Wang Q, Xu Z, Ge J, Yu K and Zhuang J. Discordant mRNA and protein expression of CXCR4 under in vitro CoCl2-induced hypoxic conditions. Biochem Biophys Res Commun. 2017; 484(2):285-291.
388. Chen G, Gharib TG, Huang CC, Taylor JM, Misek DE, Kardia SL, Giordano TJ, Iannettoni MD, Orringer MB, Hanash SM and Beer DG. Discordant protein and mRNA expression in lung adenocarcinomas. Mol Cell Proteomics. 2002; 1(4):304-313.
389. Mori S, Nada S, Kimura H, Tajima S, Takahashi Y, Kitamura A, Oneyama C and Okada M. The mTOR pathway controls cell proliferation by regulating the FoxO3a transcription factor via SGK1 kinase. PLoS One. 2014; 9(2):e88891.
390. Laplante M and Sabatini DM. mTOR signaling in growth control and disease. Cell. 2012; 149(2):274-293.
391. Graupera M, Guillermet-Guibert J, Foukas LC, Phng LK, Cain RJ, Salpekar A, Pearce W, Meek S, Millan J, Cutillas PR, Smith AJ, Ridley AJ, Ruhrberg C, Gerhardt H and Vanhaesebroeck B. Angiogenesis selectively requires the p110alpha isoform of PI3K to control endothelial cell migration. Nature. 2008; 453(7195):662-666.
392. Irie HY, Pearline RV, Grueneberg D, Hsia M, Ravichandran P, Kothari N, Natesan S and Brugge JS. Distinct roles of Akt1 and Akt2 in regulating cell migration and epithelial-mesenchymal transition. J Cell Biol. 2005; 171(6):1023-1034.
393. Xing X, Zhang L, Wen X, Wang X, Cheng X, Du H, Hu Y, Li L, Dong B, Li Z and Ji J. PP242 suppresses cell proliferation, metastasis, and angiogenesis of gastric cancer through inhibition of the PI3K/AKT/mTOR pathway. Anticancer Drugs. 2014; 25(10):1129-1140.
394. Nakao T, Shiota M, Tatemoto Y, Izumi Y and Iwao H. Pravastatin induces rat aortic endothelial cell proliferation and migration via activation of PI3K/Akt/mTOR/p70 S6 kinase signaling. J Pharmacol Sci. 2007; 105(4):334-341.
395. Courtes FC, Vardy L, Wong NS, Bardor M, Yap MG and Lee DY. Understanding translational control mechanisms of the mTOR pathway in CHO cells by polysome profiling. N Biotechnol. 2014; 31(5):514-523.
396. Wall M, Poortinga G, Hannan KM, Pearson RB, Hannan RD and McArthur GA. Translational control of c-MYC by rapamycin promotes terminal myeloid differentiation. Blood. 2008; 112(6):2305-2317.
397. Best CJ, Gillespie JW, Yi Y, Chandramouli GV, Perlmutter MA, Gathright Y, Erickson HS, Georgevich L, Tangrea MA, Duray PH, Gonzalez S, Velasco A, Linehan WM, Matusik RJ, Price DK, Figg WD, et al. Molecular alterations in primary prostate cancer after androgen ablation therapy. Clin Cancer Res. 2005; 11(19 Pt 1):6823-6834.
398. Graff JR, Konicek BW, Lynch RL, Dumstorf CA, Dowless MS, McNulty AM, Parsons SH, Brail LH, Colligan BM, Koop JW, Hurst BM, Deddens JA, Neubauer BL, Stancato LF, Carter HW, Douglass LE, et al. eIF4E activation is commonly elevated in advanced human prostate cancers and significantly related to reduced patient survival. Cancer Res. 2009; 69(9):3866-3873.
399. Pierobon M, Ramos C, Wong S, Hodge KA, Aldrich J, Byron SA, Anthony SP, Robert NJ, Northfelt DW, Jahanzeb M, Vocila L, Wulfkuhle JD, Gambara G, Gallagher RI, Dunetz B, Hoke N, et al. Enrichment of PIK3-AKT-MTOR pathway activation in hepatic metastases from breast cancer. Clin Cancer Res. 2017.
400. Cotsarelis G, Sun TT and Lavker RM. Label-retaining cells reside in the bulge area of pilosebaceous unit: implications for follicular stem cells, hair cycle, and skin carcinogenesis. Cell. 1990; 61(7):1329-1337.
401. Sampath P, Pritchard DK, Pabon L, Reinecke H, Schwartz SM, Morris DR and Murry CE. A hierarchical network controls protein translation during murine embryonic stem cell self-renewal and differentiation. Cell Stem Cell. 2008; 2(5):448-460.
402. Reya T, Morrison SJ, Clarke MF and Weissman IL. Stem cells, cancer, and cancer stem cells. Nature. 2001; 414(6859):105-111.
403. Qin J, Liu X, Laffin B, Chen X, Choy G, Jeter CR, Calhoun-Davis T, Li H, Palapattu GS, Pang S, Lin K, Huang J, Ivanov I, Li W, Suraneni MV and Tang DG. The PSA(-/lo) prostate cancer cell

population harbors self-renewing long-term tumor-propagating cells that resist castration. Cell Stem Cell. 2012; 10(5):556-569.
404. Dembinski JL and Krauss S. Characterization and functional analysis of a slow cycling stem cell-like subpopulation in pancreas adenocarcinoma. Clin Exp Metastasis. 2009; 26(7):611-623.
405. Blanco S, Bandiera R, Popis M, Hussain S, Lombard P, Aleksic J, Sajini A, Tanna H, Cortes-Garrido R, Gkatza N, Dietmann S and Frye M. Stem cell function and stress response are controlled by protein synthesis. Nature. 2016; 534(7607):335-340.
406. Hsieh AC, Nguyen HG, Wen L, Edlind MP, Carroll PR, Kim W and Ruggero D. Cell type-specific abundance of 4EBP1 primes prostate cancer sensitivity or resistance to PI3K pathway inhibitors. Sci Signal. 2015; 8(403):ra116.
407. Peng S, Chen LL, Lei XX, Yang L, Lin H, Carmichael GG and Huang Y. Genome-wide studies reveal that Lin28 enhances the translation of genes important for growth and survival of human embryonic stem cells. Stem Cells. 2011; 29(3):496-504.
408. Schott J, Reitter S, Philipp J, Haneke K, Schafer H and Stoecklin G. Translational regulation of specific mRNAs controls feedback inhibition and survival during macrophage activation. PLoS Genet. 2014; 10(6):e1004368.
409. Wong QW, Vaz C, Lee QY, Zhao TY, Luo R, Archer SK, Preiss T, Tanavde V and Vardy LA. Embryonic Stem Cells Exhibit mRNA Isoform Specific Translational Regulation. PLoS One. 2016; 11(1):e0143235.
410. Tebaldi T, Re A, Viero G, Pegoretti I, Passerini A, Blanzieri E and Quattrone A. Widespread uncoupling between transcriptome and translatome variations after a stimulus in mammalian cells. BMC Genomics. 2012; 13:220.
411. Zhu H, Shah S, Shyh-Chang N, Shinoda G, Einhorn WS, Viswanathan SR, Takeuchi A, Grasemann C, Rinn JL, Lopez MF, Hirschhorn JN, Palmert MR and Daley GQ. Lin28a transgenic mice manifest size and puberty phenotypes identified in human genetic association studies. Nat Genet. 2010; 42(7):626-630.
412. Jechlinger M, Grunert S, Tamir IH, Janda E, Ludemann S, Waerner T, Seither P, Weith A, Beug H and Kraut N. Expression profiling of epithelial plasticity in tumor progression. Oncogene. 2003; 22(46):7155-7169.
413. Bunnik EM, Chung DW, Hamilton M, Ponts N, Saraf A, Prudhomme J, Florens L and Le Roch KG. Polysome profiling reveals translational control of gene expression in the human malaria parasite Plasmodium falciparum. Genome Biol. 2013; 14(11):R128.
414. Sterne-Weiler T, Martinez-Nunez RT, Howard JM, Cvitovik I, Katzman S, Tariq MA, Pourmand N and Sanford JR. Frac-seq reveals isoform-specific recruitment to polyribosomes. Genome Res. 2013; 23(10):1615-1623.
415. Masvidal L, Hulea L, Furic L, Topisirovic I and Larsson O. mTOR-sensitive translation: Cleared fog reveals more trees. RNA Biol. 2017:1-7.
416. Jeffery CJ. An introduction to protein moonlighting. Biochem Soc Trans. 2014; 42(6):1679-1683.
417. Jeffery CJ. Molecular mechanisms for multitasking: recent crystal structures of moonlighting proteins. Curr Opin Struct Biol. 2004; 14(6):663-668.
418. Huberts DH and van der Klei IJ. Moonlighting proteins: an intriguing mode of multitasking. Biochim Biophys Acta. 2010; 1803(4):520-525.
419. Bhoumik A, Takahashi S, Breitweiser W, Shiloh Y, Jones N and Ronai Z. ATM-dependent phosphorylation of ATF2 is required for the DNA damage response. Mol Cell. 2005; 18(5):577-587.
420. Wegrzyn J, Potla R, Chwae YJ, Sepuri NB, Zhang Q, Koeck T, Derecka M, Szczepanek K, Szelag M, Gornicka A, Moh A, Moghaddas S, Chen Q, Bobbili S, Cichy J, Dulak J, et al. Function of mitochondrial Stat3 in cellular respiration. Science. 2009; 323(5915):793-797.

Appendix I: PUBLICATIONS

1. **Cánovas V,** Puñal Y, Maggio V, Redondo E, M Marín, Mellado B, Olivan M, Lleonart M**,** Planas J, Morote J, Paciucci R**. Prostate Tumor Overexpressed-1 (PTOV1) promotes docetaxel-resistance and survival of castration resistant prostate cancer cells.** Oncotarget. Published July 22, 2017
2. **Cánovas V,** Lleonart M, Morote J, Paciucci R. **The role of prostate tumor overexpressed 1 in cancer progression.** Oncotarget. 2017 Feb 14;8(7):12451-12471.
3. Mateo F, Meca-Cortés O, Celià-Terrassa T, Fernández Y, Abasolo I, Sánchez-Cid L, Bermudo R, Sagasta A, Rodríguez-Carunchio L, Pons M, **Cánovas V**, Marín-Aguilera M, Mengual L, Alcaraz A, Schwartz S Jr, Mellado B, Aguilera KY, Brekken R, Fernández PL, Paciucci R, Thomson TM. **SPARC mediates metastatic cooperation between CSC and non-CSC prostate cancer cell subpopulations.** Mol Cancer. 2014 Oct 21;13:237.
4. Marqués N*, Sesé M*, **Cánovas V**, Valente F, Bermudo R, de Torres I, Fernández Y, Abasolo I, Fernández PL, Contreras H, Castellón E, Celià-Terrassa T, Méndez R, Ramón Y Cajal S, Thomson TM, Paciucci R. **Regulation of protein translation and c-Jun expression by Prostate Tumor Overexpressed 1 (PTOV1).** Oncogene. 2014 Feb 27;33(9):1124-34.
5. Alaña L*, Sesé M*, **Cánovas V**, Punyal Y, Fernández Y, Abasolo I, de Torres I, Ruiz C, Espinosa L, Bigas A, Y Cajal SR, Fernández PL, Serras F,Corominas M, Thomson TM, Paciucci R. **Prostate Tumor OVerexpressed-1 (PTOV1) down-regulates HES1 and HEY1 Notch targets genes and promotes prostate cancer progression.** Mol Cancer. 2014 Mar 31;13(1):74.

***(**Equal contribution**)**